

AD-A182 229

THE INTERACTION OF SMALL PARTICLES WITH LASER BEAMS(U)

1/2

FLORIDA UNIV GAINESVILLE SPACE ASTRONOMY LAB

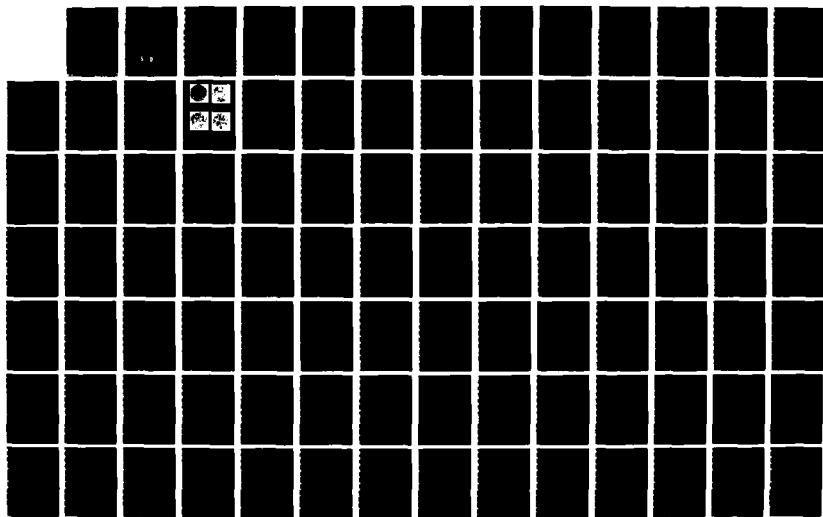
N Y MISCONI ET AL 18 FEB 87 AFOSR-TR-87-0664

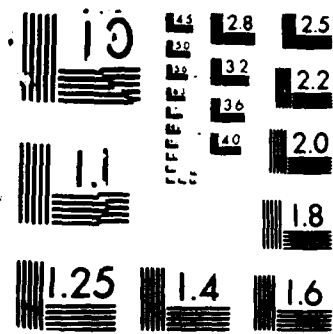
UNCLASSIFIED

F49620-85-C-0117

F/G 20/6

NL





AD-A182 229

AIR FORCE OFFICE OF SCIENTIFIC RESEARCH (AFSC)
NOTICE OF TRANSMITTAL TO DTIC
This technical report has been reviewed and is
approved for public release IAW AFR 190-12.
Distribution is unlimited.
MATTHEW J. KERPER
Chief, Technical Information Division

DTIC FILE COPY

2

AFOSR-TR- 87-0664

Approved for public release;
distribution unlimited.

ANNUAL REPORT

AFOSR CONTRACT - F49620-85-C-0117

THE INTERACTION OF SMALL PARTICLES WITH LASER BEAMS

Period of Performance:

9 July 1985 - 9 Oct. 1986

Principal Investigator:

Dr. N. Y. Misconi
Space Astronomy Laboratory
University of Florida
1810 NW 6th Street
Gainesville, Florida 32609
(904) 392-5450

Co-Investigator:

Dr. K. F. Ratcliff
Department of Physics
State University of New York
at Albany
1400 Washington Avenue
Albany, New York 12222

Scientific Collaborators:

Dr. J. P. Oliver
Department of Astronomy
University of Florida
Gainesville, Florida 32611

Dr. E. T. Rusk
Space Astronomy Laboratory
University of Florida
1810 NW 6th Street
Gainesville, Florida 32609

DTIC
ELECTE
JUN 24 1987
S D

February 18, 1987

87 5 20 129

REPORT DOCUMENTATION PAGE

1a. REPORT SECURITY CLASSIFICATION Unclassified		1b. RESTRICTIVE MARKINGS	
2a. SECURITY CLASSIFICATION AUTHORITY		3. DISTRIBUTION AVAILABILITY OF REPORT APPROVED FOR PUBLIC RELEASE DISTRIBUTION UNLIMITED	
2b. DECLASSIFICATION/DOWNGRADING SCHEDULE		5. MONITORING ORGANIZATION REPORT NUMBER(S) AFOSR-TN- 87-0664	
4. PERFORMING ORGANIZATION REPORT NUMBER(S)		7a. NAME OF MONITORING ORGANIZATION AFOSR	
6a. NAME OF PERFORMING ORGANIZATION University of Florida	6b. OFFICE SYMBOL (If applicable):	7b. ADDRESS (City, State and ZIP Code) BKA 410 Bolling AFB, D.C. 20332	
6c. ADDRESS (City, State and ZIP Code) Space Astronomy Laboratory 1810 NW 6th Street Gainesville, Florida 32609	6d. OFFICE SYMBOL (If applicable): NE	8. PROCUREMENT INSTRUMENT IDENTIFICATION NUMBER F49620-85-C-0117	
9a. NAME OF FUNDING/SPONSORING ORGANIZATION AFOSR	9b. OFFICE SYMBOL (If applicable): NE	10. SOURCE OF FUNDING NOS.	
9c. ADDRESS (City, State and ZIP Code) BKA 410 Bolling AFB, D.C. 20332		PROGRAM ELEMENT NO. 61102F	PROJECT NO. 2306
11. TITLE (Include Security Classification) The Interaction of Small Particles with Laser Beams		TASK NO. A1	WORK UNIT NO.
12. PERSONAL AUTHOR(S) Dr. N. Y. Misconi, Dr. K. F. Rateliff, and Dr. E. T. Rusk			
13a. TYPE OF REPORT Annual	13b. TIME COVERED FROM July 85 TO Oct. 86	14. DATE OF REPORT (Yr. Mo., Day) 18 Feb 87	15. PAGE COUNT
16. SUPPLEMENTARY NOTATION			
17. COSATI CODES		18. SUBJECT TERMS (Continue on reverse if necessary and identify by block number)	
FIELD	GROUP	SUB. GR.	
19. ABSTRACT (Continue on reverse if necessary and identify by block number)			
<p>This report summarizes our research under Award/Contract F49620-85-C-0117 with the interaction of a CW Argon laser beam with a variety of layers of small (few microns to a few hundred microns) particles formed out of pigments which are highly transparent over the range of wavelengths 0.35 - 0.7 μm. The known particle layers range from 0.25 mm to 2 mm. The nature of this research is to characterize the scattering of laser light by these layers. It was found that a layer of natural and synthetic laser light than suprasil, flexolite glass, fused commercial glass, or even water. Layers of irregular particles reflected more light than those of smooth surfaces. Reflectivity varied inversely with particle size. Quantitative measurements were carried out and results on thickness of layers and size of particles are tabulated. Curves of intensity vs. scattering angle are plotted for each layer.</p>			
20. DISTRIBUTION/AVAILABILITY OF ABSTRACT UNCLASSIFIED/UNLIMITED <input type="checkbox"/> SAME AS RPT <input type="checkbox"/> DTIC USERS <input type="checkbox"/>		21. ABSTRACT SECURITY CLASSIFICATION	
22a. NAME OF RESPONSIBLE INDIVIDUAL Dr. N. Y. Misconi		22b. TELEPHONE NUMBER (Include Area Code)	22c. OFFICE SYMBOL

Annual Report
AFOSR Contract - F49620-85-C-0117

PART ONE: INTRODUCTION

The research described in this report is being carried out with support of the Air Force Office of Scientific Research (AFOSR). Our efforts under this program are devoted to the degradation of a laser beam through its interaction with highly transparent particles which will not melt or evaporate. Phase One of our program focuses on the scattering and transmission of radiation through a layer* of particles. The research program will continue in Phase Two with the investigation of the scattering of radiation by single particles or by small clusters of particles suspended by laser levitation. Phase Three of the research program will investigate the dynamics of particles and clusters exposed to laser beams under conditions of high vacuum.

This report summarizes our research under the first phase of Award/Contract F49620-85-C-0117 in which we concentrated upon the interaction of a laser beam with a variety of layers of small, highly transparent particles. We utilize a 20 watt TEM₀₀ mode CW argon laser which concentrates its radiation in the blue-green region of the visible spectrum. The layer of particles is formed out of glasses or silicates which are highly transparent over the extended visible range of wavelengths (0.22 - 2.2 μ m) over which the atmosphere is also transparent. The particles which are used range in size from a few microns to a few hundred microns so that they are large compared to

* In the context of this report, the word "layer" is used to describe a sample of particles, tightly packed, many particles thick, and flattened on top and bottom surfaces.

A-1

the wavelength of the radiation and may be said to be in the geometrical optics size range.

A brief statement of our approach to the problem and summary of our results is to be found in Part 2. A description of our experimental setup and the choice of materials used in this study is contained in Parts 3 and 4 respectively. Detailed results are contained in Parts 5-8 in which we investigate the effects of particle size, particle shape, and layer thickness upon radiation transmitted through such a layer of particles. A final summary and suggestions of directions to be pursued is contained in Part 9.

PART TWO: MOTIVATION AND EXECUTIVE SUMMARY

Our approach to the problem is distinct from those envisioned under obscurants. Rather than absorbing the energy of the incident laser beam, we investigate the possibility of dispersing that beam by scattering. The utilization of highly transparent particles implies that the scattering medium remain rather than be sublimated by absorption of the laser beam. Suitability depends upon sufficiently low transmission through an ensemble of such particles.

In the current work, we have arranged our particles into samples whose thicknesses vary from 0.25 mm to 2 mm. The figure of merit (which we refer to as the 'beam suppression') for these layers is the ratio of the total intensity reflected back into the hemisphere of the side of the layer containing the incident beam (we call this the 'reflection hemisphere') to that of the intensity emerging from the side of the layer not containing the incident beam (we refer to this as the 'transmission hemisphere')(see Figure 1).

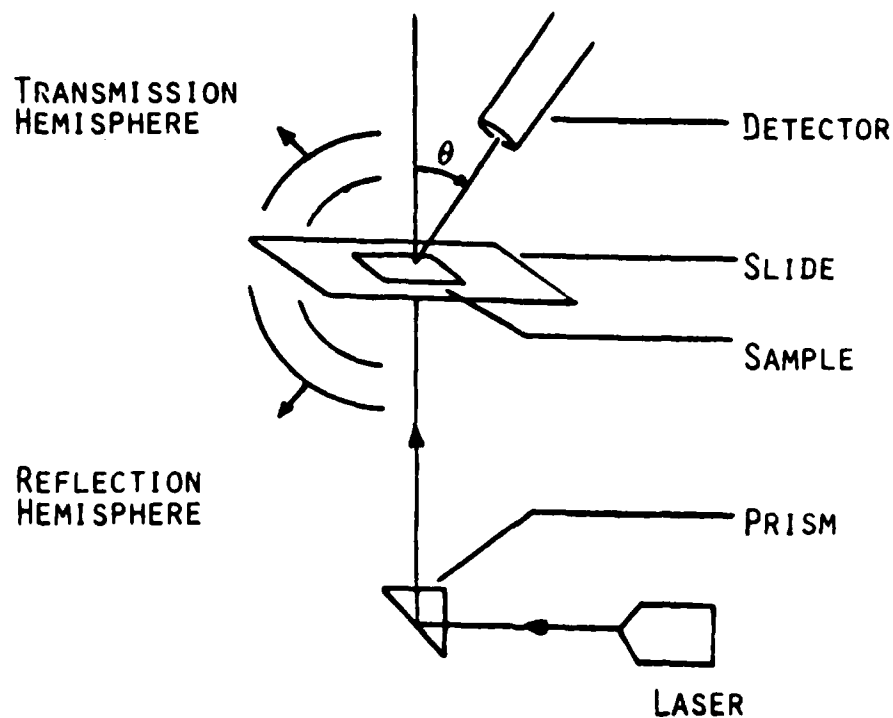


Figure 1

Figure 1. The instrument set-up used for measuring scattering of laser light from a layer of particles (the sample), which is held on a slide in a well and subjected to a laser beam. Angles (θ) are measured from the normal to the layer (and from the incident beam, since they coincide).

The primary conclusion of our work is that it is quite straightforward to achieve a beam suppression >1000 from a sample no more than 3 mm thick, with particles $< 68 \mu\text{m}$ in size (see Table 1). In fact, the results suggest that we may be able to do much better than this. A beam suppression of 1000 means that only 0.1% of the radiation incident on such a layer will be transmitted through that layer.

Table 1. Beam suppression ratios (laser light reflected/laser light transmitted; see text for details) are given for different materials and different particle sizes. Each value is listed with the corresponding layer thickness from which it was derived. V.H. signifies a beam suppression greater than 100, which could not be given a numerical value since the value of the transmitted laser light was less than the background noise of the instrument.

MATERIAL	SIZE OF PARTICLES IN (μm)					*MM = mm
	< 68	68 - 90	90 - 125	125 - 250	> 250	
SAND SAMPLE #1	.25 MM 13	0.5 MM 10	1.0 MM 14	1.0 MM 4.4	1.0 MM 3.5	
	0.5 MM 35	1.0 MM 38	1.5 MM 37	2.0 MM 17	2.0 MM 9.3	
	1.0 MM V.H.	1.5 MM V.H.	2.0 MM 73			
SAND SAMPLE #2	.25 MM 16	0.5 MM 12	1.0 MM 18	1.0 MM 18	1.0 MM 2.4	
	0.5 MM V.H.	1.0 MM 68	1.5 MM 55	2.0 MM 59	2.0 MM 7.5	
	1.0 MM V.H.	1.5 MM V.H.	2.0 MM 100			
SAND SAMPLE #13	.25 MM 8.1	0.5 MM 9.2	1.0 MM 15	1.0 MM 5		
	0.5 MM 60	1.0 MM 53	1.5 MM 33	1.5 MM 12		
	1.0 MM V.H.	1.5 MM V.H.	2.0 MM 62	2.0 MM 20		
SUPRASIL	0.5 MM 14	1.0 MM 17	1.0 MM 5.4	1.0 MM 3.6	1.0 MM 1.4	
	1.0 MM 53	1.5 MM 21	1.5 MM 8.8	1.5 MM 5.3	2.0 MM 2.4	
	1.5 MM 86	2.0 MM 37	2.0 MM 12	2.0 MM 6.8		
	2.0 MM V.H.					
FLEXOLITE GLASS	.25 MM 8.5	1.0 MM 38	1.0 MM 7.6	1.0 MM 4.2		
	0.5 MM 29	1.5 MM V.H.	2.0 MM 40	2.0 MM 8.7		
	1.0 MM V.H.					
TINTED COMMERCIAL GLASS	.25 MM 14	0.5 MM 8.1	1.0 MM 12	1.0 MM 5.8	1.0 MM 2.0	
	0.5 MM 39	1.0 MM 31	1.5 MM 28	2.0 MM 21	2.0 MM 4.7	
	1.0 MM V.H.					
CROWN GLASS	0.5 MM 2.8	1.0 MM 3.9				
	1.0 MM 7.0	1.5 MM 7.6				
		2.0 MM 14				

PART THREE: EXPERIMENTAL SYSTEM

In this investigation, we use an argon ion CW TEM₀₀ Mode laser which is rated at 18 watts total power when operated in all lines mode. This mode has two principal lines: one is the 514.5 nm green line and the other is the 488.9 nm blue line. By inserting a prism in place of the rear laser mirror, one can operate in the single line mode. However, in operating with this mode, the total power is reduced to 7.5 watts for the green line or 6.5 watts for the blue line. Since our particles are large in size compared to the wavelength of light, the classical expressions for the scattering of radiation from regular shapes such as spheres suggest little wavelength dependence. We therefore opted for operation in all lines mode. Our layer samples are prepared and packed tightly in square glass wells, 0.25 to 2.0 mm. thick, mounted on microscope slides. The laser beam can be made incident to the layer from either the bottom of the layer (i.e. passing through the microscope slide first, then the layer) or the top of the layer (i.e. passing through the layer first, then the slide). The scattering in either of these two configurations is, for all practical purposes, found to be the same. Figure 1 shows a sketch of the configuration of the experiment.

A silicon photo-diode detector was used (detector area = 0.81 mm²) to measure the scattering intensity of laser light by the sample at a fixed distance of 20 mm from the sample. The incident laser power was fixed at 65 mW during all of the scattering experiments. The detector has the freedom to move so as to measure the intensity from θ equals 0 to ± 160 degrees, where the positive angles are measured clockwise from the beam direction and the negative angles counterclockwise (see fig. 1). The angles 170° and 180° cannot be measured, since the detector, due to its finite size, is necessarily in the path of the beam. Angular distribution measurements are necessary to

investigate the symmetry of the scattering of laser light by a layer of particles. Appendix C gives the numerical values of these measurements, as well as graphical representation.

The photo-diode detector is connected to and operated by a VME/10 microprocessor that is connected to an A/D converter to digitize each measurement instantly. The data is plotted immediately and displayed by the monitor, after which a print is made of each plot. The data is then labelled and recorded for later analysis.

PART FOUR: MATERIALS USED AND THE EFFECT OF HIGH INTENSITIES

A large variety of glasses and natural silicates were investigated in this study. The samples which provided the data of this final report were constructed out of 6 different materials.

Spheres of crown glass were obtained from Duke Scientific Corporation in Palo Alto, CA. The glass particles were chosen to give us an example of a perfectly smooth surface geometry.

Glass spheres are made commercially by the Flexolite Corporation of St. Louis, MO for use in reflectors. Our sample of irregular Flexolite particles were made by crushing 500 micron-size spheres. Mixed in with the irregular particles is a subsample of spheres of the same material which had been attached to the initial set of large spheres. The absorptivity of this material is estimated to be $5 \times 10^{-2} \text{cm}^{-1}$.

Suprasil is a glass of very low absorptivity used in the manufacture of quality optical products such as lenses. We obtained a block of this material from Amerisil Company, N.Y. The block was crushed and sieved to give us particles in various size ranges. The absorptivity of this material is estimated to be $< 10^{-4} \text{cm}^{-1}$.

Natural beach sands were obtained from the panhandle region of Florida. The initial attractiveness of natural sand grains is that these grains have surface smoothness which is intermediate between the perfect spheres and those particles which are created by crushing. The beach sands of the Florida panhandle were chosen because of their small grain size and because their whiteness suggested a relatively low absorptivity.

We were not able to make direct measurements of the absorption coefficient of our sample materials. Knowledge of that coefficient is necessary to calculate the equilibrium temperature of particles exposed to laser beams. Candidate materials of interest must have good thermal properties when exposed to intense laser beams. We approached this problem in an empirical way. By focusing our laser beam to a beam waist of ~ 30 microns in diameter, our 20 watt argon laser is capable of providing a power density of $\sim 2.8 \text{ MW/cm}^2$ at the beam waist. Due to reflections off the faces of the prisms, lenses, and slide used in the apparatus the net power imparted on the sample was reduced to $\sim 1.4 \text{ MW/cm}^2$.

We then made three kinds of melting tests on the particles of each material. In the first case, we selected particles that are of the same or smaller size than our beam waist. By isolating particles in the beam waist we ensured that the particle was exposed to the same radiation environment that might be expected in vacuum. In the second case, we formed a layer of particles and then brought the beam focus onto the layer. Only the particles of a very small neighborhood were thus exposed to a high laser intensity. In the third case a sample was exposed to a beam focused to a diameter of 500 microns, thus encompassing many particles. At this beam diameter, the power density was 5 kW/cm^2 . In all cases, we sought evidence for melting under a microscope.

Suprasil Glass and the natural beach sands passed all three tests with no evidence of melting. Crown Glass Spheres and crushed Flexolite glass showed no evidence of melting in the case of isolated particles but there was melting of both materials when a layer sample was exposed. We have some ideas but no confident explanation as to the contrast between the results of these different melting tests.

A number of melting tests of layers showed evidence of cratering in the layer, a few times even showing the kind of central peak seen in lunar impact craters. We believe that all cases of cratering we have seen can be traced to thermal stress (sometimes even cracking) of the glass slide that supports the layers of particles. Strong evidence that this is so is the reduction in both the frequency and magnitude of the cratering when the laser power is raised and lowered over a more extended period of time (>3 minutes).

PART FIVE: ANGULAR DISTRIBUTIONS

The shape of the angular distribution from a layer of particles is rather simple to characterize provided that the width of the incident laser beam at the layer is much larger than the size of the particles making up that layer. Under these circumstances the resulting angular distribution is the summed effect of the contributions of many particles. This largely averages out any dependence of the angular distribution upon particle size, shape, or surface roughness - quite in contrast to what you would expect in the case of scattering from isolated particles in the geometrical limit.

In Figure 2a we show a typical angular distribution. Here 0° corresponds to the direction of the normal to the layer in the transmitted hemisphere whereas $\pm 180^\circ$ corresponds to the direction of the normal in the reflected

hemisphere. The angles of $\pm 90^\circ$ correspond to directions in the plane of the layer. Positive and negative angles correspond to angular distributions measured along azimuth directions that differ by 180° (see Figure 1). The similarity of the angular distributions for positive and negative angles reflects our observation that, to an accuracy of few percent, the angular distribution is cylindrically symmetric about the normal to the layer.

The angular distribution is seen to fall rapidly from peaks occasionally in the forward direction and always in the backward direction. The intensity becomes very small in the vicinity of 90° . This small value is to be expected given the increase in the effective thickness of the layer as we approach directions that lie in the plane of the layer. In Figure 2b we plot the angular distribution divided by the cosine of the angle θ . This weighted angular distribution is still similar to the measured angular distribution since it only corrects for the geometrical effect resulting from the method of detection; namely, it eliminates that reduction of power caused solely by the decrease in projected surface of the sample as viewed from the photodiode. A constant value of the weighted angular distribution either from 0° to 90° or from 90° to 180° would indicate uniform scattering into either hemisphere. We observe that our angular distributions are not uniform (see Appendix C).

Throughout this discussion of angular distributions we have emphasized that the angle in question is measured with respect to the normal to the layer. In conventional discussions of optical scattering, the scattering angle is measured with respect to the direction of the incident beam. Only since our incident beam is normal to the layers of particles does the angle relative to the normal coincide with the conventionally defined scattering angle.

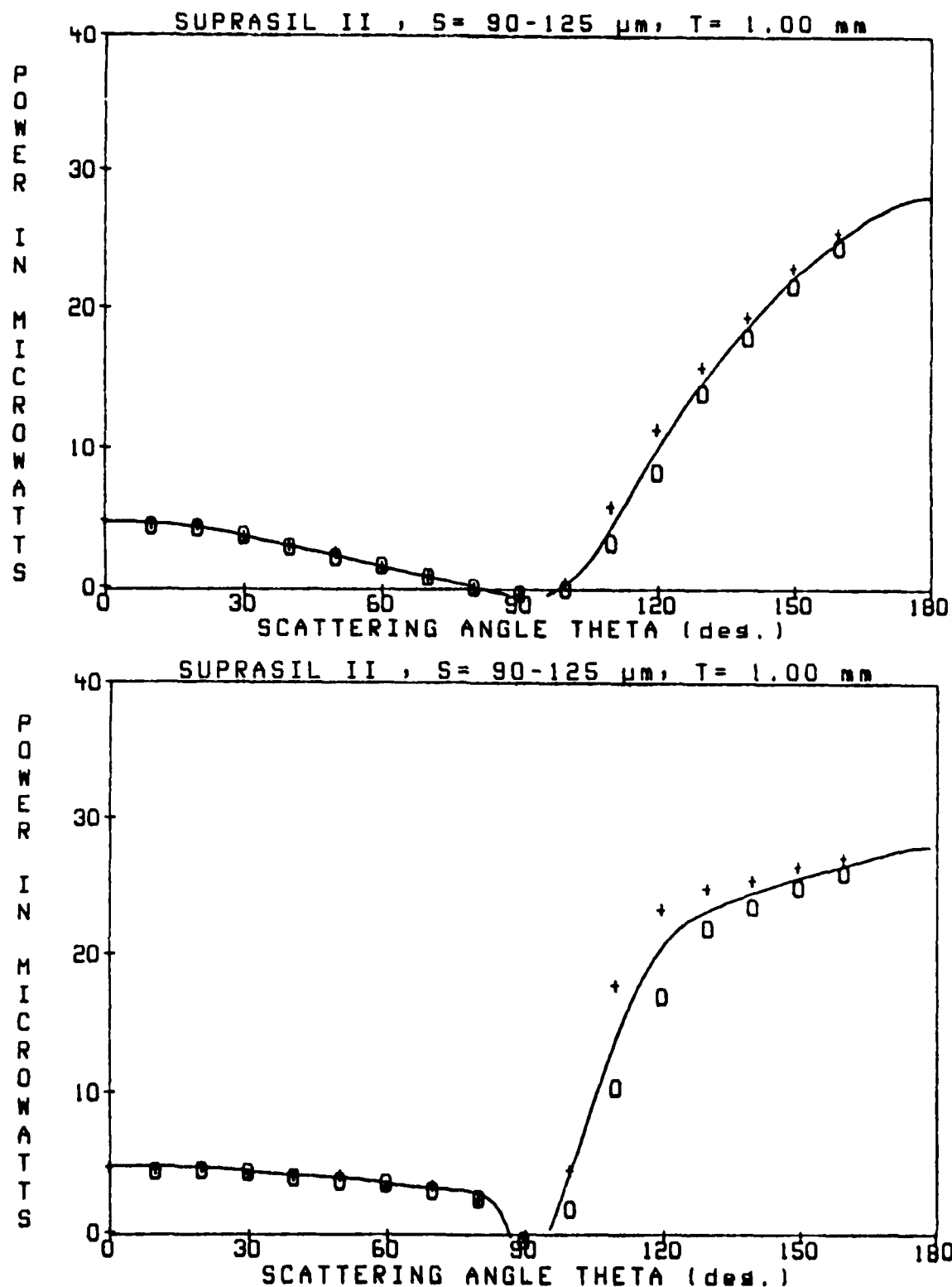


Figure 2. Angular distribution of laser light scattered by a 1.0 mm thick layer of Suprasil particles, 90-125 μ in size. The input power was 65 mW, and the .81 mm² detector surface was 2.0 cm from the sample. Angles were measured from the normal to the sample, which was also the direction of the incident beam. In the lower plot (2b), the power at the detector has been divided by the cosine of θ , to compensate for the variation in projected surface area of the sample as "seen" by the detector. Crosses (+) represent angles measured clockwise and circles (O) represent angles measured counterclockwise. Other materials and size ranges can be found in Appendix C.

In all our experiments, the measurement of the scattering angle θ was with respect to the incident beam, since this coincided with the normal to the sample. We now show that it is the angle with respect to the normal and not the conventional scattering angle which is significant in characterizing angular distributions from layers of such particles. In Fig. 3 we compare angular distributions for a case of normal incidence (3a) to a case where the detector is fixed with respect to the incident beam direction but in which the plane of the layer is rotated (3b). We obtain the same intensity when the angle between the detector and the normal to the plane is the same in the two cases. In Table 2 we vary both θ and the angle between the normal to the layer and the incident beam direction, but keep constant the angle between the detector and the normal to the plate. We find that the detector output remains fixed with good accuracy. The same result is found for angles in the reflection hemisphere.

One final concern about the angular distributions is to question the influence of the layer support upon our measurements. The layer of particles is supported by a glass slide. However, the incident beam can either be brought into the layer from below the layer, in which case the support plate is in the reflection hemisphere, or it can be brought into the layer from above, in which case the support plate is in the transmission hemisphere. Comparison of these two cases shows no difference in the angular distribution.

We summarize our measurements of the angular distribution by saying that a layer of small transparent particles acts in many ways like a diffuse reflector. The radiation pattern is independent of the incident direction and depends only on the angle with respect to the normal to the layer. The angular distributions on both sides of the layer are close to identical. The

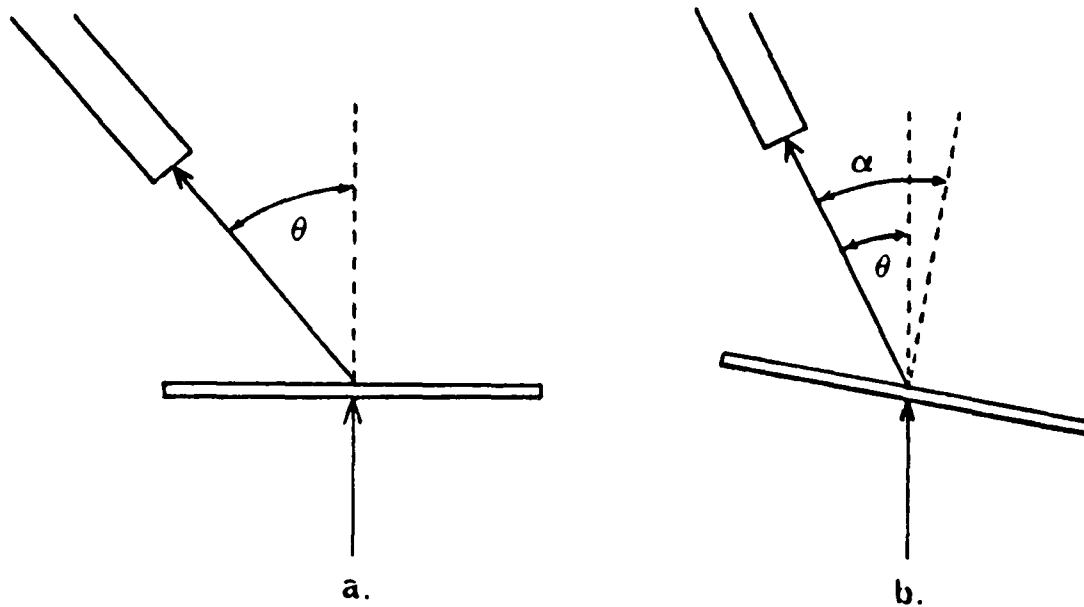


Figure 3. In figure 3a, we show our standard setup where the layer is normal to the beam direction. Here the scattering angle is measured from the beam. In figure 3b, we have tilted the plate so that it is no longer normal to the beam. We then measure two angles to the detector; θ is measured from the beam direction and α is measured from the plate normal.

common distribution is furthermore close to being uniform except for suppression in directions close to the plane of the layer. This set of results is very simple and indicates that the effect of such a layer would be largely independent of the direction of a laser beam incident upon it.

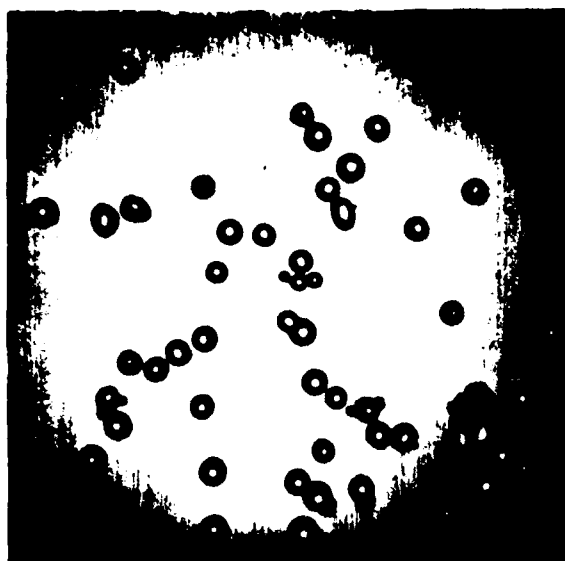
Table 2. A demonstration that the scattering of laser light from a layer of highly transmitting particles depends on the angle measured with respect to the normal to the layer and is independent of the beam direction. For the data in this table, the angle between the detector and the beam direction (θ) was varied over a range of 80° while the angle between the detector and the normal to the layer (α) was held constant at 40° . The diode voltage remained constant to within 7%. For comparison, the change in diode voltage for a 10° change in α was 21%.

<u>θ</u>	<u>Diode Voltage ($\times 10^{-6}$)</u>
0°	1.17
10°	1.19
20°	1.18
30°	1.22
40°	1.22
50°	1.24
60°	1.11
70°	1.09
80°	1.13

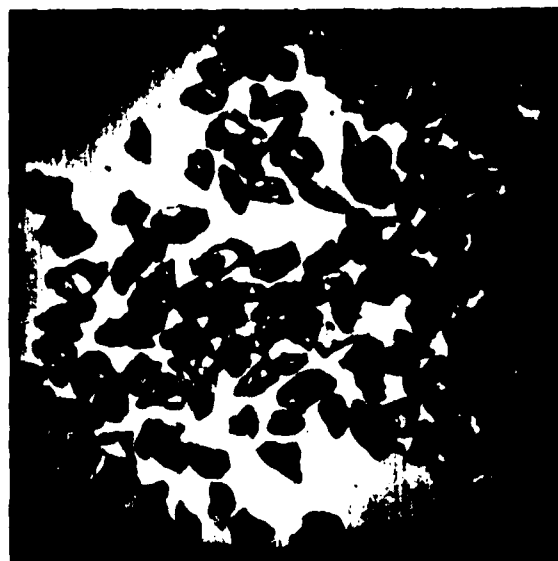
PART SIX: THE EFFECT OF PARTICLE SHAPE

One objective of our study has been to determine if particle shape played a major role in beam suppression. We have employed a variety of particles of varying degrees of surface roughness. Pictures showing examples of four classes of particles are to be seen in Fig. 4.

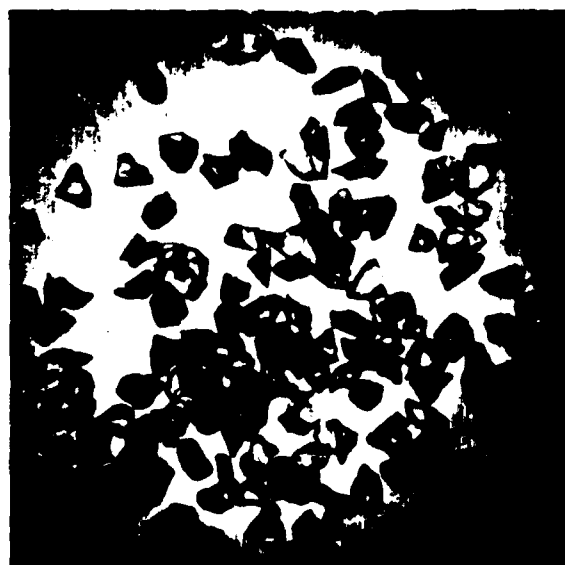
Sizing spheres of crown glass are perfectly smooth - we refer to these as having surface class one. Particles of natural sand have been ground down slowly by nature. Such particles have rather smooth surfaces and tend to have all three of their linear dimensions of the same size - we call these surface class two. The next two degrees of roughness are produced by the crushing of larger particles. This tends to produce fractured surfaces on larger particles that are more angular than natural sand. Furthermore, there is some



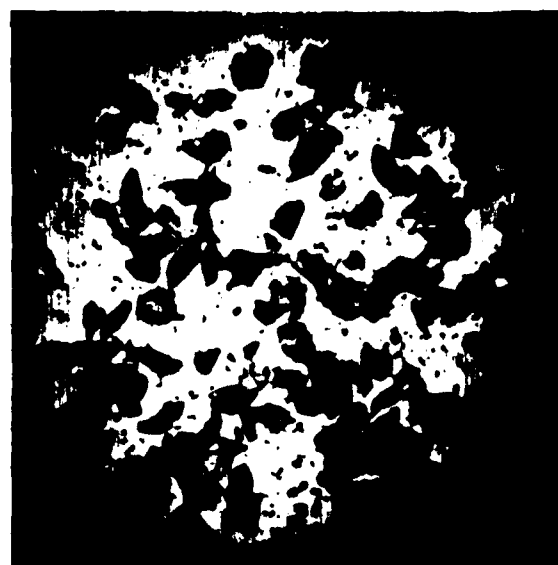
a.



b.



c.



d.

Figure 4. Photographs showing the variation in roughness for four different classes of particles. Class 1 (smooth) particles are shown in Figure 4a, class 2 (semi-smooth) particles are shown in 4b. By crushing, we achieve roughnesses such as class 3 (4c) which are irregular particles with no smaller particles adhering to their surfaces and class 4 (4d) which do have smaller particles attached to them.

tendency for particles that are plate-like or needle-like with much smaller particles attached to the surface of the larger ones. Surface class three particles are the larger particles left over from crushing and which have the smaller particles cleaned from their surfaces by a washing process. In the absence of washing the fragments from such particles, we have surface class four particles which mimic particles with a very complex surface geometry.

PART SEVEN: THE EFFECT OF PARTICLE SIZE

The small particles we use in constructing our layers are still large on the scale of the wavelength of the incident radiation and so we are well within the regime of geometrical optics. The effect of decreasing the size of the particles is to increase the density of particle surfaces in the layer. We would expect that this increase should yield an increase in beam suppression.

Table 3: Beam Suppression of Several Materials for 4 Ranges of Particle Size. Each Sample is 1.0 mm thick.

Material	Particle size in microns			
	< 68	68-90	90-125	125-250
Crown Glass Spheres	7.0	3.9		
Irregular Flexolite Glass	V.H.*	38		
Suprasil	53	17	5.4	3.6
Beach Sand #1	V.H.	38	14	4.4
Beach Sand #2	V.H.	68	18	15
Beach Sand #13	V.H.	53	15	5

* V.H. stands for very high beam suppression. For sand samples this was >>100.

The results are displayed in Table 3 where the evidence is rather clear that the beam suppression does increase with decreasing particle size. Figure 5 displays histograms of beam suppression vs. particle size for Suprasil (5a) and beach sand sample #2 (5b). Various sample thicknesses are represented for each material. See also Appendix A, for histograms showing beam suppression of other materials.

PART EIGHT: THE EFFECT OF LAYER THICKNESS

As we increase the thickness of the layer, we are increasing the number of particle surfaces in our sample. We summarize our findings on the effect of sample thickness on beam suppression in the histograms of Appendix B, each of which focuses on one size range of particles for a variety of materials. An example of this is shown in figure 6.

As we would expect, beam suppression always grows with increasing layer thickness but the rate of growth is not simple to characterize. In the case of no absorption, however, an expression can be derived.

Rapid increases in beam suppression with increasing thickness are seen with samples such as Sand sample #2, crown glass spheres, and crushed Flexolite spheres. In contrast, Suprasil shows only a doubling of beam suppression with a doubling of thickness of the layer. The beam suppression of a non-absorbing layer will vary linearly with the thickness of the layer. This can easily be demonstrated for the case of doubling the thickness of a layer. A double-thick layer can be thought to consist of two layers of single thickness, one above the other. Then the problem is one of multiple reflections between the two layers (see figure 7). If a beam of initial

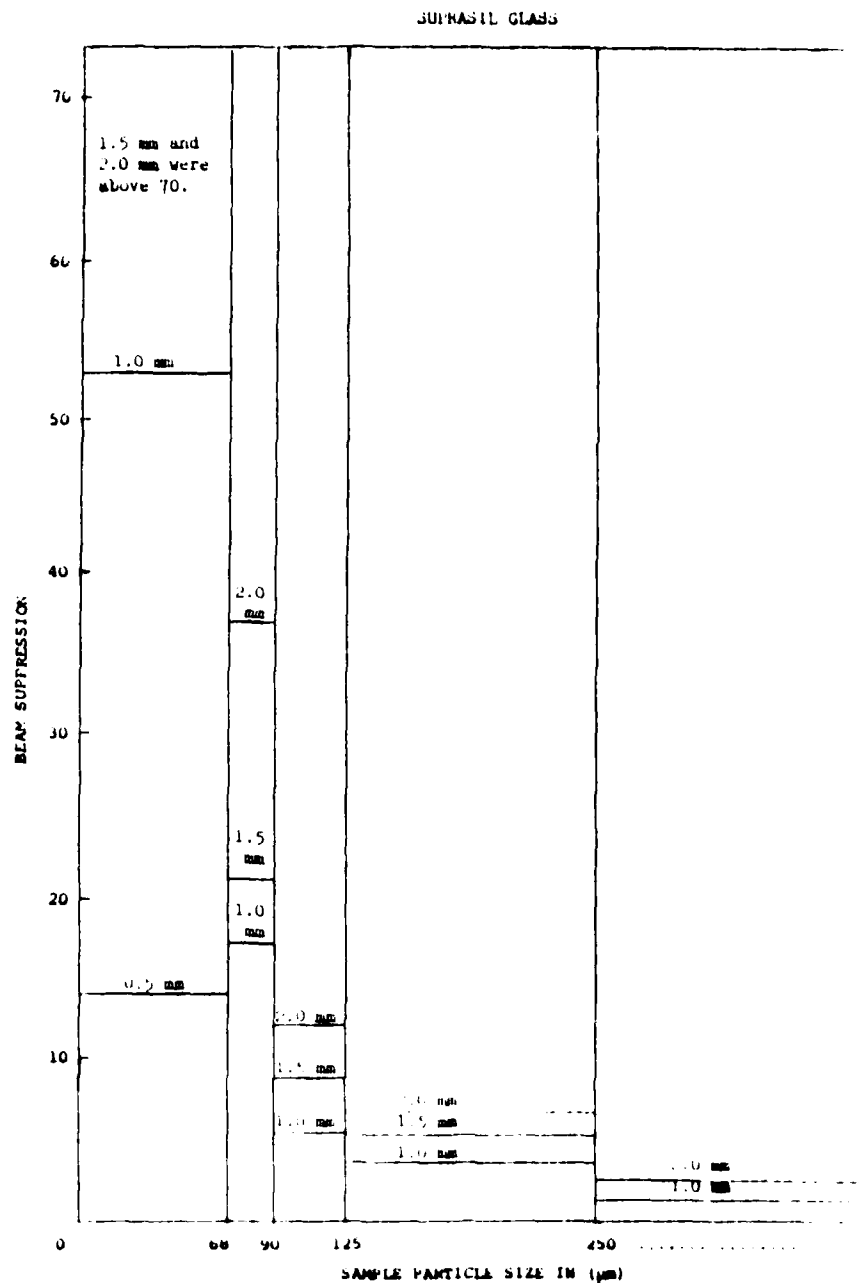


Figure 5. Beam suppression (laser light reflected/laser light transmitted) is given as a function of particle size for Suprasil glass. Different sample thicknesses give different levels in the histogram. Thicknesses which give a beam suppression greater than 70 are not plotted, but are noted. Histograms for other materials can be found in Appendix A.

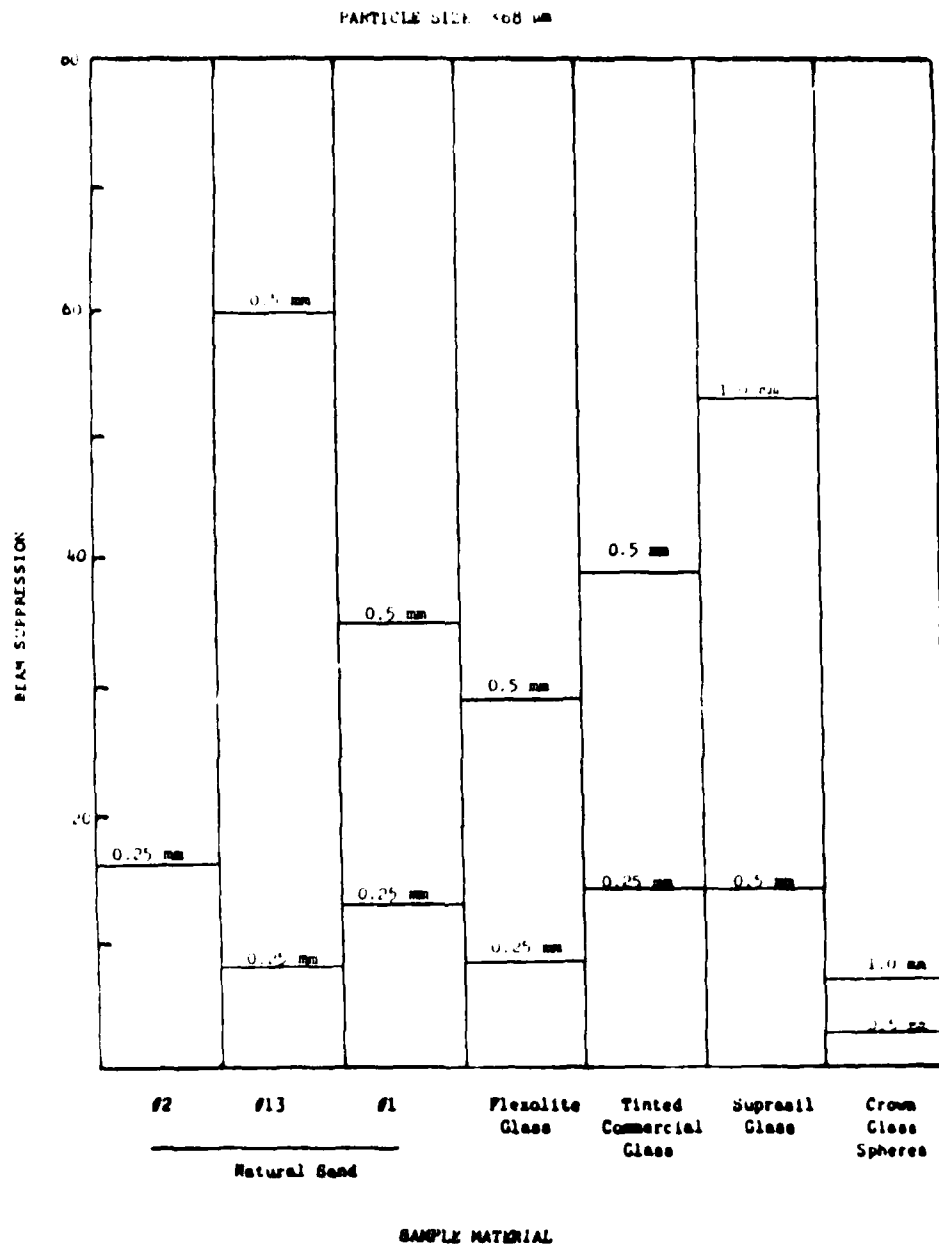


Figure 6. beam suppression vs. type of material, for particles less than 60 μ m in size. Different sample thicknesses were represented by two separate horizontal lines in the same column.

intensity I_0 strikes a single-thick layer, the intensity transmitted is $I_0 T$ and the intensity reflected is $I_0 R$. If two such layers were stacked as in figure 7, then the total transmitted intensity (T_2) is the sum of all multiple reflections which eventually pass through the top of the double layer. From figure 7 this is seen to be

$$T_2 = I_0 T^2 + I_0 R^2 T^2 + I_0 R^4 T^2 + \dots$$

$$= I_0 T^2 \left(1 + \sum_{i=1}^{\infty} R^{2i} \right).$$

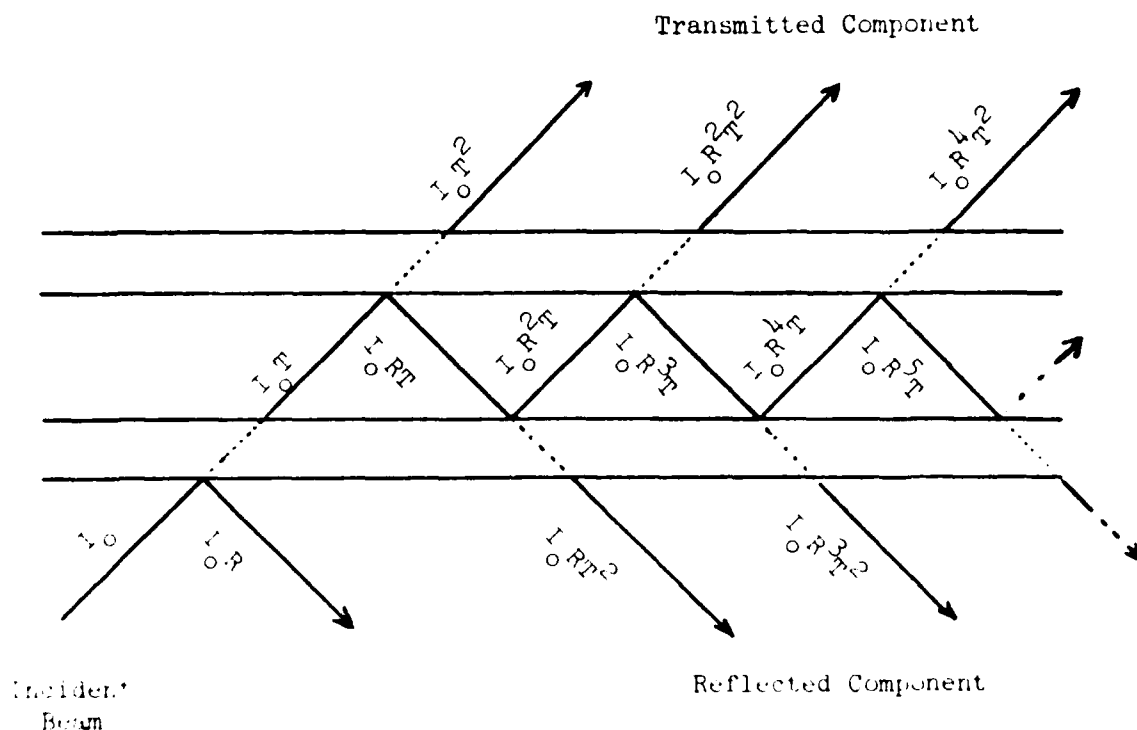


Figure 7. Transmission and reflection of two layers stacked one above the other. Multiple reflections between the two layers result in a converging infinite sum in each hemisphere. The distance between the layers does not affect the result; likewise the angle of the incident beam is not a factor. Here, an incident beam of 45° was used for convenience.

Likewise the total reflected intensity (R_2) is the sum of all the arrows leaving the bottom of figure 7, or

$$\begin{aligned} R_2 &= I_0 R + I_0 R T^2 + I_0 R^3 T^2 + I_0 R^5 T^2 + \dots \\ &= I_0 R + I_0 R T^2 \left(1 + \sum_{i=1}^{\infty} R^{2i} \right). \end{aligned}$$

In both equations, the expression in parentheses is an infinite series equal to $(1 - R^2)^{-1}$. By substituting this and dividing, we get the beam suppression B_2 of a double thick layer,

$$\begin{aligned} B_2 &= \frac{R_2}{T_2} = \frac{I_0 R + I_0 R T^2 / (1 - R^2)}{I_0 T^2 / (1 - R^2)} \\ &= \frac{I_0 R (1 - R^2) + I_0 R T^2}{I_0 T^2}. \end{aligned}$$

Since there is no absorption, $R + T = 1$, so $T = 1 - R$. Using this, and eliminating I_0 , we get

$$B_2 = \frac{R(1 - R^2) + R(1 - R)^2}{T(1 - R)}$$

$$B_2 = \frac{R(1 - R)(1 + R) + R(1 - R)(1 - R)}{T(1 - R)}$$

$$B_2 = \frac{2R}{T}.$$

The beam suppression of a double-thick non-absorbing layer is exactly twice the beam suppression of a single thick layer!

Applying the above expression, our results for Suprasil then make perfect sense, since Suprasil is highly non-absorbing. Likewise, this implies that the non-linearity in beam suppression with respect to thickness of a layer, that we found in some materials, results from absorption.

At least in the case of slightly absorbing materials such as the beach sands, there appears to be a limit to the thickness needed to block very nearly 100% of the transmitted light. For some very thick samples (> 3 mm thick) no evidence of transmission of laser light could be seen visually. Even materials that suppressed the beam poorly at thin thicknesses blocked the beam to this degree when a sample 9 mm thick was created. In the future, we hope to determine that thickness for each material and particle size where the above condition occurs, such that any additional increase in layer thickness does not increase the suppression.

PART NINE: CONCLUSION

This investigation has yielded a number of answers to a fundamental question: can we reduce the power of a laser beam by using the scattering from highly transparent particles which are not destroyed in the process. These answers are summarized below.

1. Highly transparent silica particles (for wavelengths from 0.22 to $2.2 \mu\text{m}$) can easily reduce a laser beam to much less than 1% of its intensity before leaving the medium, through scattering of the beam. This beam suppression can be achieved by transmittance of the beam through a layer of irregular particles on the order of 1 mm thick and of sizes $100 \mu\text{m}$ and less.
2. Among several kinds of silica particles (see Part Four), it was found that natural beach sand (obtained from the Florida Panhandle) is by far the best laser beam suppressor, followed by suprasil (see table 2 for beam suppression ratios).

3. Our results show that irregularly shaped particles suppress the beam much better than spheres (by at least a factor of two) of the same material. This is probably due to the many surfaces created by crushing the material which in turn enhances the multiple scattering process. There is clear evidence from our experiments (table 2) that smaller size particles (68 μm and below) suppress the beam far better than bigger sizes.
4. It is essential for these materials to suppress the beam while not being destroyed (melting, evaporation). From the material used in this study, only the natural beach sands and suprasil survived melting tests when subjected to laser beam power of 1.4 MW/cm^2 . It is very important to note here that, in the form of single particles or particles layed unpiled on a microscope slide, we could not melt any of the silica materials that we used in our experiments when we subjected them to 1.4 MW/cm^2 laser power. This means that materials that melted in a layer form will not melt in a cloud. Even when melting occurred in our layer samples (e.g. flexolite particles), the suppression of the laser beam by the layer remained high regardless of the melted region inside the sample. We hope to pursue studies of the effect of melting on beam suppression in the future, if funds become available to us.
5. Angular distribution measurements (see Part Five) show that there is a very close symmetry between the intensities measured at the positive scattering angles and the negative ones, which suggests cylindrical symmetry. In all of the angular distribution measurements, taken with the scattering angle measured from the direction of the incident laser beam, the beam was normal to the sample layer. In cases where the laser beam is

not normal to the layer, we have found that the angular distribution measurements will still be valid if the scattering angle (θ) is replaced by the angle measured with respect to the normal to the layer. In such a case, the scattering is symmetric about this normal.

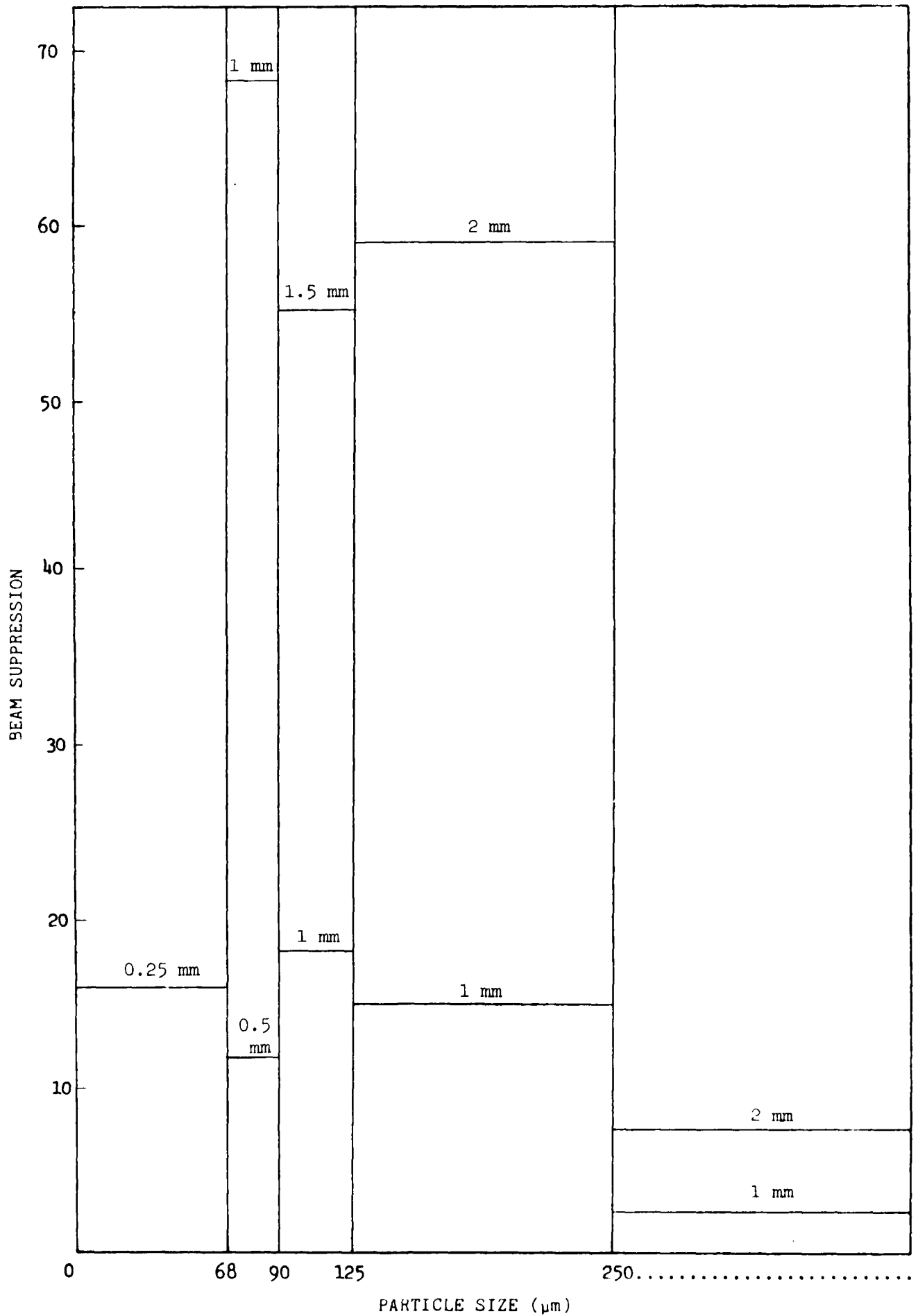
APPENDIX A

APPENDIX A

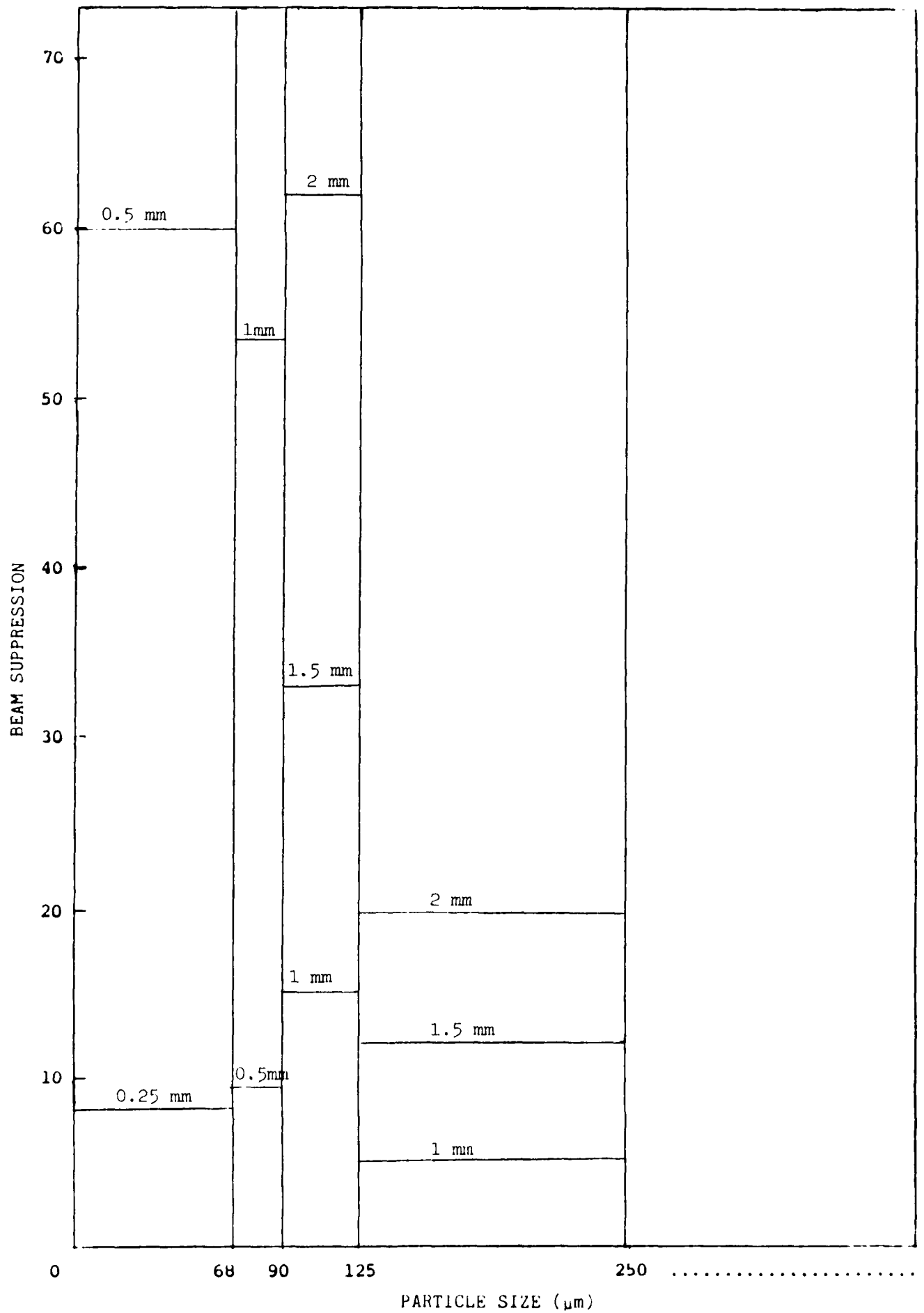
Beam Suppression vs Particle Size Range of Various Materials

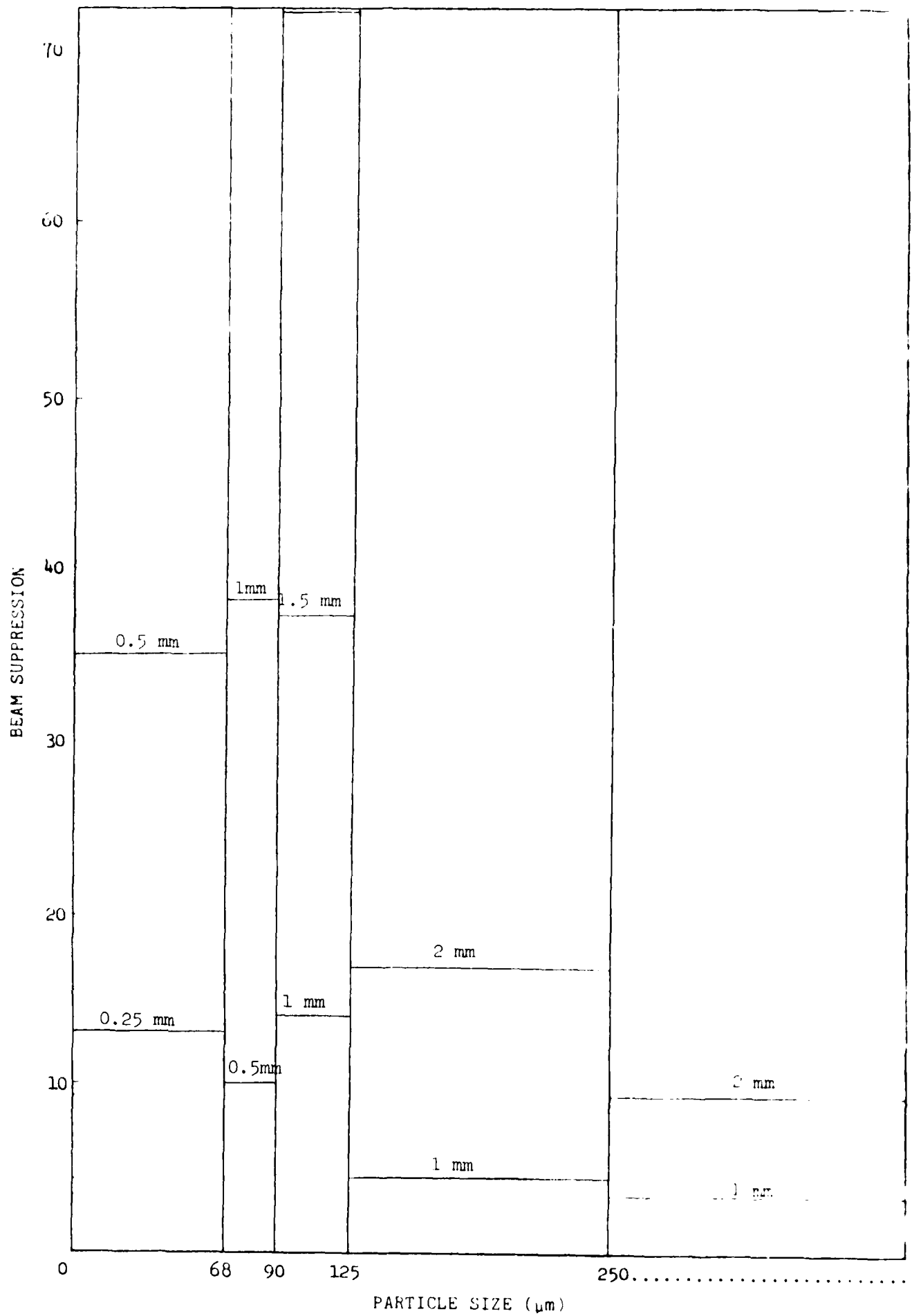
Histograms of Beam Suppression (laser light reflected/laser light transmitted) vs. particle size range are plotted for the materials studied in the layer scattering measurement program. Several layer thicknesses are represented in each column. Beam suppressions above 70, found for many materials, in the noise level of the instrument.

SAND SAMPLE #2

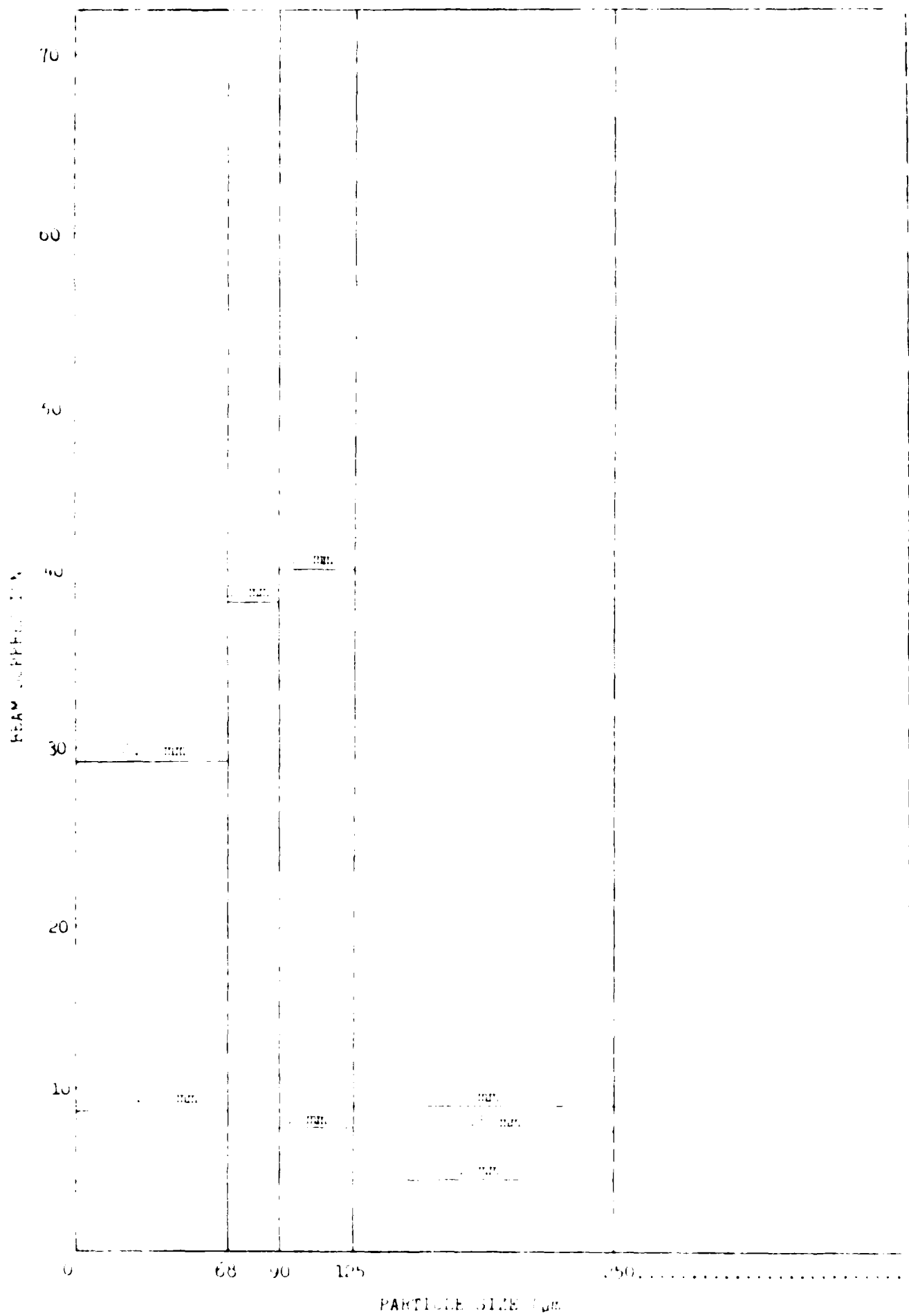


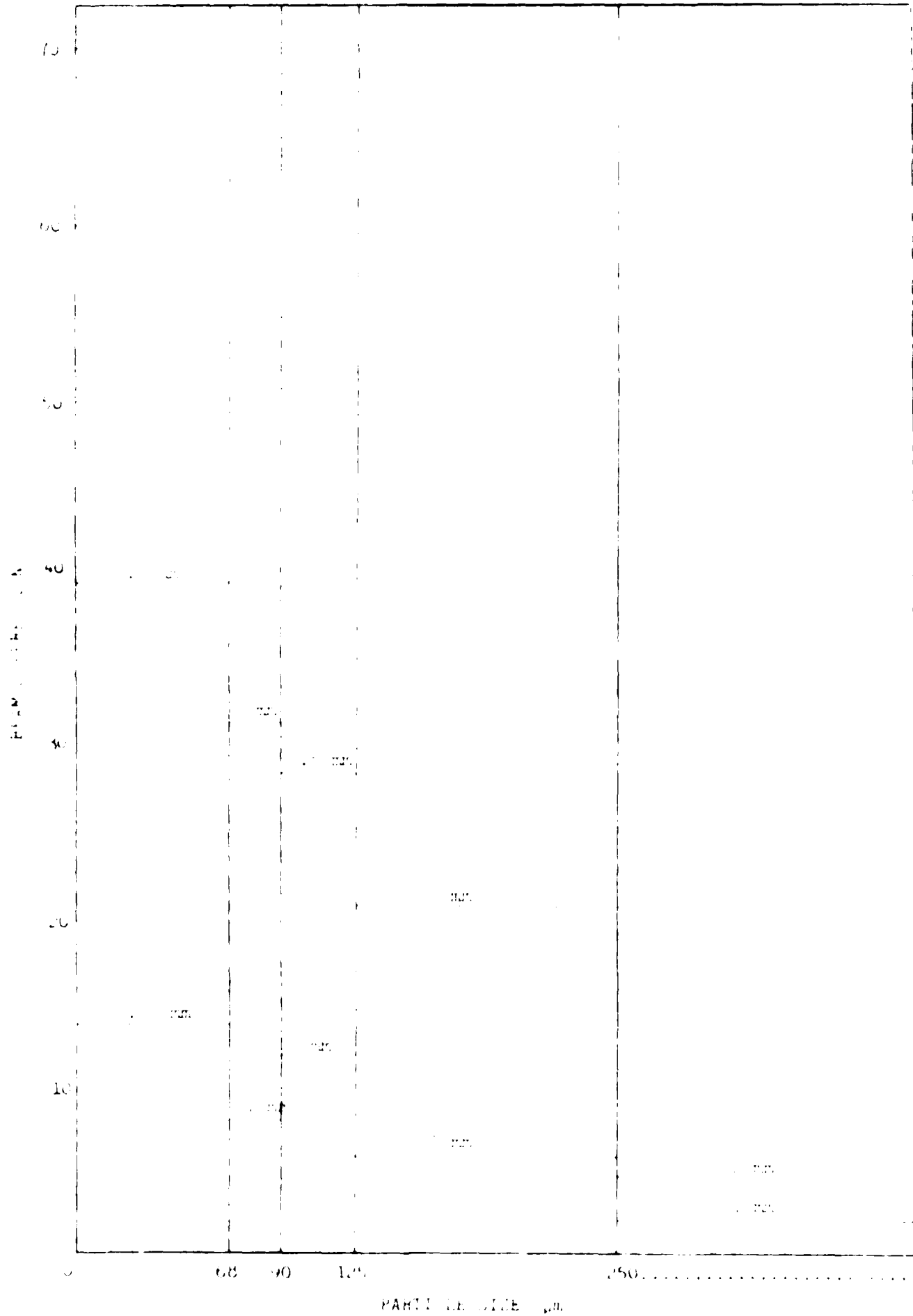
SAND SAMPLE #13

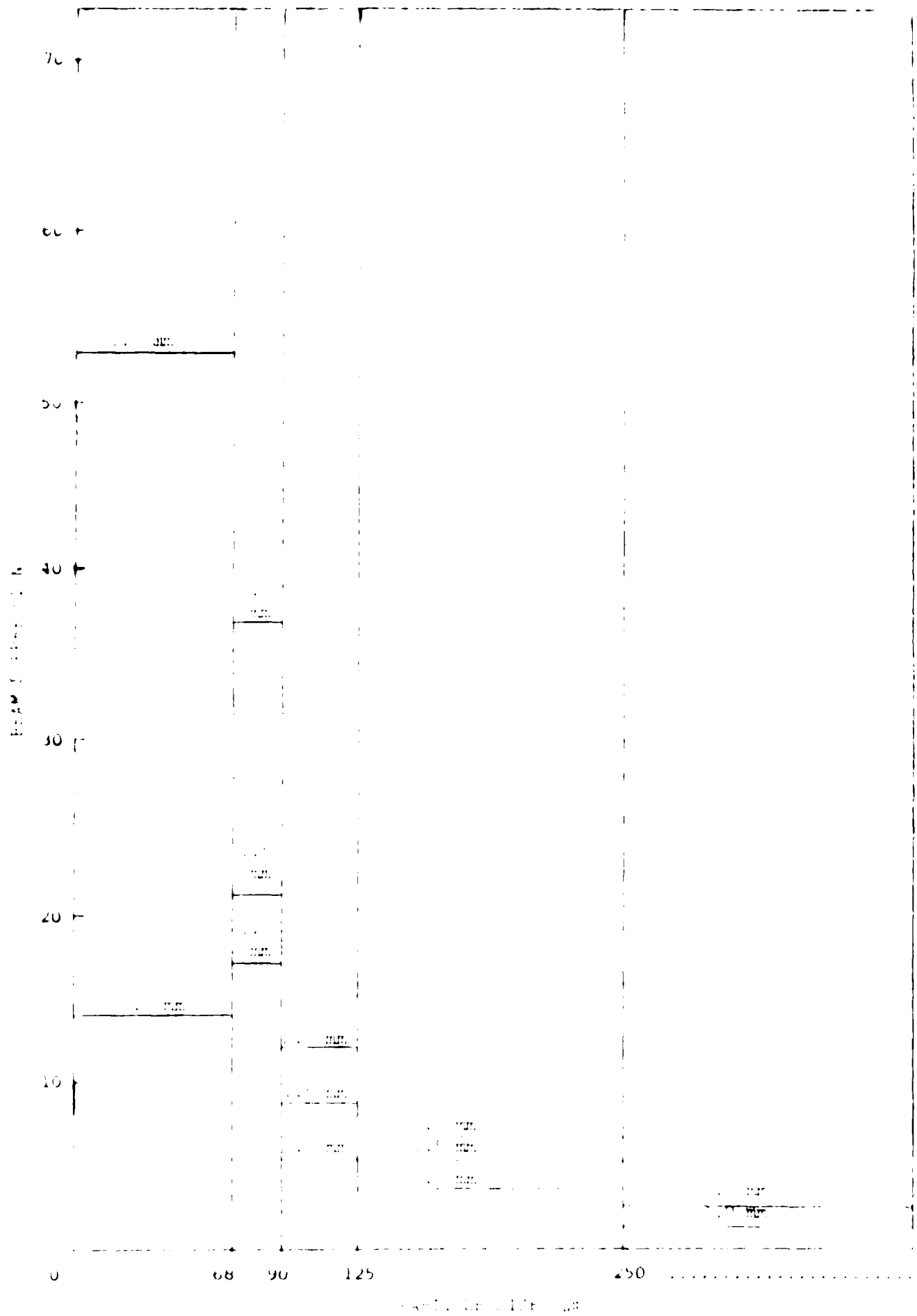




PIEXOMITE MASS







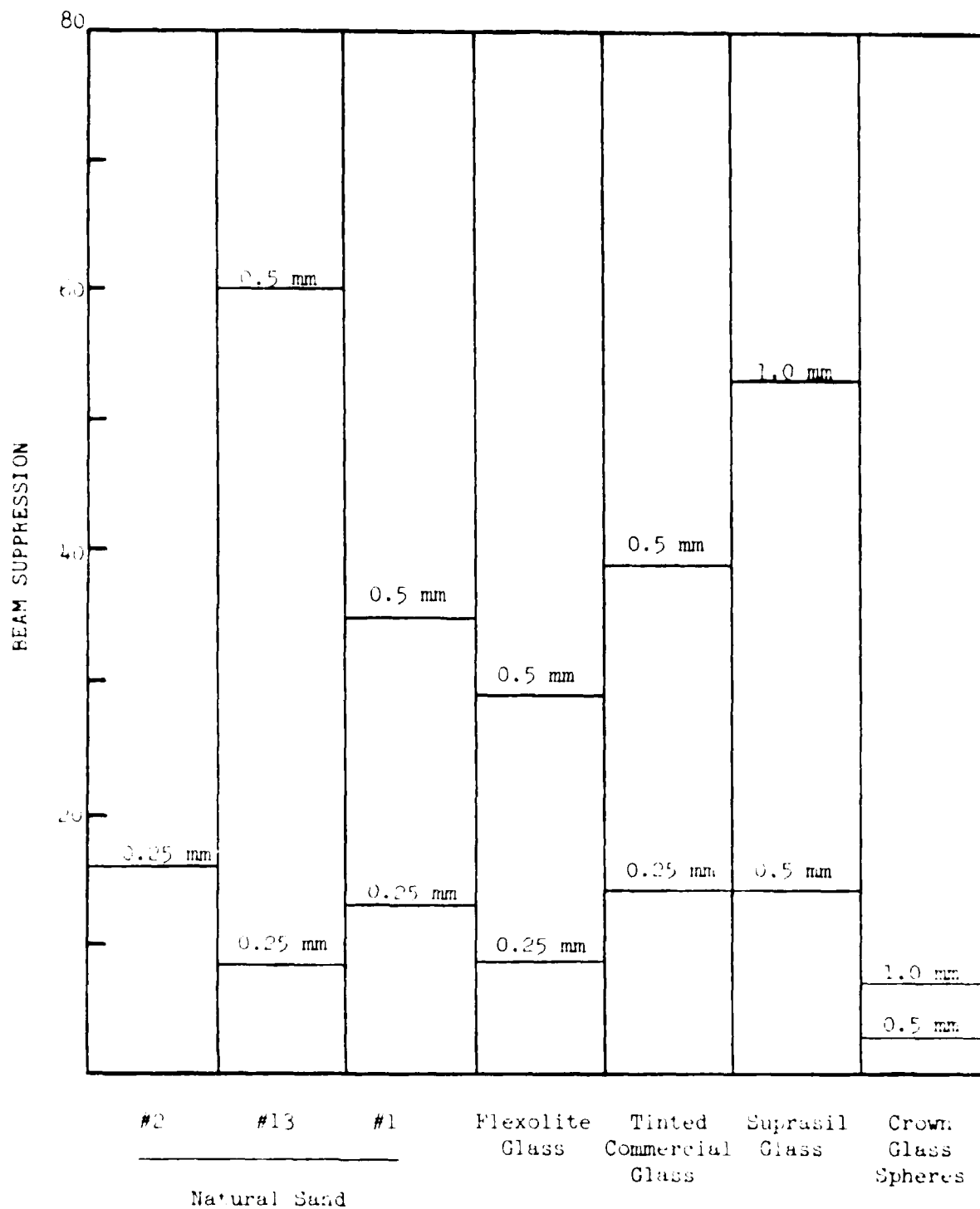
APPENDIX B

APPENDIX B

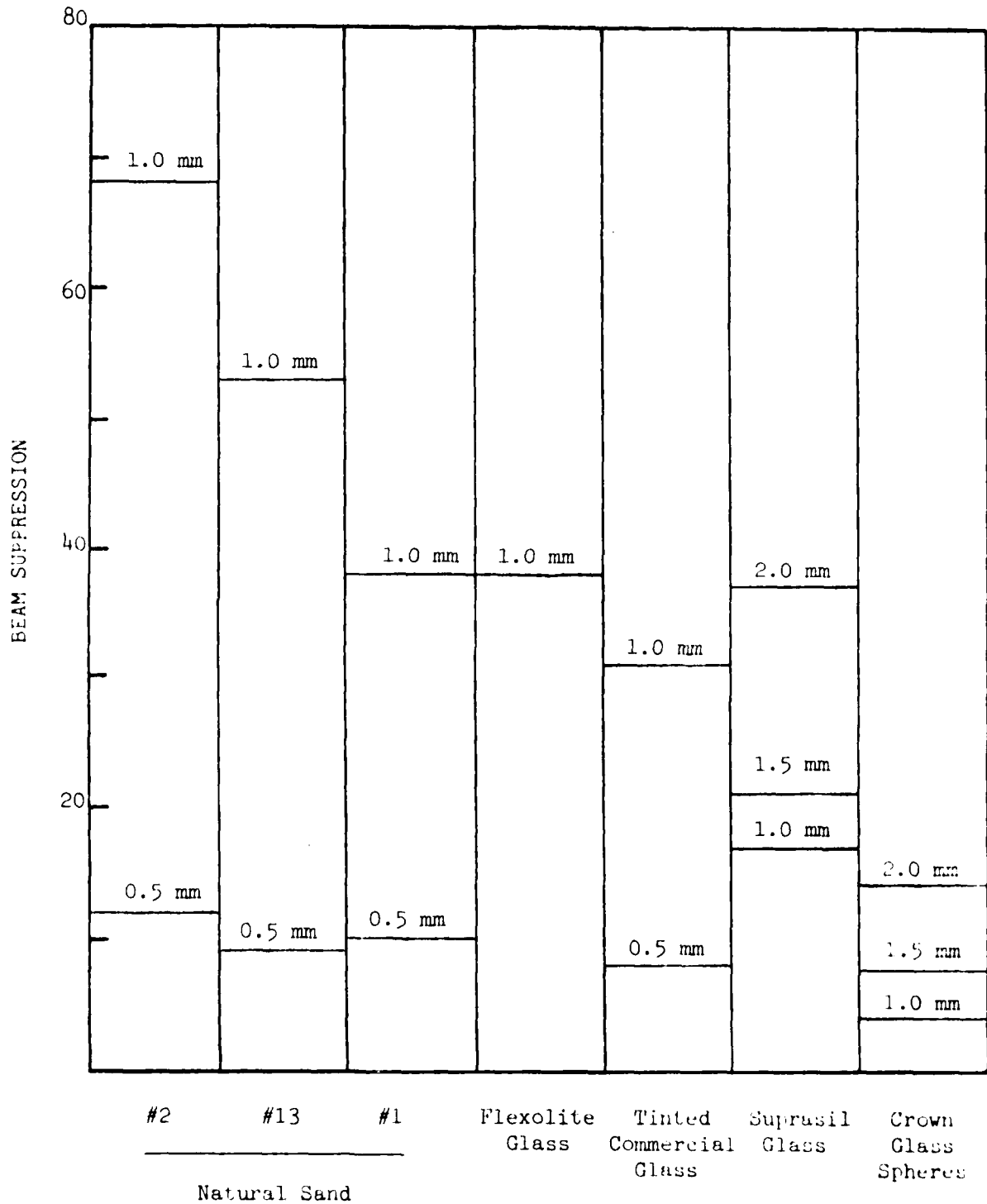
Beam Suppression vs Type of Material for Various Particle Size Ranges

Histograms of beam suppression (laser light reflected/laser light transmitted) vs. type of material are plotted for the particle size ranges stated in the layer scattering measurement program. Several layer thicknesses are represented in each column. Those thicknesses with a beam suppression greater than 5% are considered in the noise level of the instrument.

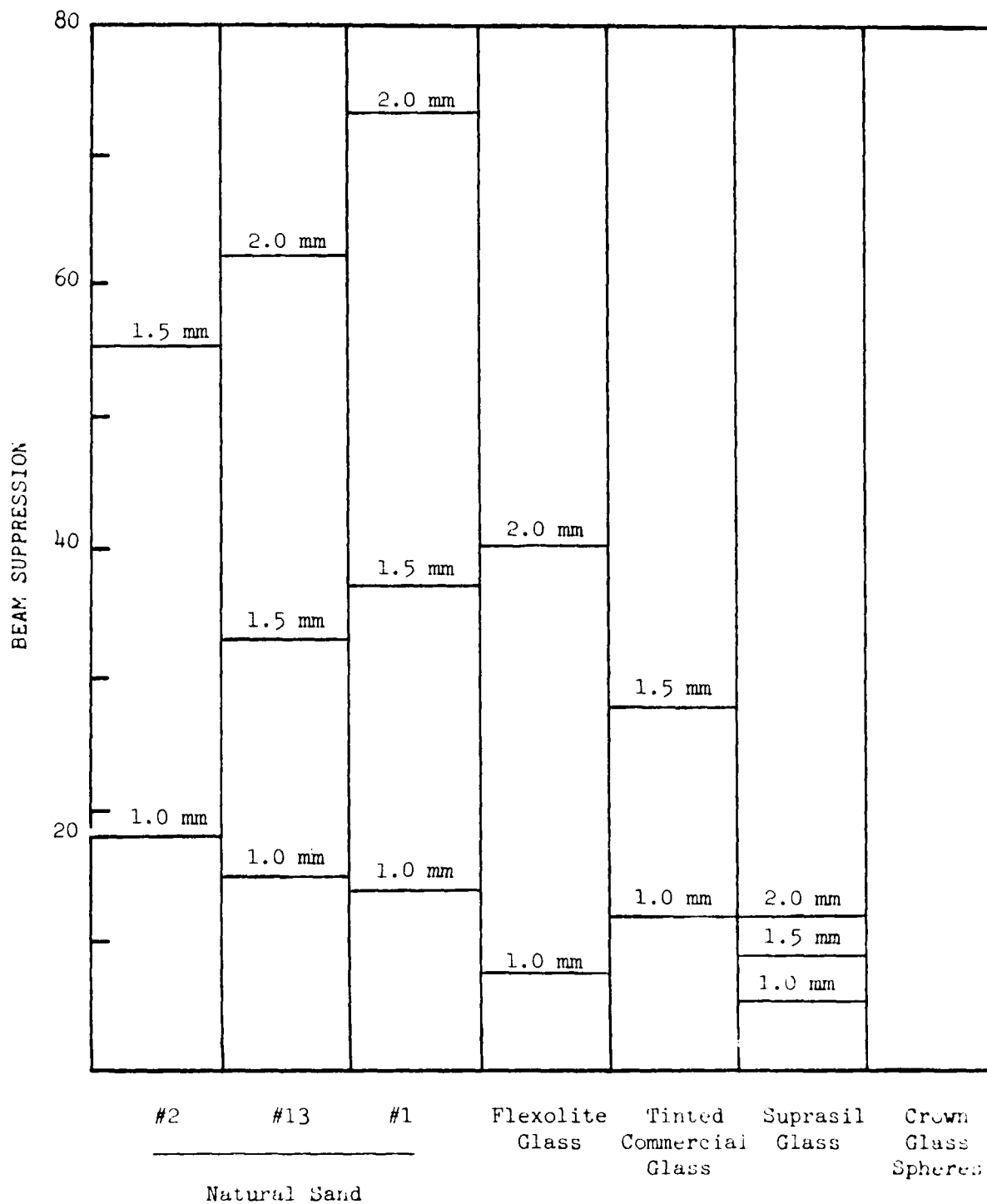
PARTICLE SIZE <68 μm



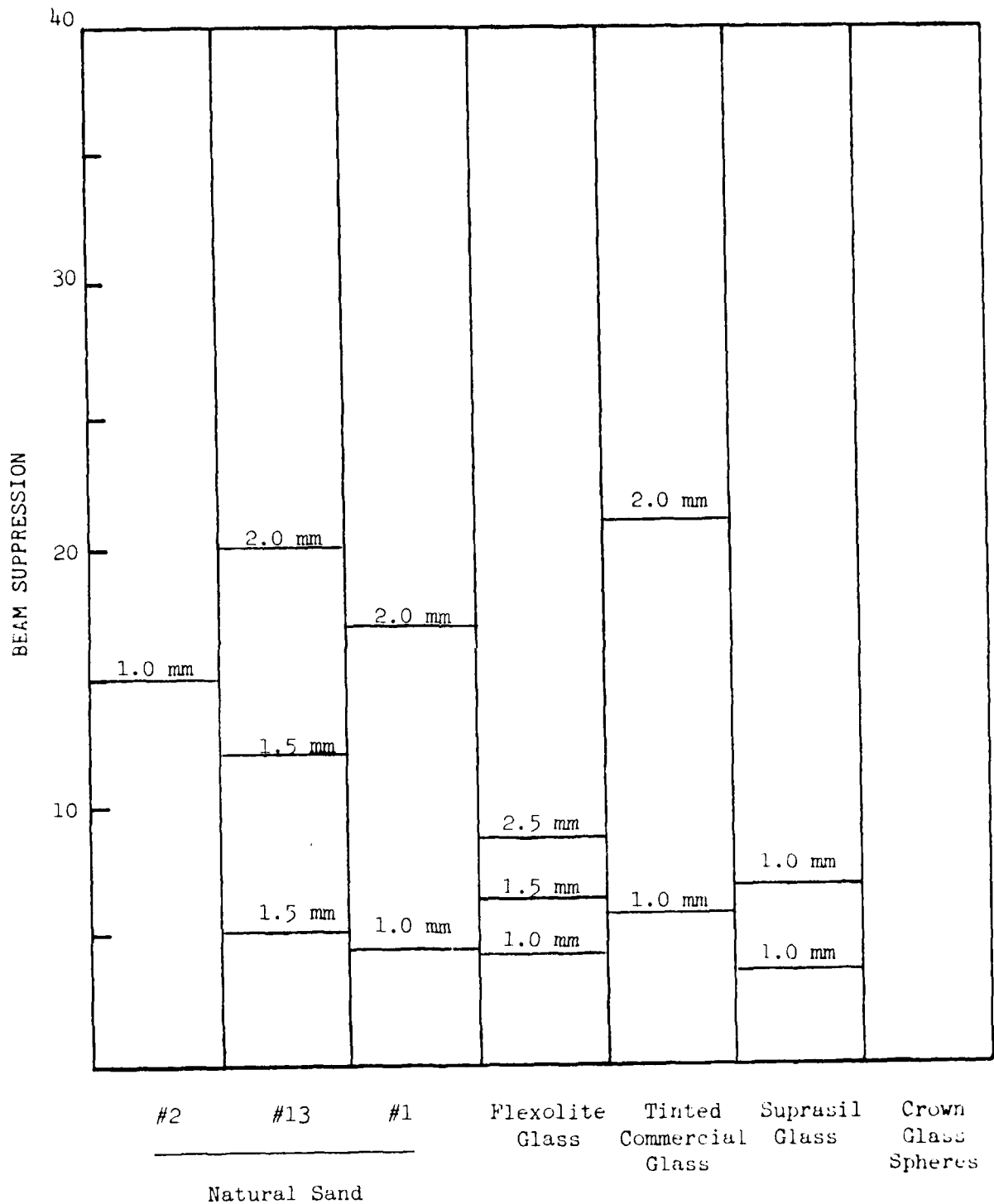
PARTICLE SIZE 68-90



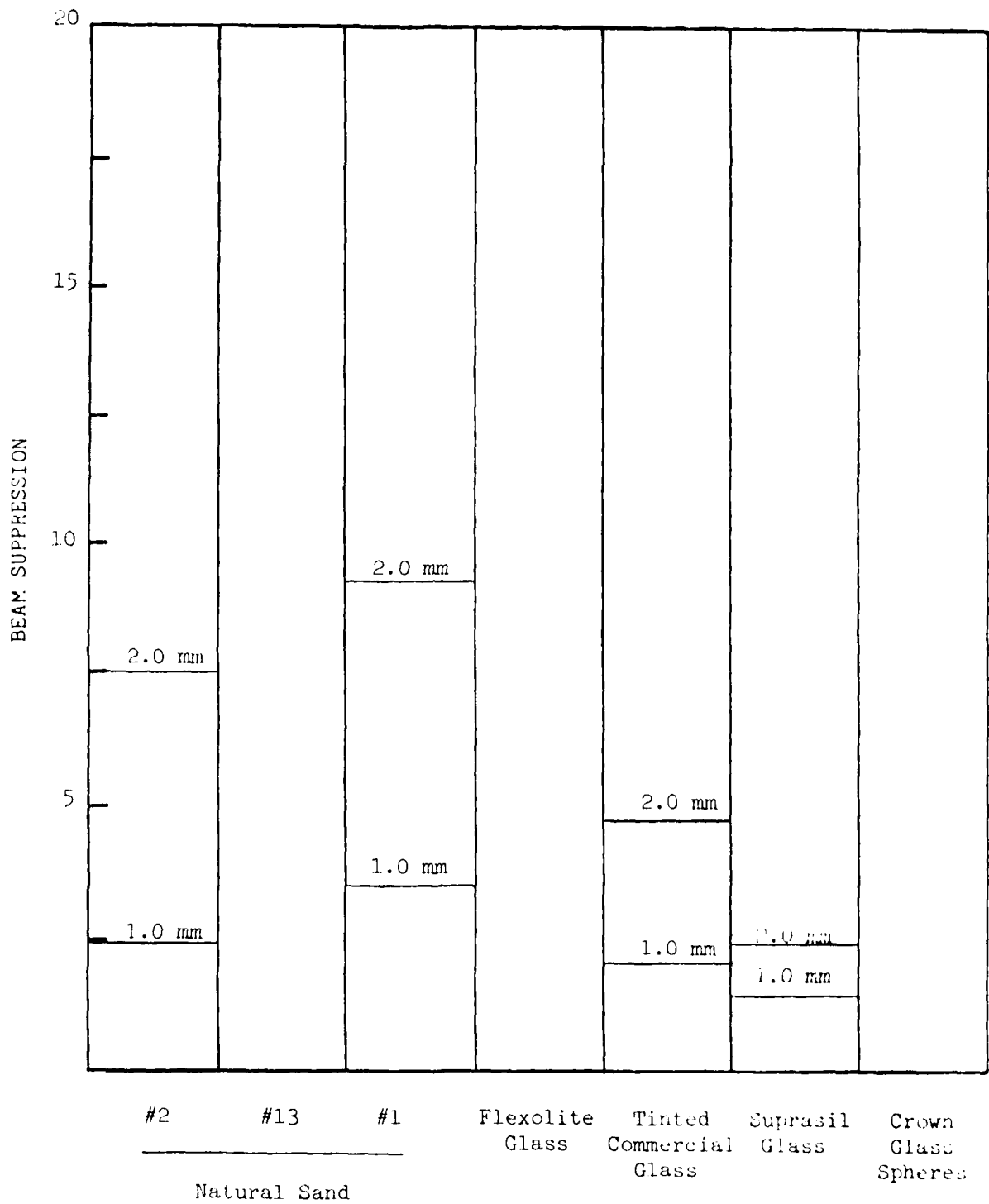
PARTICLE SIZE 90-125



PARTICLE SIZE 125-250



PARTICLE SIZE >250



APPENDIX C

APPENDIX C

Scattering Measurements of Particle Layer Samples

Each page consists of two graphs. Each graph is labelled at the top; showing the material, the particle size range, and the thickness of the sample which the graph represents. The power readings were taken using a silicon photo-diode with a surface area of 0.81 mm^2 . The detector was fixed 2.0 cm. from the point where the center of the incident beam first entered the sample, and the input power was set to 65 mW. The upper graph is a plot of laser power, measured at the detector, vs. scattering angle (θ) measured with respect to the plate normal (also the beam direction, since they coincide; see figure 1). In the lower graph, the diode measurements have been divided by the cosine of θ to eliminate that reduction of power caused solely by the decrease in projected surface of the sample as viewed from the photodiode.

In both cases, crosses correspond to positive values of θ (measured clockwise from the beam direction) and circles to negative values of θ (measured counter-clockwise). Each curve is a least-square fit based on a 12th order Fourier approximation. Projections of the curves beyond 160° are extrapolations and may not represent the true energy flux in that range. The numerical readings of the diode voltage output and corresponding light power measured by the detector are given on the facing pages.

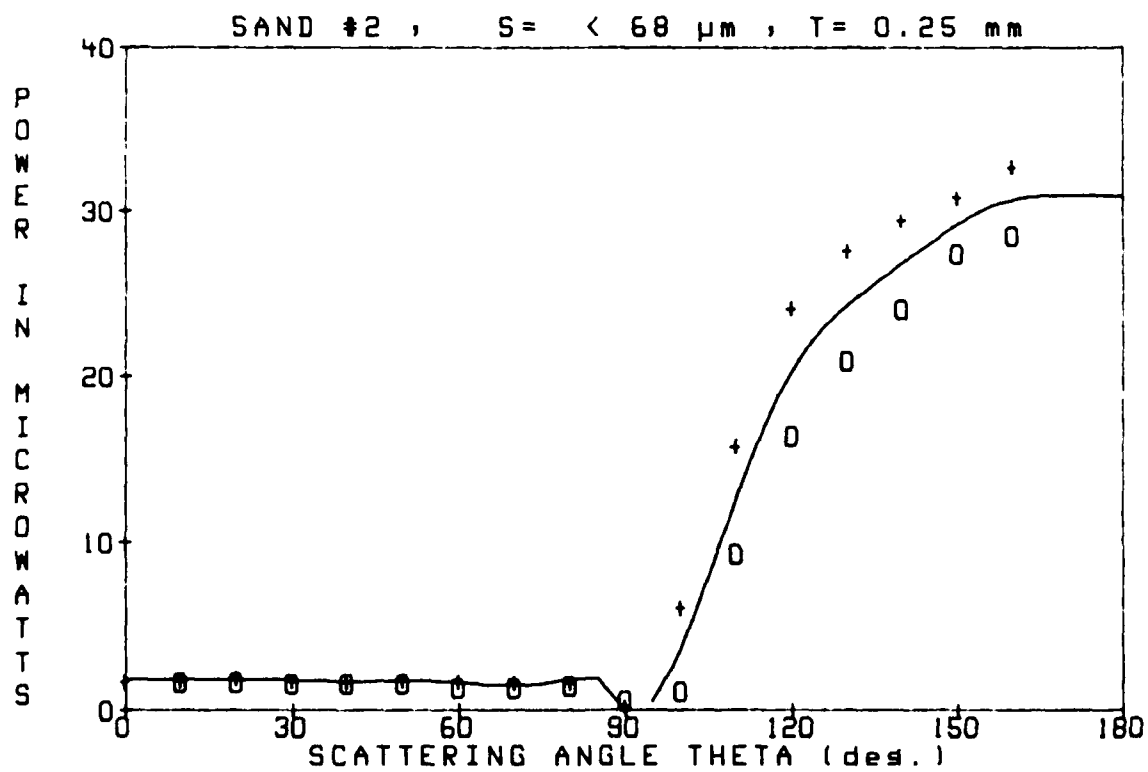
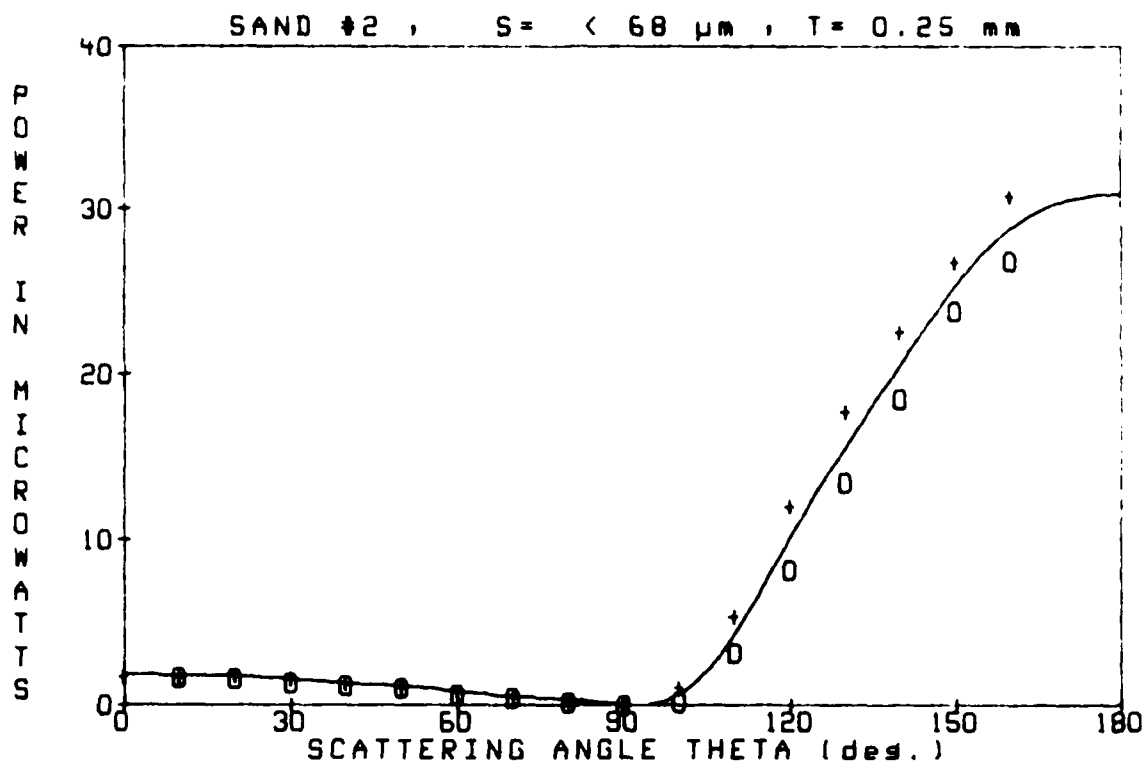
SAND 12

S

68 um

T= 0.175 mm

SCATTERING ANGLE	DIODE VOLTAGE	POWER (microwatts)
160	4.49	29.7
150	3.96	22.78
140	3.03	13.47
130	2.21	7.47
120	1.35	1.22
110	0.53	3.21
100	0.03	0.21
90	0.00	0.00
80	0.04	0.26
70	0.08	0.48
60	0.11	0.6
50	0.17	1.07
40	0.21	1.27
30	0.23	1.49
20	0.26	1.66
10	0.28	1.70
0	0.29	1.79
10	0.29	1.79
20	0.30	1.84
30	0.28	1.80
40	0.27	1.37
50	0.19	1.16
60	0.15	0.87
70	0.10	0.57
80	0.05	0.17
90	0.00	0.00
100	0.17	1.07
110	0.89	5.42
120	1.98	12.10
130	2.91	17.76
140	3.70	22.08
150	4.39	26.75
160	5.05	30.81



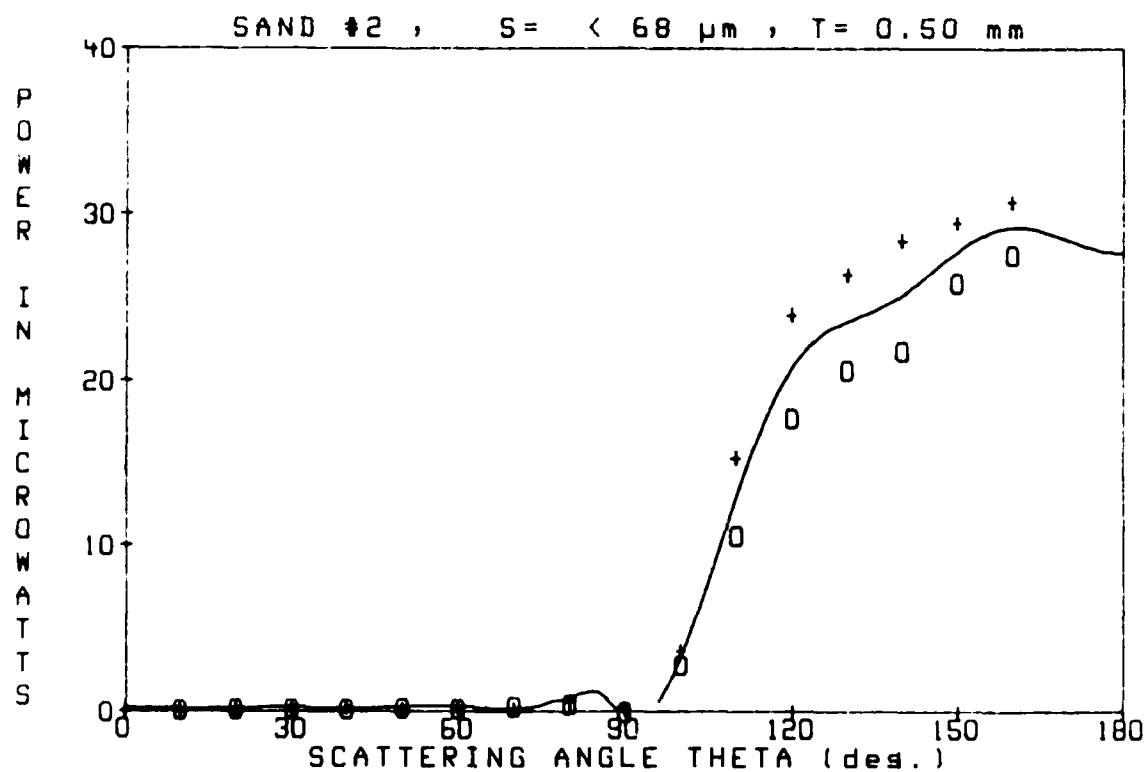
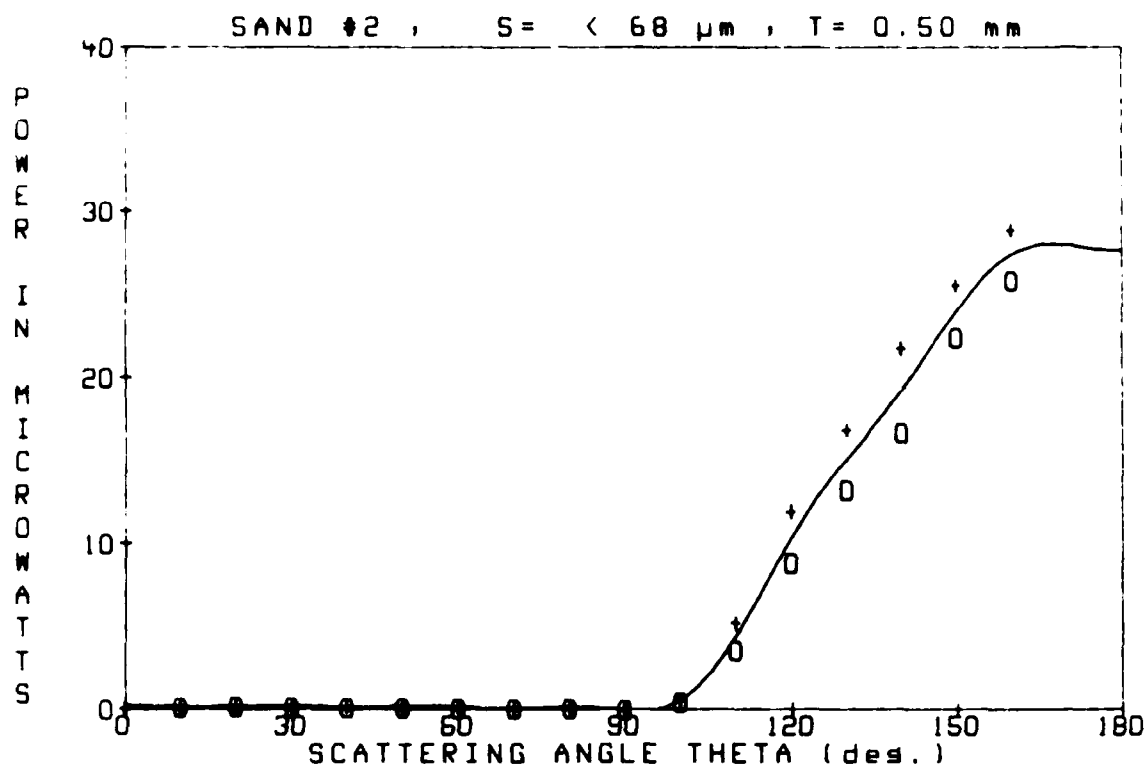
SAND #2

S=

0.8 um

T= 0.50 mm

SCATTERING ANGLE	DIODE VOLTAGE	POWER (microwatts)
-150	4.25	20.92
-150	3.67	22.41
-140	2.74	18.74
-130	2.18	13.27
-120	1.45	8.88
-110	0.60	3.63
-100	0.08	0.51
-90	0.00	0.00
-80	0.01	0.07
-70	0.02	0.12
-60	0.02	0.11
-50	0.03	0.16
-40	0.03	0.11
-30	0.03	0.18
-20	0.03	0.21
-10	0.03	0.18
0	0.03	0.18
10	0.03	0.18
20	0.03	0.21
30	0.03	0.18
40	0.03	0.21
50	0.02	0.15
60	0.02	0.15
70	0.01	0.09
80	0.02	0.12
90	0.00	0.00
100	0.11	0.65
110	0.86	5.27
120	1.97	12.00
130	2.78	16.98
140	3.58	21.81
150	4.20	25.63
160	4.75	28.96



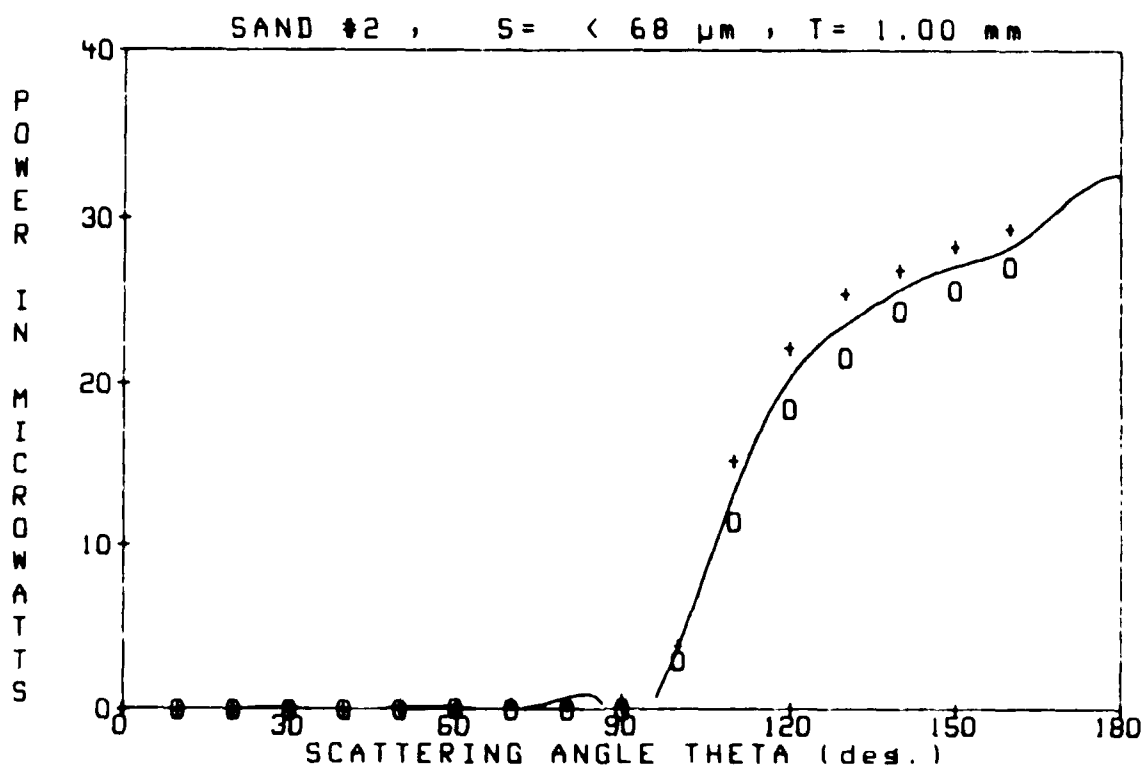
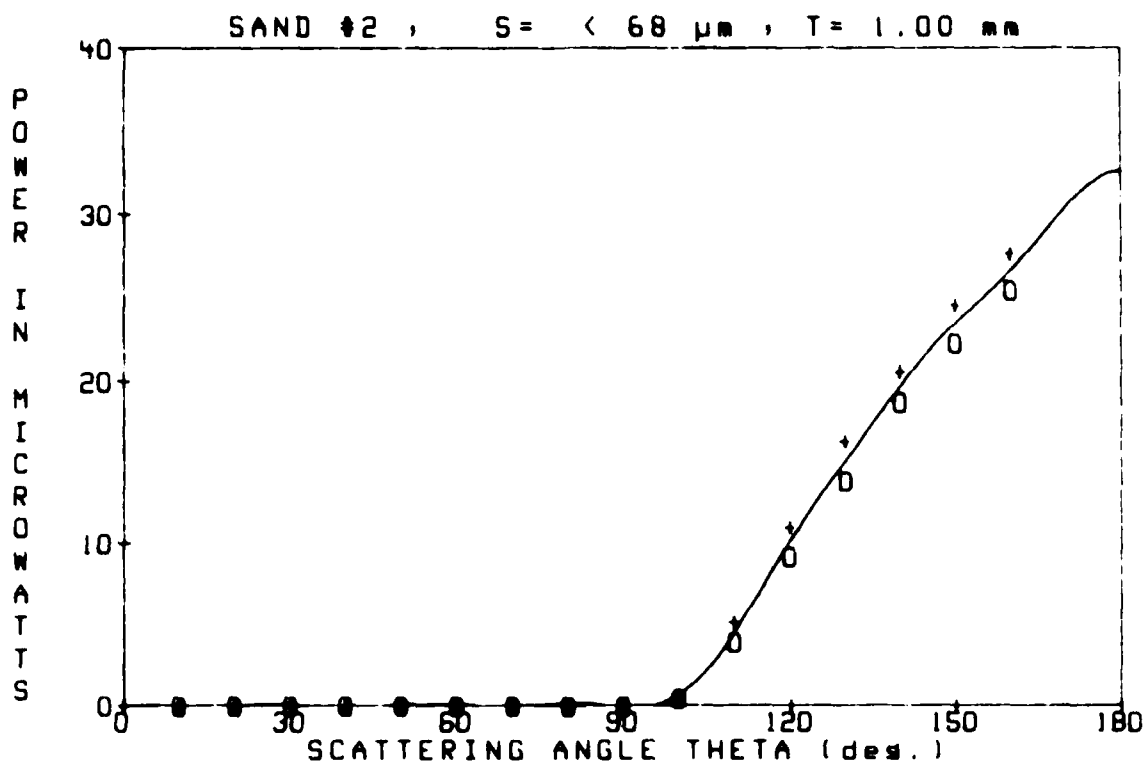
SAND #2

S-

68 um

T- 1.00 mm

SCATTERING ANGLE	DIODE VOLTAGE	POWER (microwatts)
-160	4.18	25.51
-150	3.65	22.29
-140	3.08	19.77
-130	2.28	13.91
-120	1.51	9.24
-110	0.65	3.98
-100	0.09	0.53
-90	0.00	0.00
-80	0.00	0.00
-70	0.00	0.00
-60	0.00	0.00
-50	0.00	0.00
-40	0.00	0.00
-30	0.00	0.00
-20	0.00	0.00
-10	0.00	0.00
0	0.00	0.00
10	0.00	0.00
20	0.00	0.00
30	0.00	0.00
40	0.00	0.00
50	0.00	0.00
60	0.00	0.00
70	0.02	0.12
80	0.00	0.00
90	0.00	0.00
100	0.11	0.68
110	0.86	5.24
120	1.82	11.11
130	2.69	16.42
140	3.39	20.65
150	4.04	24.64
160	4.54	27.71

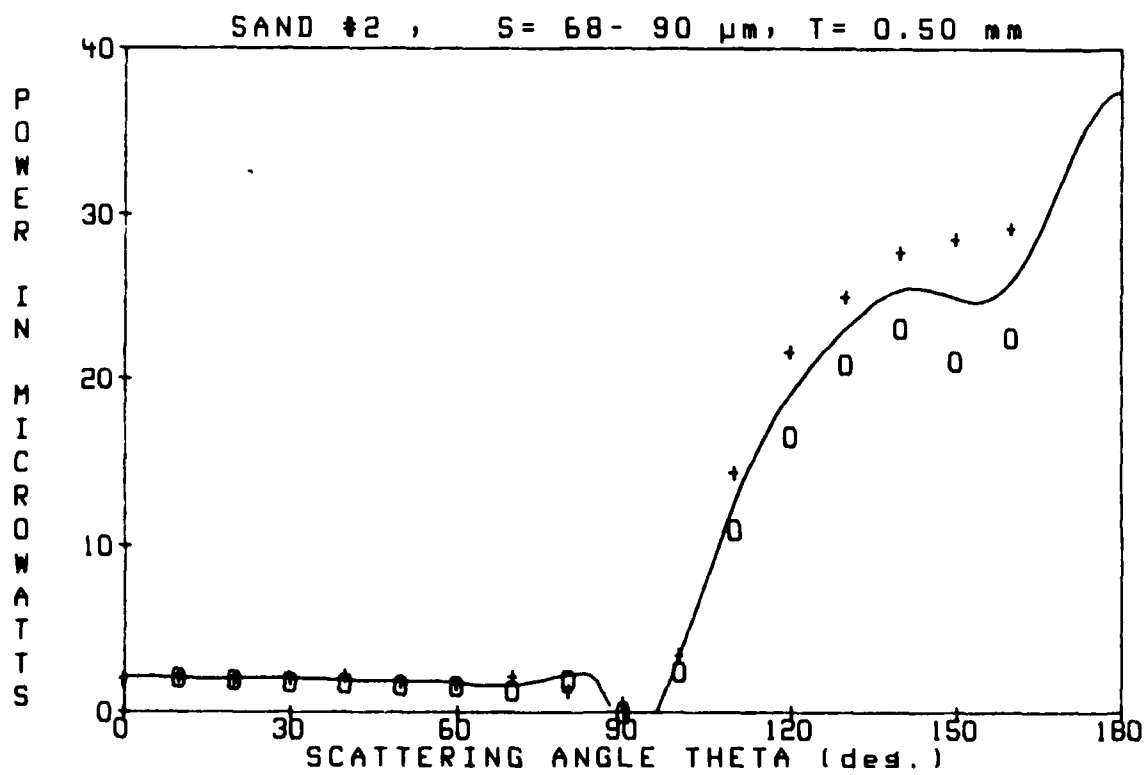
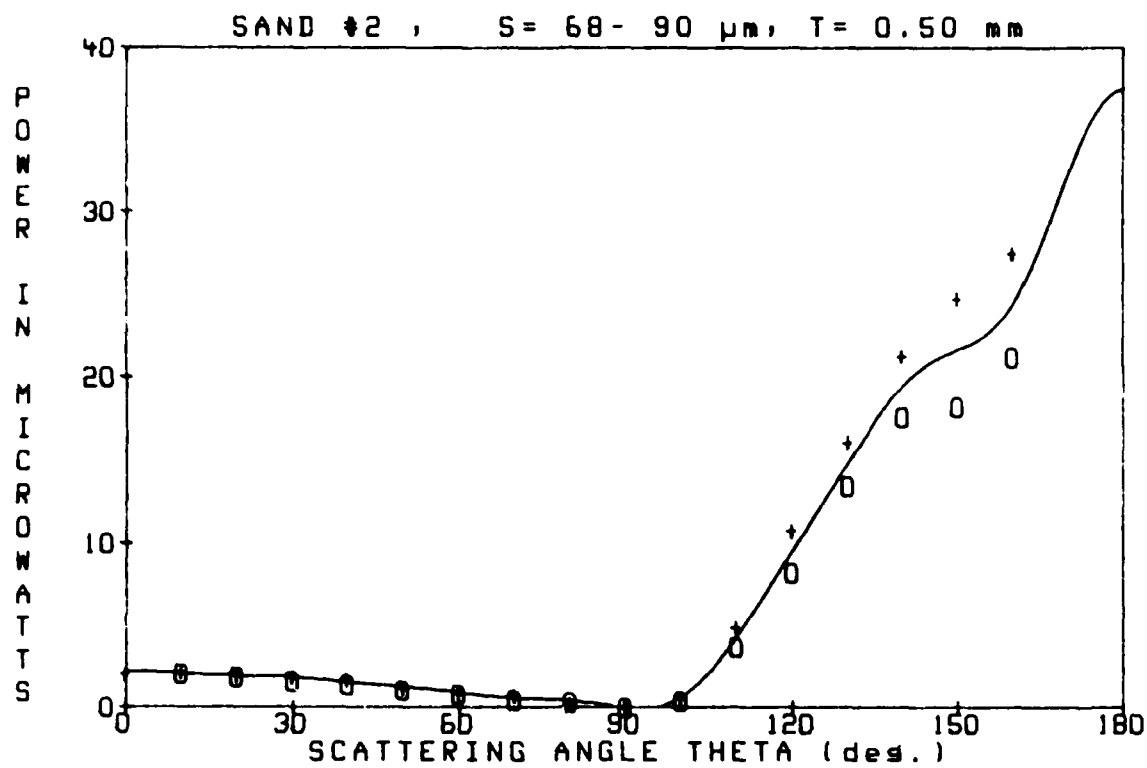


SAND #2

S- 68- 90 μ m

T- 0.50 mm

SCATTERING ANGLE	DIODE VOLTAGE	POWER (microwatts)
160	3.46	21.22
150	3.00	18.32
140	2.90	17.70
130	2.21	13.47
120	1.36	8.31
110	0.62	3.76
100	0.07	0.45
90	0.00	0.00
80	0.06	0.35
70	0.08	0.46
60	0.14	0.83
50	0.18	1.10
40	0.23	1.43
30	0.27	1.67
20	0.31	1.90
10	0.35	2.11
0	0.35	2.11
10	0.37	2.23
20	0.33	2.03
30	0.31	1.87
40	0.29	1.79
50	0.21	1.25
60	0.15	0.92
70	0.13	0.77
80	0.04	0.24
90	0.00	0.00
100	0.10	0.67
110	0.81	4.94
120	1.78	10.85
130	2.65	16.15
140	3.49	21.28
150	4.06	24.79
160	4.51	27.53

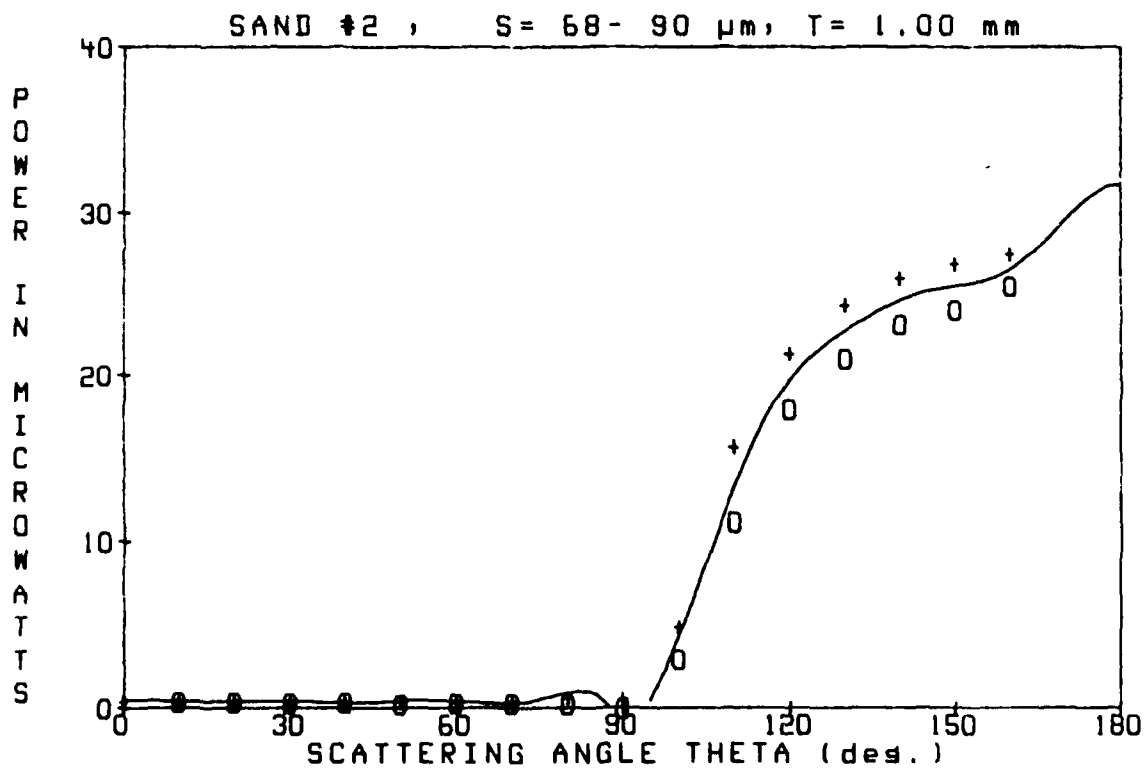
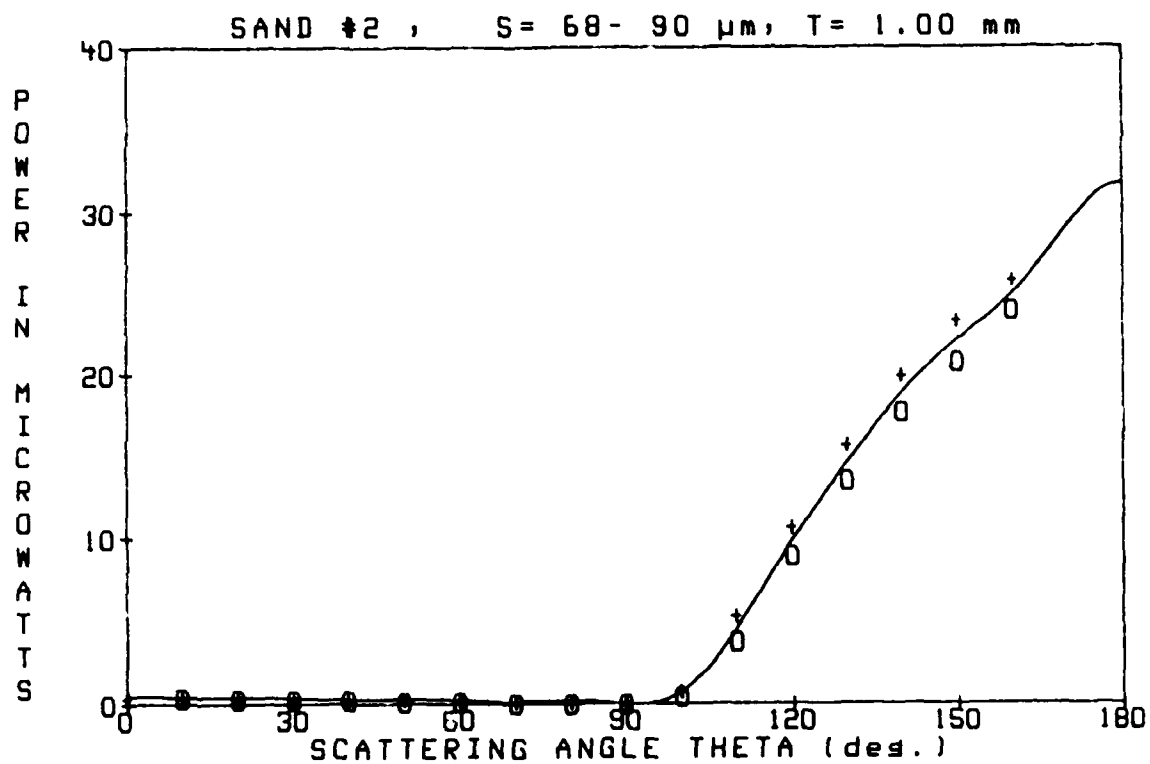


SAND #2

S= 68- 90 um

T= 1.00 mm

SCATTERING ANGLE	DIODE VOLTAGE	POWER (microwatts)
-160	3.93	23.95
-150	3.41	20.79
-140	2.90	17.70
-130	2.22	13.52
-120	1.48	9.00
-110	0.63	3.84
-100	0.09	0.53
-90	0.00	0.00
-80	0.00	0.00
-70	0.02	0.12
-60	0.03	0.18
-50	0.03	0.18
-40	0.05	0.29
-30	0.05	0.29
-20	0.06	0.38
-10	0.07	0.41
0	0.07	0.45
10	0.07	0.41
20	0.07	0.41
30	0.05	0.32
40	0.05	0.29
50	0.05	0.32
60	0.03	0.21
70	0.03	0.18
80	0.02	0.12
90	0.00	0.00
100	0.14	0.86
110	0.88	5.36
120	1.75	10.69
130	2.57	15.67
140	3.27	19.97
150	3.82	23.30
160	4.24	25.86

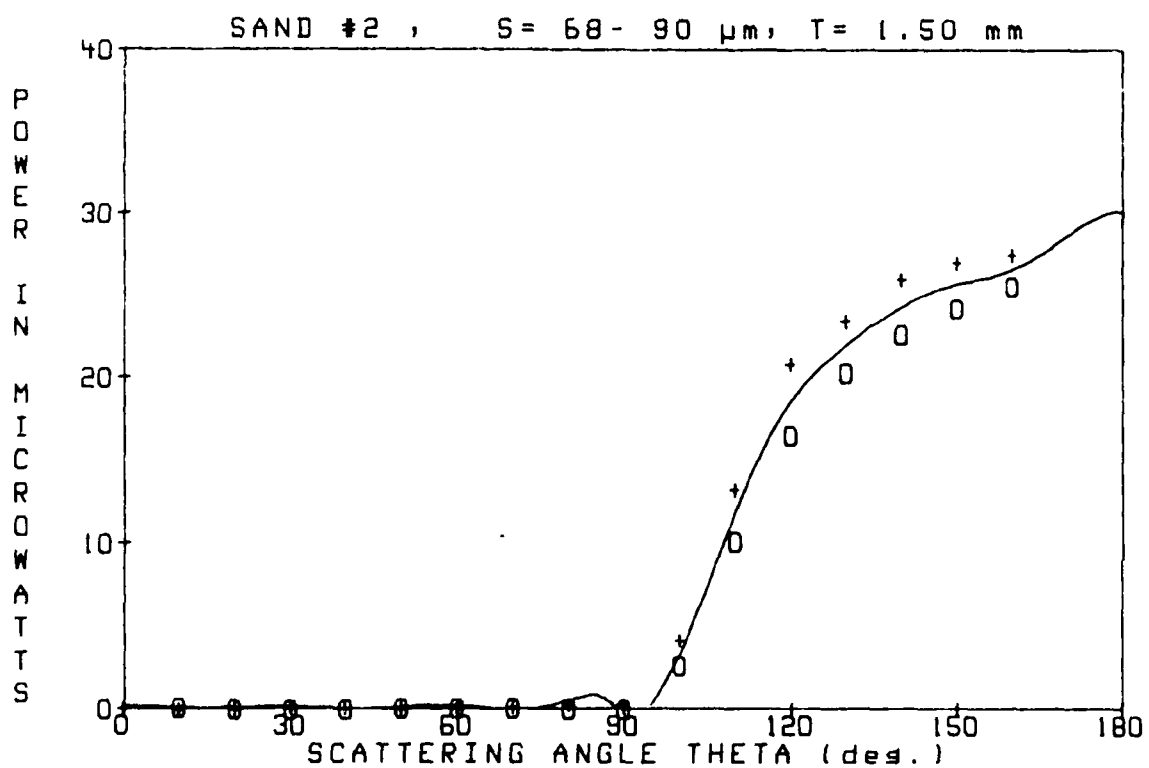
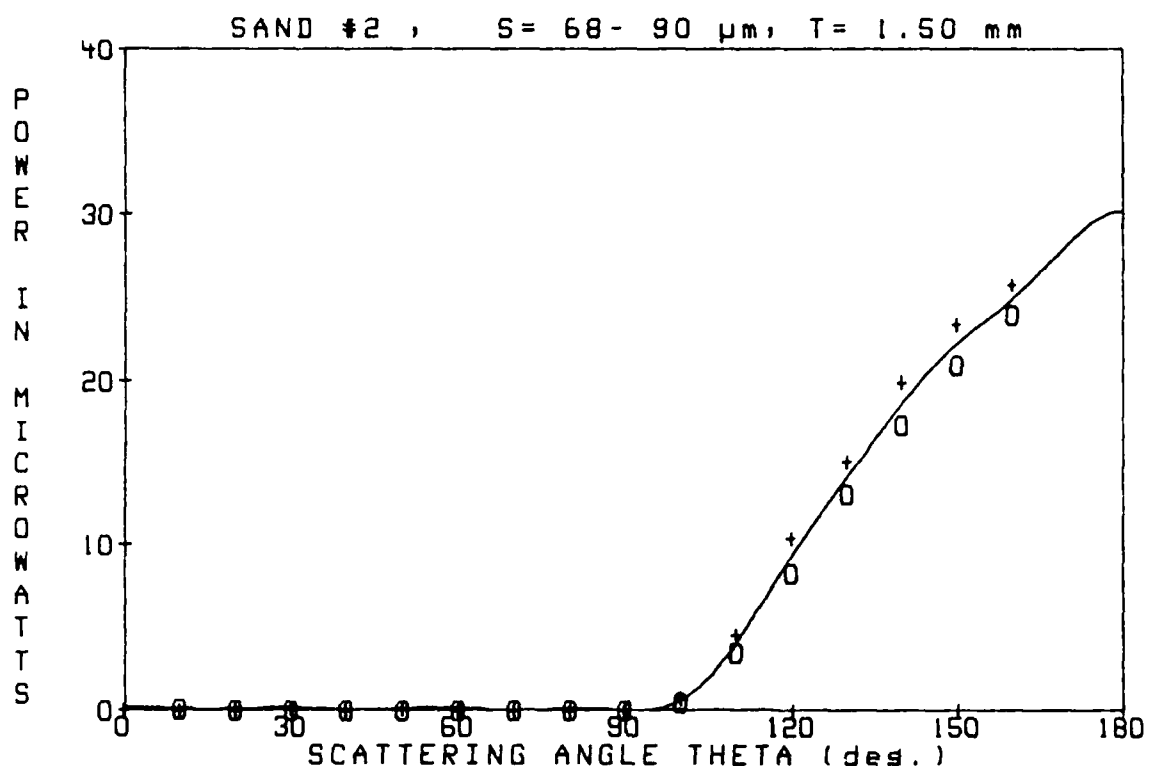


SAND #2

S= 68- 90 um

T= 1.50 mm

SCATTERING ANGLE	DIODE VOLTAGE	POWER (microwatts)
-160	3.94	24.02
-150	3.44	20.98
-140	2.84	17.34
-130	2.14	13.08
-120	1.36	8.28
-110	0.57	3.48
-100	0.08	0.48
-90	0.00	0.00
-80	0.00	0.00
-70	0.00	0.00
-60	0.00	0.00
-50	0.00	0.00
-40	0.00	0.00
-30	0.00	0.00
-20	0.00	0.00
-10	0.02	0.12
0	0.02	0.12
10	0.00	0.00
20	0.00	0.00
30	0.02	0.12
40	0.00	0.00
50	0.01	0.09
60	0.00	0.00
70	0.00	0.00
80	0.00	0.00
90	0.00	0.00
100	0.12	0.74
110	0.75	4.56
120	1.71	10.46
130	2.47	15.07
140	3.27	19.93
150	3.84	23.42
160	4.24	25.86

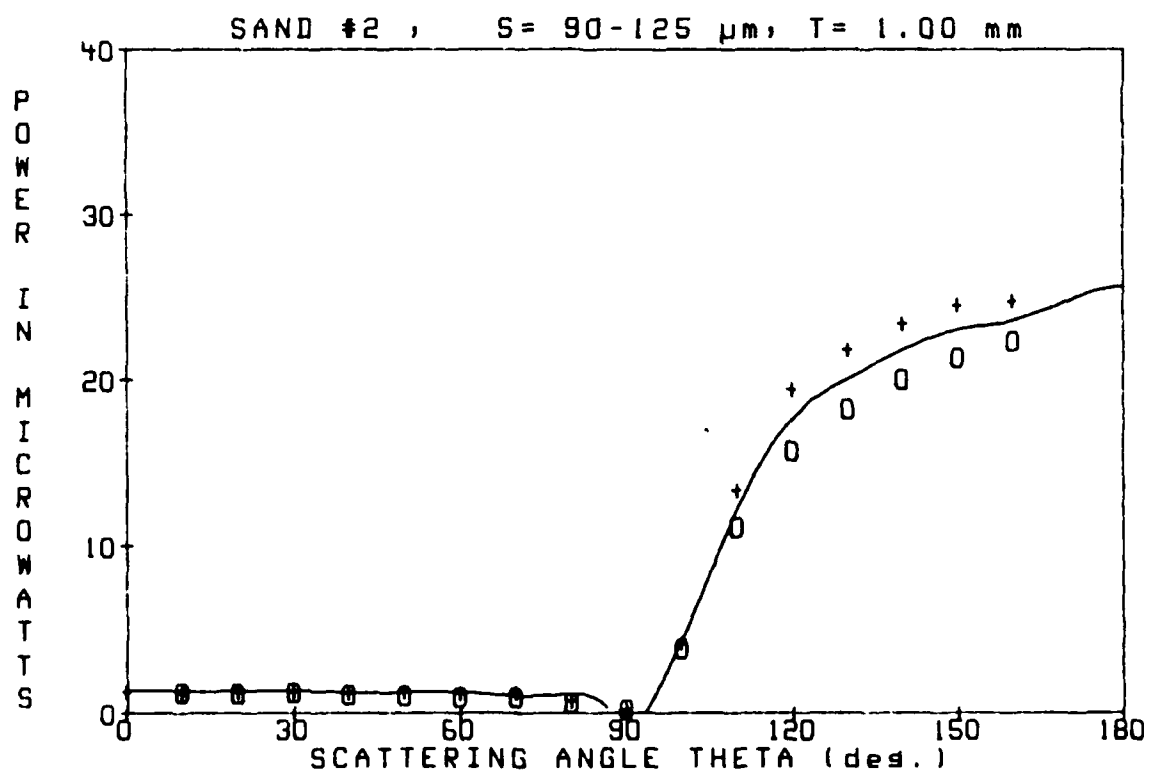
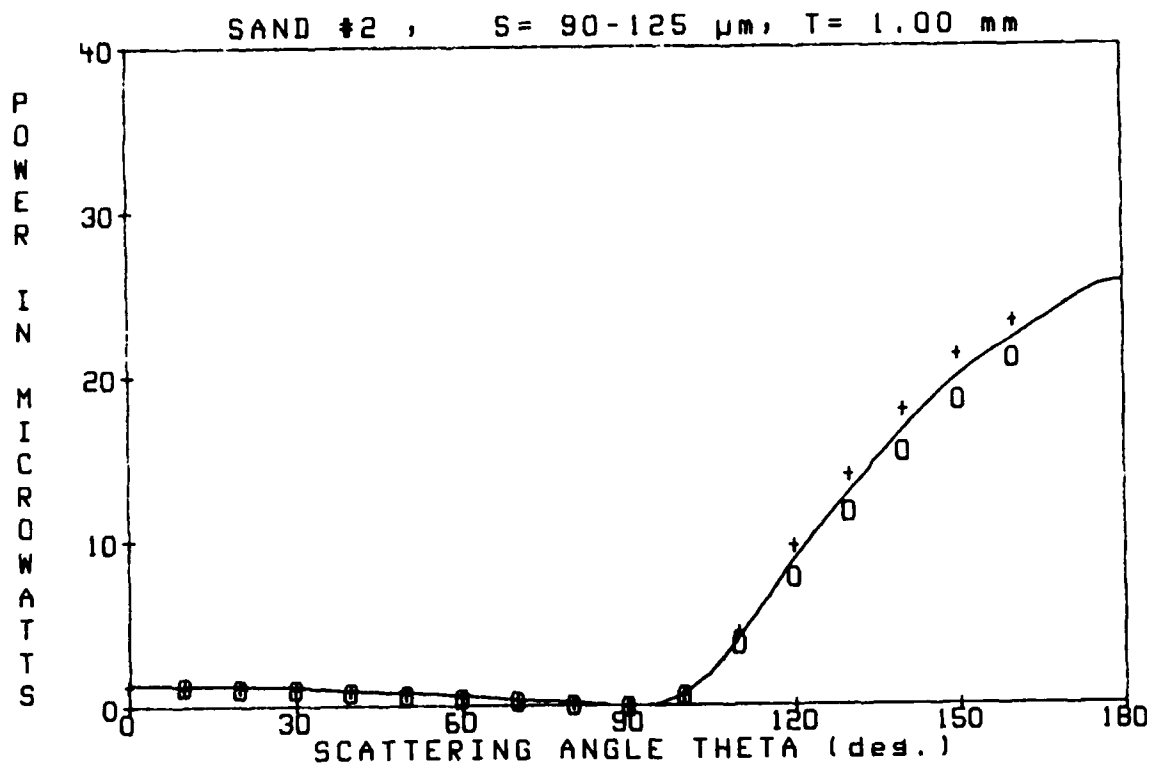


SAND #2

S= 90-125 μm

T= 1.00 mm

SCATTERING ANGLE	DIODE VOLTAGE	POWER (microwatts)
-160	3.45	21.03
-150	3.04	18.53
-140	2.53	15.40
-130	1.93	11.77
-120	1.30	7.92
-110	0.63	3.84
-100	0.11	0.68
-90	0.00	0.00
-80	0.02	0.12
-70	0.06	0.35
-60	0.09	0.53
-50	0.12	0.71
-40	0.15	0.89
-30	0.18	1.10
-20	0.19	1.19
-10	0.21	1.28
0	0.22	1.34
10	0.21	1.31
20	0.21	1.31
30	0.19	1.16
40	0.17	1.01
50	0.14	0.86
60	0.11	0.65
70	0.07	0.45
80	0.02	0.15
90	0.00	0.00
100	0.12	0.74
110	0.75	4.59
120	1.60	9.74
130	2.30	14.06
140	2.95	17.96
150	3.49	21.28
160	3.83	23.33

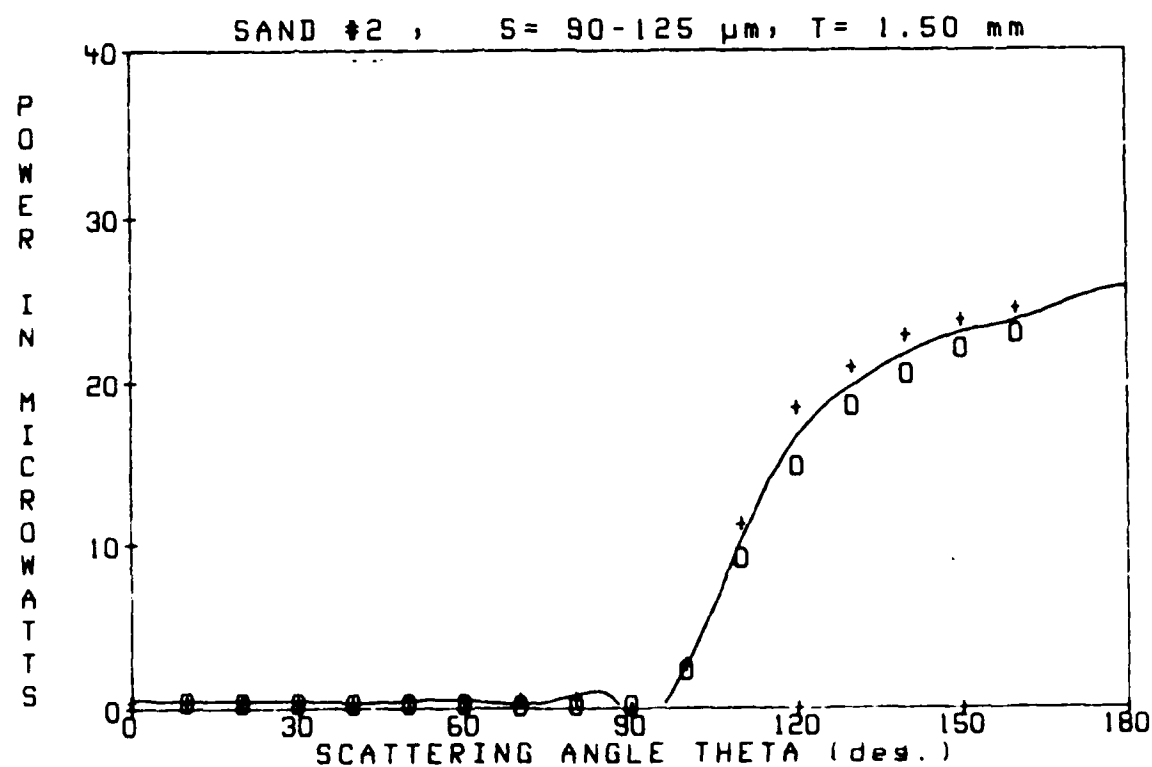
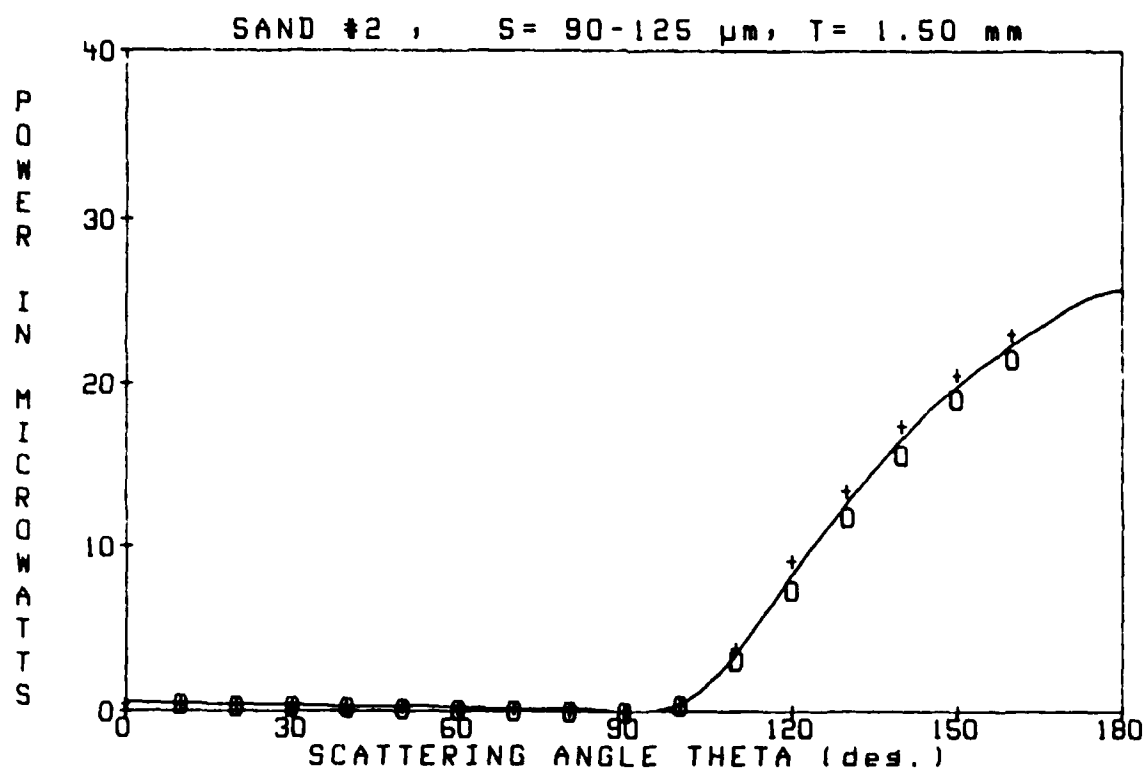


SAND #2

S= 90-125 μ m

T= 1.50 mm

SCATTERING ANGLE	DIODE VOLTAGE	POWER (microwatts)
-160	3.54	21.57
-150	3.14	19.13
-140	2.58	15.73
-130	1.95	11.92
-120	1.22	7.42
-110	0.52	3.15
-100	0.07	0.41
-90	0.00	0.00
-80	0.00	0.00
-70	0.01	0.09
-60	0.03	0.18
-50	0.04	0.24
-40	0.05	0.29
-30	0.06	0.35
-20	0.06	0.38
-10	0.08	0.48
0	0.08	0.48
10	0.08	0.48
20	0.08	0.48
30	0.06	0.38
40	0.05	0.29
50	0.06	0.35
60	0.04	0.24
70	0.03	0.21
80	0.02	0.12
90	0.00	0.00
100	0.08	0.48
110	0.64	3.90
120	1.52	9.27
130	2.21	13.47
140	2.87	17.52
150	3.39	20.65
160	3.79	23.09

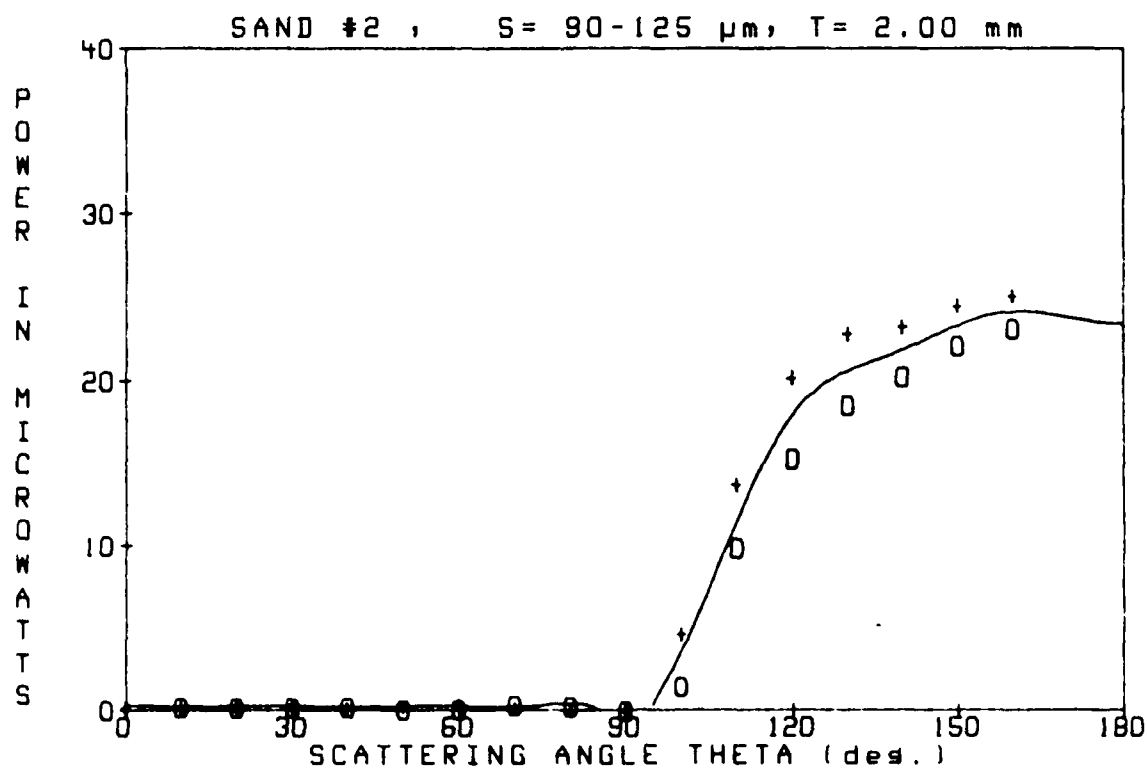
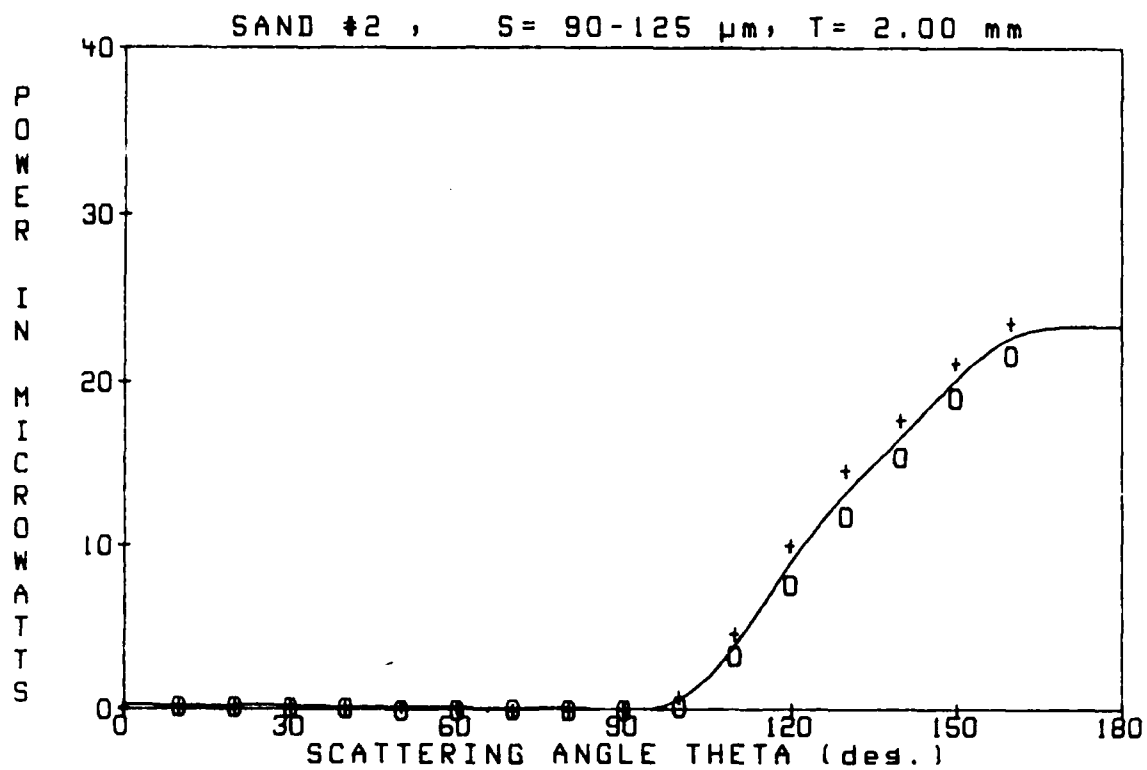


SAND #2

S= 90-125 μ m

T= 2.00 mm

SCATTERING ANGLE		DIODE VOLTAGE		POWER (microwatts)
-160		3.56		21.59
-150		3.14		19.13
-140		2.55		15.56
-130		1.95		11.92
-120		1.26		7.69
-110		0.56		3.39
-100		0.04		0.26
-90		0.00		0.00
-80		0.00		0.00
-70		0.02		0.12
-60		0.00		0.00
-50		0.00		0.00
-40		0.03		0.18
-30		0.03		0.18
-20		0.04		0.24
-10		0.03		0.21
0		0.04		0.24
10		0.04		0.24
20		0.04		0.24
30		0.04		0.24
40		0.02		0.15
50		0.03		0.21
60		0.03		0.18
70		0.00		0.00
80		0.00		0.00
90		0.00		0.00
100		0.14		0.83
110		0.77		4.70
120		1.66		10.13
130		2.41		14.69
140		2.92		17.82
150		3.48		21.22
160		3.87		23.60

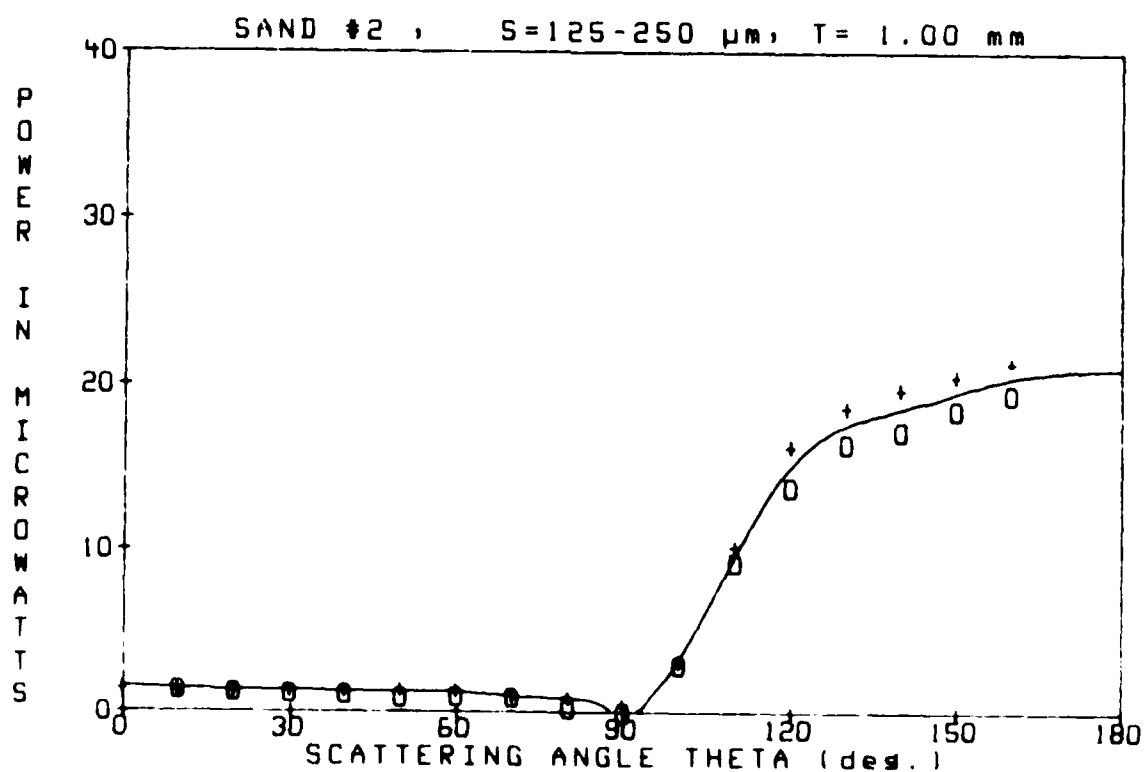
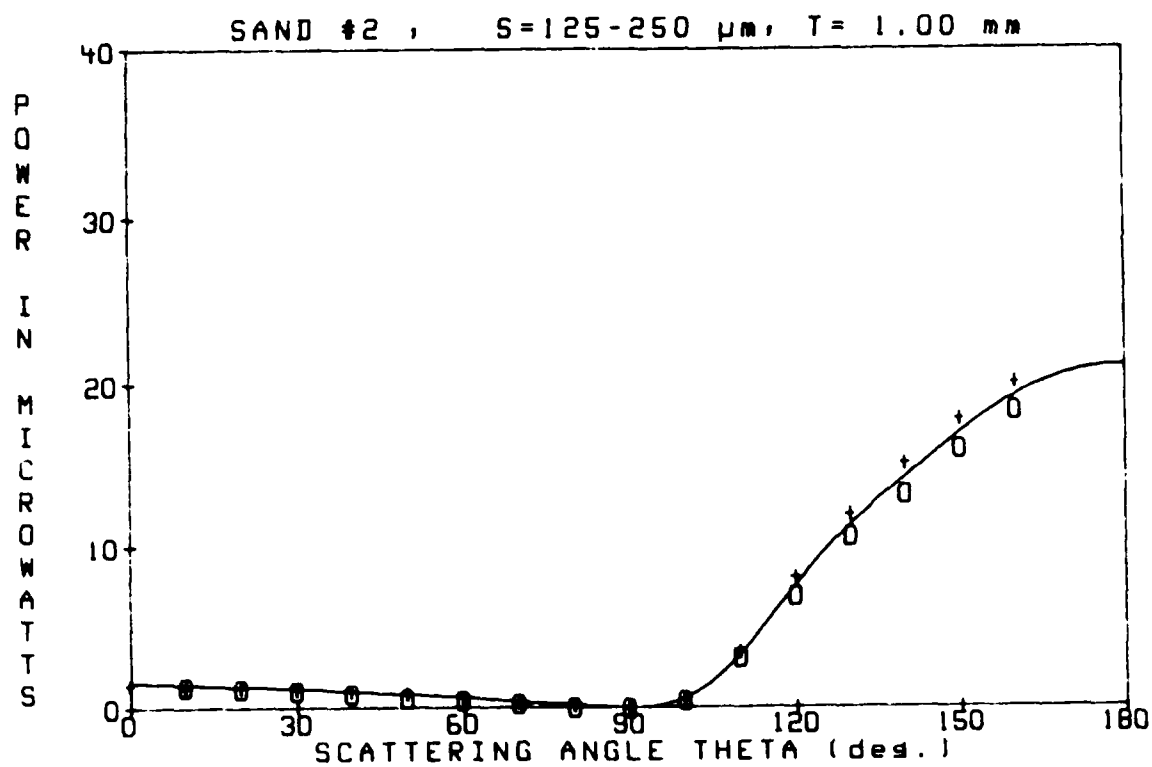


SAND 42

S=125-250 μ m

T= 1.00 mm

SCATTERING ANGLE	DIODE VOLTAGE	POWER (microwatts)
-160	3.01	18.35
-150	2.63	16.06
-140	2.17	13.26
-130	1.74	10.84
-120	1.14	8.94
-110	0.52	3.18
-100	0.09	0.53
-90	0.00	0.00
-80	0.00	0.00
-70	0.05	0.32
-60	0.08	0.51
-50	0.10	0.62
-40	0.15	0.89
-30	0.17	1.07
-20	0.21	1.25
-10	0.23	1.40
0	0.25	1.52
10	0.23	1.40
20	0.22	1.34
30	0.20	1.22
40	0.18	1.10
50	0.16	0.95
60	0.12	0.71
70	0.06	0.38
80	0.03	0.18
90	0.00	0.00
100	0.09	0.56
110	0.58	3.51
120	1.34	8.19
130	1.97	12.00
140	2.49	15.20
150	2.93	17.88
160	3.30	20.11

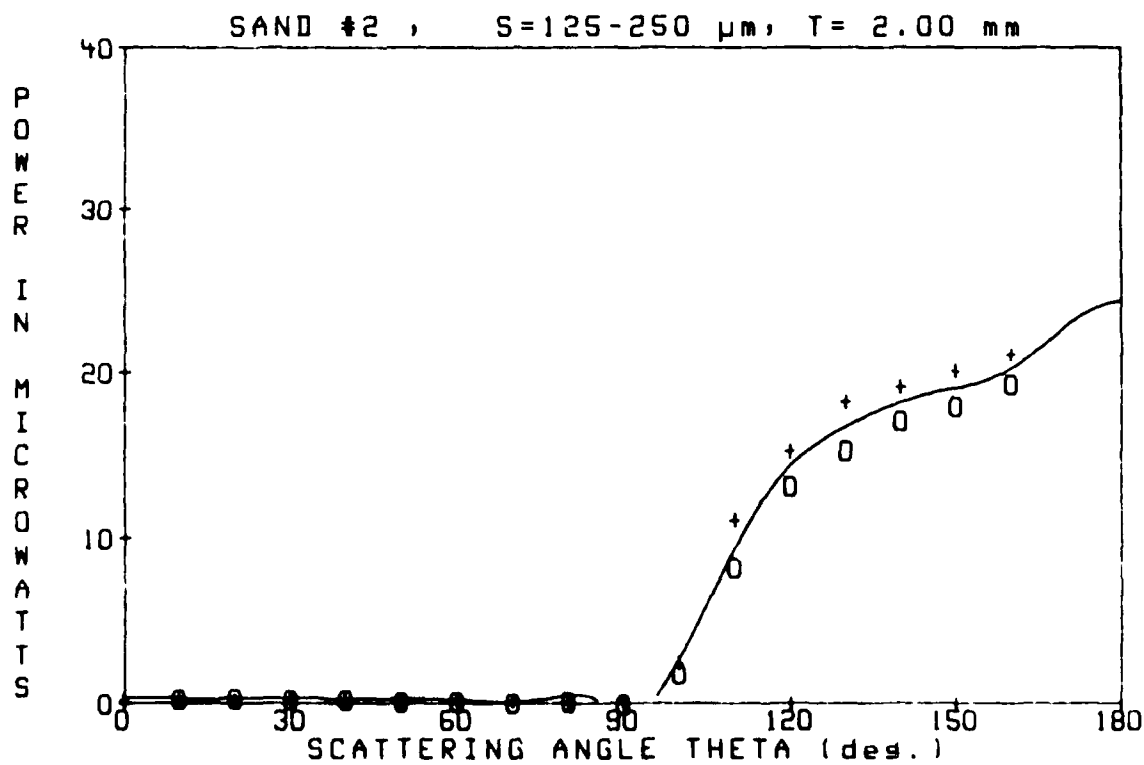
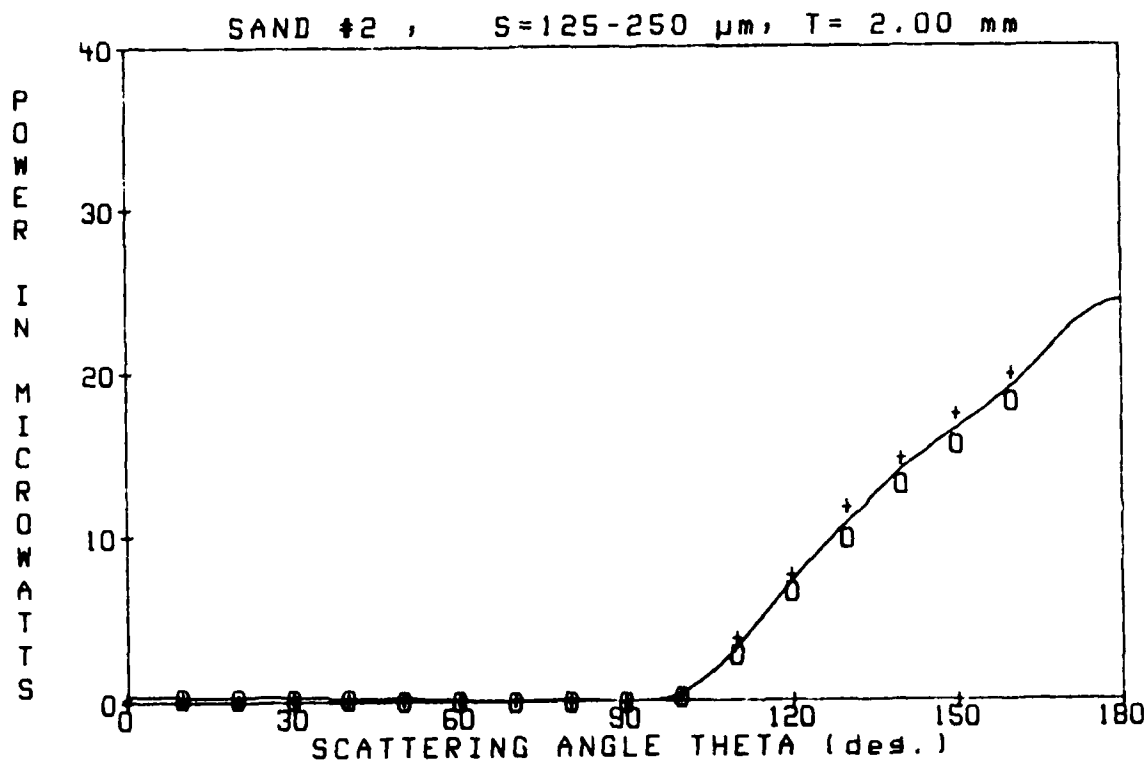


SAND #2

S=125-250 μ m

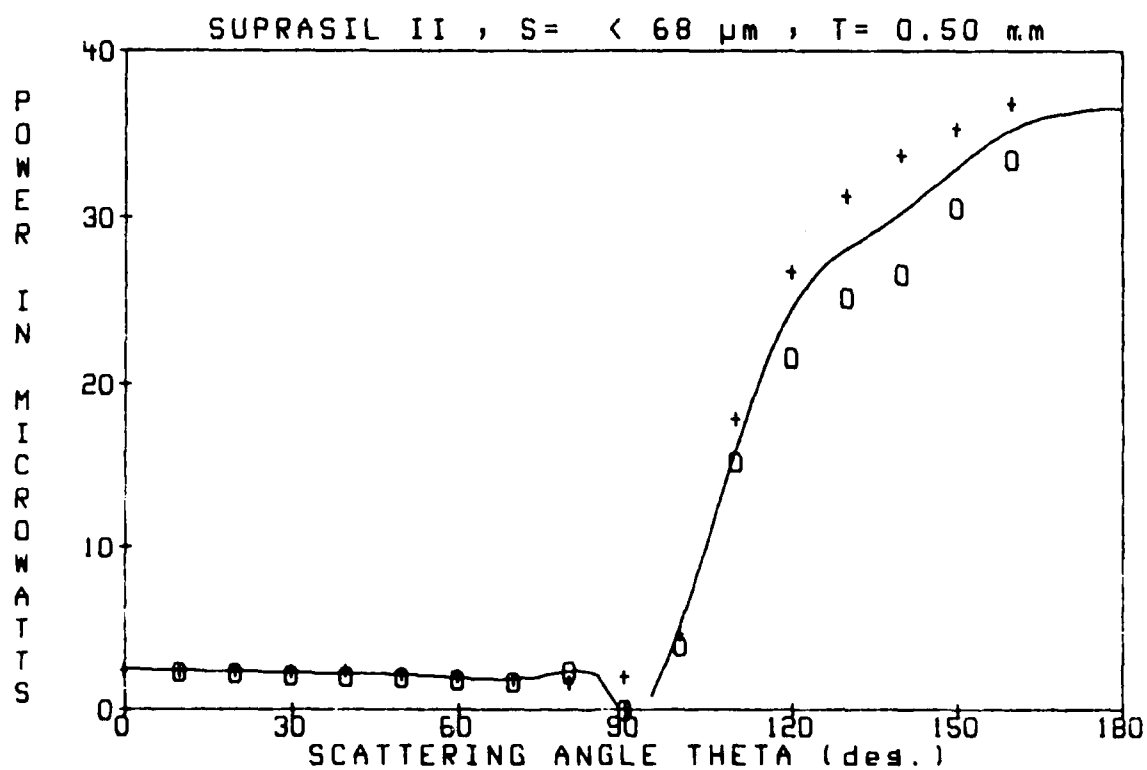
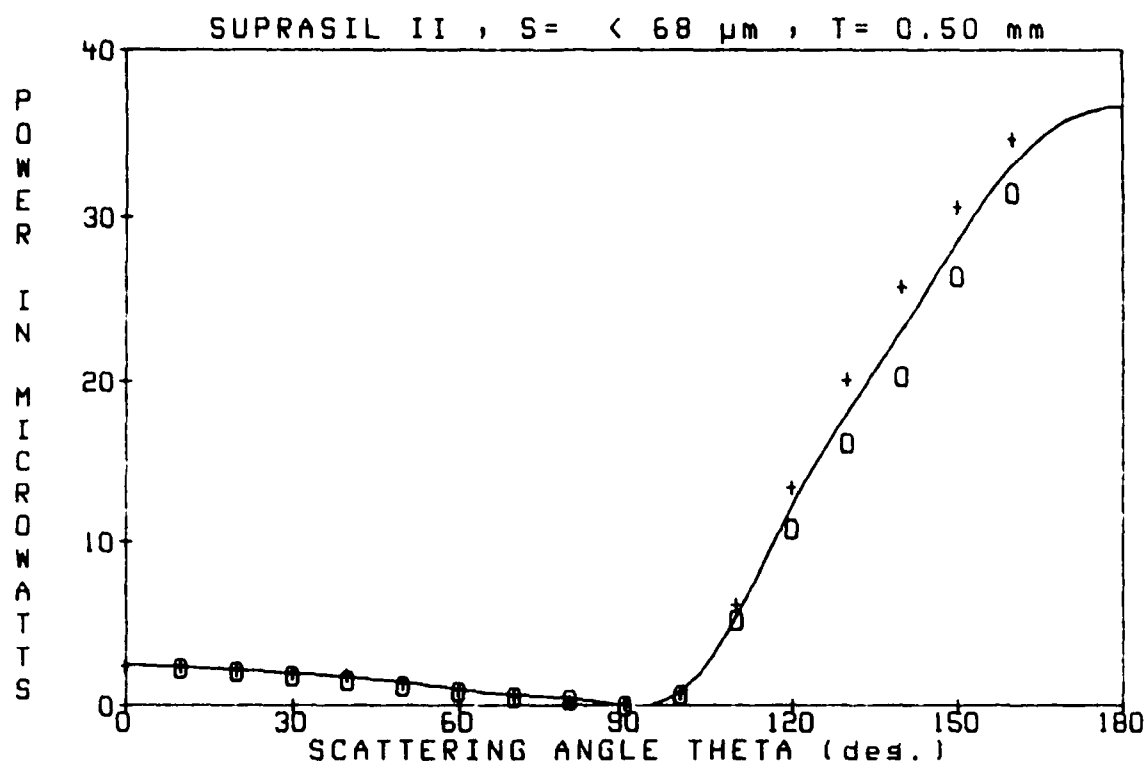
T= 2.00 mm

SCATTERING ANGLE	DIODE VOLTAGE	POWER (microwatts)
-160	2.97	18.15
-150	2.55	15.56
-140	2.15	13.11
-130	1.62	9.86
-120	1.08	6.53
-110	0.46	2.83
-100	0.05	0.32
-90	0.00	0.00
-80	0.00	0.00
-70	0.00	0.00
-60	0.01	0.09
-50	0.02	0.12
-40	0.04	0.24
-30	0.04	0.24
-20	0.05	0.32
-10	0.05	0.32
0	0.05	0.29
10	0.05	0.32
20	0.04	0.26
30	0.05	0.29
40	0.04	0.26
50	0.02	0.15
60	0.02	0.15
70	0.01	0.09
80	0.00	0.00
90	0.00	0.00
100	0.07	0.45
110	0.63	3.81
120	1.26	7.66
130	1.93	11.77
140	2.41	14.69
150	2.86	17.46
160	3.26	19.90



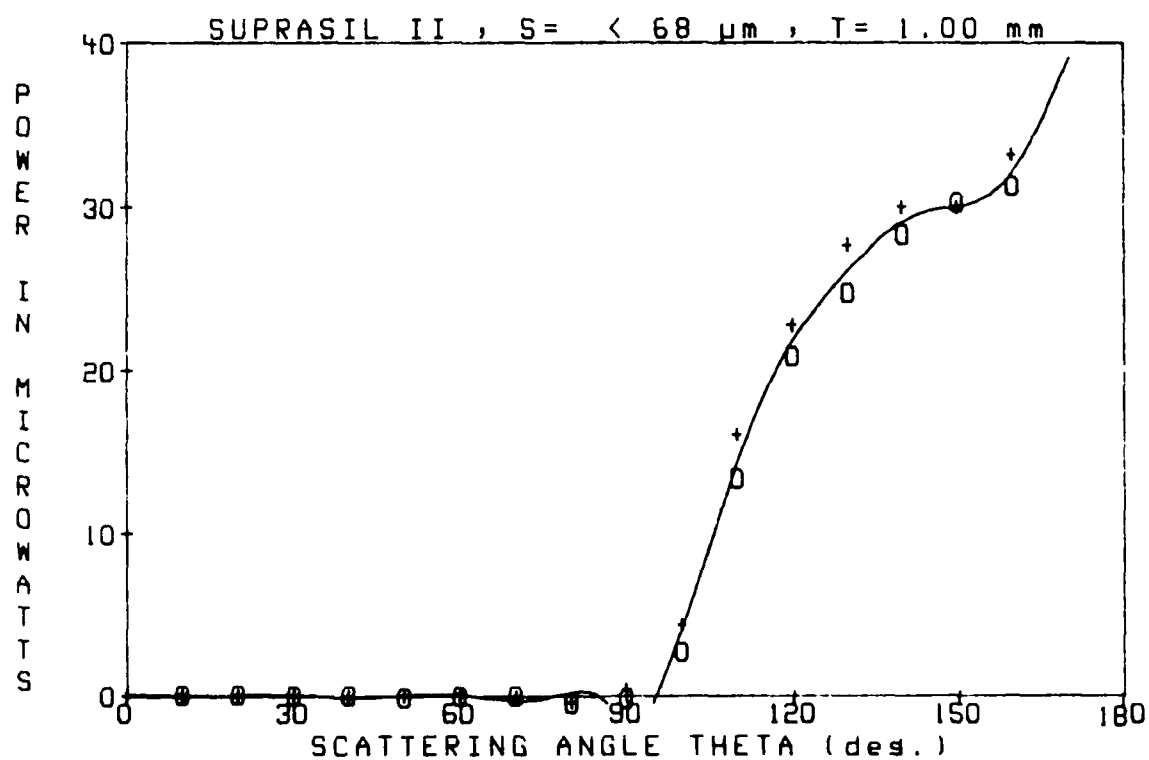
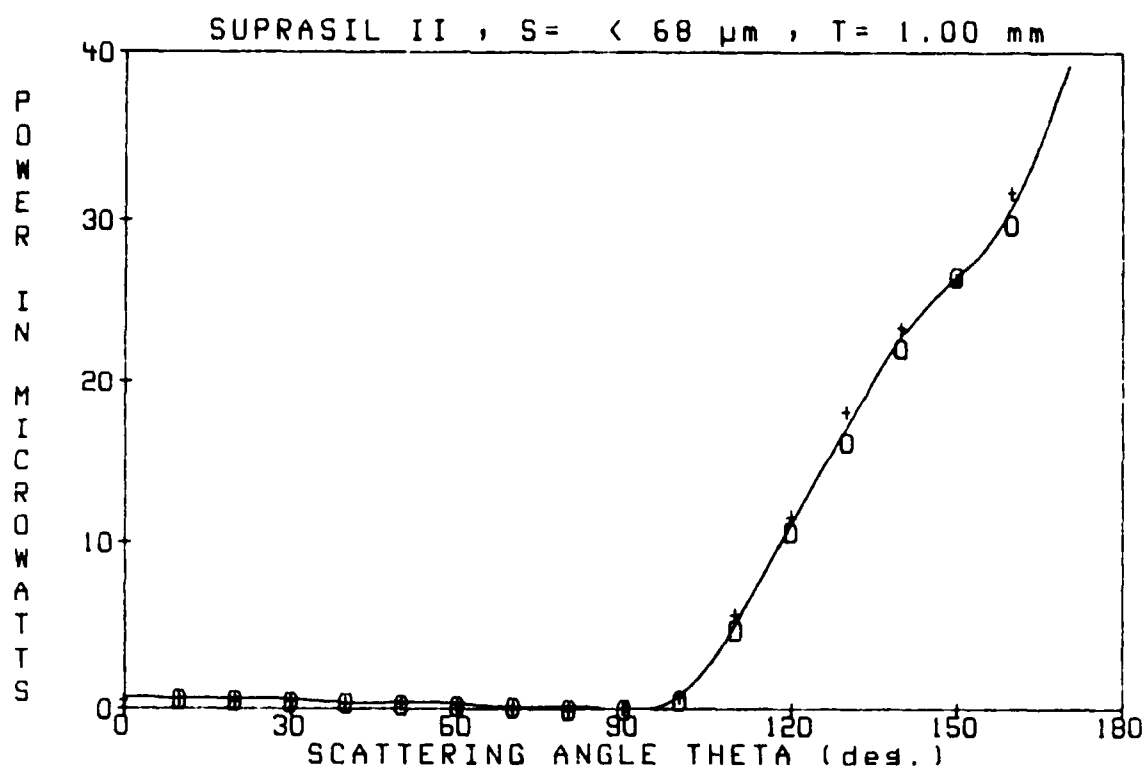
SUPRASIL II S= < 68 μ m T= 0.50 mm

SCATTERING ANGLE	DIODE VOLTAGE	POWER (microwatts)
-160	5.17	31.52
-150	4.35	26.52
-140	3.34	20.38
-130	2.66	16.24
-120	1.77	10.82
-110	0.85	5.21
-100	0.11	0.68
-90	0.00	0.00
-80	0.07	0.41
-70	0.10	0.59
-60	0.15	0.92
-50	0.21	1.25
-40	0.25	1.55
-30	0.30	1.84
-20	0.35	2.11
-10	0.38	2.29
0	0.40	2.44
10	0.39	2.41
20	0.37	2.26
30	0.34	2.06
40	0.31	1.87
50	0.23	1.43
60	0.17	1.04
70	0.11	0.65
80	0.05	0.29
90	0.03	0.18
100	0.14	0.83
110	1.01	6.14
120	2.20	13.41
130	3.30	20.14
140	4.24	25.89
150	5.03	30.69
160	5.70	34.75



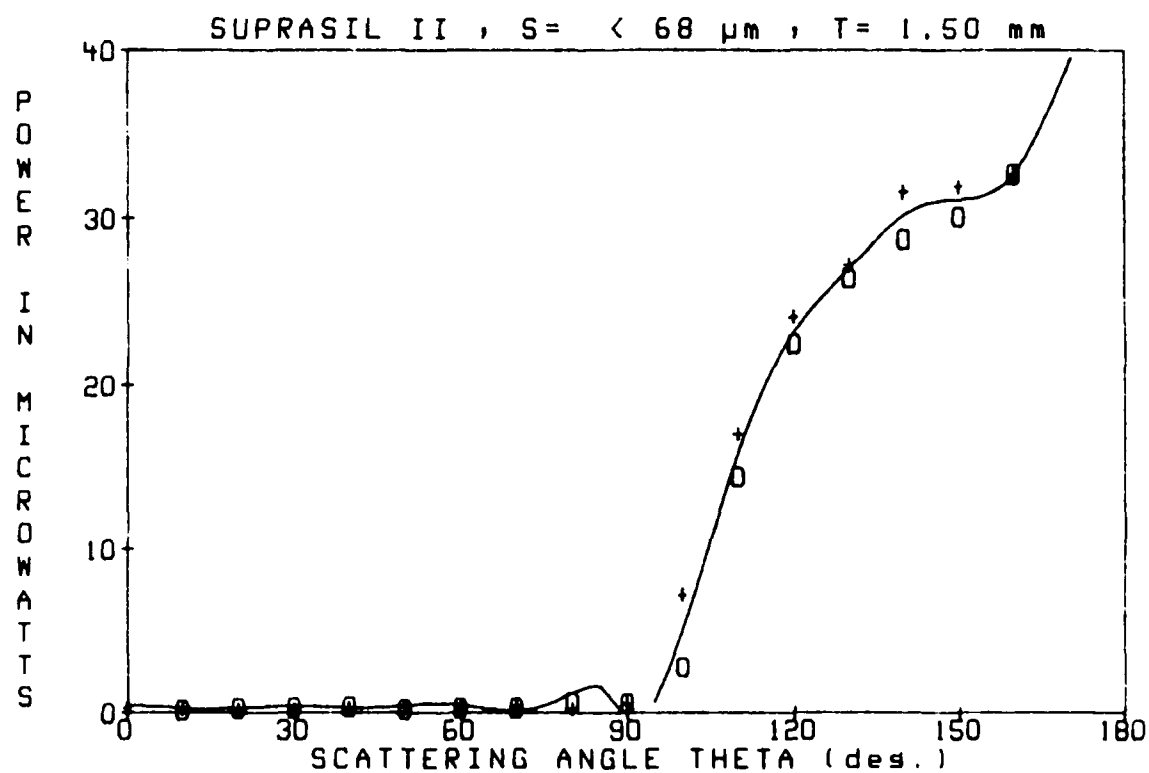
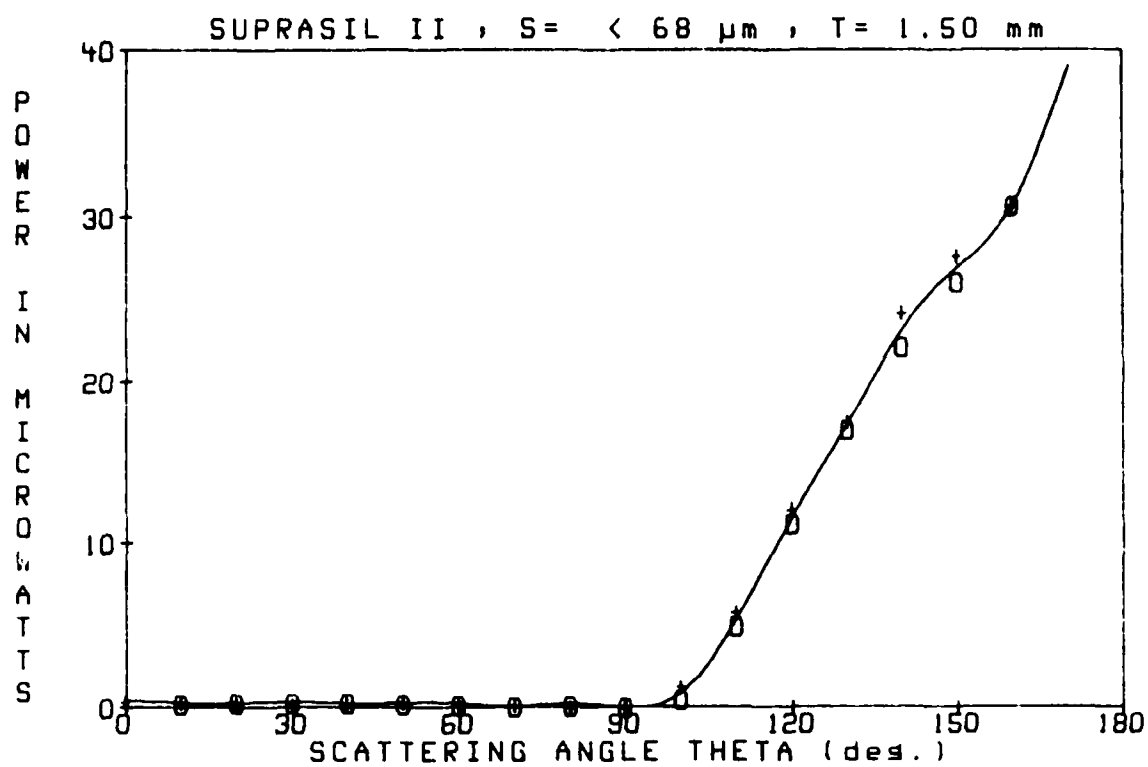
SUPRASIL II S= < 68 μ m T= 1.00 mm

SCATTERING ANGLE	DIODE VOLTAGE	POWER (microwatts)
-160	4.89	29.85
-150	4.37	26.64
-140	3.62	22.11
-130	2.67	16.27
-120	1.75	10.69
-110	0.78	4.73
-100	0.09	0.56
-90	0.00	0.00
-80	0.00	0.00
-70	0.03	0.18
-60	0.04	0.24
-50	0.05	0.29
-40	0.07	0.41
-30	0.08	0.48
-20	0.10	0.59
-10	0.11	0.65
0	0.10	0.59
10	0.11	0.65
20	0.10	0.59
30	0.09	0.56
40	0.07	0.41
50	0.07	0.41
60	0.06	0.35
70	0.03	0.18
80	0.00	0.00
90	0.01	0.09
100	0.14	0.86
110	0.93	5.69
120	1.91	11.68
130	2.98	18.20
140	3.84	23.45
150	4.35	26.52
160	5.21	31.79



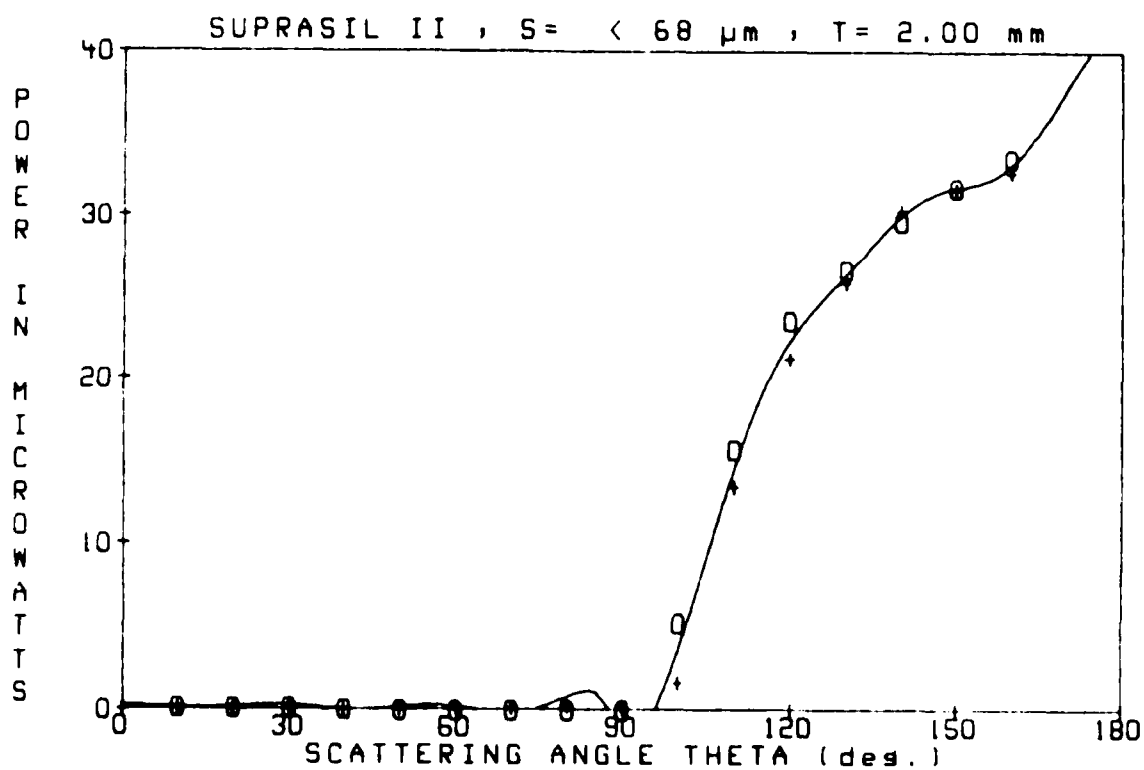
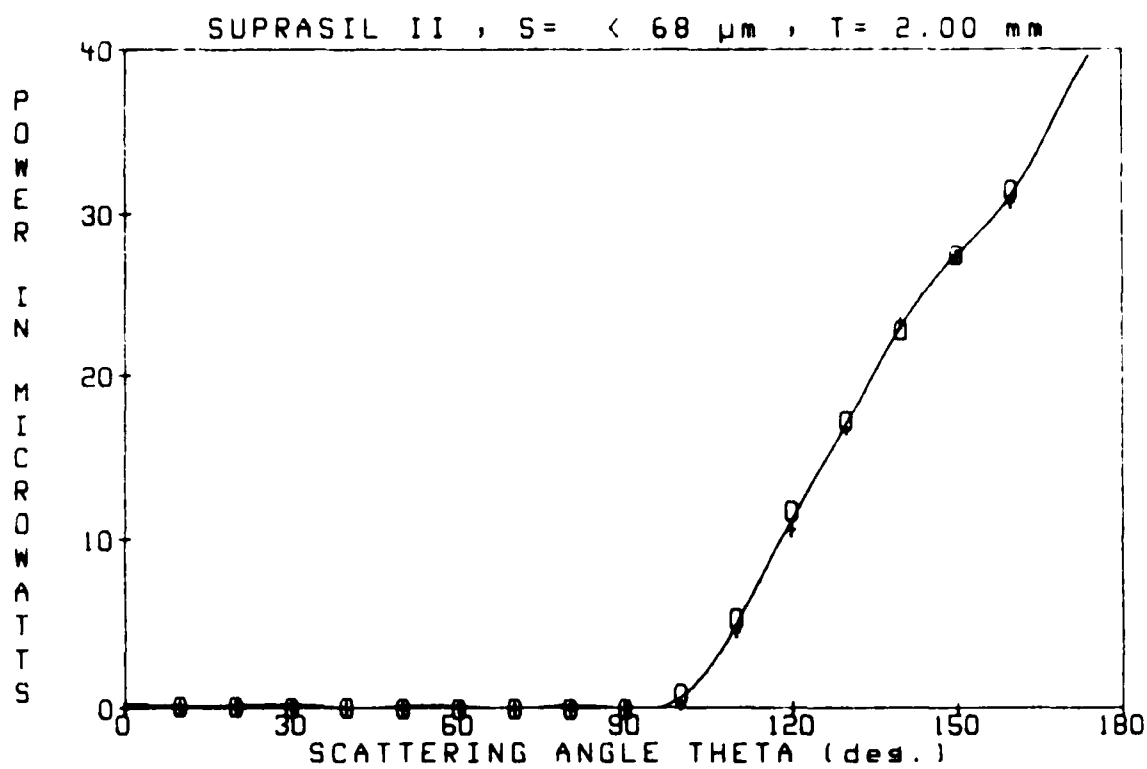
SUPRASIL II S = < 68 μ m T = 1.50 mm

SCATTERING ANGLE	DIODE VOLTAGE	POWER (microwatts)
-160	5.04	30.72
-150	4.28	26.13
-140	3.62	22.11
-130	2.79	17.04
-120	1.85	11.26
-110	0.81	4.94
-100	0.08	0.51
-90	0.00	0.00
-80	0.02	0.12
-70	0.02	0.12
-60	0.03	0.13
-50	0.03	0.21
-40	0.05	0.32
-30	0.05	0.29
-20	0.05	0.32
-10	0.04	0.24
0	0.06	0.35
10	0.05	0.29
20	0.05	0.29
30	0.04	0.26
40	0.05	0.29
50	0.05	0.29
60	0.03	0.18
70	0.03	0.18
80	0.00	0.00
90	0.00	0.00
100	0.21	1.28
110	0.96	5.84
120	1.98	12.10
130	2.88	17.55
140	3.97	24.22
150	4.54	27.68
160	5.03	30.69



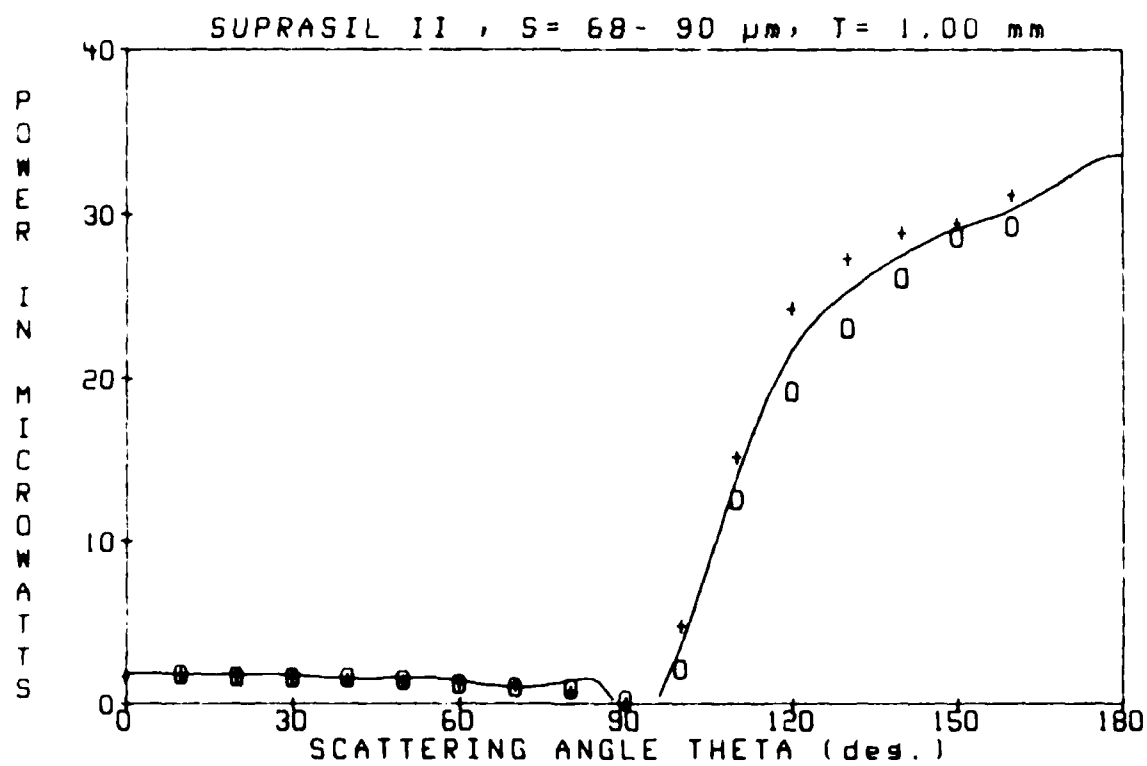
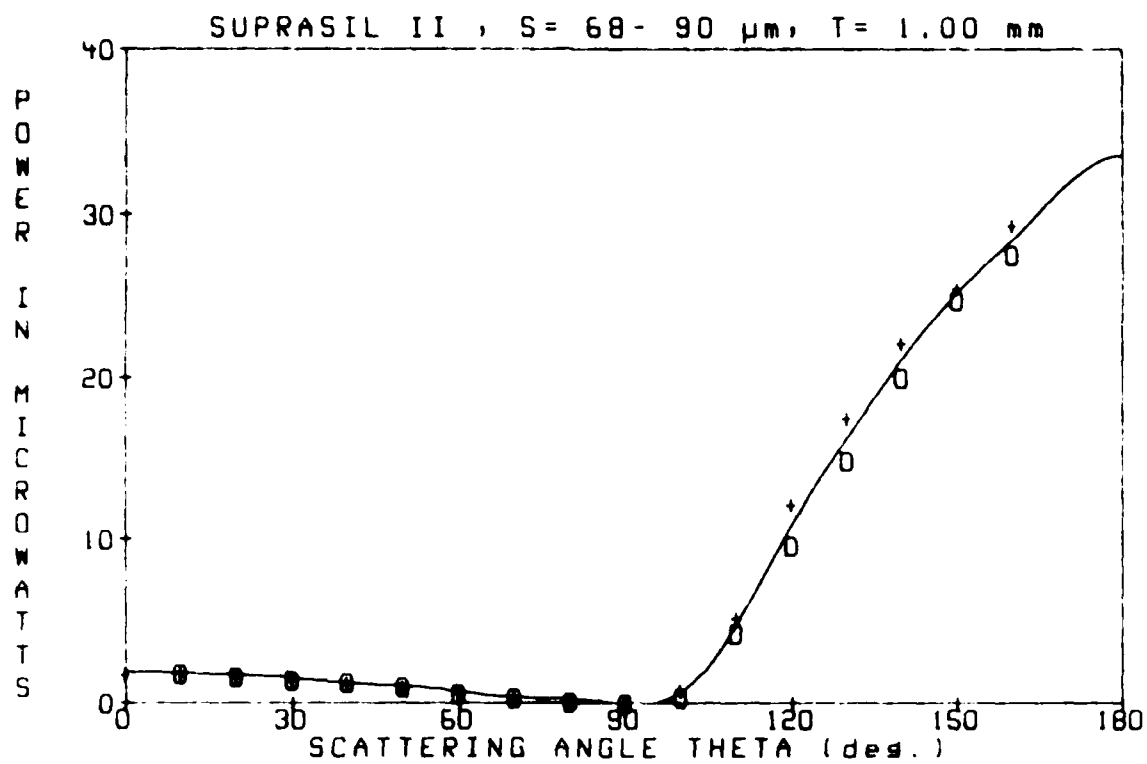
SUPRASIL II S = 68 μ m T = 2.00 mm

SCATTERING ANGLE	DIODE VOLTAGE	POWER (microwatts)
-160	5.17	31.52
-150	4.51	27.50
-140	3.73	22.73
-130	2.82	17.22
-120	1.93	11.80
-110	0.88	5.39
-100	0.15	0.92
-90	0.00	0.00
-80	0.00	0.00
-70	0.00	0.00
-60	0.00	0.00
-50	0.00	0.00
-40	0.01	0.09
-30	0.02	0.12
-20	0.02	0.15
-10	0.03	0.18
0	0.01	0.09
10	0.03	0.18
20	0.03	0.18
30	0.03	0.18
40	0.01	0.09
50	0.00	0.00
60	0.02	0.15
70	0.00	0.00
80	0.00	0.00
90	0.00	0.00
100	0.05	0.29
110	0.76	4.62
120	1.74	10.64
130	2.74	16.74
140	3.82	23.30
150	4.50	27.44
160	5.05	30.78



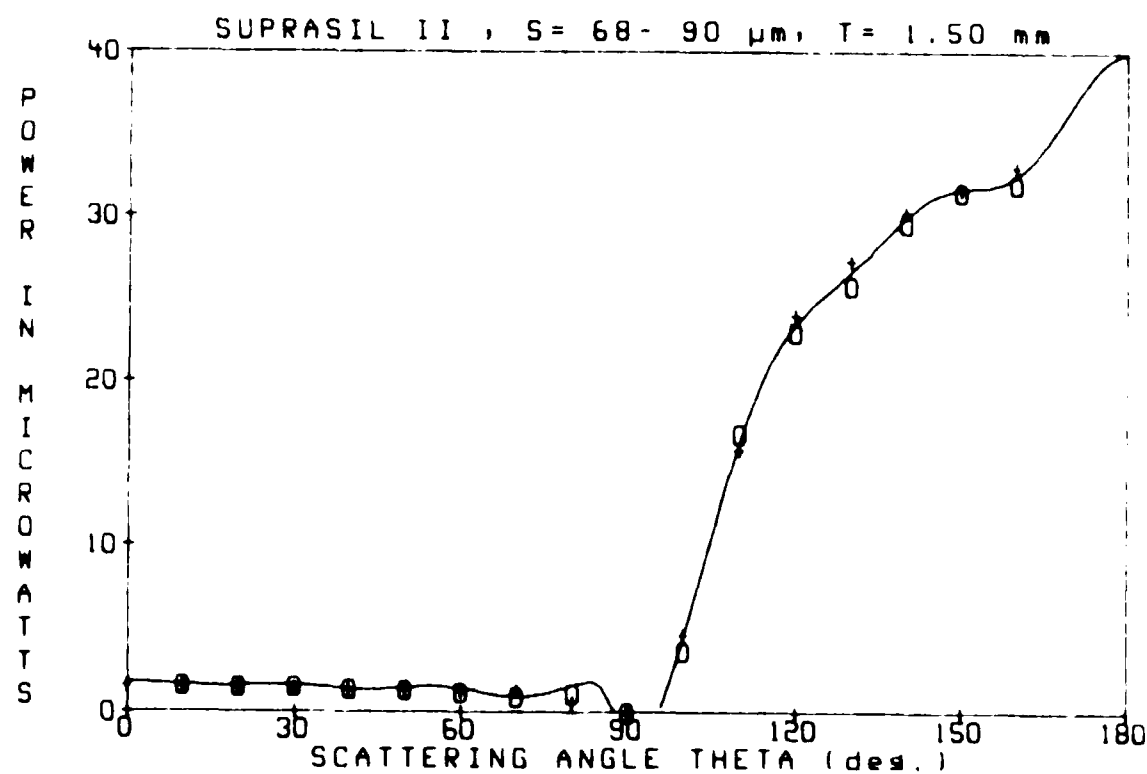
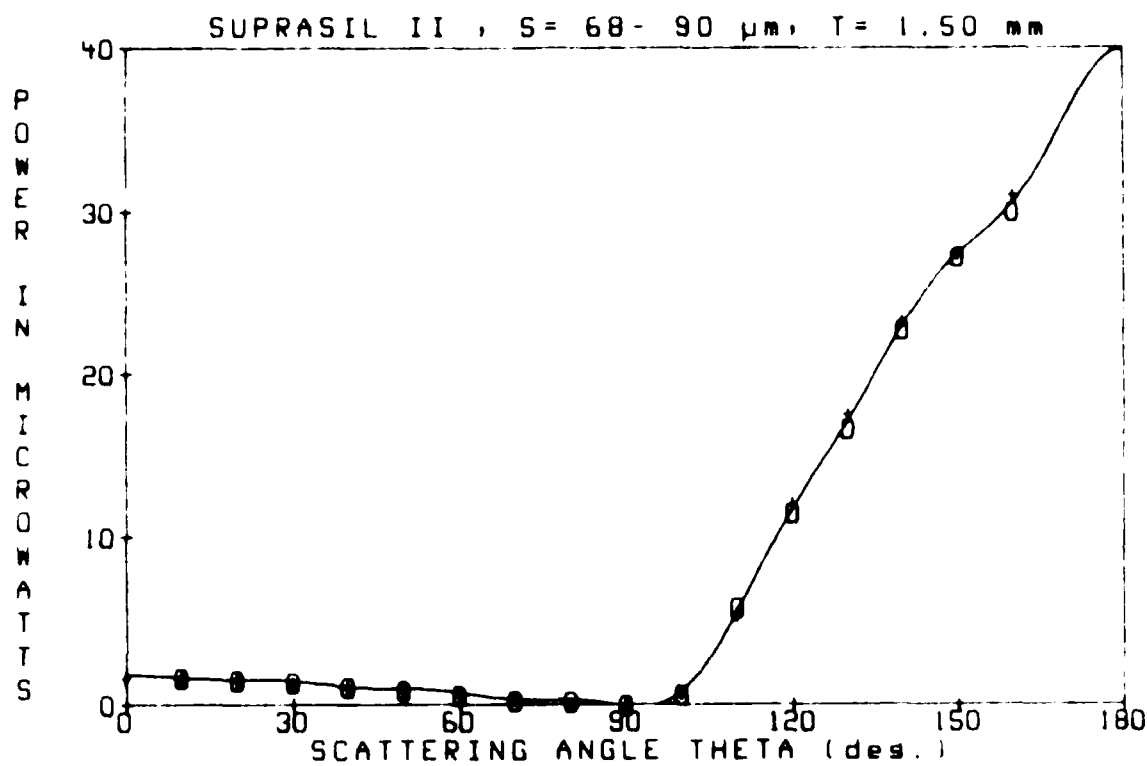
SUPRASIL II S- 68- 90 μ m T= 1.00 mm

SCATTERING ANGLE	DIODE VOLTAGE	POWER (microwatts)
-160	4.52	27.59
-150	4.07	24.85
-140	3.29	20.05
-130	2.43	14.84
-120	1.58	9.62
-110	0.71	4.31
-100	0.06	0.38
-90	0.00	0.00
-80	0.03	0.13
-70	0.06	0.38
-60	0.11	0.65
-50	0.17	1.01
-40	0.21	1.23
-30	0.24	1.46
-20	0.27	1.67
-10	0.30	1.84
0	0.29	1.79
10	0.31	1.87
20	0.28	1.70
30	0.24	1.49
40	0.20	1.22
50	0.16	0.98
60	0.12	0.71
70	0.07	0.45
80	0.02	0.15
90	0.00	0.00
100	0.14	0.86
110	0.85	5.21
120	1.99	12.16
130	2.88	17.56
140	3.63	22.17
150	4.20	25.60
160	4.82	29.41



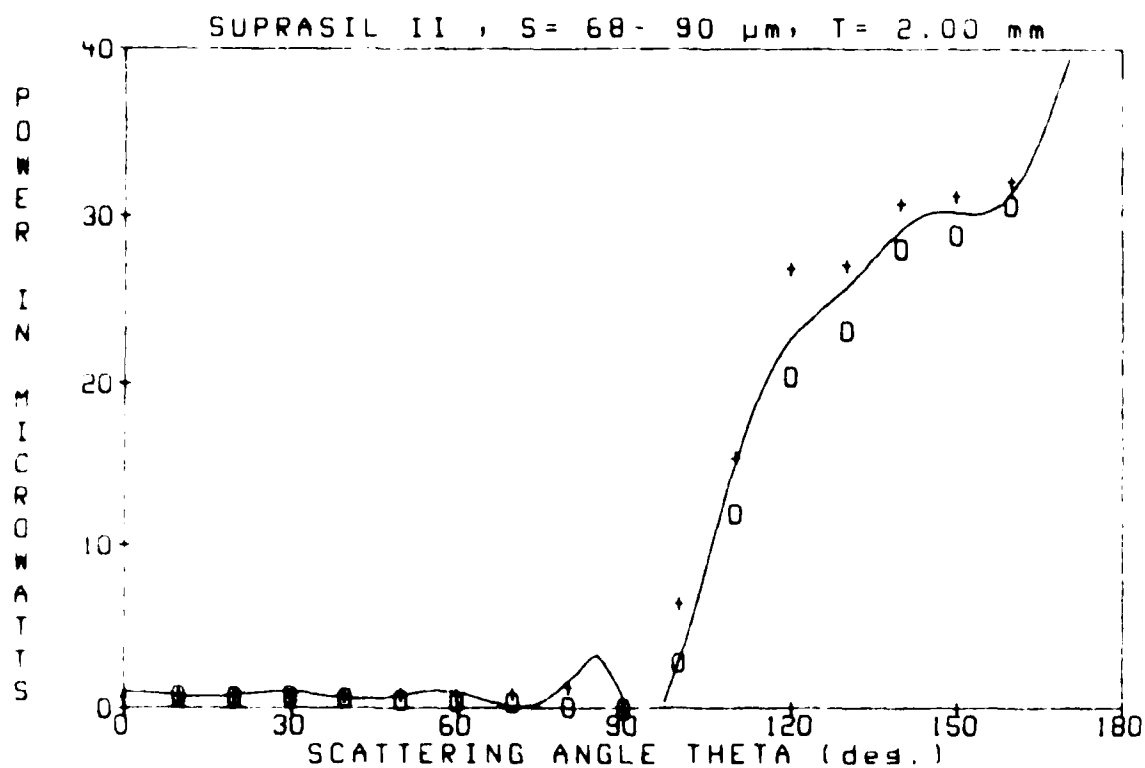
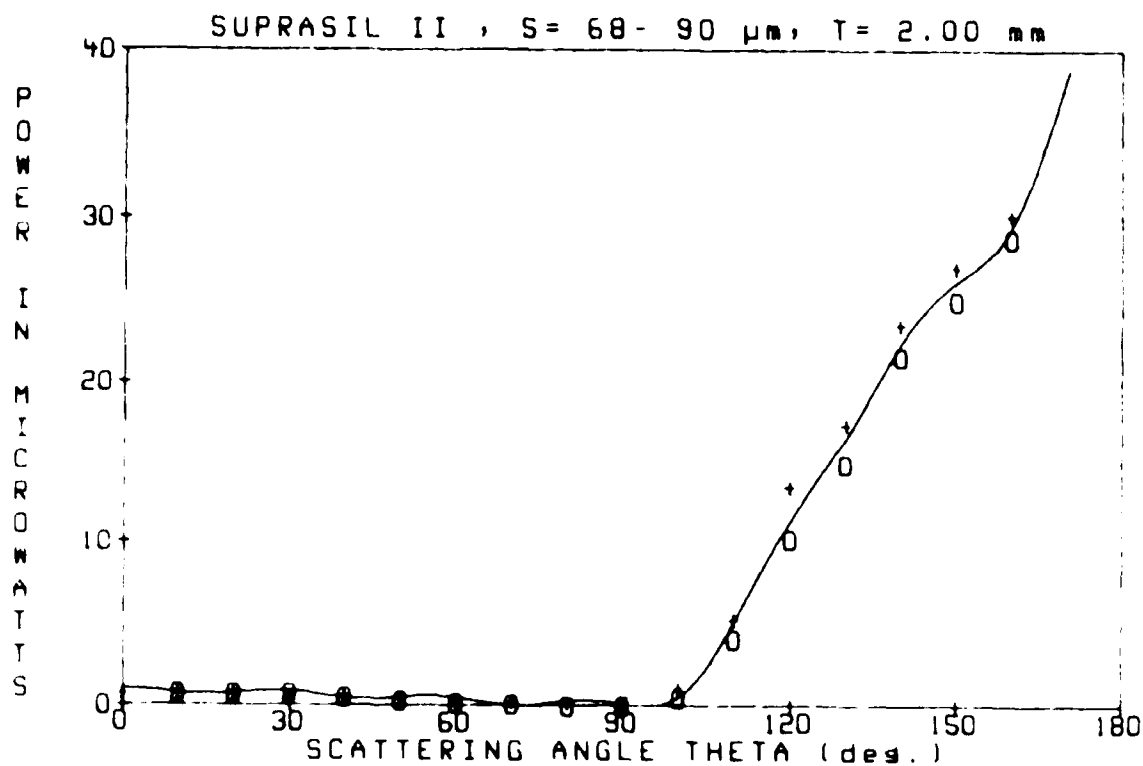
SUPRASIL II S = 68- 90 μ m T = 1.50 mm

SCATTERING ANGLE	DIODE VOLTAGE	POWER (microwatts)
-160	4.92	30.04
-150	4.47	27.26
-140	3.72	22.70
-130	2.72	16.62
-120	1.89	11.50
-110	0.94	5.75
-100	0.11	0.66
-90	0.00	0.00
-80	0.03	0.21
-70	0.05	0.32
-60	0.10	0.62
-50	0.15	0.89
-40	0.18	1.10
-30	0.22	1.37
-20	0.24	1.49
-10	0.26	1.60
0	0.27	1.67
10	0.27	1.63
20	0.24	1.49
30	0.21	1.31
40	0.18	1.10
50	0.15	0.92
60	0.11	0.68
70	0.08	0.48
80	0.02	0.12
90	0.00	0.00
100	0.14	0.83
110	0.89	5.45
120	1.97	12.04
130	2.88	17.58
140	3.82	23.27
150	4.51	27.53
160	5.09	31.08



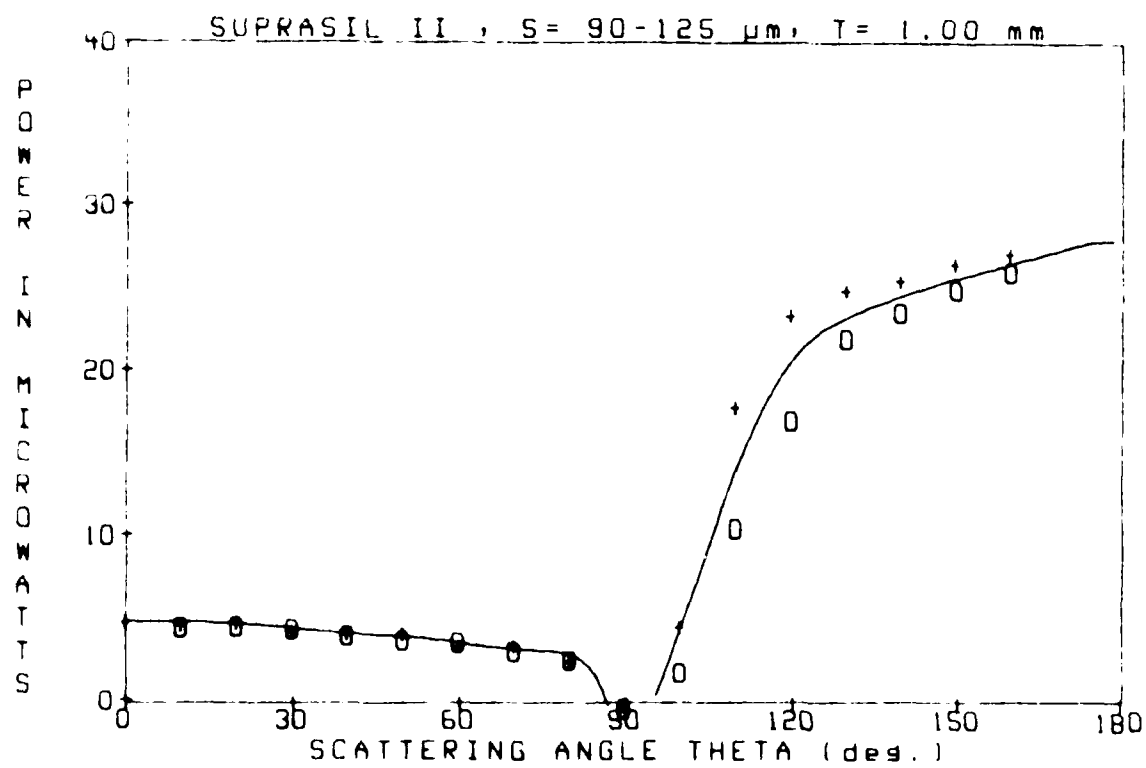
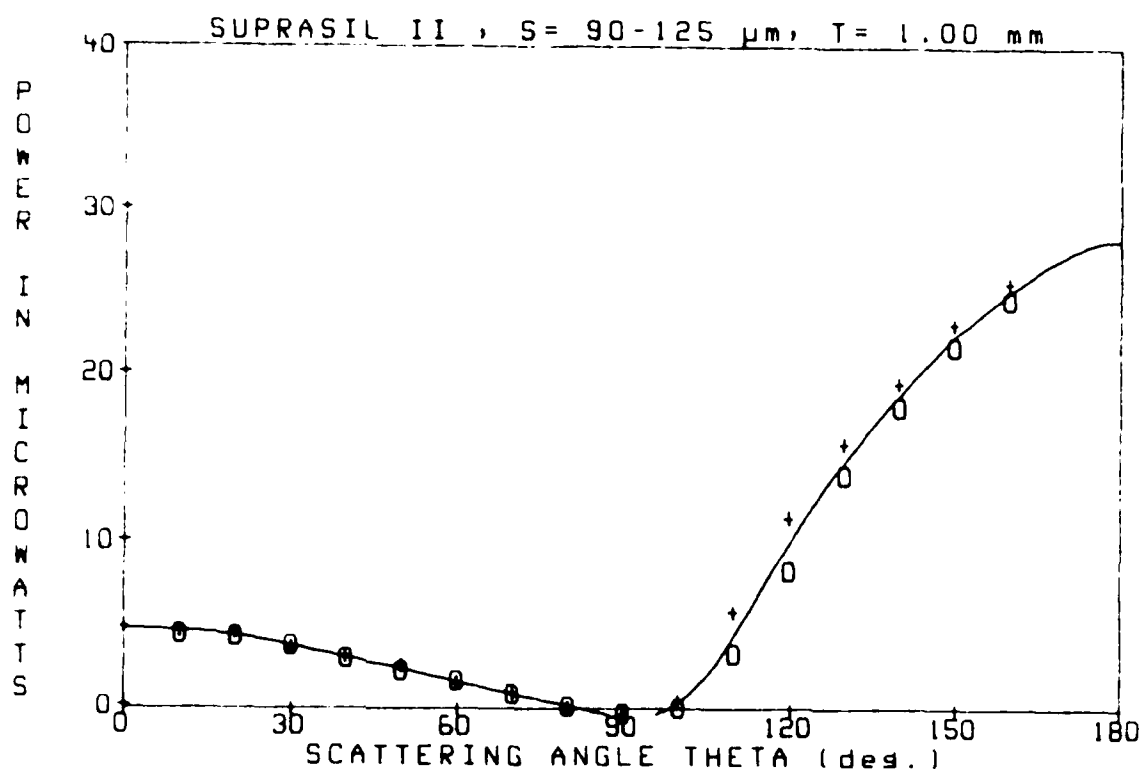
SUPRASIL II S= 68- 90 um T= 2.00 mm

SCATTERING ANGLE	DIODE VOLTAGE	POWER (microwatts)
-160	4.23	28.84
-150	4.11	25.69
-140	3.54	21.80
-130	2.45	14.93
-120	1.58	10.25
-110	0.87	4.11
-100	0.68	0.51
-90	0.00	0.00
-80	0.00	0.00
-70	0.02	0.15
-60	0.04	0.27
-50	0.05	0.38
-40	0.09	0.56
-30	0.12	0.74
-20	0.12	0.74
-10	0.13	0.80
0	0.13	0.80
10	0.14	0.87
20	0.13	0.80
30	0.11	0.65
40	0.11	0.65
50	0.09	0.56
60	0.07	0.45
70	0.05	0.32
80	0.04	0.24
90	0.00	0.00
100	0.17	1.13
110	0.87	5.30
120	2.21	13.47
130	2.86	17.46
140	3.8	23.60
150	4.44	27.08
160	4.95	30.21



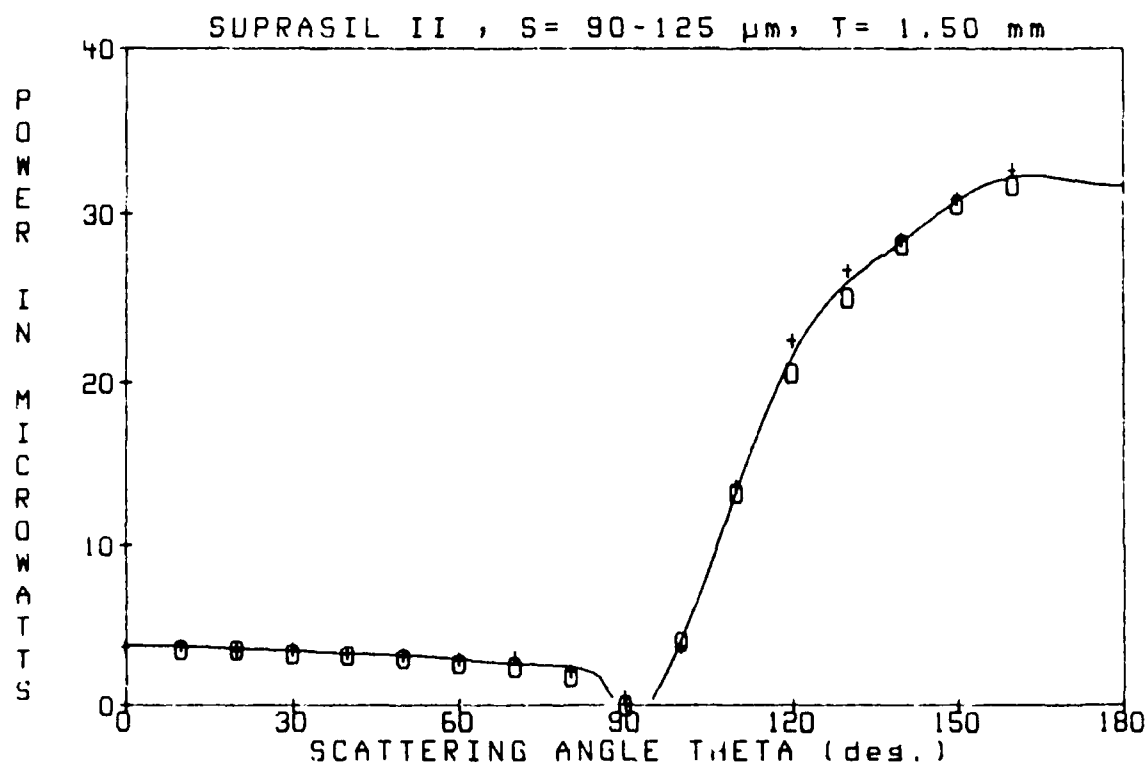
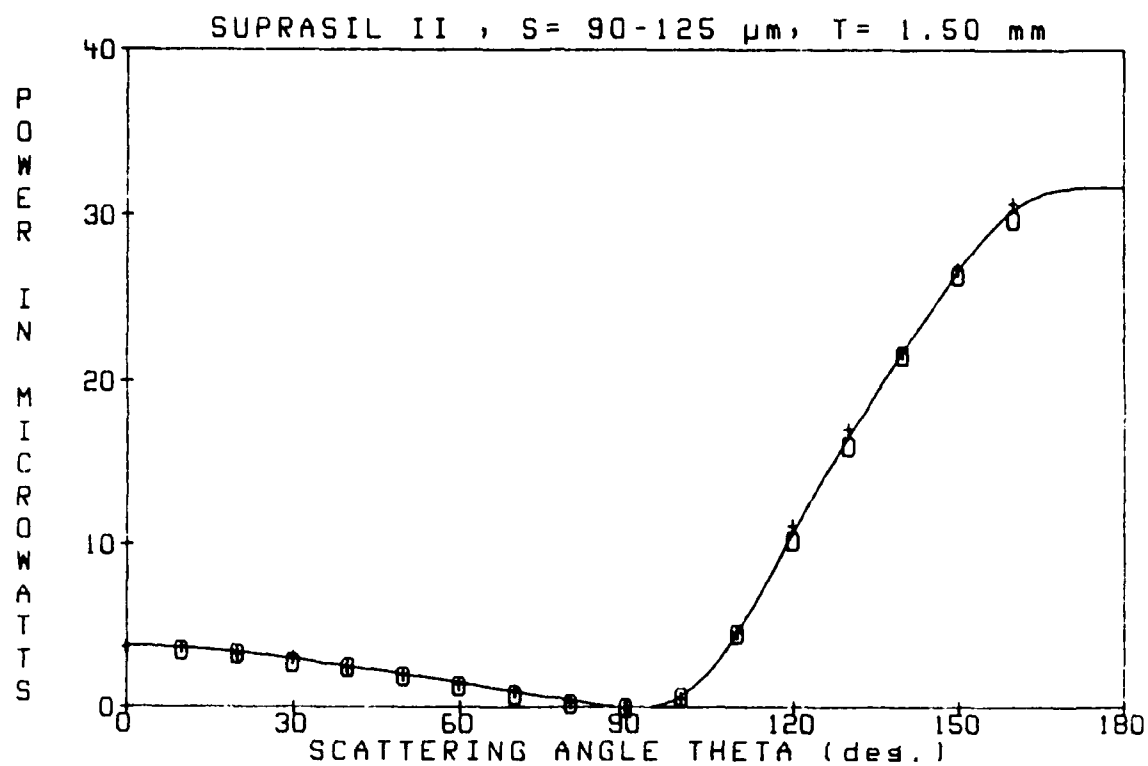
SUPRASIL 11 S- 90-125 μ m T- 1.00 mm

SCATTERING ANGLE	DIODE VOLTAGE	POWER (microwatts)
-150	4.07	24.85
-150	3.60	21.96
-140	3.01	18.35
-130	2.36	14.39
-120	1.43	8.73
-110	0.61	3.72
-100	0.06	0.38
-90	0.00	0.00
-80	0.09	0.53
-70	0.20	1.22
-60	0.34	2.06
-50	0.44	2.71
-40	0.56	3.42
-30	0.70	4.26
-20	0.78	4.73
-10	0.81	4.92
0	0.87	5.33
10	0.84	5.09
20	0.82	5.00
30	0.68	4.14
40	0.59	3.57
50	0.49	3.01
60	0.32	1.96
70	0.22	1.37
80	0.09	0.53
90	0.00	0.00
100	0.15	0.89
110	1.03	6.26
120	1.96	11.94
130	2.68	16.35
140	3.22	19.93
150	3.84	23.42
150	4.26	26.01



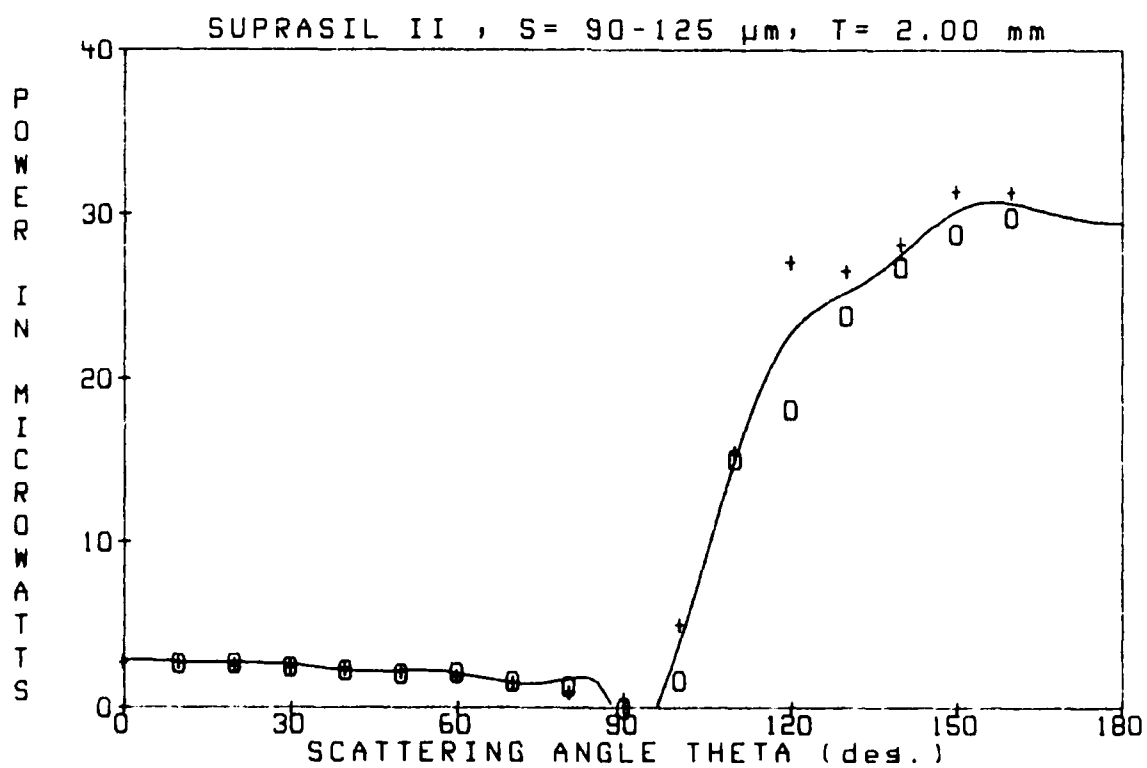
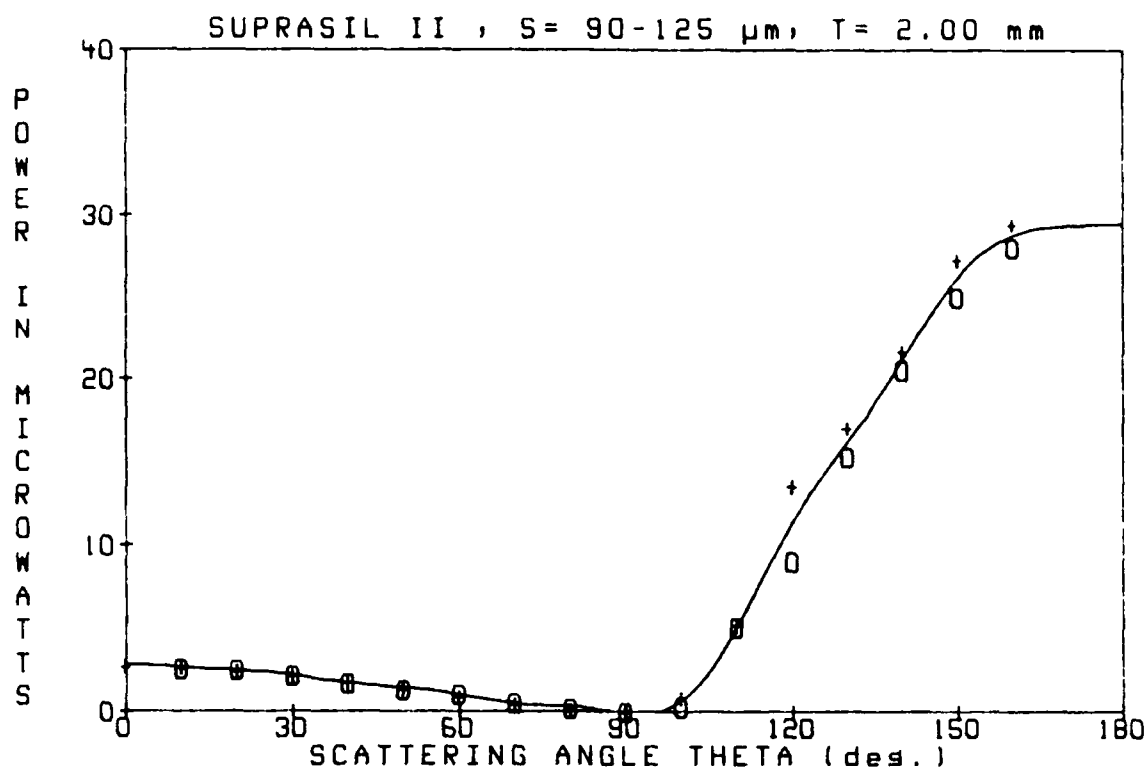
SUPRASIL II S= 90-125 μ m T= 1.50 mm

SCATTERING ANGLE	DIODE VOLTAGE	POWER (microwatts)
-160	4.89	29.85
-150	4.35	26.52
-140	3.55	21.66
-130	2.65	16.15
-120	1.69	10.31
-110	0.75	4.56
-100	0.12	0.71
-90	0.00	0.00
-80	0.05	0.32
-70	0.14	0.83
-60	0.22	1.37
-50	0.32	1.96
-40	0.40	2.47
-30	0.46	2.83
-20	0.55	3.37
-10	0.58	3.54
0	0.62	3.75
10	0.62	3.75
20	0.55	3.37
30	0.50	3.07
40	0.43	2.59
50	0.34	2.08
60	0.24	1.49
70	0.17	1.07
80	0.06	0.38
90	0.00	0.00
100	0.11	0.65
110	0.77	4.70
120	1.85	11.29
130	2.82	17.22
140	3.59	21.90
150	4.41	26.88
160	5.05	30.81



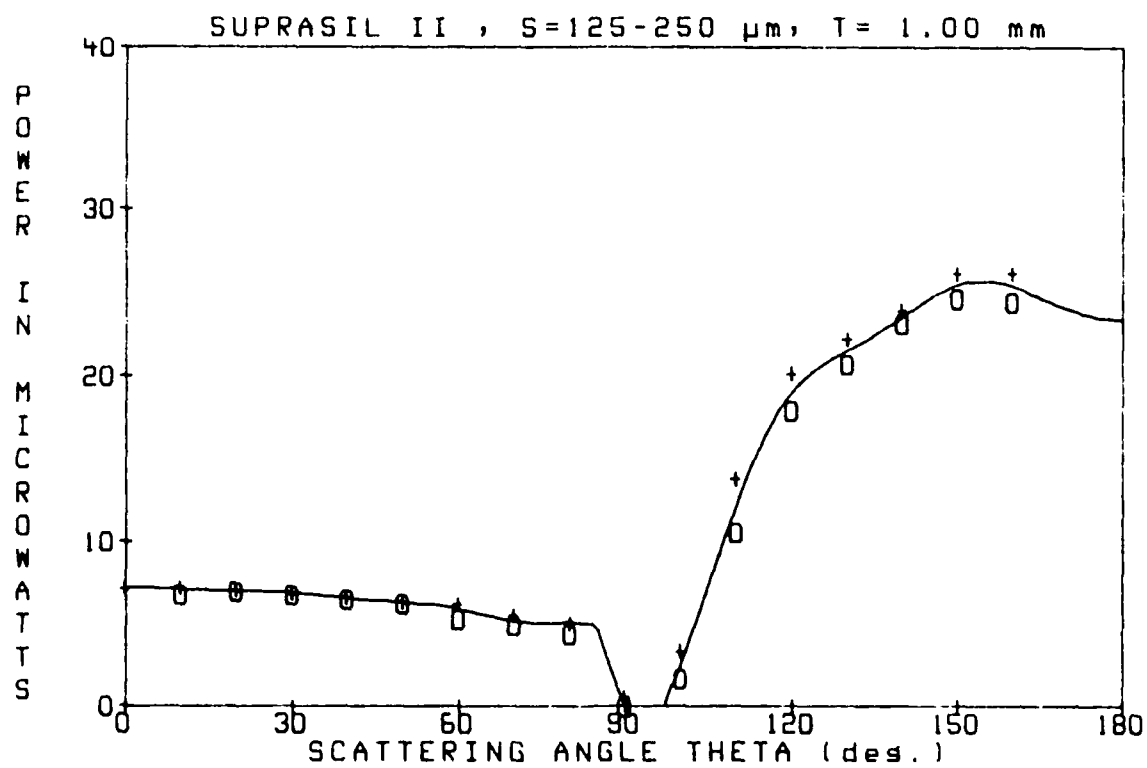
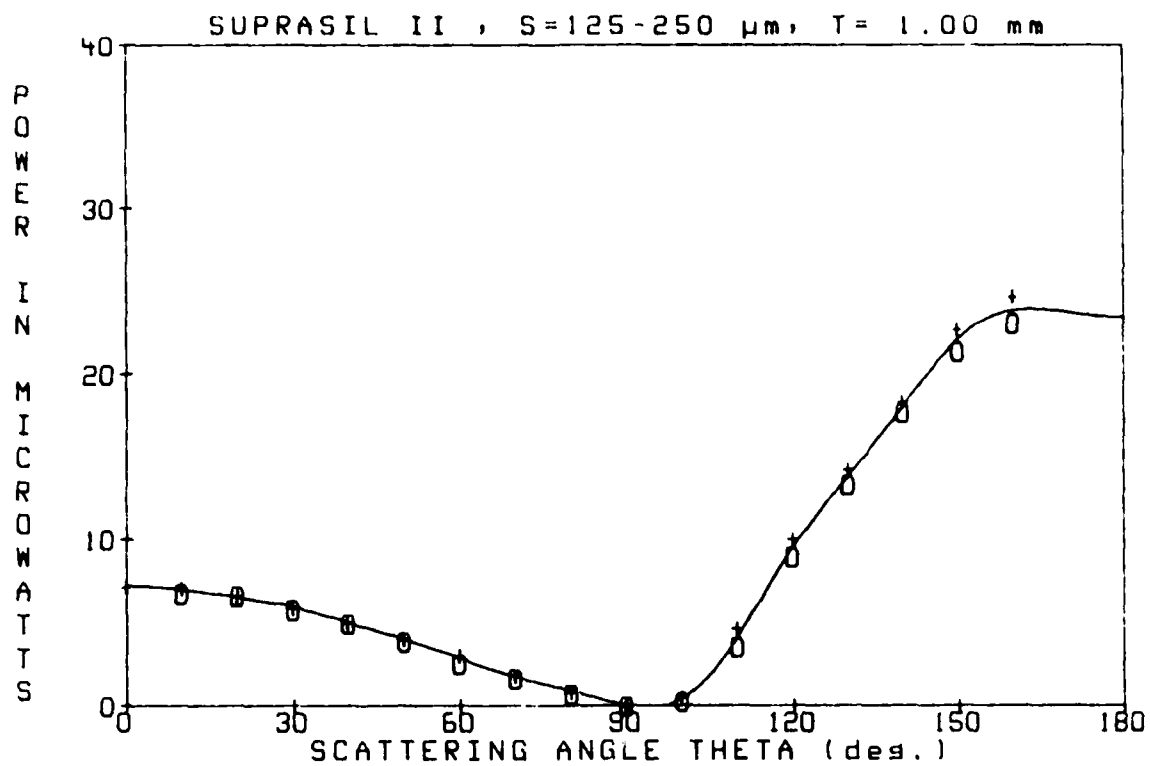
SUPRASIL II S= 90-125 μ m T= 2.00 mm

SCATTERING ANGLE		DIODE VOLTAGE		POWER (microwatts)
-160		4.60		28.07
-150		4.10		25.03
-140		3.37		20.56
-130		2.52		15.37
-120		1.49		9.08
-110		0.85		5.15
-100		0.05		0.29
-90		0.00		0.00
-80		0.04		0.24
-70		0.09		0.56
-60		0.17		1.07
-50		0.22		1.37
-40		0.29		1.76
-30		0.37		2.23
-20		0.43		2.62
-10		0.44		2.71
0		0.46		2.83
10		0.45		2.77
20		0.41		2.50
30		0.36		2.20
40		0.30		1.84
50		0.23		1.43
60		0.16		0.98
70		0.09		0.53
80		0.03		0.18
90		0.00		0.00
100		0.15		0.89
110		0.87		5.33
120		2.23		13.58
130		2.81		17.13
140		3.56		21.69
150		4.47		27.29
160		4.84		29.53



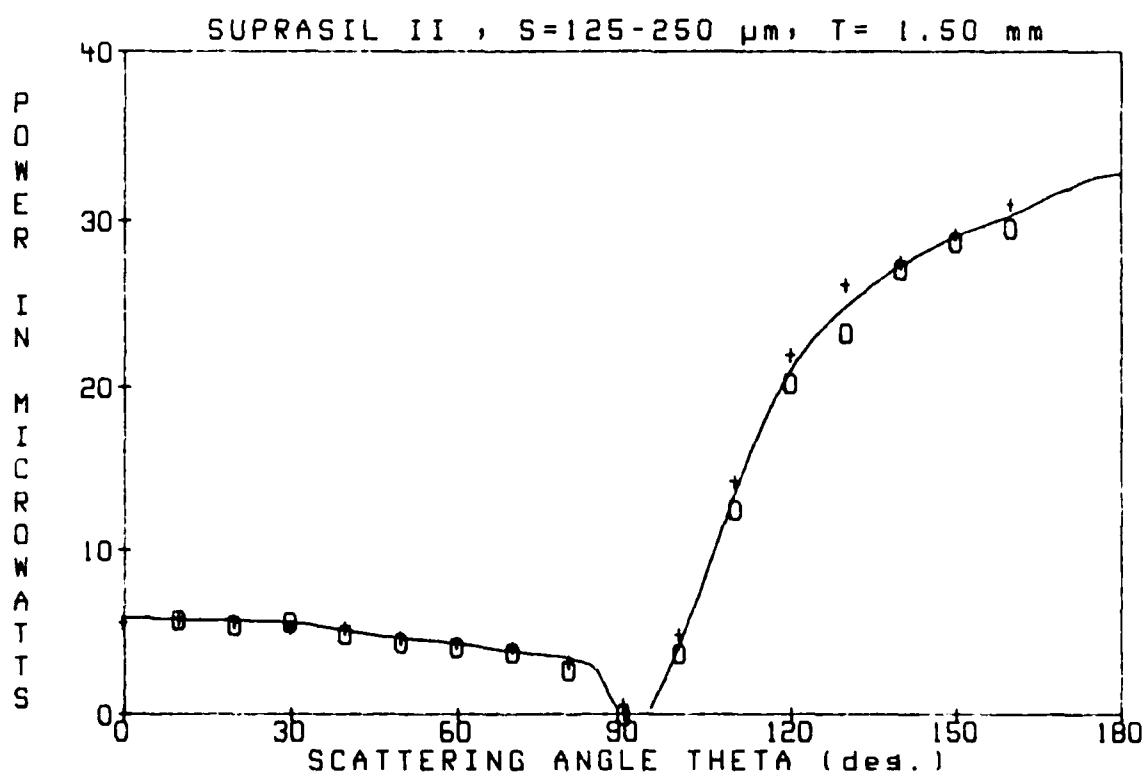
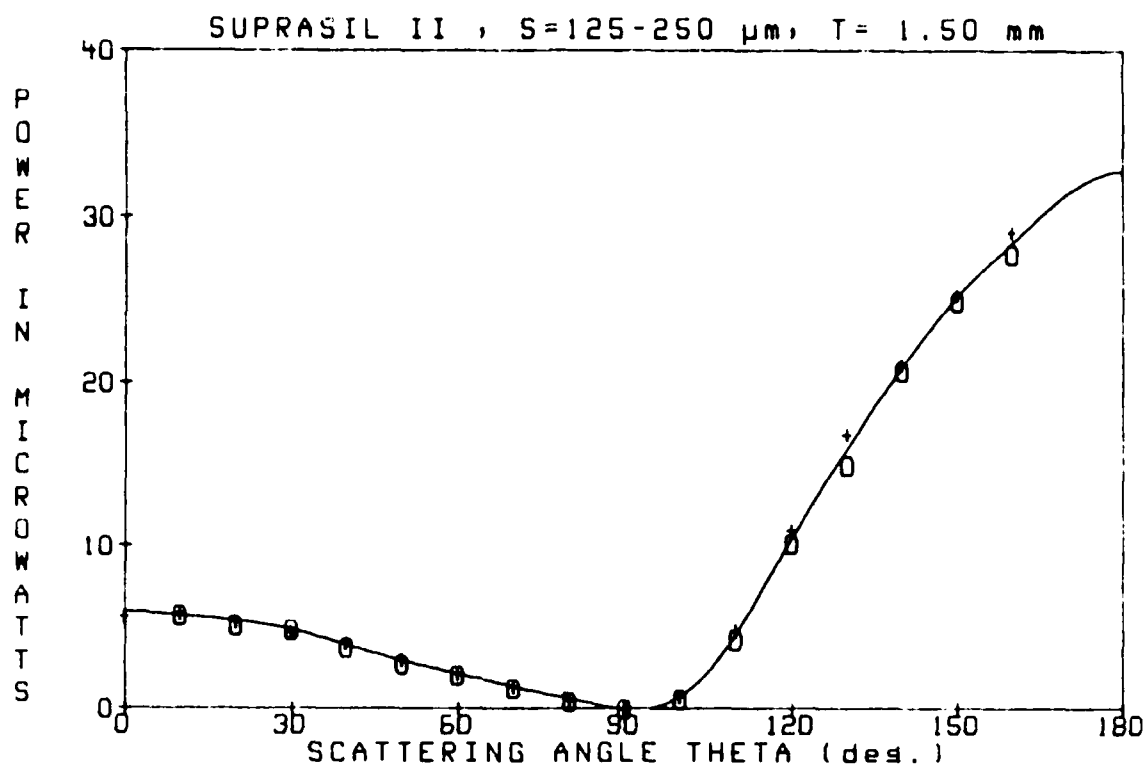
SUPRASIL II S=125-250 μ m T= 1.00 mm

SCATTERING ANGLE	DIODE VOLTAGE	POWER (microwatts)
-160	3.77	23.00
-150	3.51	21.39
-140	2.91	17.73
-130	2.19	13.35
-120	1.47	8.97
-110	0.60	3.63
-100	0.05	0.29
-90	0.00	0.00
-80	0.13	0.77
-70	0.28	1.70
-60	0.43	2.65
-50	0.65	3.99
-40	0.82	5.00
-30	0.96	5.84
-20	1.08	6.61
-10	1.10	6.73
0	1.19	7.27
10	1.17	7.12
20	1.09	6.64
30	0.98	5.98
40	0.84	5.09
50	0.67	4.11
60	0.51	3.12
70	0.31	1.90
80	0.15	0.89
90	0.00	0.00
100	0.10	0.59
110	0.78	4.76
120	1.66	10.13
130	2.35	14.33
140	3.01	18.39
150	3.72	22.70
160	4.04	24.67



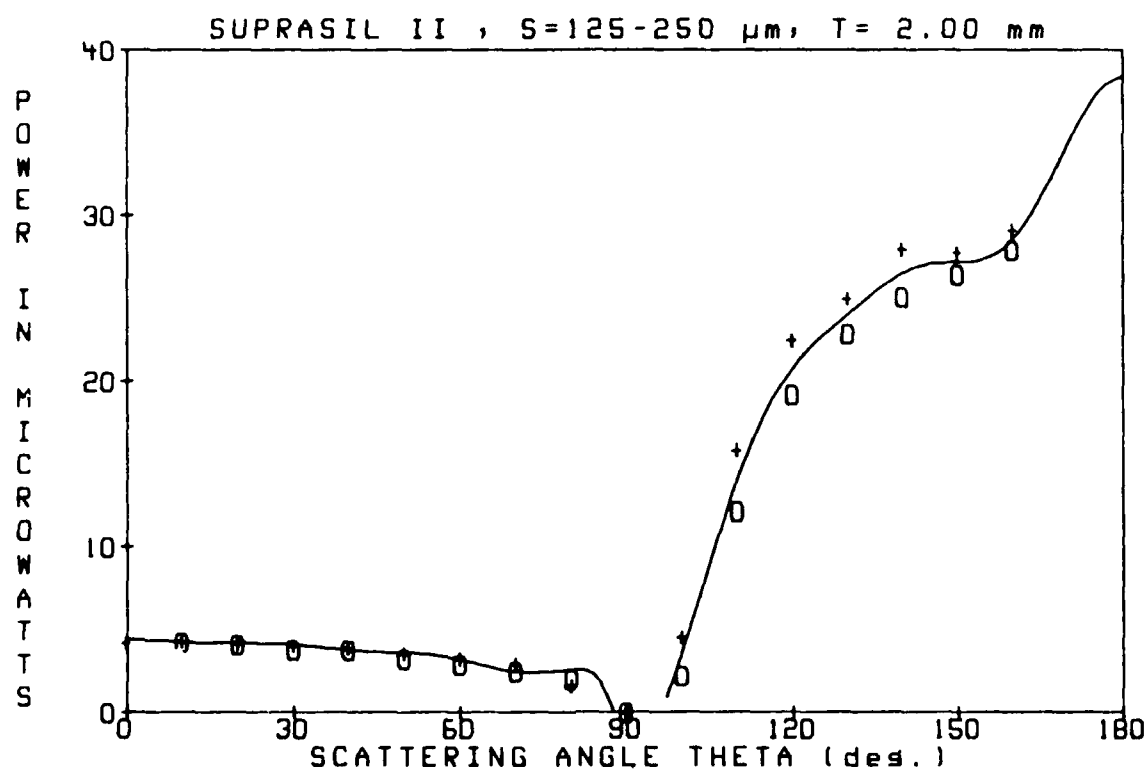
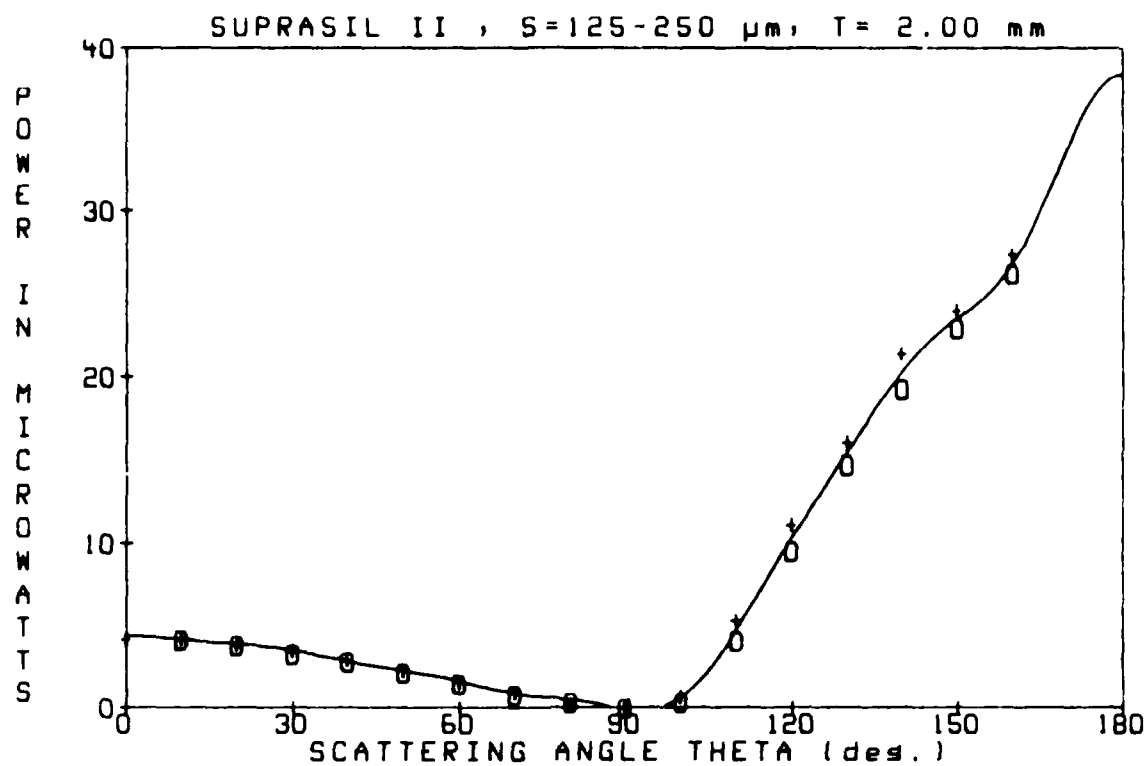
SUPRASIL II S=125-250 μ m T= 1.50 mm

SCATTERING ANGLE		DIODE VOLTAGE		POWER (microwatts)
-160		4.56		27.83
-150		4.09		24.97
-140		3.41		20.79
-130		2.46		14.99
-120		1.67		10.16
-110		0.70		4.29
-100		0.11		0.65
-90		0.00		0.00
-80		0.08		0.48
-70		0.21		1.31
-60		0.34		2.08
-50		0.46		2.83
-40		0.63		3.81
-30		0.81		4.92
-20		0.85		5.19
-10		0.94		5.75
0		0.94		5.72
10		0.96		5.87
20		0.89		5.42
30		0.78		4.73
40		0.67		4.11
50		0.50		3.07
60		0.36		2.20
70		0.23		1.43
80		0.09		0.56
90		0.00		0.00
100		0.14		0.86
110		0.80		4.89
120		1.81		11.02
130		2.77		16.89
140		3.47		21.19
150		4.16		25.39
160		4.79		29.20



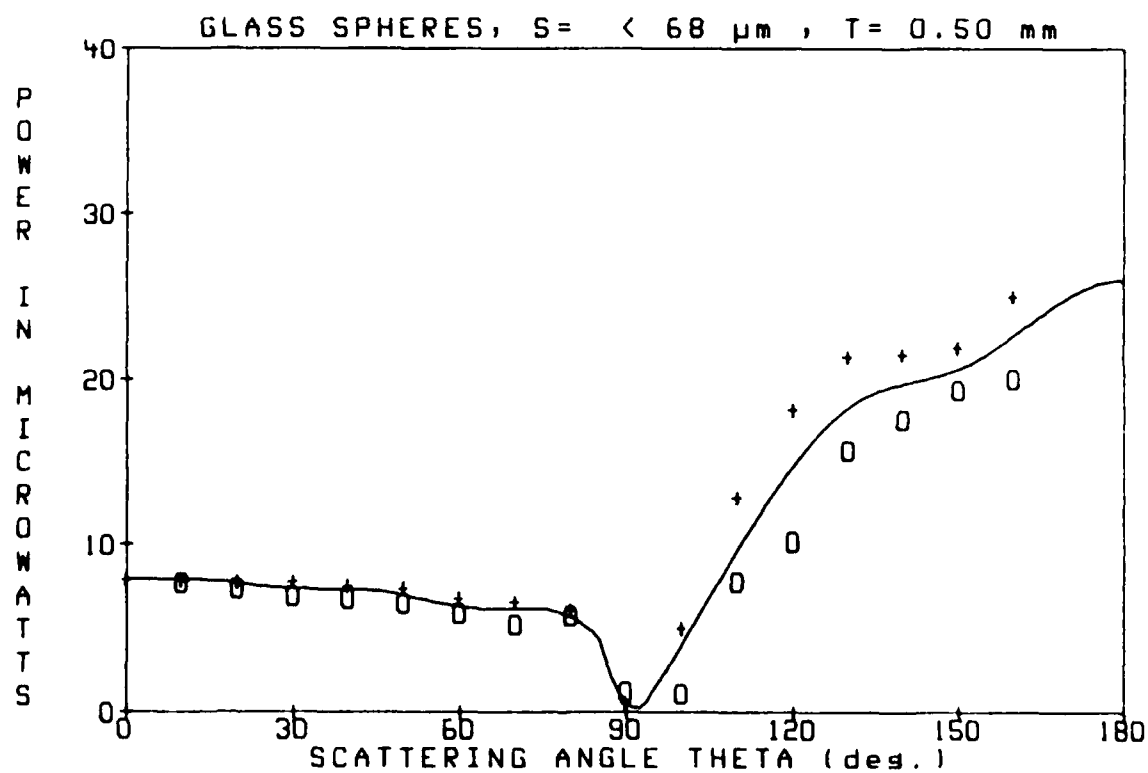
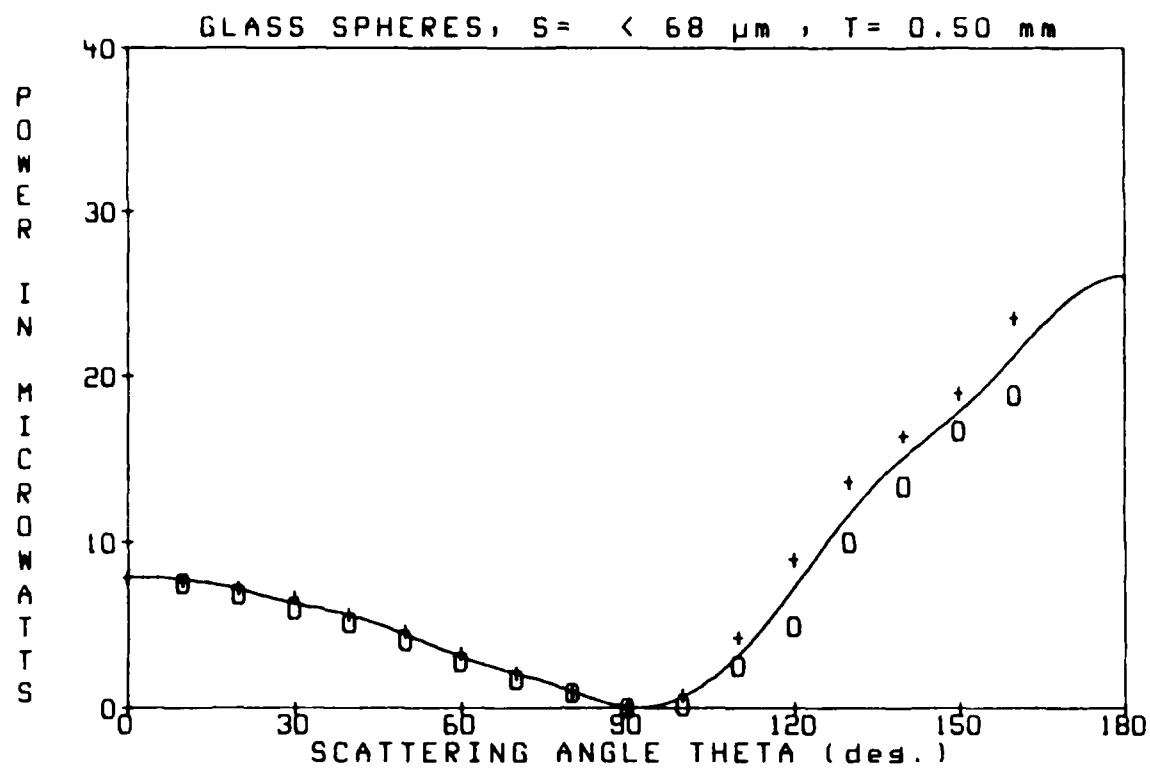
SUPRASIL II S-125-250 μm $t = 2.00 \text{ mm}$

SCATTERING ANGLE	DIODE VOLTAGE	POWER (microwatts)
-160	4.30	26.22
-150	3.75	22.88
-140	3.15	19.22
-130	2.41	14.69
-120	1.57	9.60
-110	0.68	4.17
-100	0.06	0.38
-90	0.00	0.00
-80	0.06	0.35
-70	0.14	0.86
-60	0.24	1.49
-50	0.35	2.14
-40	0.48	2.92
-30	0.55	3.34
-20	0.64	3.90
-10	0.69	4.23
0	0.70	4.29
10	0.70	4.29
20	0.65	3.96
30	0.59	3.57
40	0.50	3.04
50	0.39	2.35
60	0.27	1.67
70	0.17	1.01
80	0.05	0.29
90	0.00	0.00
100	0.13	0.80
110	0.89	5.45
120	1.85	11.26
130	2.64	16.09
140	3.51	21.42
150	3.94	24.05
160	4.49	27.41



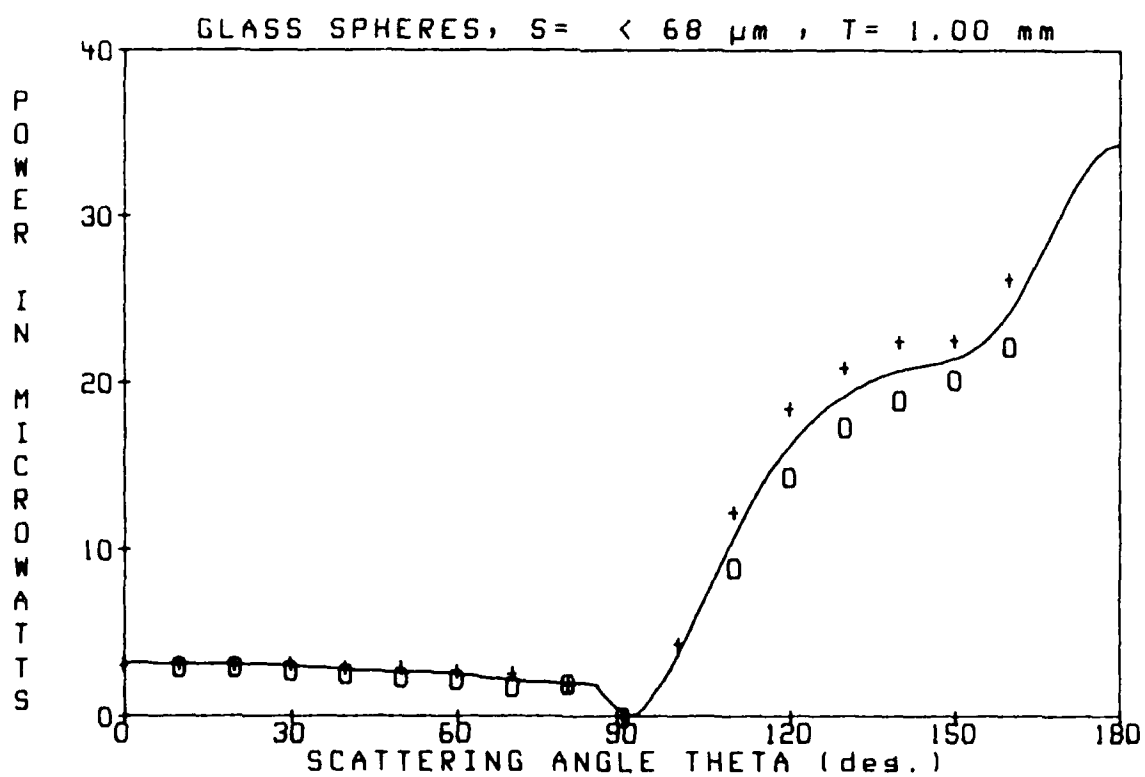
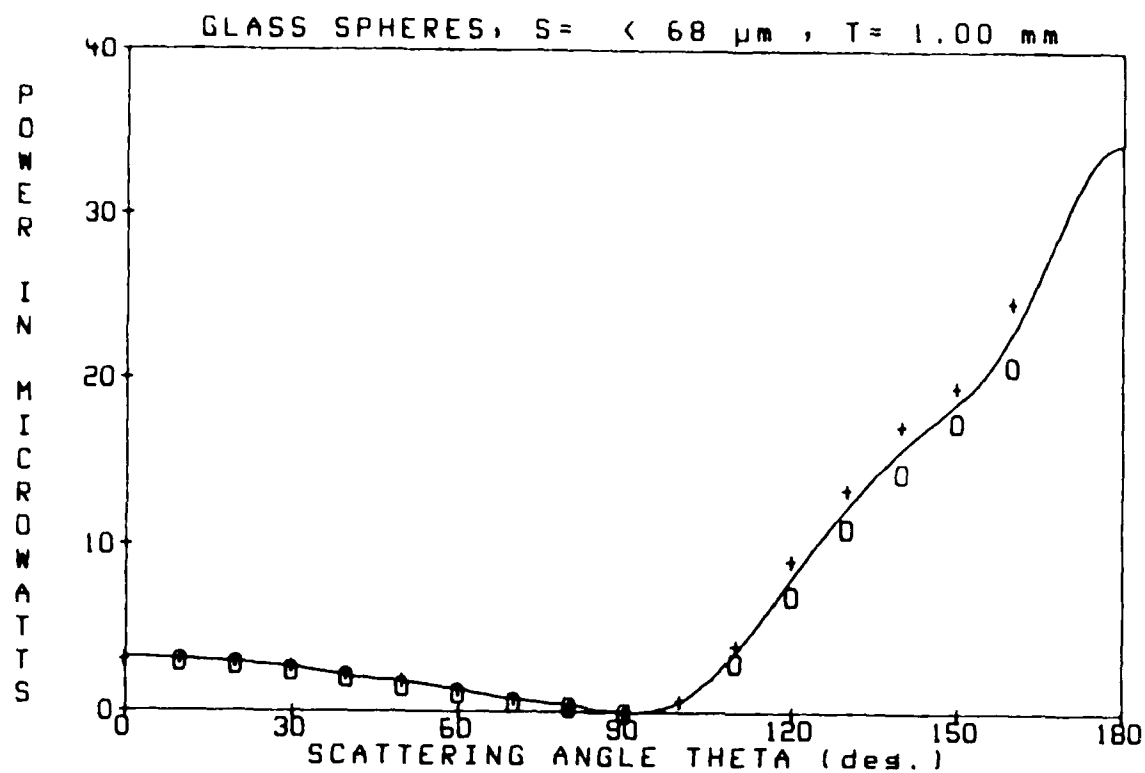
GLASS SPHERES S- 0.68 μ m T- 0.50 mm

SCATTERING ANGLE	DIODE VOLTAGE	POWER (microwatts)
-150	3.10	18.87
-150	2.74	16.74
-140	2.22	13.52
-130	1.66	10.13
-120	0.84	5.12
-110	0.44	2.71
-100	0.03	0.21
-90	0.02	0.12
-80	0.17	1.01
-70	0.30	1.81
-60	0.49	2.98
-50	0.69	4.23
-40	0.86	5.27
-30	1.00	6.11
-20	1.16	7.06
-10	1.27	7.72
0	1.32	8.05
10	1.28	7.83
20	1.21	7.39
30	1.12	6.85
40	0.96	5.84
50	0.79	4.83
60	0.57	3.45
70	0.37	2.26
80	0.17	1.07
90	0.00	0.00
100	0.15	0.89
110	0.72	4.41
120	1.49	9.11
130	2.26	13.79
140	2.71	16.51
150	3.12	19.04
160	3.86	23.57



GLASS SPHERES S- 0.68 μ m T- 1.00 mm

SCATTERING ANGLE	DIODE VOLTAGE	POWER (microwatts)
-160	3.43	20.92
-150	2.87	17.52
-140	2.38	14.51
-130	1.83	11.14
-120	1.18	7.18
-110	0.50	3.07
-100		
-90	0.00	0.00
-80	0.06	0.35
-70	0.10	0.62
-60	0.19	1.16
-50	0.25	1.55
-40	0.34	2.08
-30	0.42	2.53
-20	0.47	2.89
-10	0.50	3.07
0	0.53	3.21
10	0.54	3.28
20	0.50	3.07
30	0.46	2.83
40	0.39	2.35
50	0.32	1.96
60	0.23	1.43
70	0.15	0.92
80	0.06	0.35
90	0.00	0.00
100	0.13	0.77
110	0.69	4.20
120	1.51	9.24
130	2.21	13.47
140	2.84	17.31
150	3.21	19.61
160	4.06	24.79



GLASS SPHERES S = 68- 90 μ m T = 1.00 mm

SCATTERING ANGLE	DIODE VOLTAGE	POWER (microwatts)
-160	3.02	18.42
-150	2.57	15.67
-140	2.18	13.29
-130	1.62	9.89
-120	1.07	6.55
-110	0.56	3.39
-100	0.08	0.48
-90	0.00	0.00
-80	0.07	0.41
-70	0.15	0.92
-60	0.29	1.79
-50	0.42	2.56
-40	0.54	3.28
-30	0.65	3.99
-20	0.77	4.70
-10	0.83	5.06
0	0.86	5.27
10	0.85	5.21
20	0.82	5.00
30	0.75	4.59
40	0.64	3.93
50	0.51	3.12
60	0.38	2.32
70	0.25	1.52
80	0.10	0.62
90	0.00	0.00
100	0.11	0.68
110	0.66	4.02
120	1.39	8.46
130	2.00	12.21
140	2.48	15.13
150	2.89	17.64
160	3.63	22.17

AD-A182 229

THE INTERACTION OF SMALL PARTICLES WITH LASER BEAMS(U)

212

FLORIDA UNIV GAINESVILLE SPACE ASTRONOMY LAB

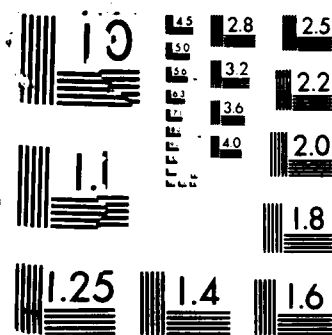
N Y MISCONI ET AL 18 FEB 87 AFOSR-TR-87-0664

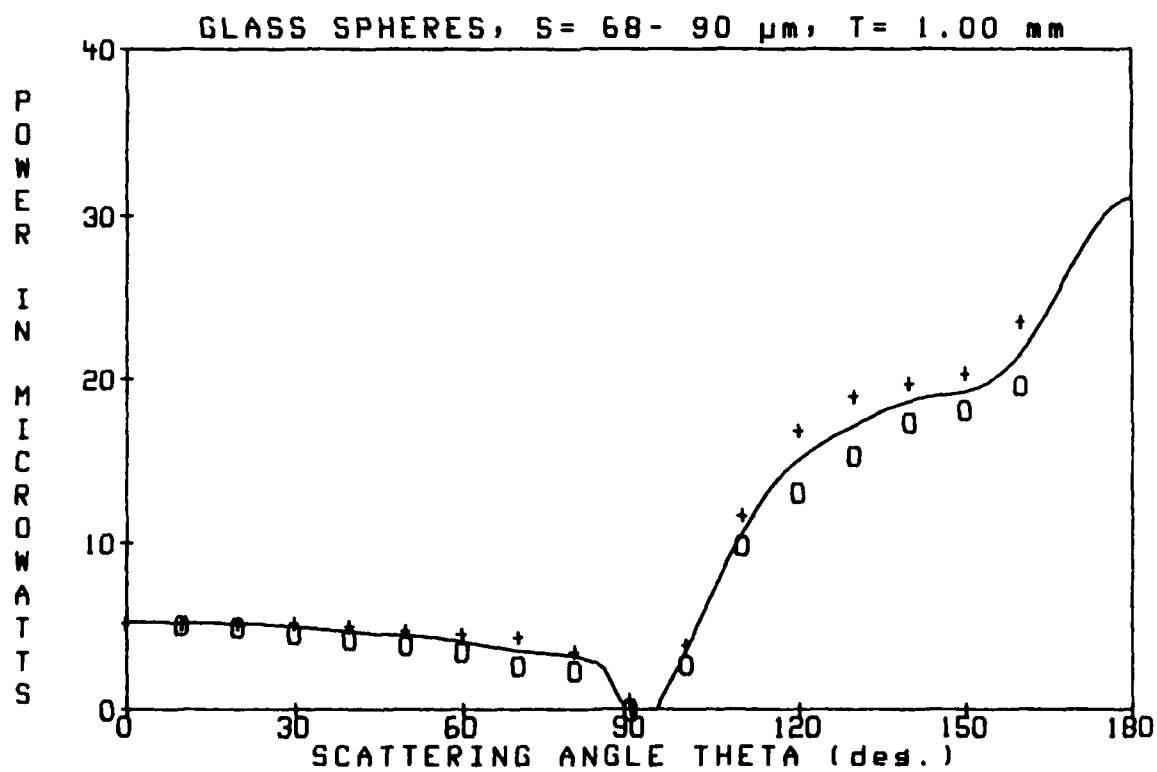
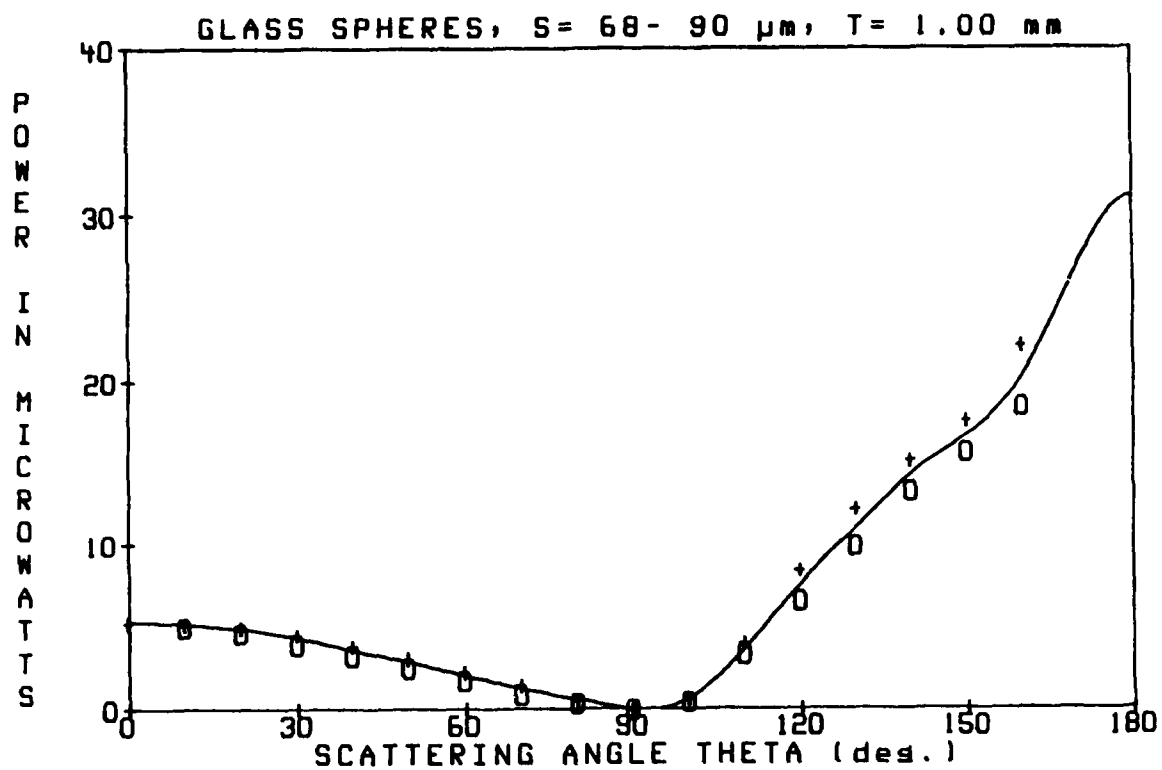
UNCLASSIFIED

F49620-85-C-0117

F/G 28/6

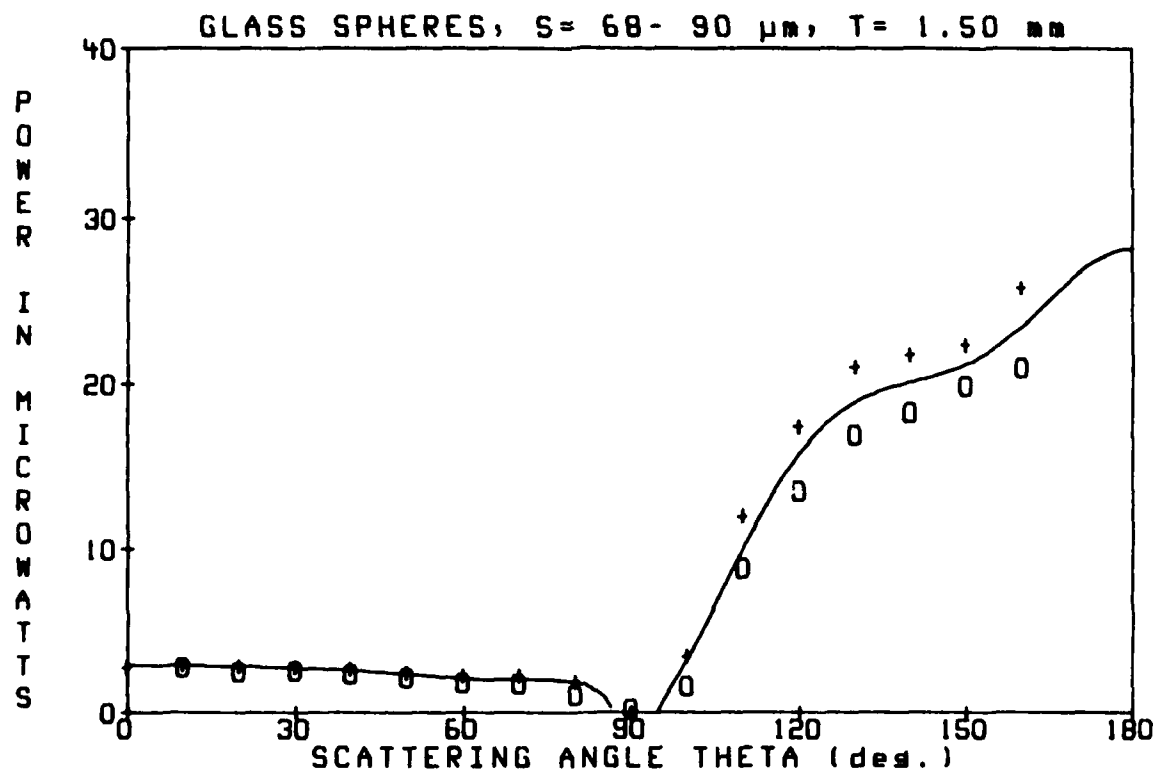
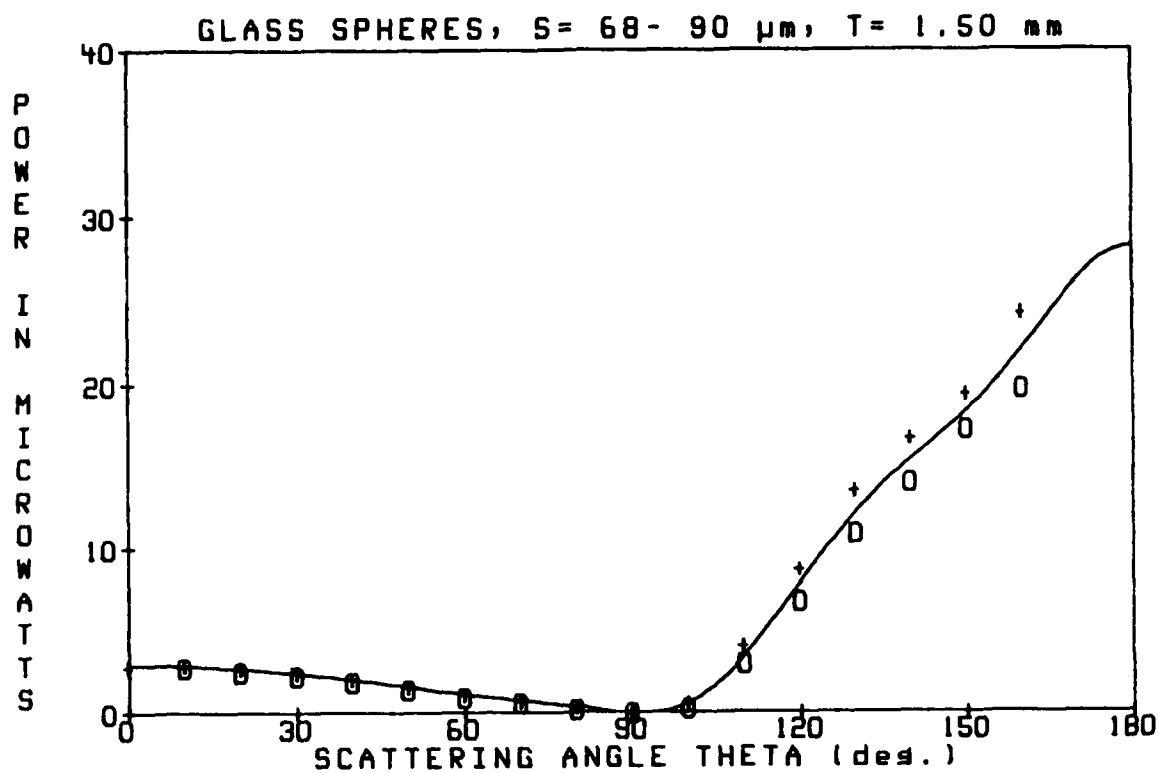
NL





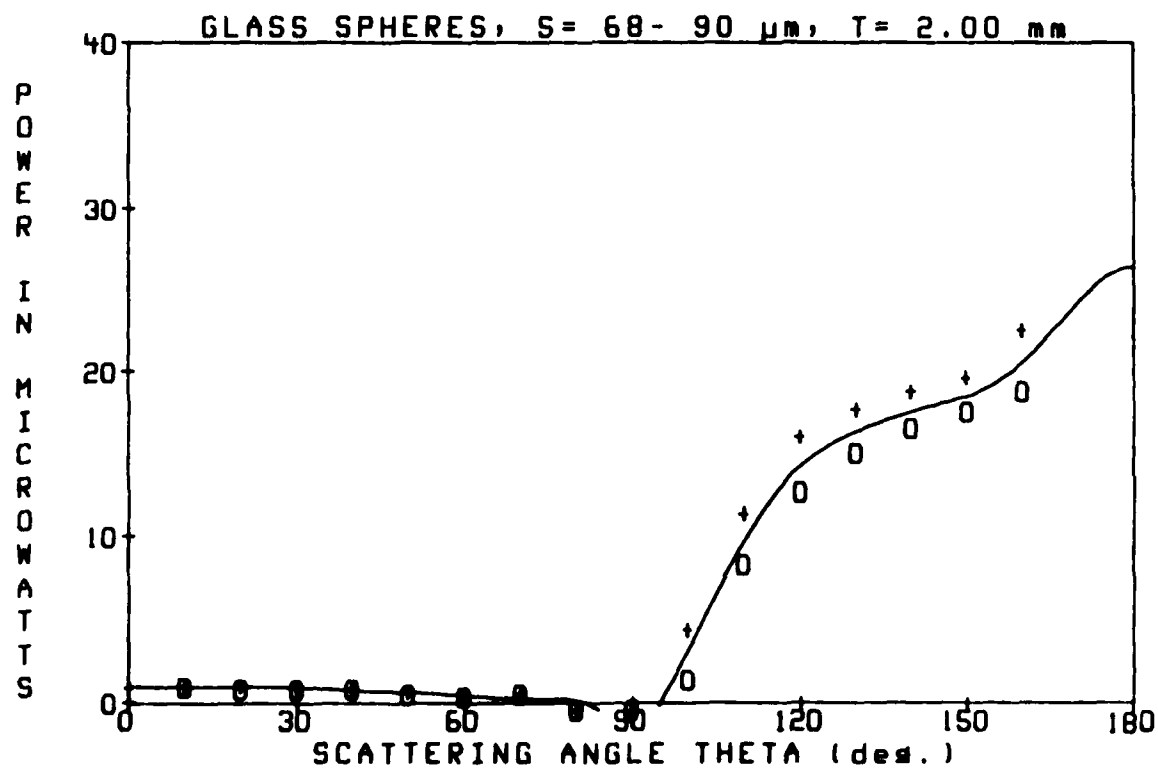
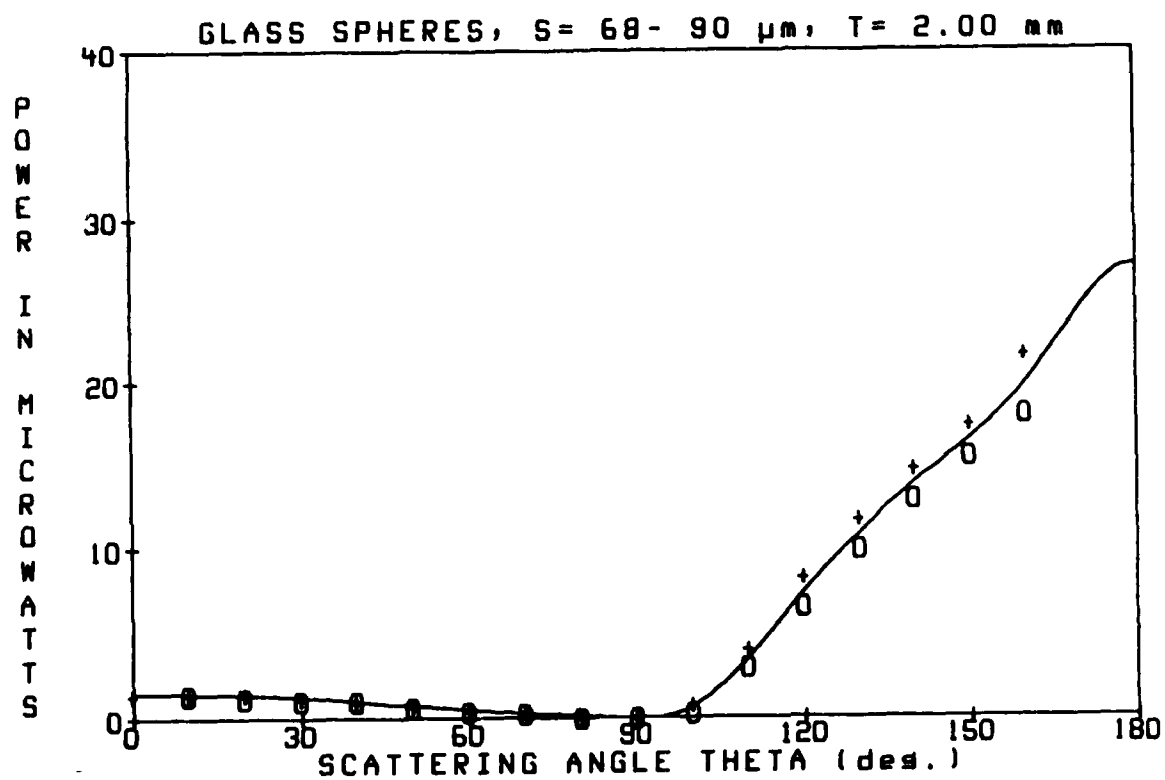
GLASS SPHERES S= 68- 90 μ m T= 1.50 mm

SCATTERING ANGLE	DIODE VOLTAGE	POWER (microwatts)
-160	3.24	19.75
-150	2.83	17.28
-140	2.30	14.01
-130	1.79	10.90
-120	1.11	6.79
-110	0.50	3.04
-100	0.05	0.29
-90	0.00	0.00
-80	0.03	0.21
-70	0.10	0.62
-60	0.16	0.95
-50	0.23	1.43
-40	0.31	1.87
-30	0.38	2.32
-20	0.41	2.50
-10	0.47	2.85
0	0.48	2.92
10	0.49	2.98
20	0.46	2.80
30	0.42	2.53
40	0.35	2.11
50	0.27	1.67
60	0.19	1.19
70	0.13	0.80
80	0.06	0.35
90	0.00	0.00
100	0.10	0.62
110	0.67	4.11
120	1.44	8.76
130	2.22	13.55
140	2.74	16.74
150	3.18	19.43
160	3.99	24.31



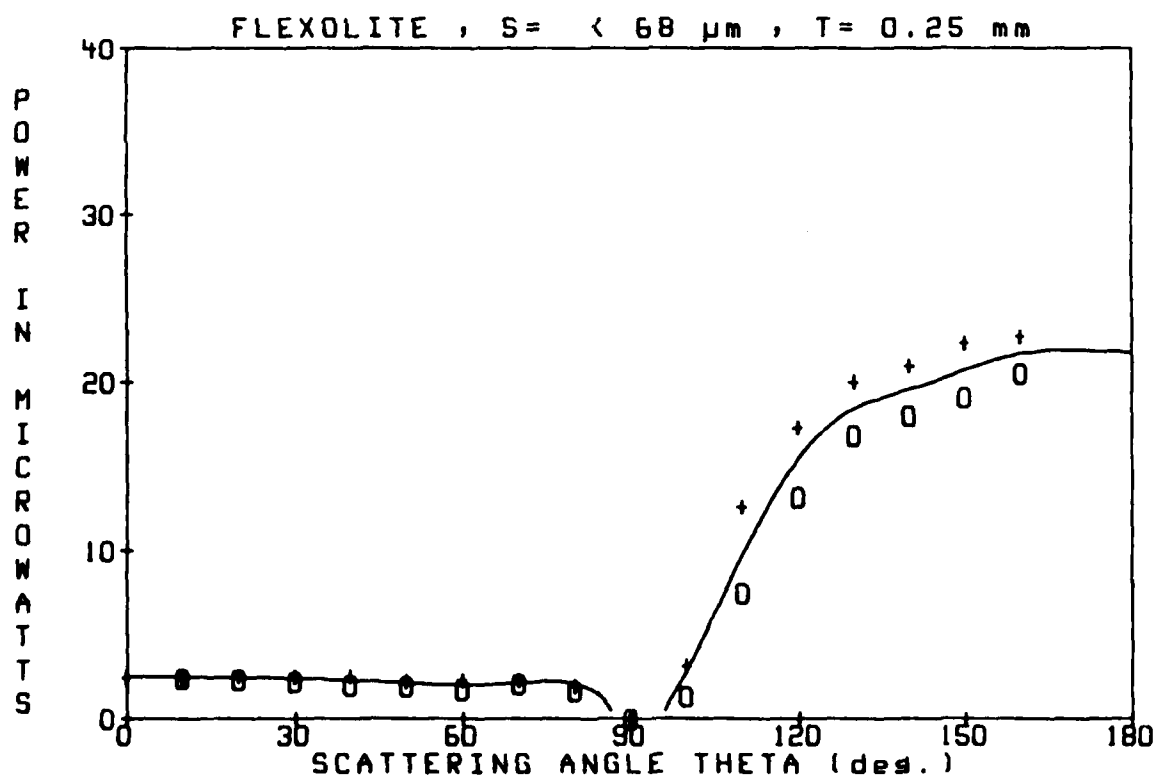
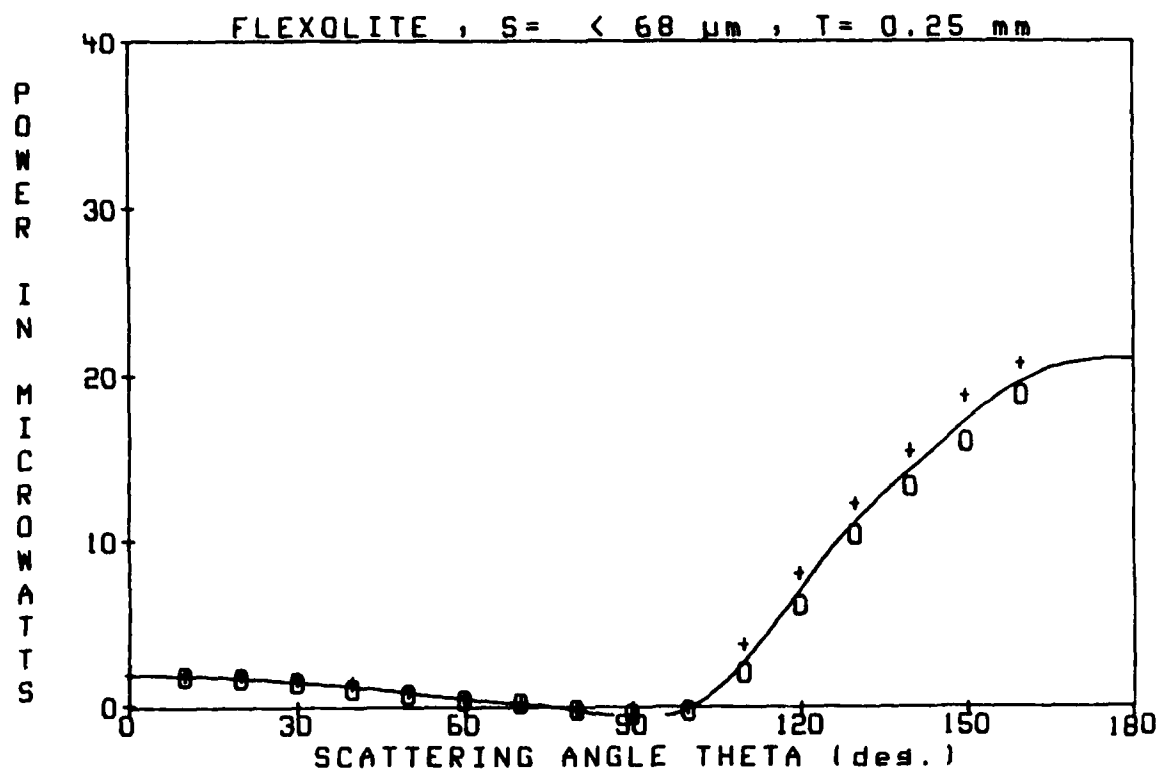
GLASS SPHERES S= 68- 90 μ m T= 2.00 mm

SCATTERING ANGLE		DIODE VOLTAGE		POWER (microwatts)
-160		2.96		18.03
-150		2.55		15.56
-140		2.13		12.99
-130		1.63		9.95
-120		1.07		6.55
-110		0.49		3.01
-100		0.05		0.32
-90		0.00		0.00
-80		0.00		0.00
-70		0.05		0.32
-60		0.07		0.41
-50		0.10		0.62
-40		0.17		1.01
-30		0.18		1.10
-20		0.21		1.25
-10		0.23		1.43
0		0.23		1.43
10		0.24		1.49
20		0.24		1.49
30		0.21		1.25
40		0.17		1.04
50		0.13		0.77
60		0.08		0.48
70		0.06		0.35
80		0.00		0.00
90		0.00		0.00
100		0.14		0.86
110		0.67		4.08
120		1.36		8.28
130		1.92		11.74
140		2.42		14.78
150		2.86		17.46
160		3.55		21.63



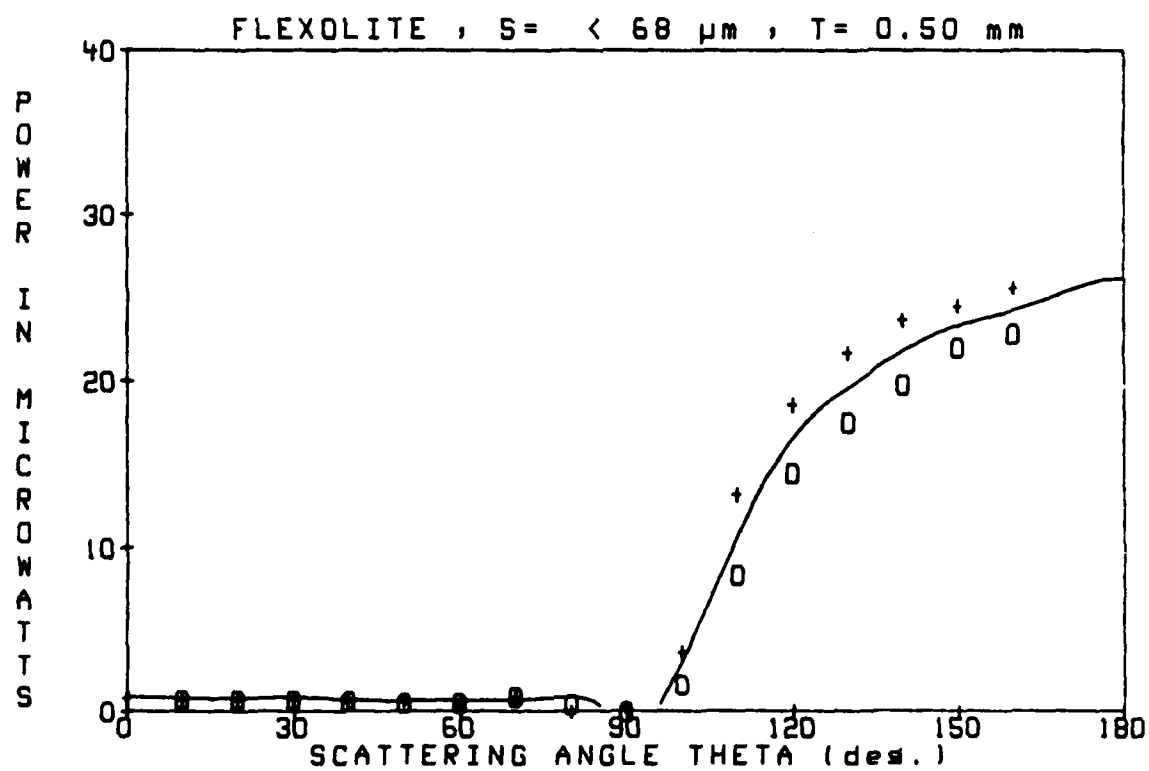
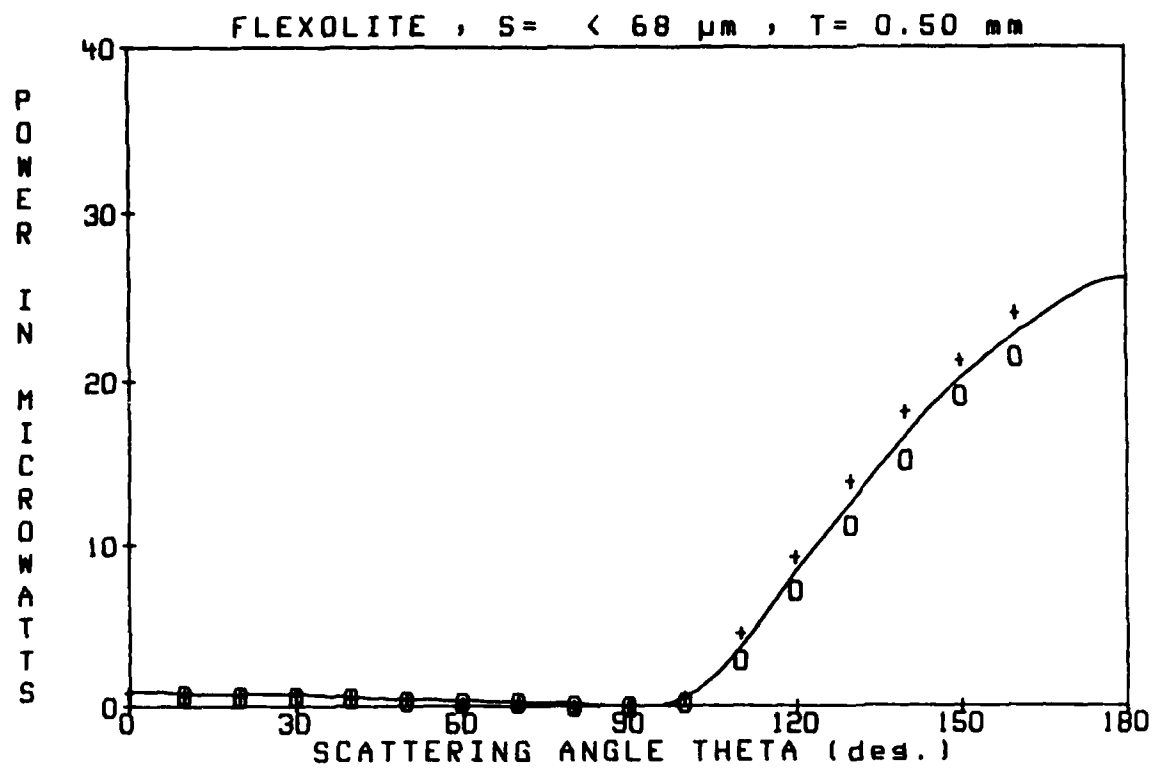
FLEXOLITE S = < 68 μ m T = 0.25 mm

SCATTERING ANGLE	DIODE VOLTAGE	POWER (microwatts)
-160	3.16	19.31
-150	2.71	16.54
-140	2.27	13.82
-130	1.78	10.88
-120	1.08	6.61
-110	0.43	2.59
-100	0.04	0.24
-90	0.00	0.00
-80	0.05	0.29
-70	0.12	0.71
-60	0.15	0.89
-50	0.21	1.25
-40	0.26	1.57
-30	0.32	1.93
-20	0.37	2.23
-10	0.39	2.38
0	0.42	2.56
10	0.41	2.50
20	0.40	2.47
30	0.37	2.23
40	0.33	1.99
50	0.24	1.49
60	0.19	1.19
70	0.13	0.80
80	0.06	0.35
90	0.00	0.00
100	0.09	0.56
110	0.71	4.35
120	1.42	8.67
130	2.12	12.93
140	2.64	16.12
150	3.17	19.37
160	3.51	21.39



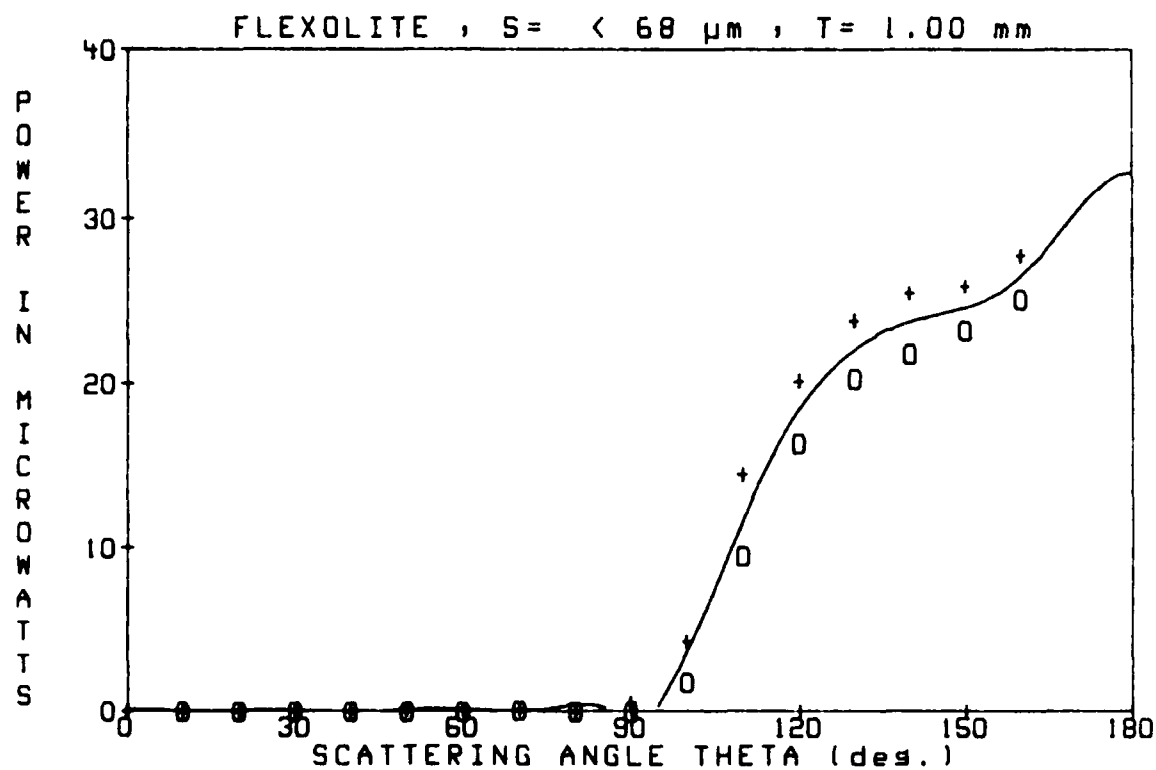
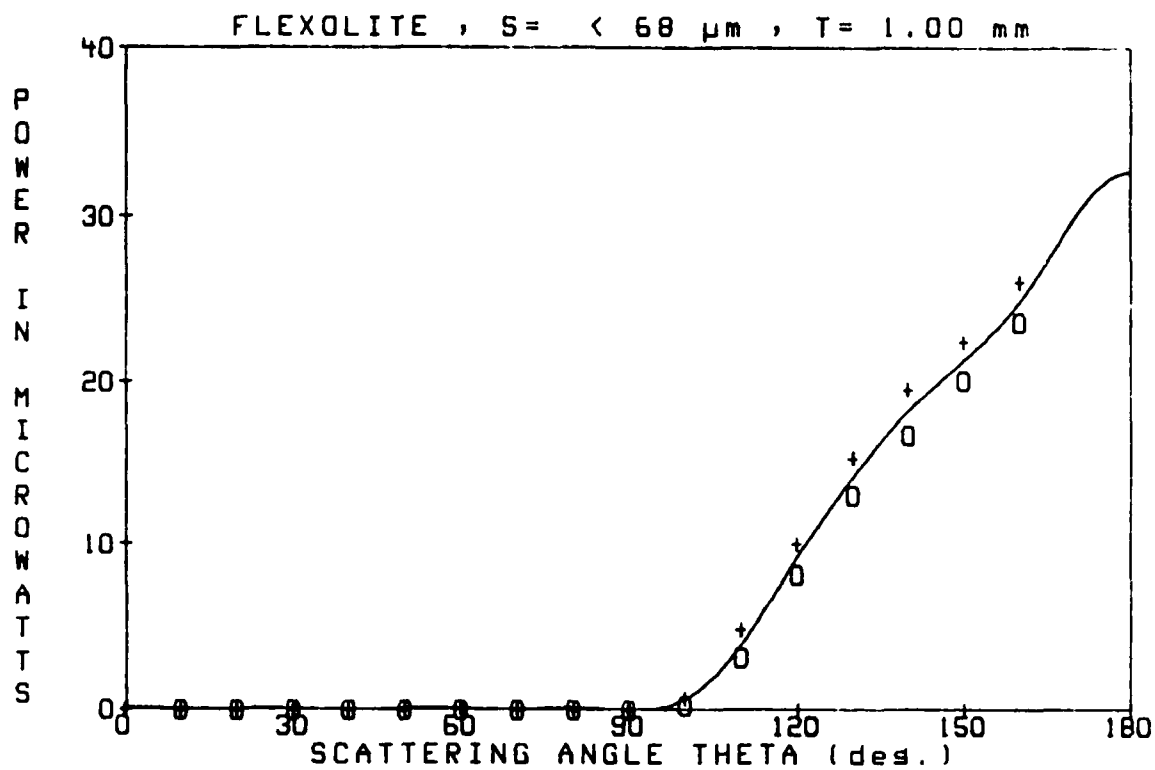
FLEXOLITE S = < 68 μ m T = 0.50 mm

SCATTERING ANGLE	DIODE VOLTAGE	POWER (microwatts)
-160	3.52	21.48
-150	3.13	19.07
-140	2.49	15.20
-130	1.85	11.29
-120	1.19	7.24
-110	0.47	2.89
-100	0.05	0.29
-90	0.00	0.00
-80	0.01	0.09
-70	0.05	0.32
-60	0.05	0.29
-50	0.06	0.35
-40	0.09	0.56
-30	0.11	0.65
-20	0.12	0.71
-10	0.13	0.77
0	0.15	0.89
10	0.13	0.80
20	0.13	0.80
30	0.12	0.74
40	0.09	0.56
50	0.08	0.48
60	0.04	0.26
70	0.05	0.32
80	0.00	0.00
90	0.00	0.00
100	0.11	0.65
110	0.75	4.56
120	1.53	9.33
130	2.29	13.98
140	2.97	18.15
150	3.49	21.30
160	3.95	24.08



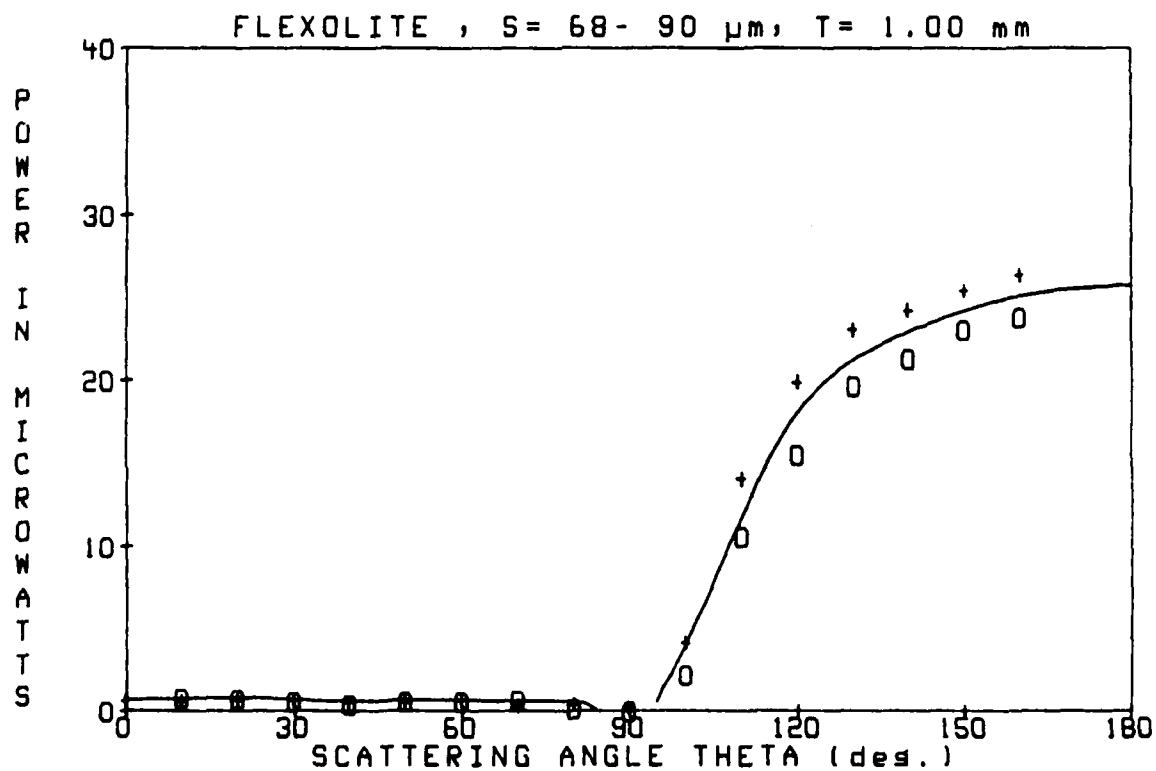
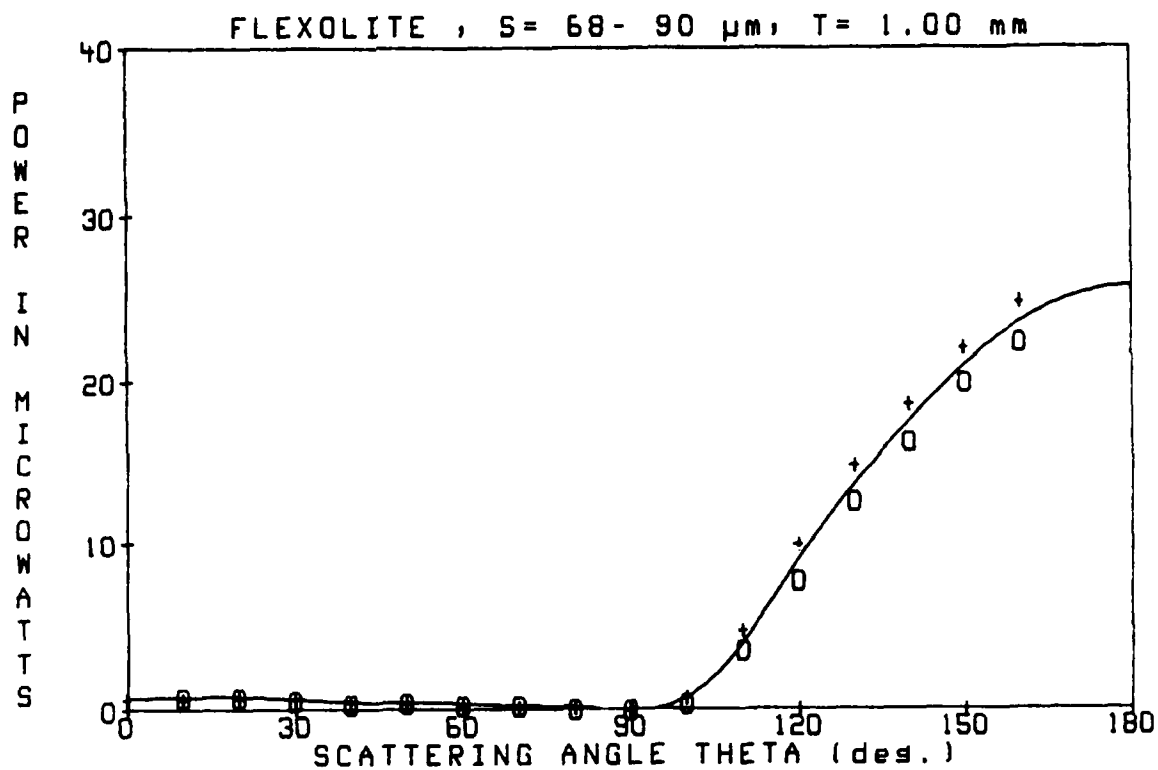
FLEXOLITE S= < 68 um T= 1.00 mm

SCATTERING ANGLE		DIODE VOLTAGE		POWER (microwatts)
-160		3.88		23.66
-150		3.30		20.14
-140		2.74		16.74
-130		2.14		13.08
-120		1.35		8.22
-110		0.54		3.28
-100		0.05		0.32
-90		0.00		0.00
-80		0.00		0.00
-70		0.00		0.00
-60		0.00		0.00
-50		0.00		0.00
-40		0.00		0.00
-30		0.00		0.00
-20		0.00		0.00
-10		0.00		0.00
0		0.00		0.00
10		0.00		0.00
20		0.00		0.00
30		0.00		0.00
40		0.00		0.00
50		0.00		0.00
60		0.01		0.09
70		0.00		0.00
80		0.00		0.00
90		0.00		0.00
100		0.13		0.77
110		0.82		4.97
120		1.66		10.13
130		2.52		15.37
140		3.21		19.61
150		3.69		22.50
160		4.29		26.16



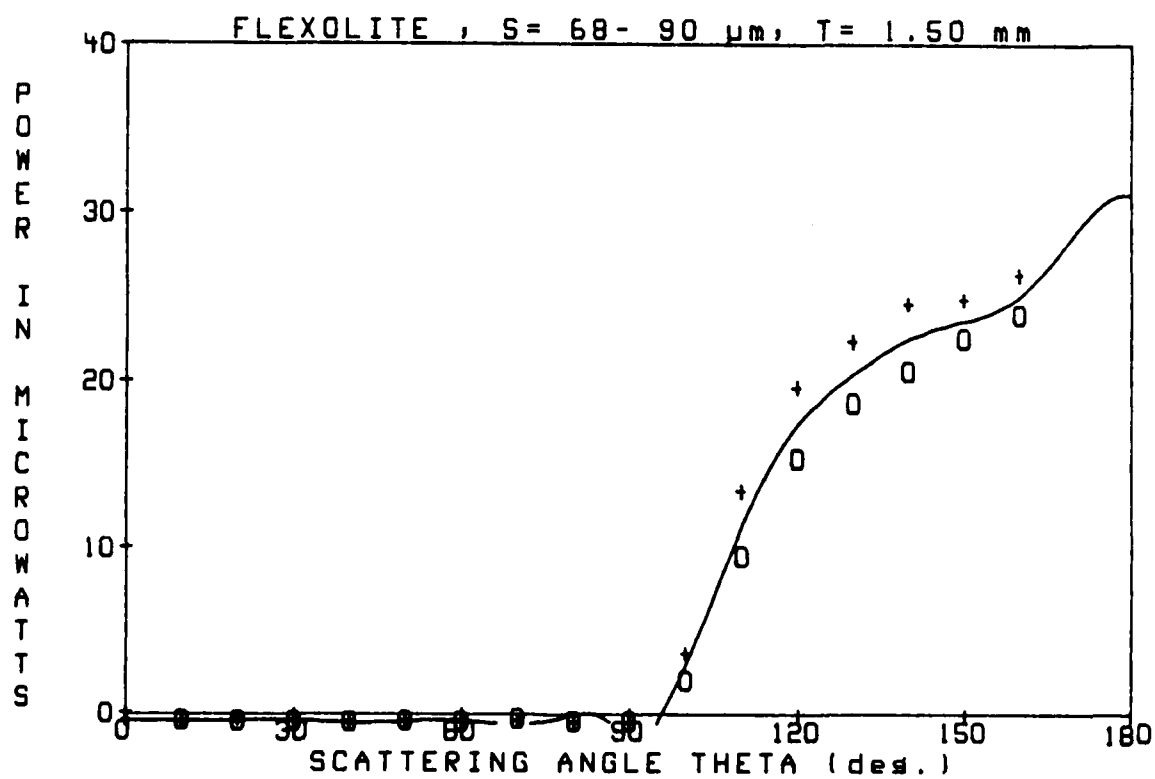
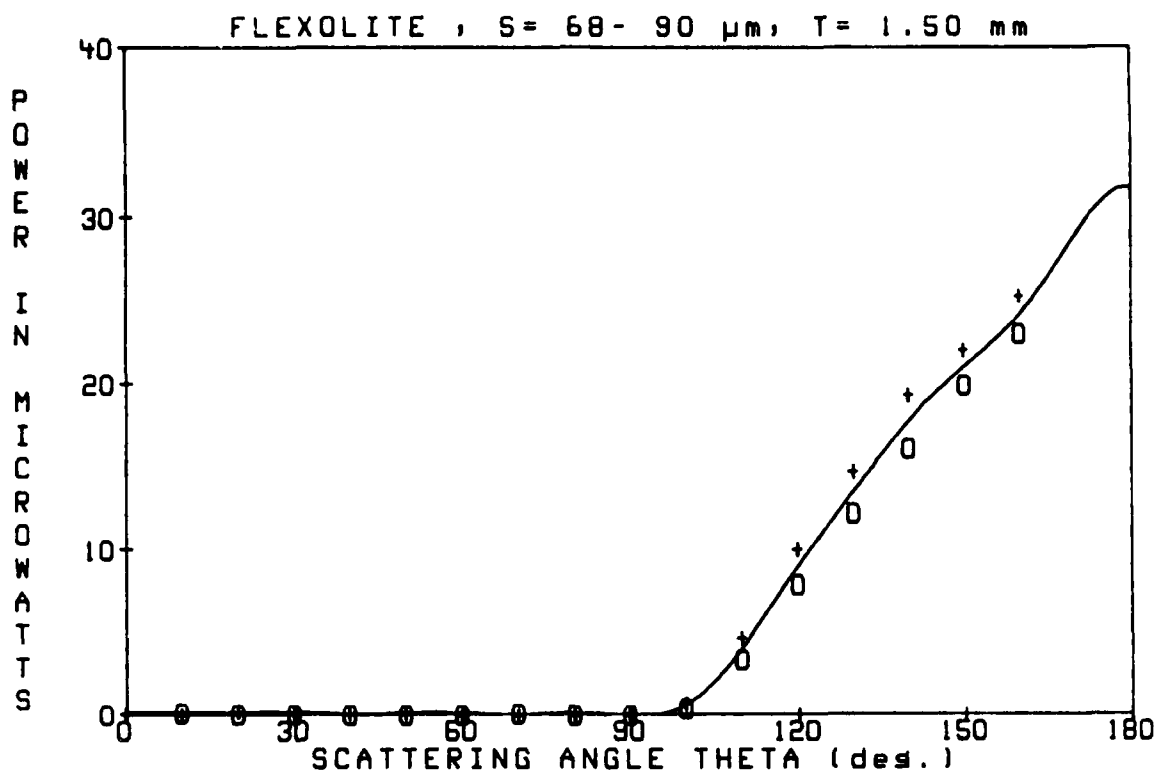
FLEXOLITE S= 68- 90 um T= 1.00 mm

SCATTERING ANGLE	DIODE VOLTAGE	POWER (microwatts)
-160	3.66	22.34
-150	3.27	19.93
-140	2.67	16.30
-130	2.08	12.66
-120	1.27	7.78
-110	0.60	3.63
-100	0.06	0.38
-90	0.00	0.00
-80	0.00	0.00
-70	0.04	0.24
-60	0.05	0.32
-50	0.07	0.41
-40	0.06	0.35
-30	0.09	0.56
-20	0.12	0.74
-10	0.13	0.80
0	0.11	0.68
10	0.12	0.71
20	0.12	0.74
30	0.11	0.68
40	0.08	0.51
50	0.07	0.41
60	0.06	0.38
70	0.02	0.15
80	0.01	0.09
90	0.00	0.00
100	0.12	0.74
110	0.80	4.86
120	1.64	9.98
130	2.44	14.87
140	3.05	18.62
150	3.62	22.08
160	4.07	24.82



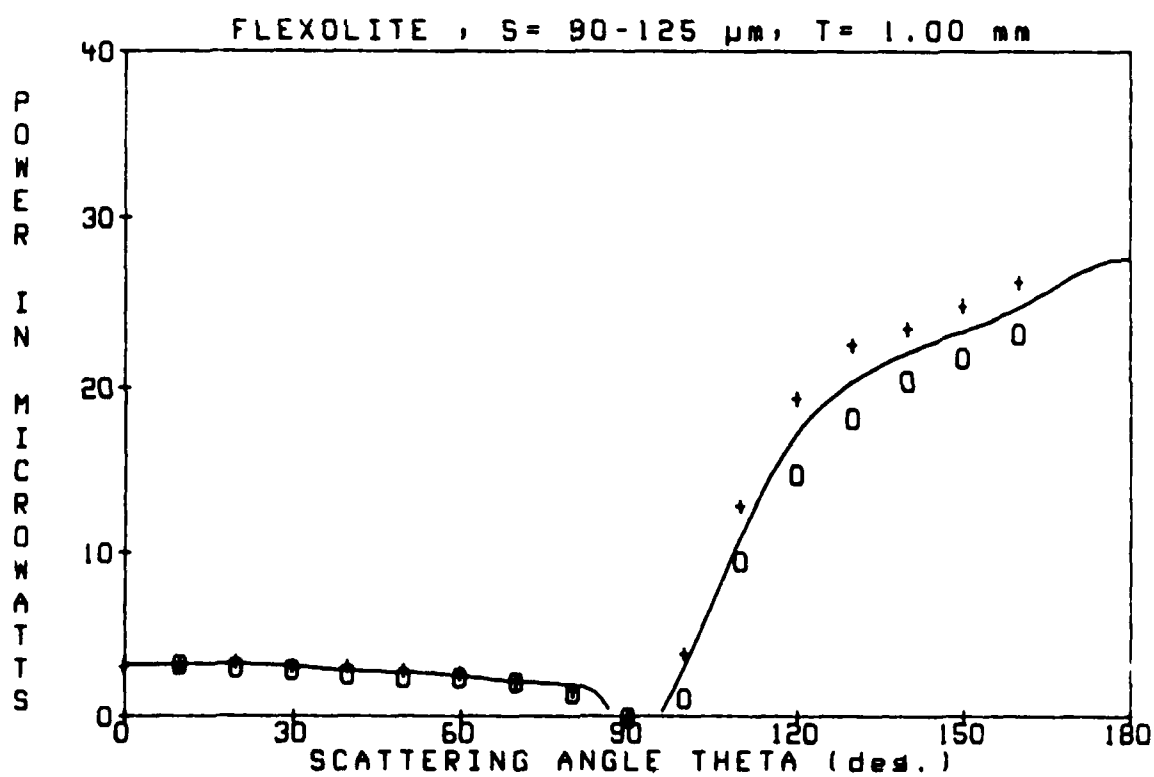
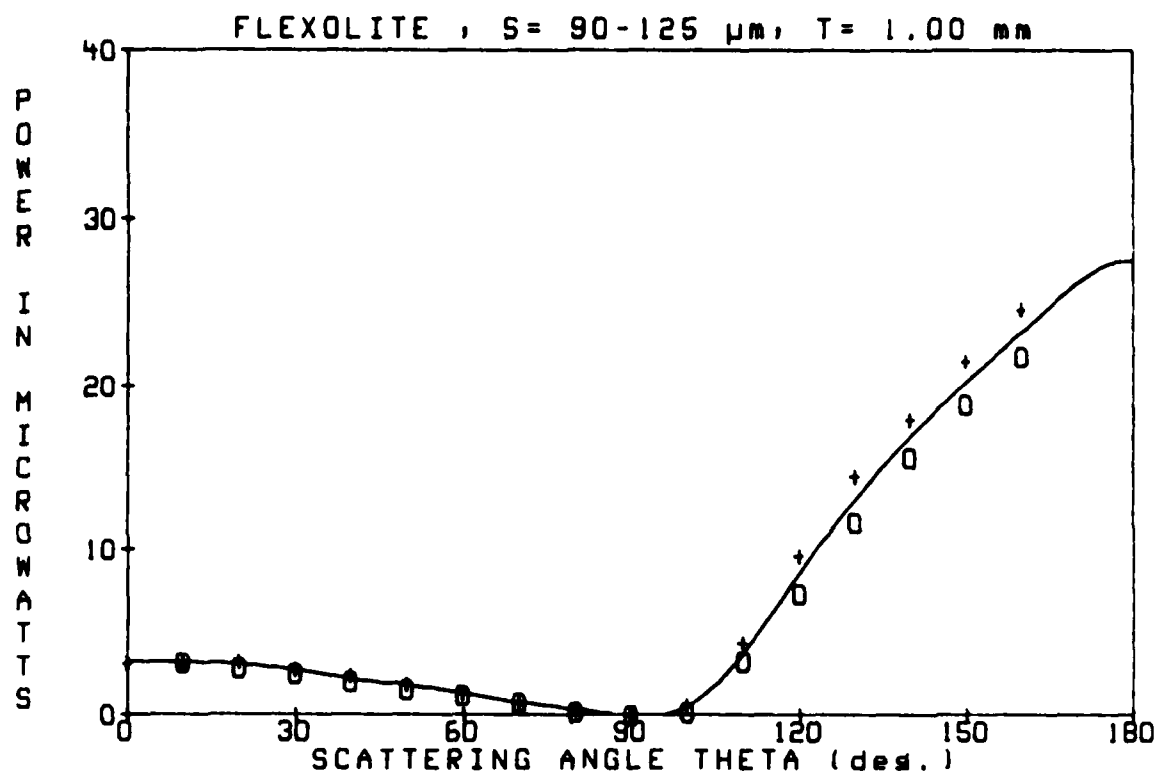
FLEXOLITE S= 68- 90 um T= 1.50 mm

SCATTERING ANGLE	DIODE VOLTAGE	POWER (microwatts)
-160	3.77	23.00
-150	3.27	19.93
-140	2.65	16.15
-130	2.02	12.30
-120	1.30	7.95
-110	0.56	3.42
-100	0.07	0.45
-90	0.00	0.00
-80	0.00	0.00
-70	0.01	0.09
-60	0.00	0.00
-50	0.00	0.00
-40	0.00	0.00
-30	0.01	0.09
-20	0.01	0.09
-10	0.02	0.15
0	0.02	0.15
10	0.01	0.09
20	0.04	0.24
30	0.02	0.15
40	0.01	0.09
50	0.02	0.12
60	0.00	0.00
70	0.00	0.00
80	0.00	0.00
90	0.00	0.00
100	0.12	0.74
110	0.79	4.79
120	1.66	10.13
130	2.42	14.75
140	3.17	19.34
150	3.62	22.08
160	4.16	25.36



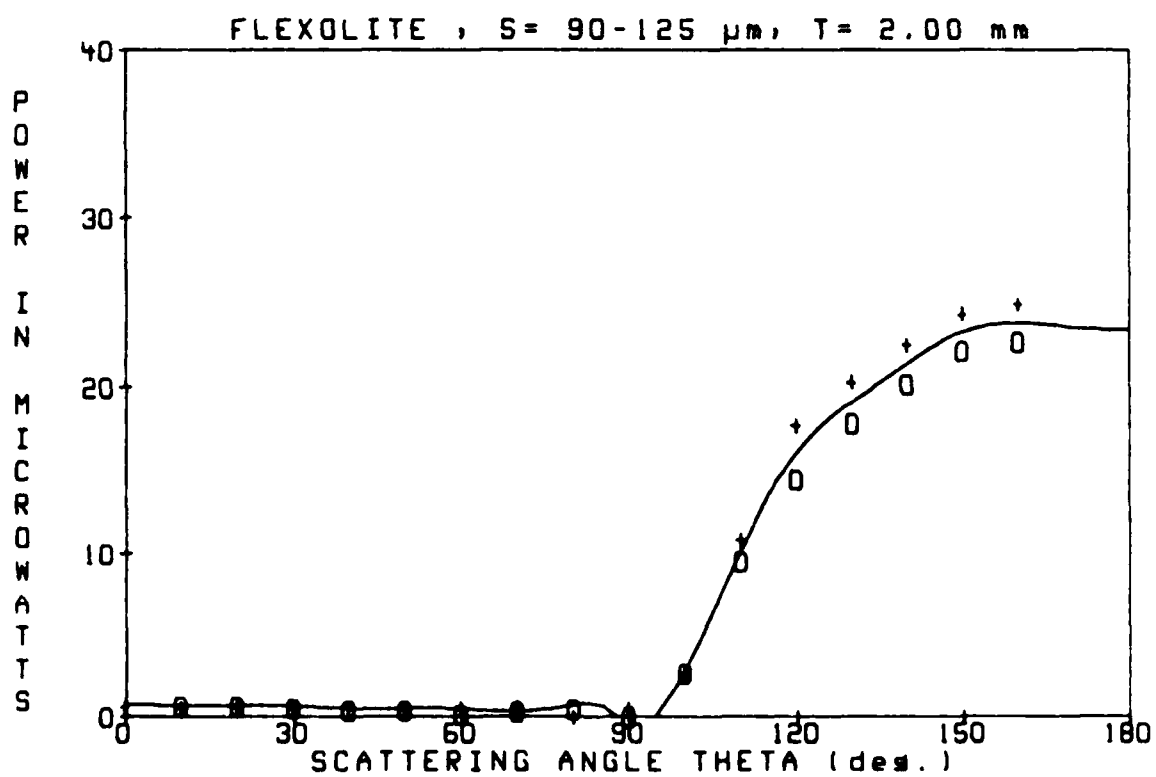
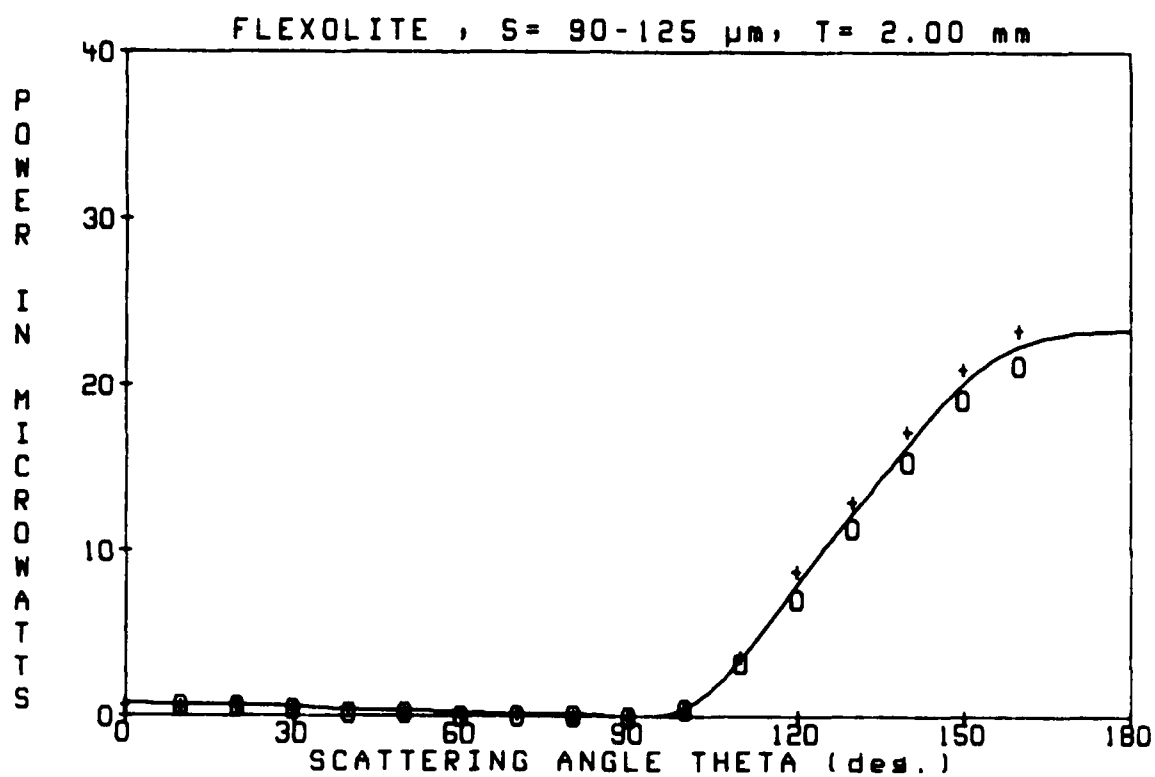
FLEXOLITE S= 90-125 um T= 1.00 mm

SCATTERING ANGLE	DIODE VOLTAGE	POWER (microwatts)
-160	3.58	21.81
-150	3.10	18.92
-140	2.57	15.70
-130	1.92	11.74
-120	1.22	7.42
-110	0.54	3.28
-100	0.03	0.21
-90	0.00	0.00
-80	0.04	0.26
-70	0.12	0.74
-60	0.20	1.22
-50	0.25	1.55
-40	0.34	2.06
-30	0.42	2.56
-20	0.47	2.89
-10	0.53	3.25
0	0.52	3.18
10	0.52	3.18
20	0.53	3.21
30	0.45	2.77
40	0.39	2.41
50	0.31	1.87
60	0.22	1.34
70	0.13	0.77
80	0.05	0.29
90	0.00	0.00
100	0.11	0.68
110	0.73	4.43
120	1.59	9.71
130	2.39	14.57
140	2.96	18.06
150	3.53	21.54
160	4.05	24.70



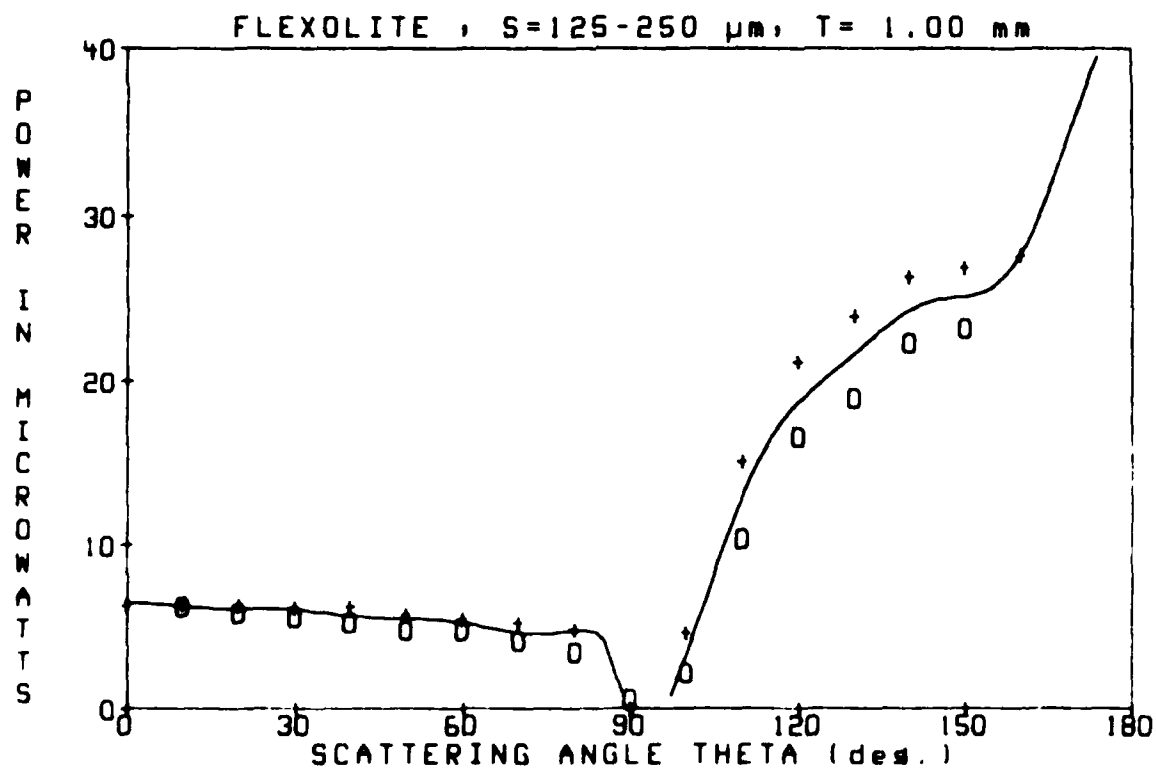
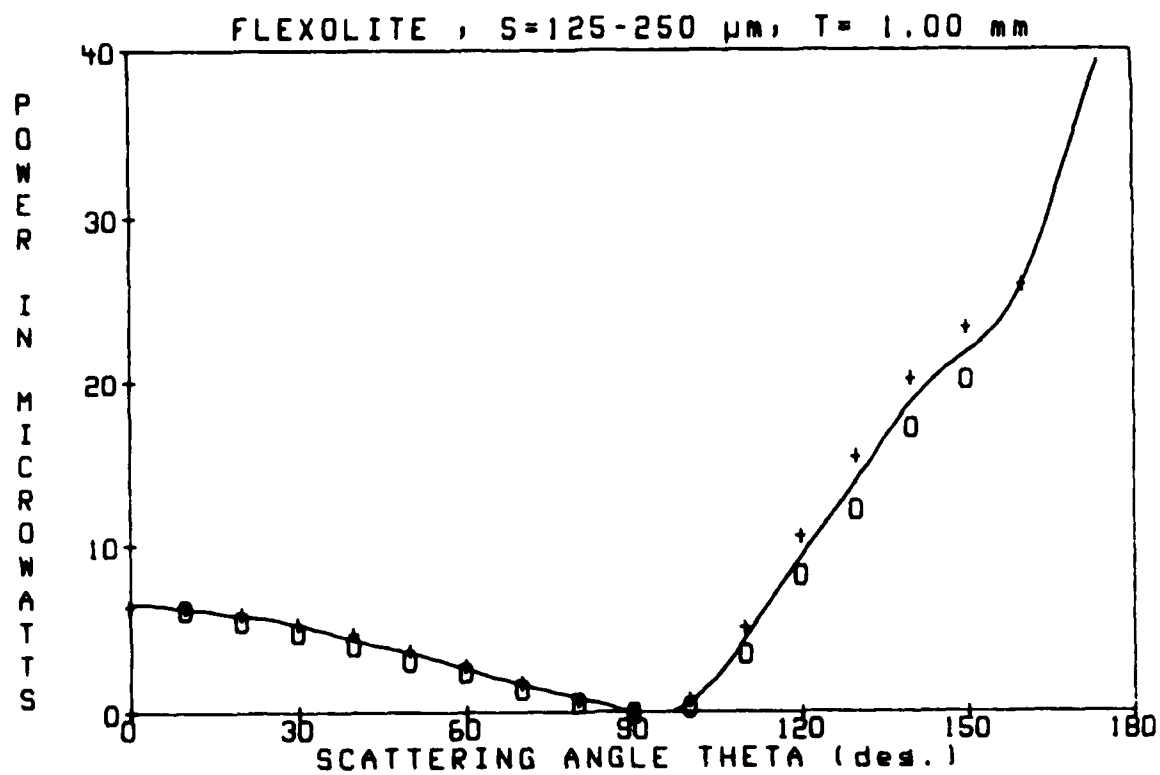
FLEXOLITE S= 90-125 μm T= 2.00 mm

SCATTERING ANGLE	DIODE VOLTAGE	POWER (microwatts)
-160	3.49	21.30
-150	3.15	19.19
-140	2.54	15.52
-130	1.89	11.50
-120	1.19	7.27
-110	0.54	3.28
-100	0.08	0.48
-90	0.00	0.00
-80	0.01	0.09
-70	0.02	0.12
-60	0.01	0.09
-50	0.05	0.29
-40	0.05	0.32
-30	0.08	0.48
-20	0.11	0.65
-10	0.12	0.71
0	0.11	0.68
10	0.11	0.65
20	0.11	0.65
30	0.09	0.53
40	0.09	0.53
50	0.05	0.32
60	0.05	0.32
70	0.04	0.24
80	0.00	0.00
90	0.00	0.00
100	0.08	0.48
110	0.61	3.72
120	1.46	8.91
130	2.15	13.11
140	2.84	17.31
150	3.46	21.09
160	3.84	23.45



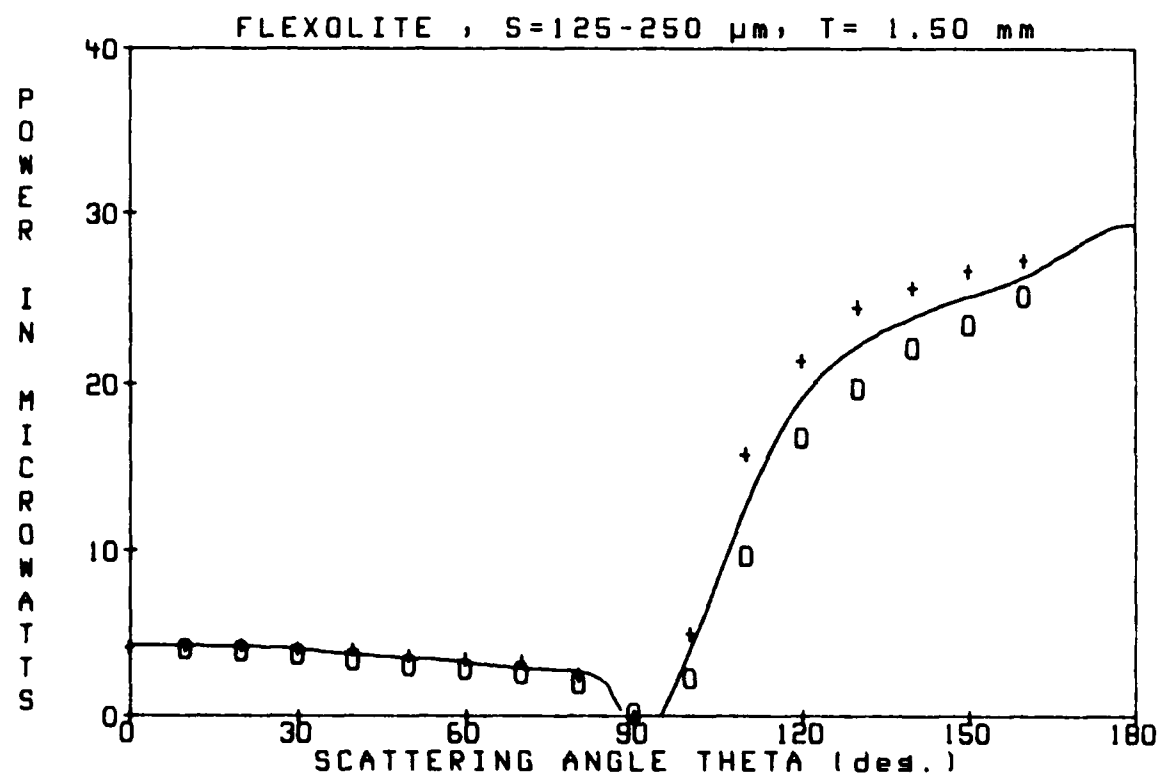
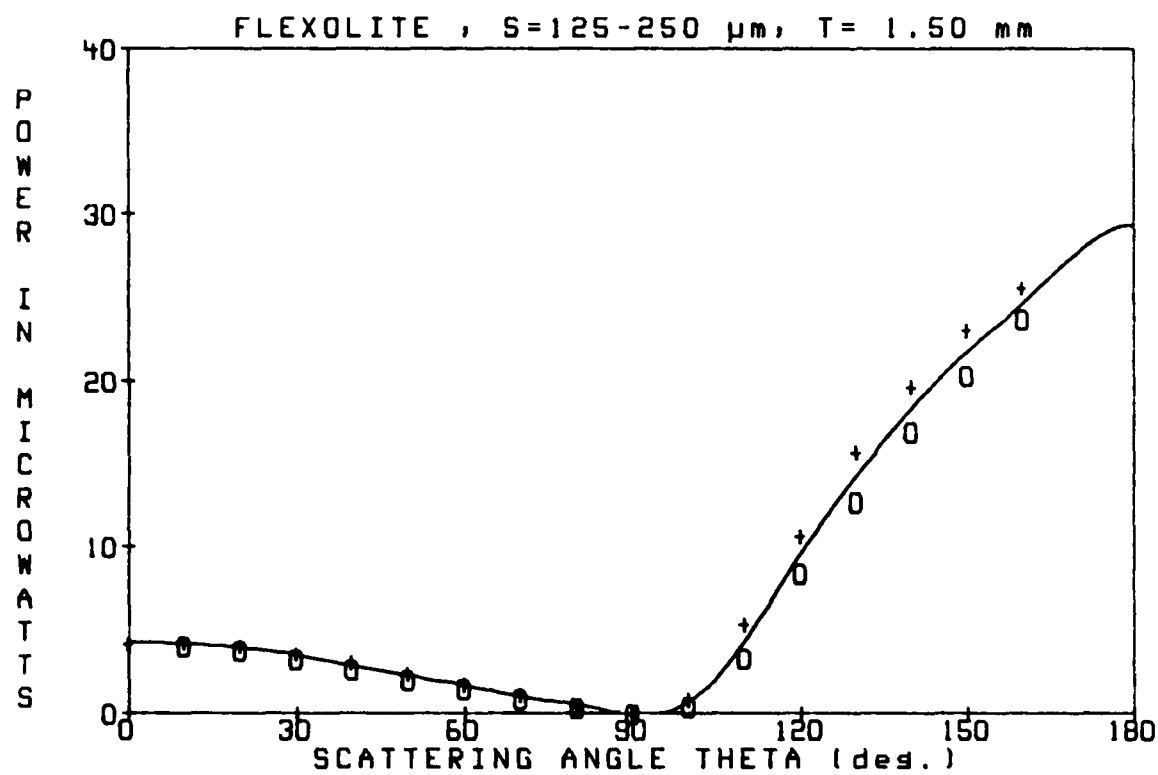
FLEXOLITE S=125-250 μ m T= 1.00 mm

SCATTERING ANGLE	DIODE VOLTAGE	POWER (microwatts)
-160		
-150	3.30	20.14
-140	2.81	17.16
-130	2.00	12.21
-120	1.36	8.31
-110	0.59	3.57
-100	0.06	0.38
-90	0.00	0.00
-80	0.10	0.62
-70	0.24	1.46
-60	0.40	2.44
-50	0.52	3.15
-40	0.67	4.11
-30	0.81	4.92
-20	0.92	5.60
-10	1.02	6.25
0	1.05	6.44
10	1.05	6.44
20	0.99	6.01
30	0.89	5.45
40	0.80	4.86
50	0.63	3.81
60	0.46	2.83
70	0.30	1.84
80	0.14	0.86
90	0.00	0.00
100	0.14	0.83
110	0.85	5.15
120	1.74	10.61
130	2.53	15.43
140	3.32	20.26
150	3.83	23.36
160	4.27	26.04



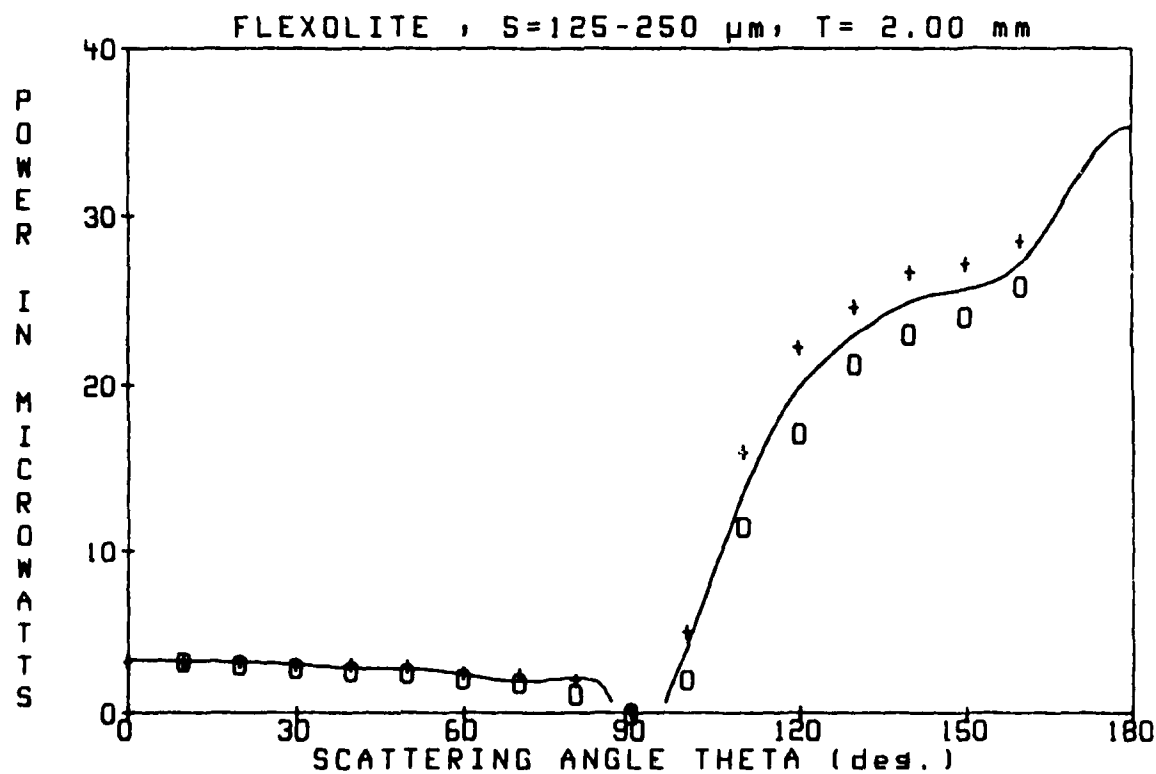
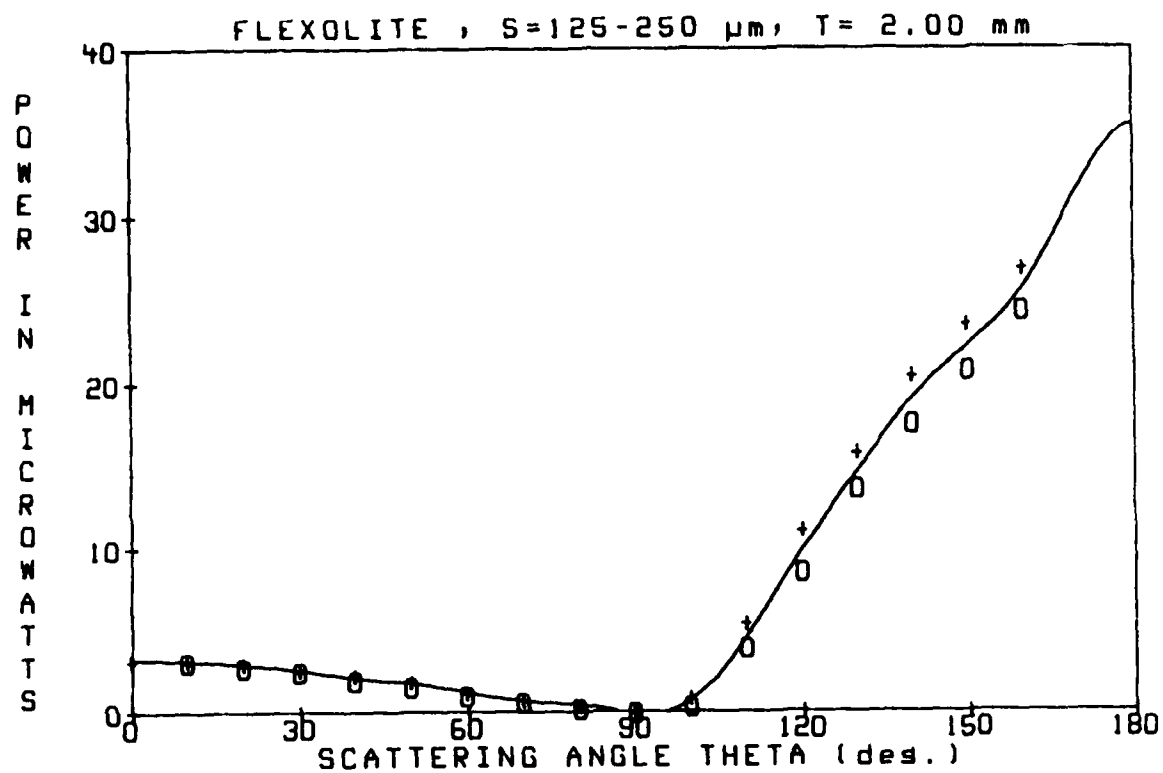
FLEXOLITE S=125-250 μ m T= 1.50 mm

SCATTERING ANGLE	DIODE VOLTAGE	POWER (microwatts)
-160	3.88	23.69
-150	3.34	20.38
-140	2.78	16.93
-130	2.09	12.75
-120	1.39	8.46
-110	0.55	3.34
-100	0.07	0.41
-90	0.00	0.00
-80	0.06	0.35
-70	0.15	0.92
-60	0.24	1.49
-50	0.34	2.06
-40	0.44	2.68
-30	0.54	3.31
-20	0.63	3.81
-10	0.67	4.11
0	0.69	4.23
10	0.71	4.32
20	0.67	4.08
30	0.60	3.63
40	0.51	3.12
50	0.39	2.41
60	0.29	1.76
70	0.19	1.16
80	0.07	0.45
90	0.00	0.00
100	0.15	0.89
110	0.89	5.45
120	1.76	10.72
130	2.59	15.79
140	3.23	19.70
150	3.79	23.09
160	4.20	25.63



FLEXOLITE S=125-250 μ m T= 2.00 mm

SCATTERING ANGLE	DIODE VOLTAGE	POWER (microwatts)
-160	3.99	24.35
-150	3.42	20.86
-140	2.89	17.64
-130	2.24	13.68
-120	1.41	8.58
-110	0.65	3.96
-100	0.06	0.35
-90	0.00	0.00
-80	0.03	0.21
-70	0.10	0.62
-60	0.17	1.04
-50	0.26	1.57
-40	0.33	1.99
-30	0.40	2.47
-20	0.46	2.83
-10	0.52	3.18
0	0.53	3.21
10	0.53	3.21
20	0.50	3.04
30	0.43	2.65
40	0.38	2.32
50	0.31	1.87
60	0.21	1.25
70	0.13	0.80
80	0.06	0.35
90	0.00	0.00
100	0.15	0.89
110	0.90	5.51
120	1.83	11.14
130	2.60	15.88
140	3.36	20.53
150	3.86	23.57
160	4.41	26.91

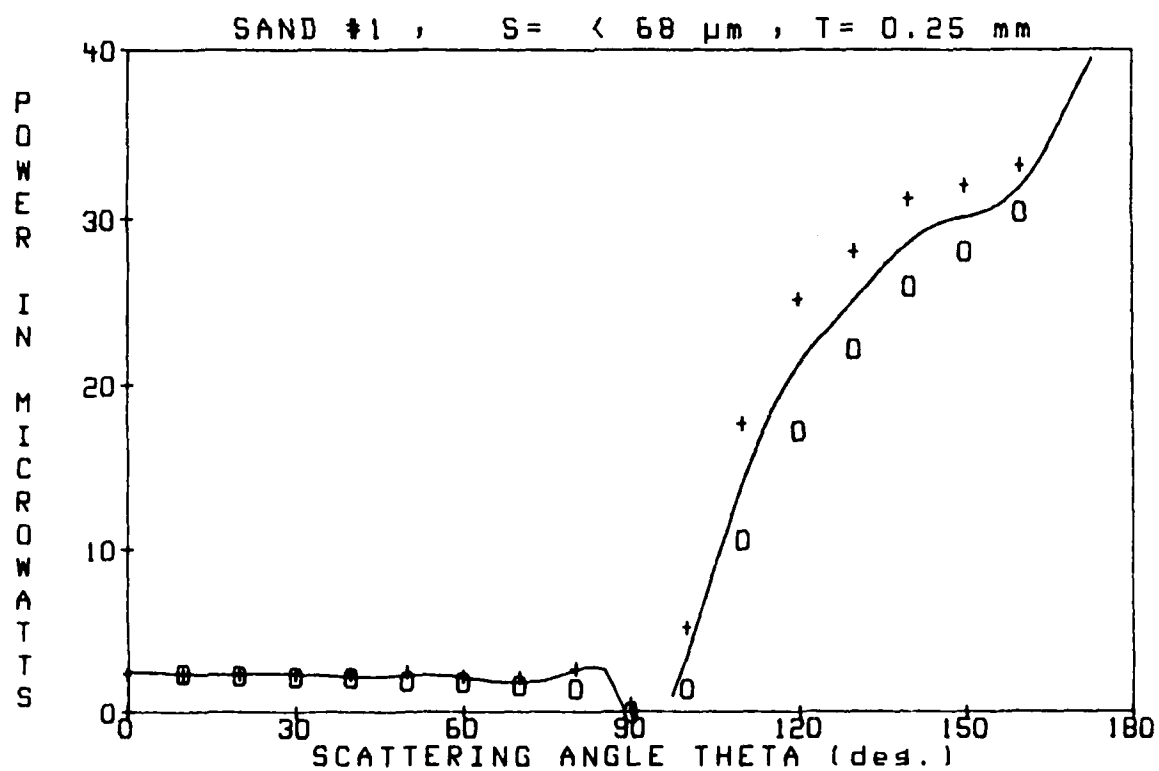
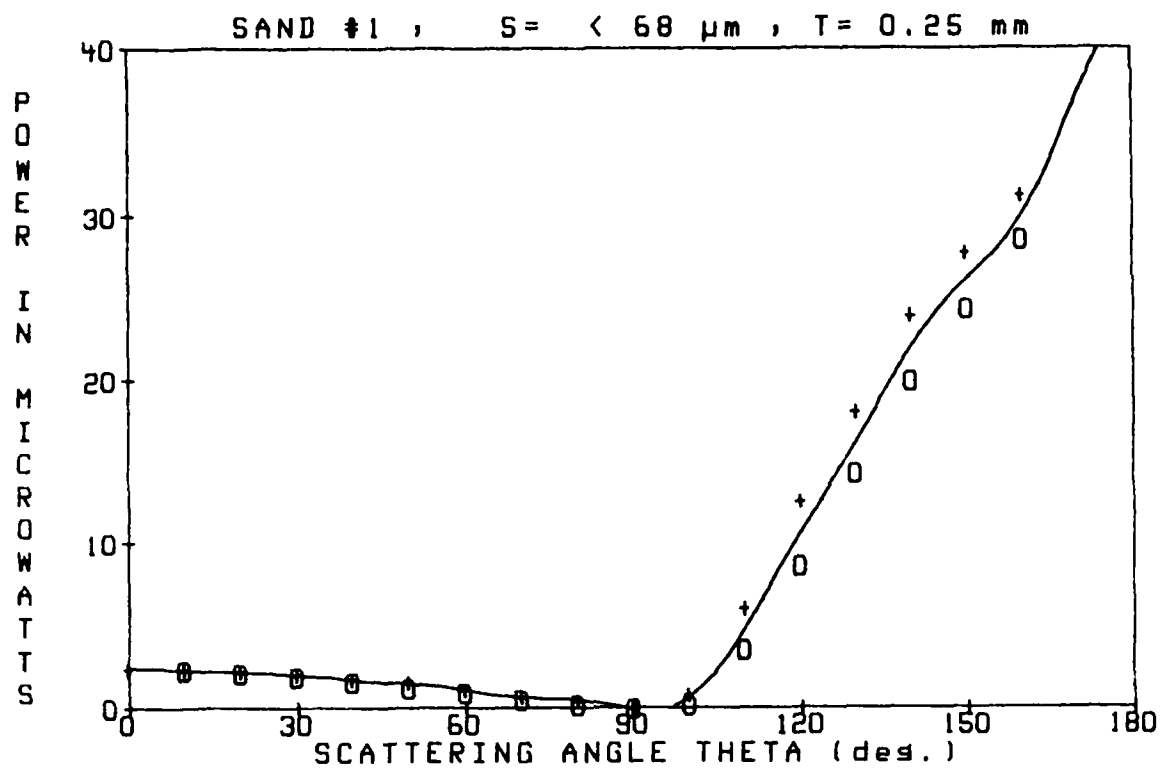


SAND #1

S= < 68 μ m

T= 0.25 mm

SCATTERING ANGLE	DIODE VOLTAGE	POWER (microwatts)
-160	4.70	28.66
-150	4.00	24.38
-140	3.27	19.97
-130	2.34	14.27
-120	1.42	8.64
-110	0.60	3.63
-100	0.04	0.26
-90	0.00	0.00
-80	0.04	0.26
-70	0.10	0.59
-60	0.16	0.95
-50	0.21	1.25
-40	0.27	1.63
-30	0.32	1.93
-20	0.35	2.14
-10	0.39	2.38
0	0.40	2.44
10	0.39	2.41
20	0.38	2.29
30	0.35	2.11
40	0.30	1.84
50	0.27	1.63
60	0.19	1.16
70	0.13	0.77
80	0.08	0.48
90	0.00	0.00
100	0.15	0.92
110	1.00	6.08
120	2.08	12.66
130	2.97	18.09
140	3.93	23.95
150	4.56	27.83
160	5.13	31.32

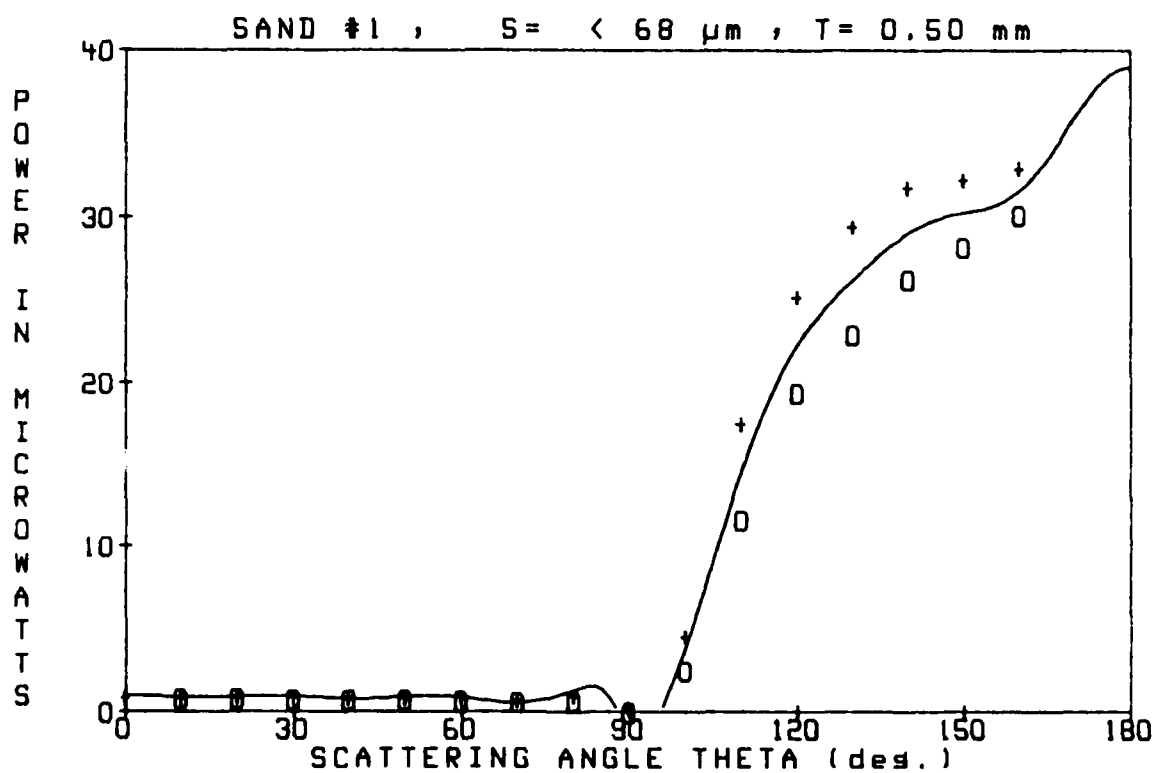
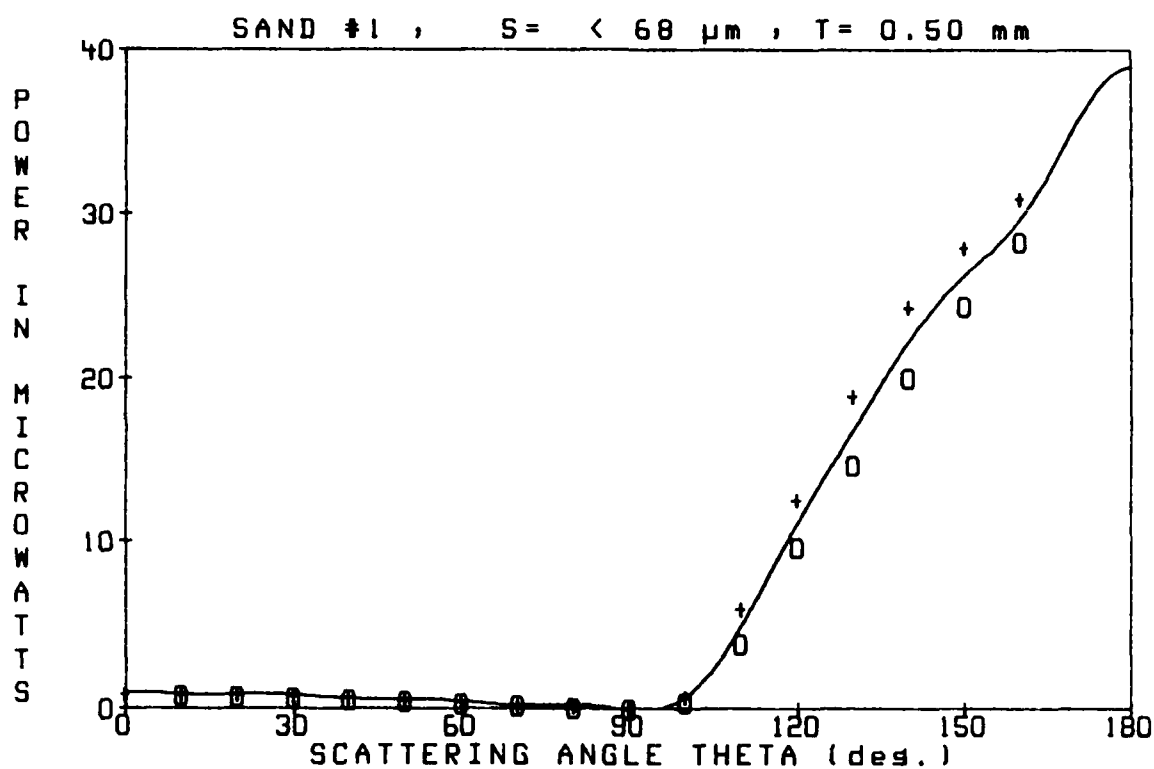


SAND #1

S= < 68 um

T= 0.50 mm

SCATTERING ANGLE	DIODE VOLTAGE	POWER (microwatts)
-160	4.65	28.33
-150	4.01	24.43
-140	3.30	20.11
-130	2.41	14.72
-120	1.59	9.68
-110	0.65	3.99
-100	0.07	0.45
-90	0.00	0.00
-80	0.02	0.12
-70	0.03	0.21
-60	0.06	0.35
-50	0.08	0.48
-40	0.10	0.59
-30	0.11	0.68
-20	0.13	0.77
-10	0.14	0.83
0	0.15	0.92
10	0.15	0.89
20	0.15	0.92
30	0.14	0.83
40	0.11	0.68
50	0.10	0.59
60	0.08	0.48
70	0.04	0.26
80	0.03	0.18
90	0.00	0.00
100	0.13	0.80
110	0.99	6.01
120	2.07	12.60
130	3.11	18.98
140	4.00	24.38
150	4.59	27.98
160	5.09	31.05

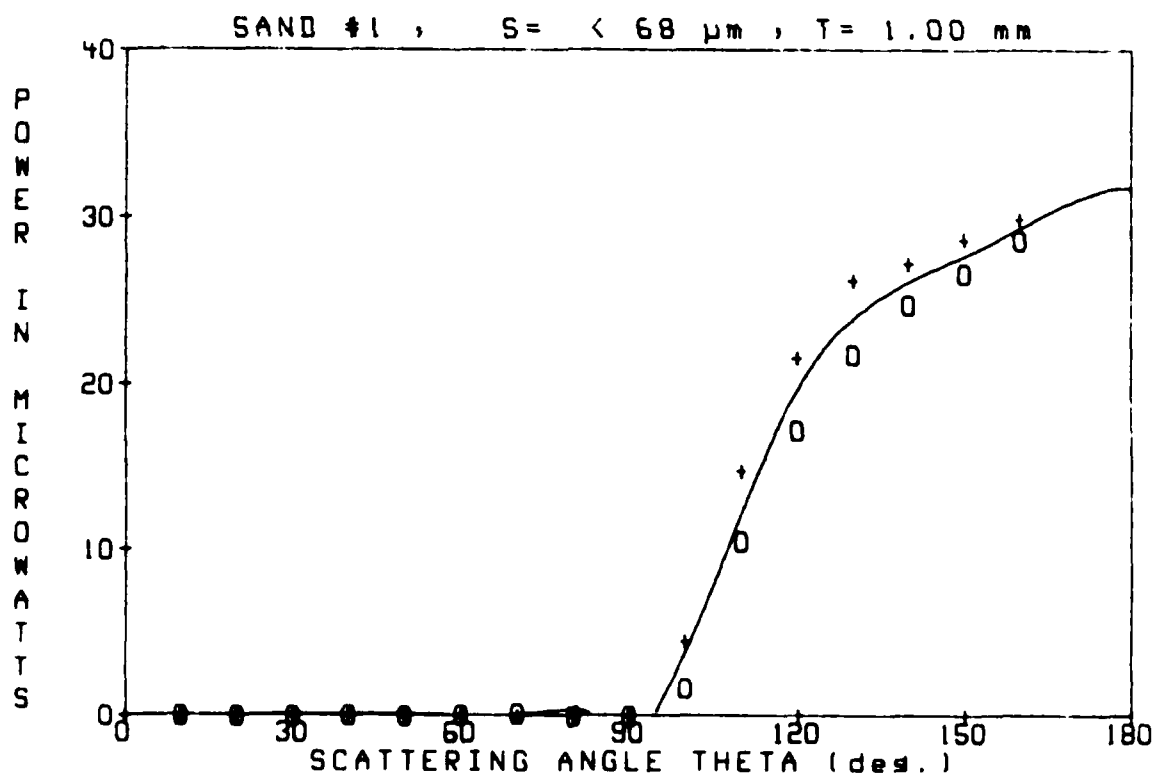
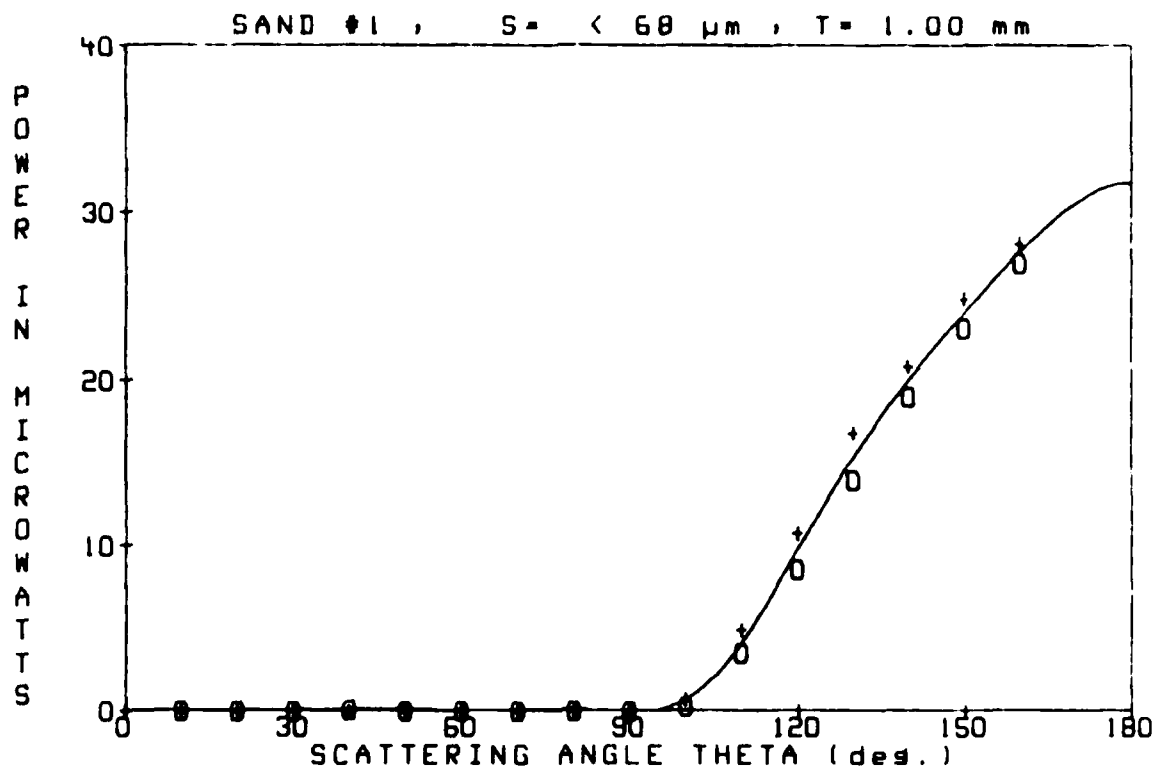


SAND #1

S = < 68 μ m

T = 1.00 mm

SCATTERING ANGLE	DIODE VOLTAGE	POWER (microwatts)
-160	4.42	26.97
-150	3.79	23.12
-140	3.12	19.01
-130	2.30	14.03
-120	1.42	8.64
-110	0.59	3.61
-100	0.05	0.29
-90	0.00	0.00
-80	0.00	0.00
-70	0.00	0.00
-60	0.00	0.00
-50	0.00	0.00
-40	0.01	0.09
-30	0.00	0.00
-20	0.00	0.00
-10	0.00	0.00
0	0.00	0.00
10	0.00	0.00
20	0.00	0.00
30	0.00	0.00
40	0.00	0.00
50	0.00	0.00
60	0.00	0.00
70	0.00	0.00
80	0.00	0.00
90	0.00	0.00
100	0.13	0.80
110	0.83	5.06
120	1.77	10.82
130	2.77	16.92
140	3.43	20.92
150	4.08	24.91
160	4.62	28.19

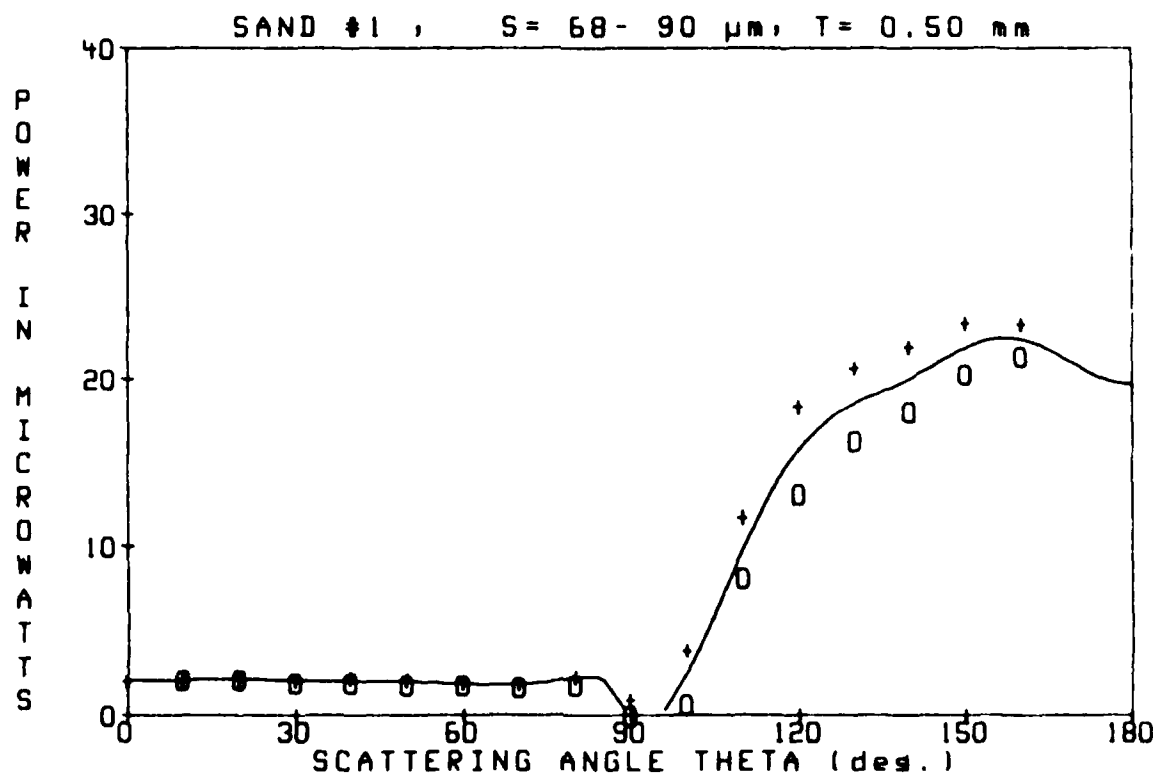
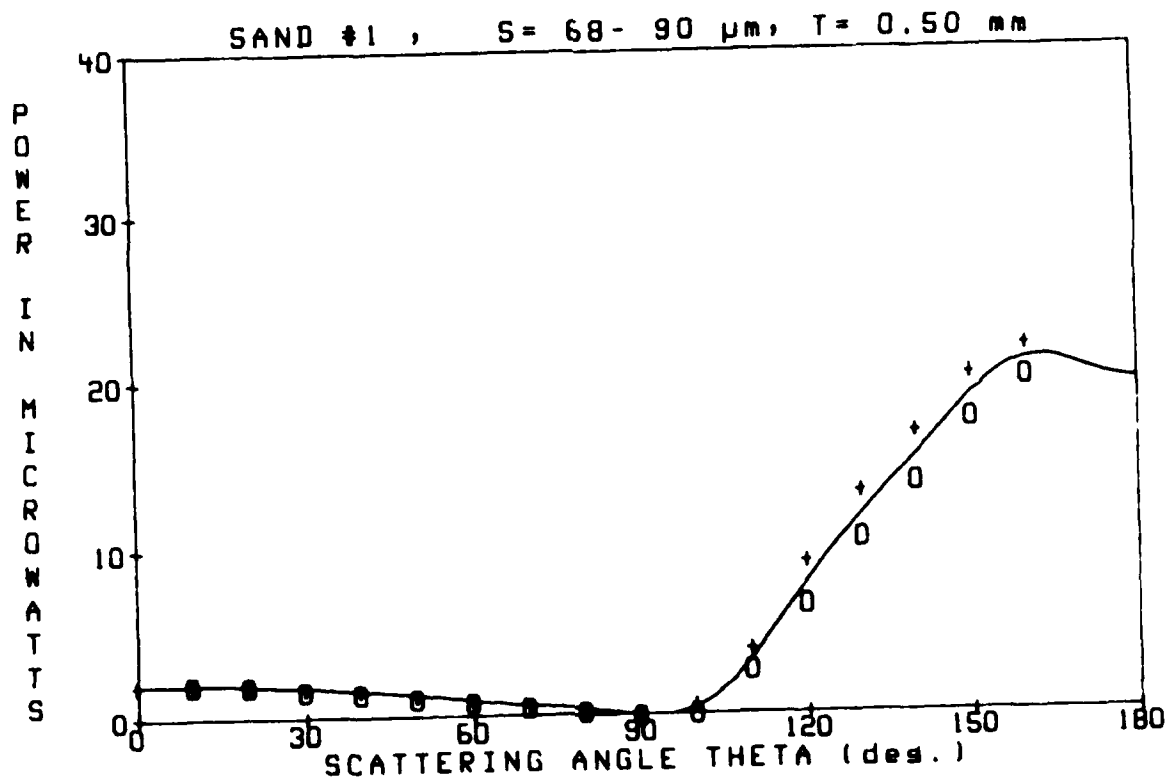


SAND #1

S= 68- 90 μ m

T= 0.50 mm

SCATTERING ANGLE	DIODE VOLTAGE	POWER (microwatts)
-160	3.29	20.05
-150	2.88	17.58
-140	2.27	13.82
-130	1.72	10.49
-120	1.07	6.55
-110	0.46	2.80
-100	0.02	0.12
-90	0.00	0.00
-80	0.05	0.32
-70	0.10	0.59
-60	0.15	0.92
-50	0.19	1.16
-40	0.24	1.49
-30	0.28	1.73
-20	0.33	2.03
-10	0.35	2.11
0	0.34	2.08
10	0.36	2.17
20	0.35	2.11
30	0.31	1.87
40	0.29	1.79
50	0.23	1.40
60	0.17	1.01
70	0.11	0.68
80	0.07	0.41
90	0.01	0.09
100	0.11	0.68
110	0.66	4.02
120	1.50	9.17
130	2.18	13.32
140	2.76	16.84
150	3.32	20.23
160	3.59	21.90

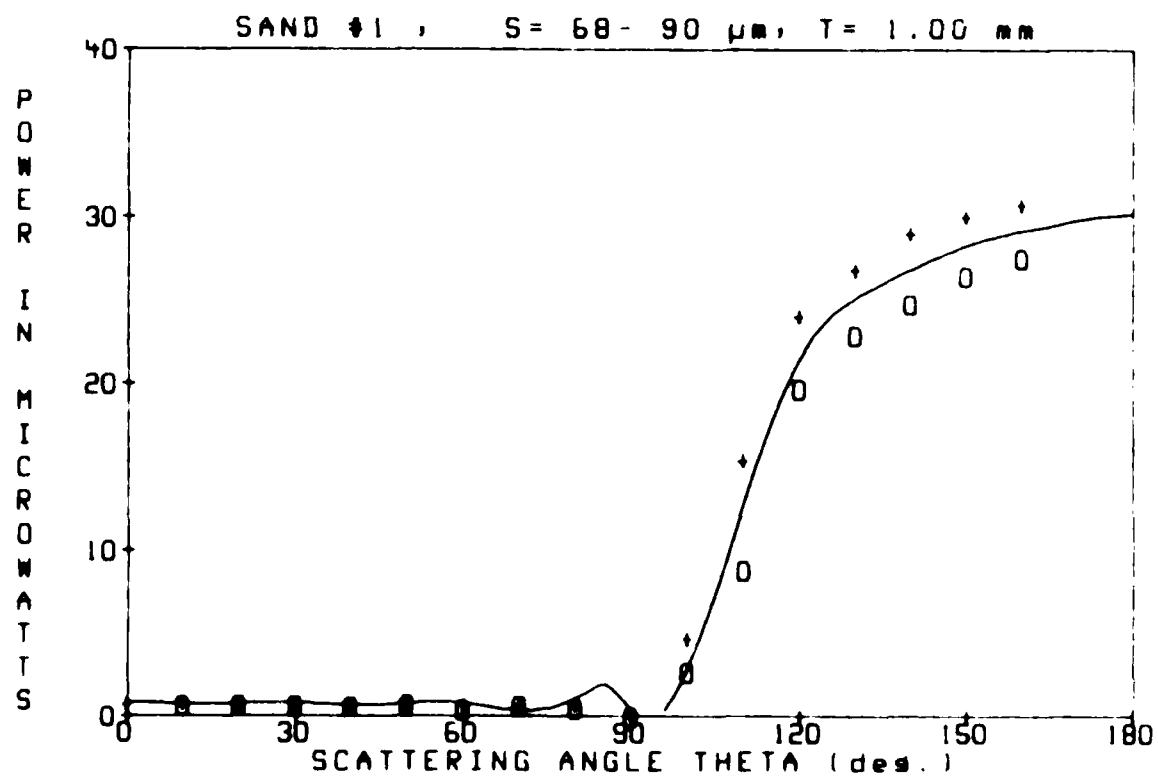
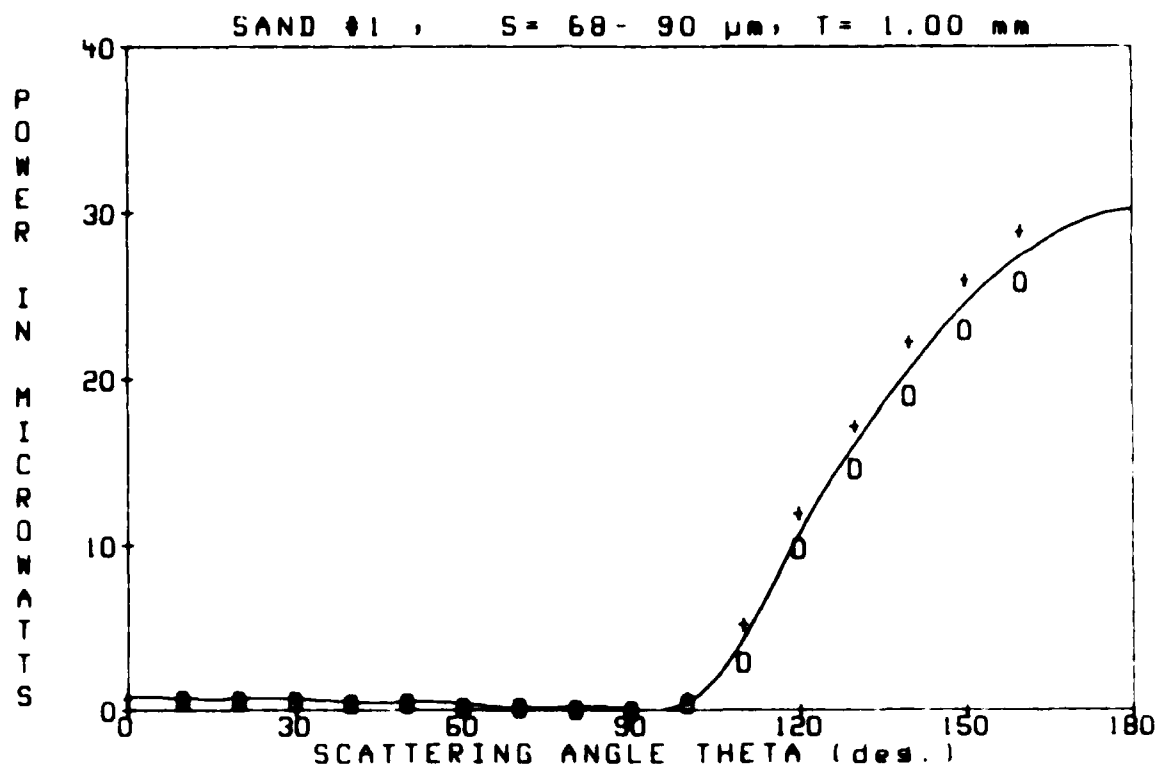


SAND #1

S= 68- 90 um

T= 1.00 mm

SCATTERING ANGLE	DIODE VOLTAGE	POWER (microwatts)
-160	4.25	25.92
-150	3.76	22.94
-140	3.12	19.04
-130	2.41	14.72
-120	1.62	9.89
-110	0.50	3.04
-100	0.08	0.48
-90	0.00	0.00
-80	0.01	0.09
-70	0.04	0.24
-60	0.03	0.21
-50	0.08	0.48
-40	0.08	0.48
-30	0.10	0.62
-20	0.11	0.65
-10	0.11	0.68
0	0.12	0.74
10	0.14	0.86
20	0.13	0.77
30	0.11	0.68
40	0.10	0.59
50	0.10	0.59
60	0.06	0.38
70	0.04	0.24
80	0.02	0.15
90	0.00	0.00
100	0.14	0.83
110	0.87	5.30
120	1.98	12.07
130	2.83	17.28
140	3.65	22.29
150	4.27	26.04
160	4.75	28.99

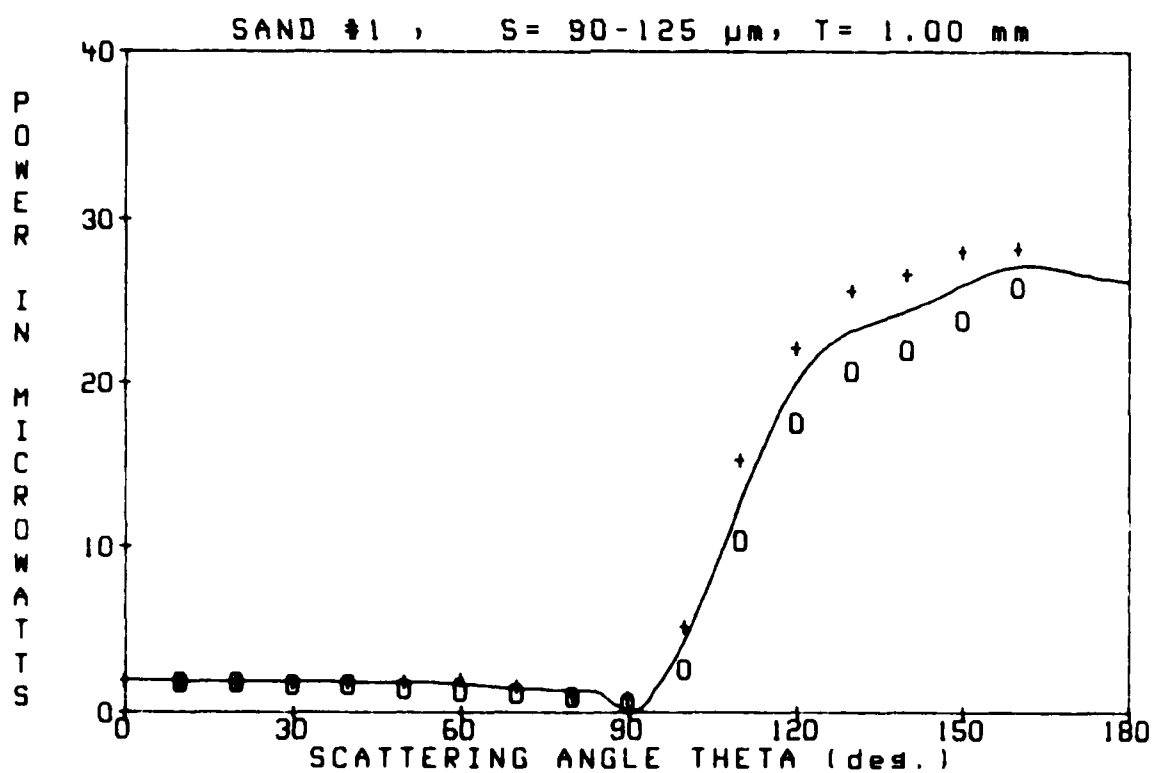
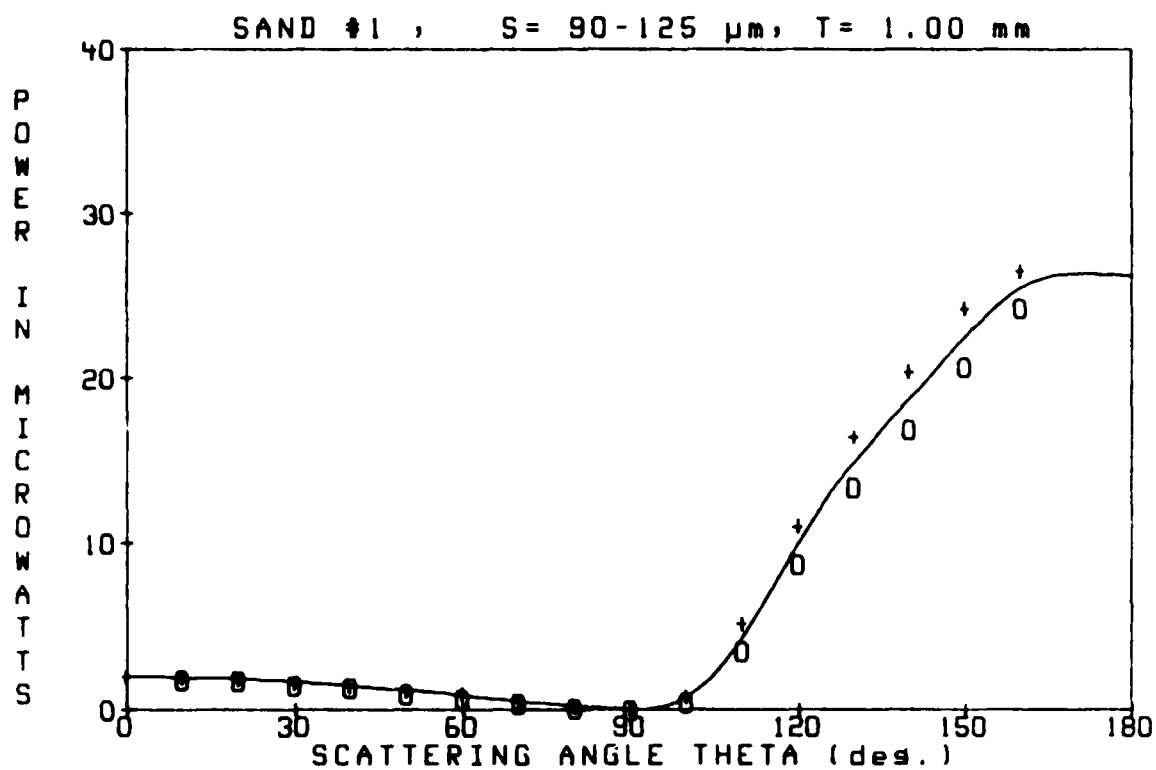


SAND #1

S= 90-125 μ m

T= 1.00 mm

SCATTERING ANGLE	DIODE VOLTAGE	POWER (microwatts)
-160	3.99	24.31
-150	3.39	20.68
-140	2.77	16.89
-130	2.19	13.35
-120	1.44	8.79
-110	0.59	3.57
-100	0.08	0.48
-90	0.00	0.00
-80	0.03	0.18
-70	0.07	0.41
-60	0.11	0.68
-50	0.16	0.98
-40	0.22	1.37
-30	0.25	1.52
-20	0.29	1.79
-10	0.30	1.84
0	0.33	2.03
10	0.33	2.03
20	0.31	1.87
30	0.28	1.73
40	0.24	1.49
50	0.21	1.25
60	0.17	1.04
70	0.10	0.59
80	0.03	0.21
90	0.01	0.09
100	0.15	0.92
110	0.86	5.24
120	1.82	11.08
130	2.71	16.51
140	3.35	20.44
150	3.99	24.31
160	4.36	26.58

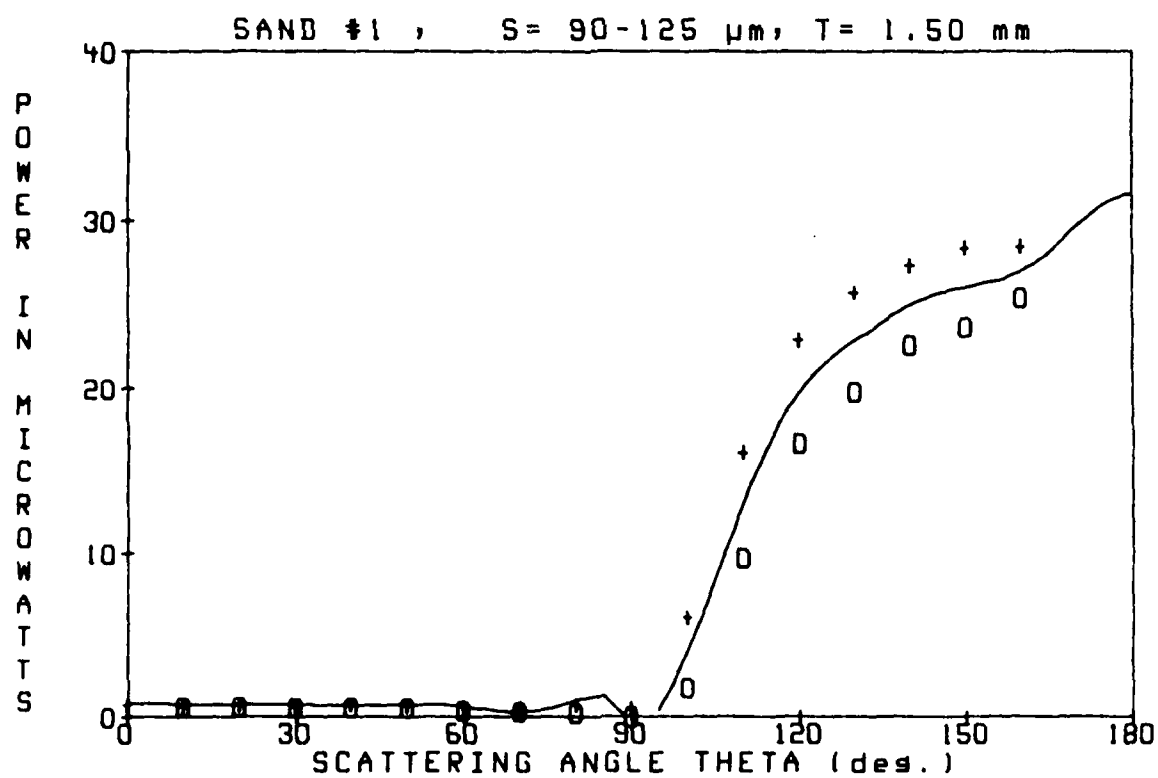
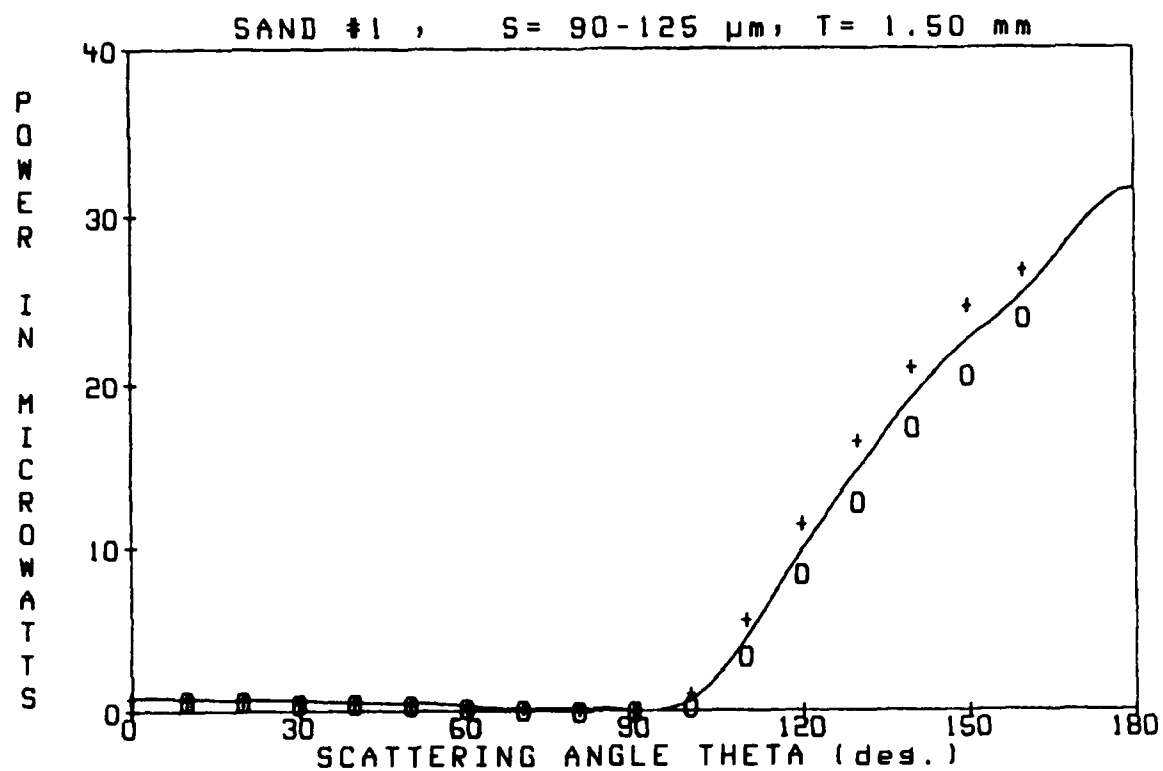


SAND #1

S= 90-125 μ m

T= 1.50 mm

SCATTERING ANGLE	DIODE VOLTAGE	POWER (microwatts)
-160	3.93	23.99
-150	3.36	20.50
-140	2.84	17.34
-130	2.09	12.75
-120	1.37	8.34
-110	0.55	3.34
-100	0.05	0.32
-90	0.00	0.00
-80	0.00	0.00
-70	0.02	0.12
-60	0.03	0.21
-50	0.07	0.41
-40	0.08	0.48
-30	0.09	0.53
-20	0.11	0.65
-10	0.11	0.68
0	0.14	0.83
10	0.12	0.74
20	0.13	0.80
30	0.10	0.59
40	0.11	0.65
50	0.08	0.48
60	0.06	0.35
70	0.03	0.21
80	0.02	0.15
90	0.00	0.00
100	0.17	1.07
110	0.91	5.54
120	1.89	11.50
130	2.72	16.60
140	3.44	21.01
150	4.04	24.67
160	4.40	26.82

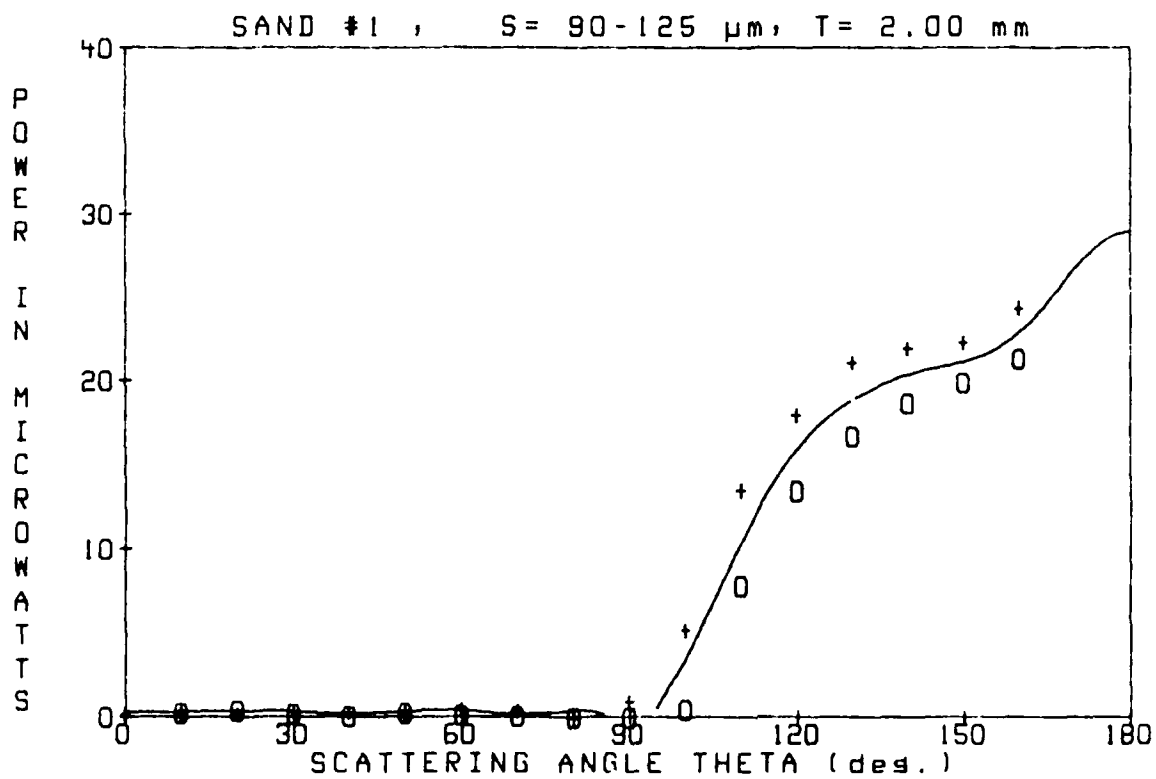
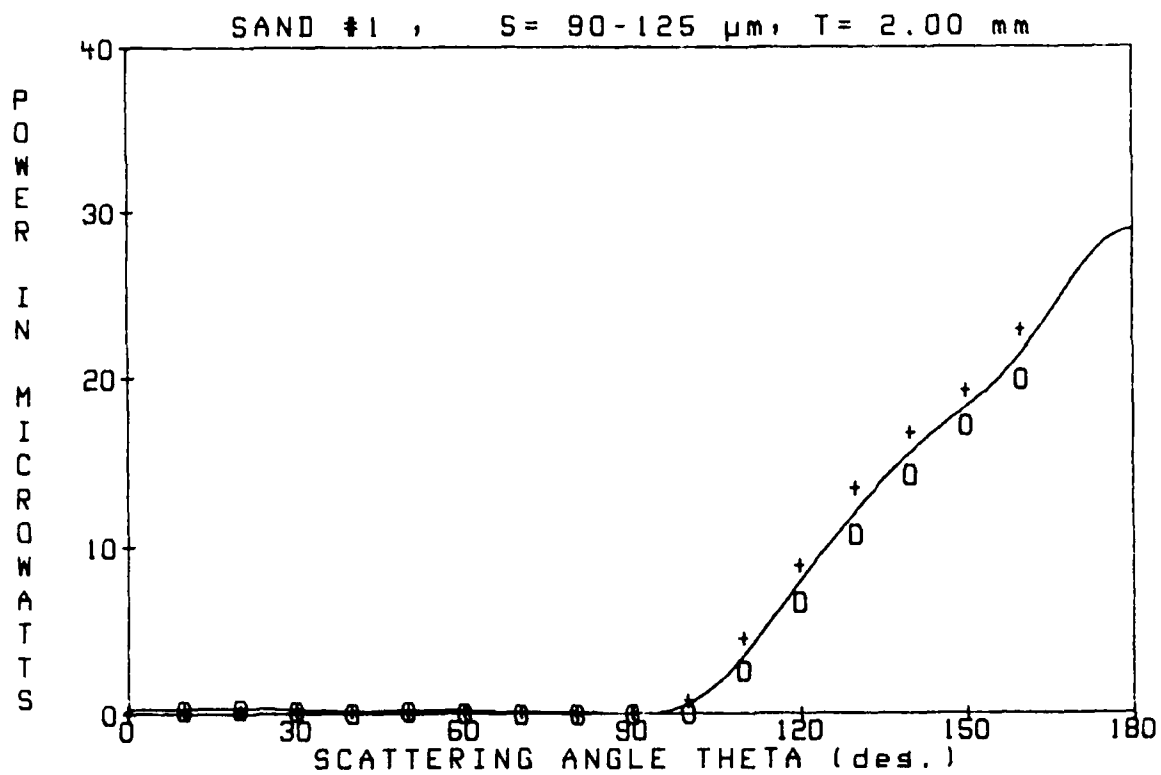


SAND #1

S= 90-125 μ m

T= 2.00 mm

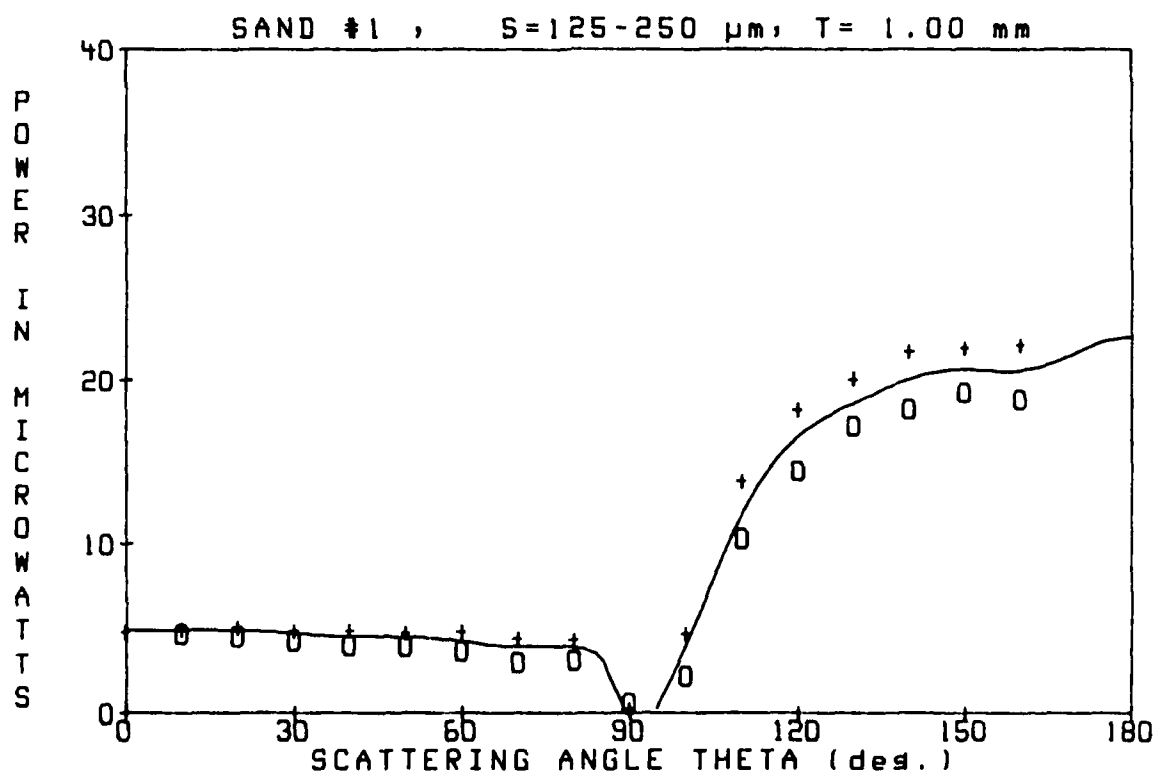
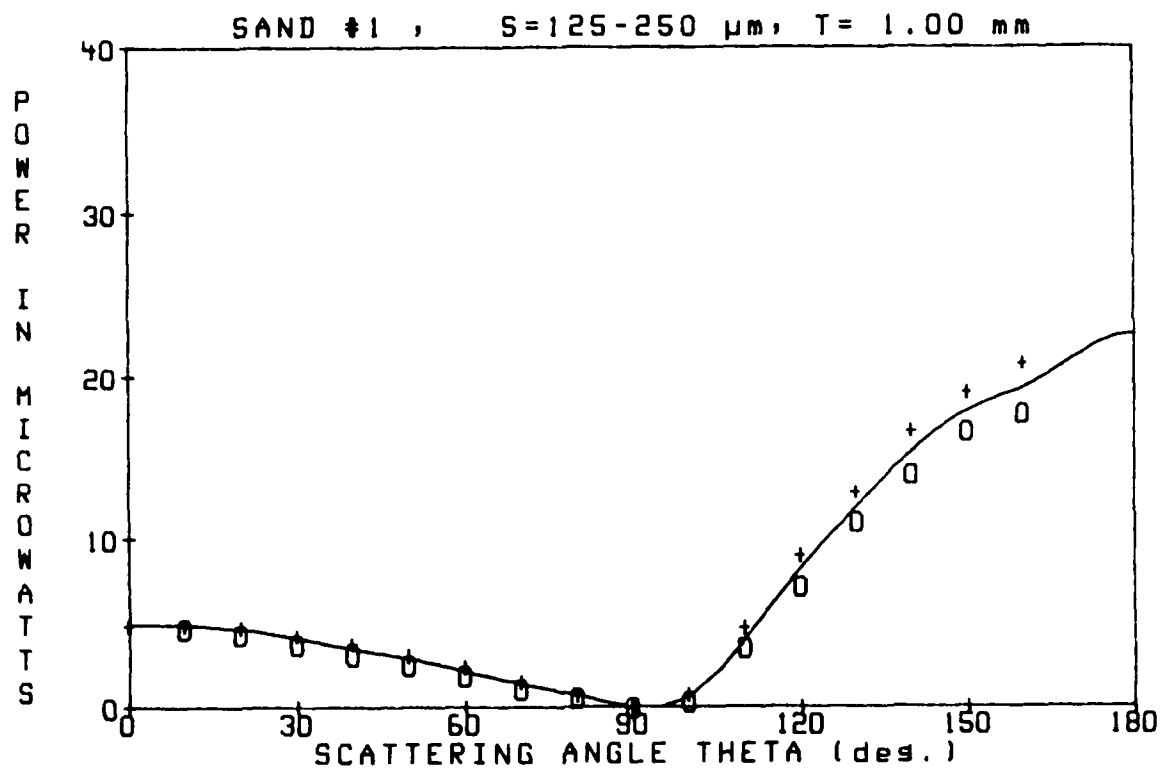
SCATTERING ANGLE	DIODE VOLTAGE	POWER (microwatts)
-160	3.28	19.99
-150	2.82	17.22
-140	2.34	14.27
-130	1.76	10.75
-120	1.10	6.70
-110	0.44	2.71
-100	0.01	0.09
-90	0.00	0.00
-80	0.00	0.00
-70	0.00	0.00
-60	0.01	0.09
-50	0.03	0.21
-40	0.01	0.09
-30	0.03	0.21
-20	0.06	0.38
-10	0.05	0.32
0	0.04	0.26
10	0.05	0.32
20	0.04	0.24
30	0.05	0.29
40	0.04	0.24
50	0.03	0.21
60	0.04	0.26
70	0.02	0.15
80	0.00	0.00
90	0.01	0.09
100	0.15	0.92
110	0.76	4.62
120	1.48	9.00
130	2.22	13.55
140	2.76	16.81
150	3.16	19.31
160	3.76	22.91



SAND #1

S=125-250 μm T= 1.00 mm

SCATTERING ANGLE	DIODE VOLTAGE	POWER (microwatts)
-160	2.91	17.73
-150	2.73	16.65
-140	2.29	13.94
-130	1.82	11.08
-120	1.18	7.21
-110	0.58	3.54
-100	0.06	0.38
-90	0.00	0.00
-80	0.09	0.56
-70	0.17	1.07
-60	0.31	1.87
-50	0.43	2.59
-40	0.52	3.15
-30	0.62	3.78
-20	0.71	4.35
-10	0.77	4.70
0	0.80	4.89
10	0.81	4.94
20	0.79	4.83
30	0.71	4.32
40	0.63	3.81
50	0.51	3.10
60	0.40	2.44
70	0.25	1.55
80	0.13	0.77
90	0.00	0.00
100	0.14	0.83
110	0.78	4.73
120	1.49	9.11
130	2.12	12.93
140	2.73	16.68
150	3.12	19.04
160	3.42	20.86

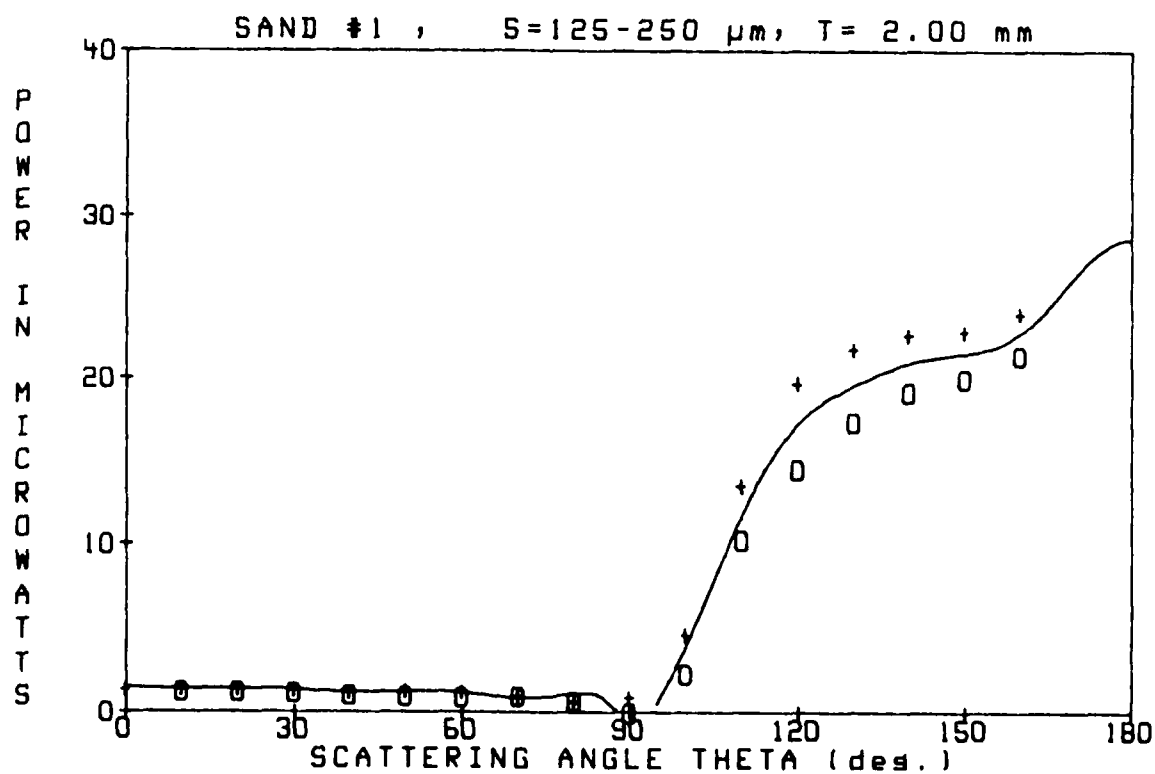
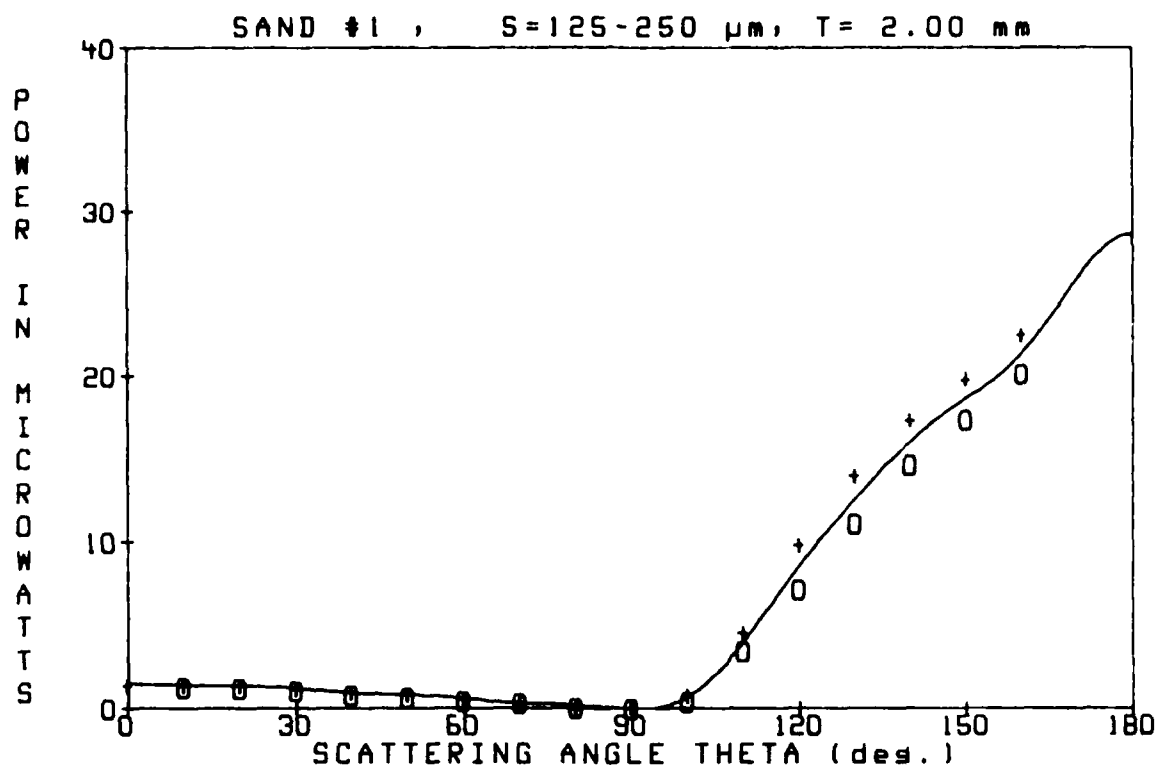


SAND #1

S=125-250 μ m

T= 2.00 mm

SCATTERING ANGLE	DIODE VOLTAGE	POWER (microwatts)
-160	3.30	20.14
-150	2.85	17.37
-140	2.40	14.66
-130	1.83	11.17
-120	1.19	7.27
-110	0.58	3.51
-100	0.07	0.41
-90	0.00	0.00
-80	0.02	0.12
-70	0.06	0.35
-60	0.08	0.48
-50	0.11	0.66
-40	0.14	0.86
-30	0.17	1.07
-20	0.21	1.25
-10	0.21	1.31
0	0.23	1.43
10	0.24	1.46
20	0.23	1.43
30	0.21	1.25
40	0.17	1.01
50	0.15	0.89
60	0.11	0.65
70	0.06	0.35
80	0.02	0.12
90	0.01	0.09
100	0.14	0.83
110	0.76	4.65
120	1.62	9.89
130	2.30	14.03
140	2.85	17.37
150	3.25	19.84
160	3.70	22.58

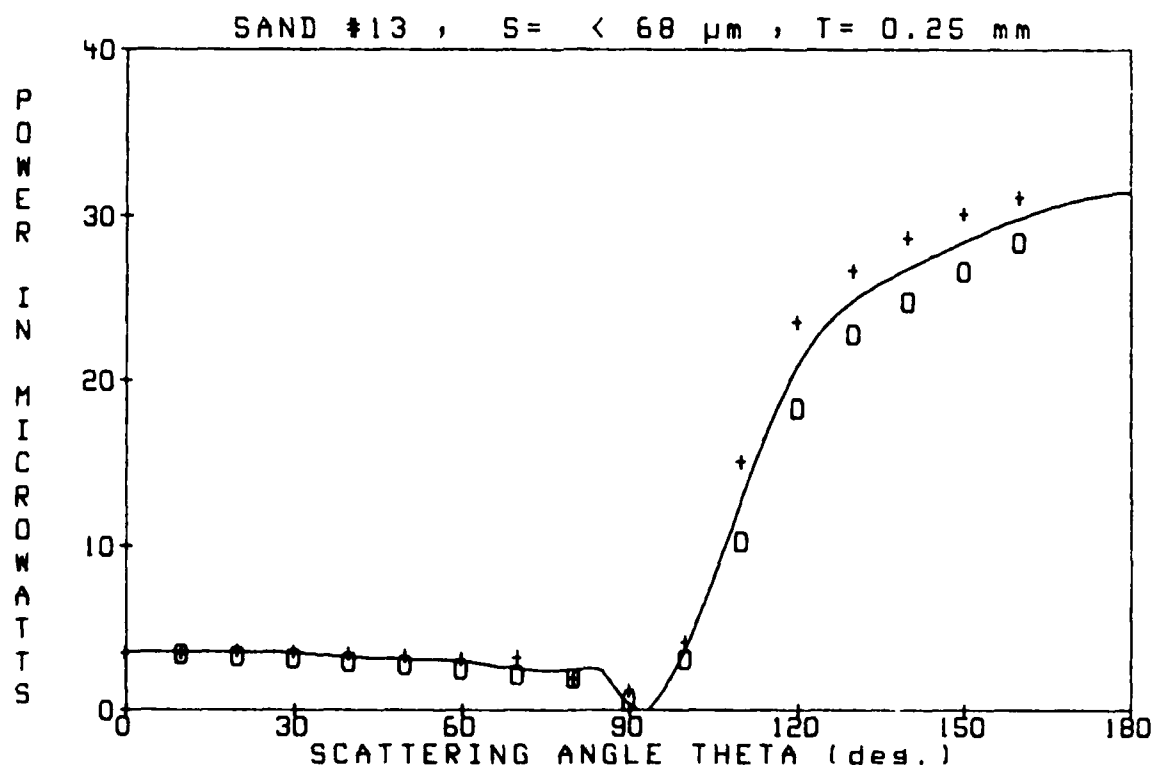
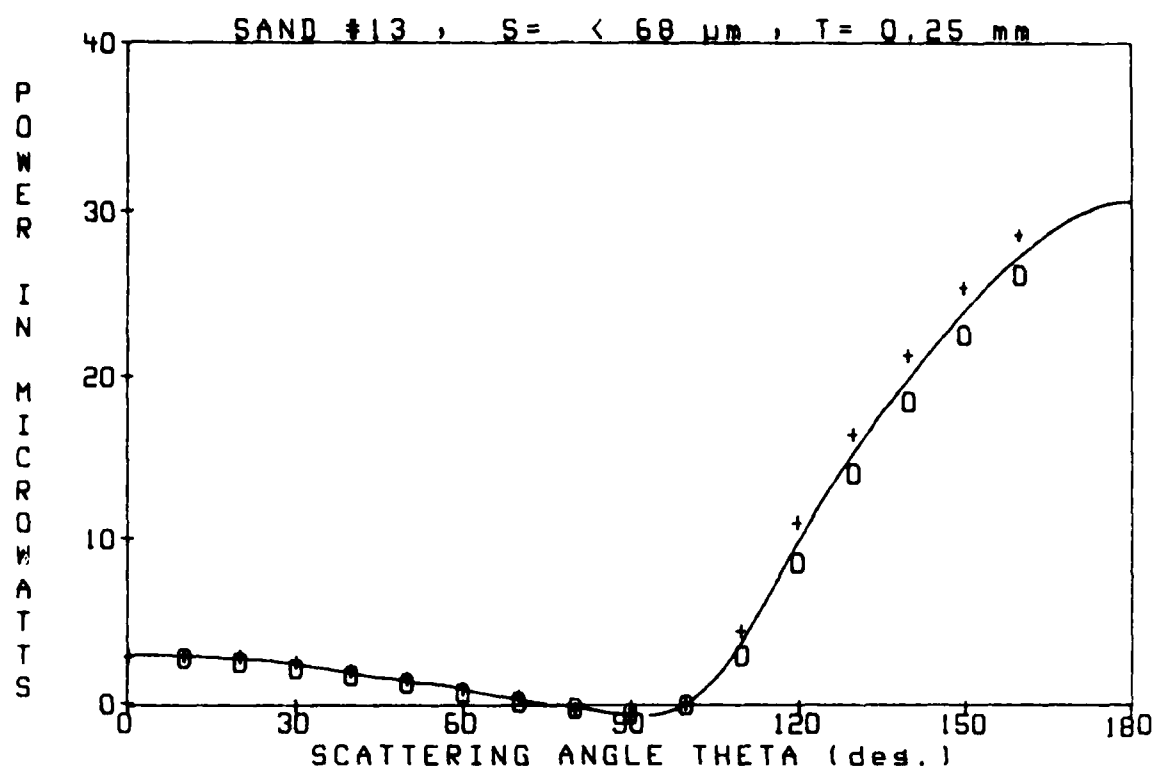


SAND #13

S= < 68 μ m

T= 0.25 mm

SCATTERING ANGLE	DIODE VOLTAGE	POWER (microwatts)
-160	4.39	26.75
-150	3.79	23.09
-140	3.12	19.04
-130	2.40	14.66
-120	1.50	9.17
-110	0.58	3.54
-100	0.09	0.56
-90	0.00	0.00
-80	0.06	0.35
-70	0.13	0.77
-60	0.21	1.31
-50	0.31	1.87
-40	0.39	2.38
-30	0.46	2.83
-20	0.53	3.25
-10	0.57	3.48
0	0.59	3.61
10	0.59	3.61
20	0.58	3.54
30	0.53	3.21
40	0.44	2.71
50	0.36	2.20
60	0.26	1.60
70	0.19	1.16
80	0.06	0.35
90	0.02	0.12
100	0.12	0.74
110	0.85	5.19
120	1.93	11.80
130	2.82	17.19
140	3.61	22.05
150	4.29	26.16
160	4.82	29.38

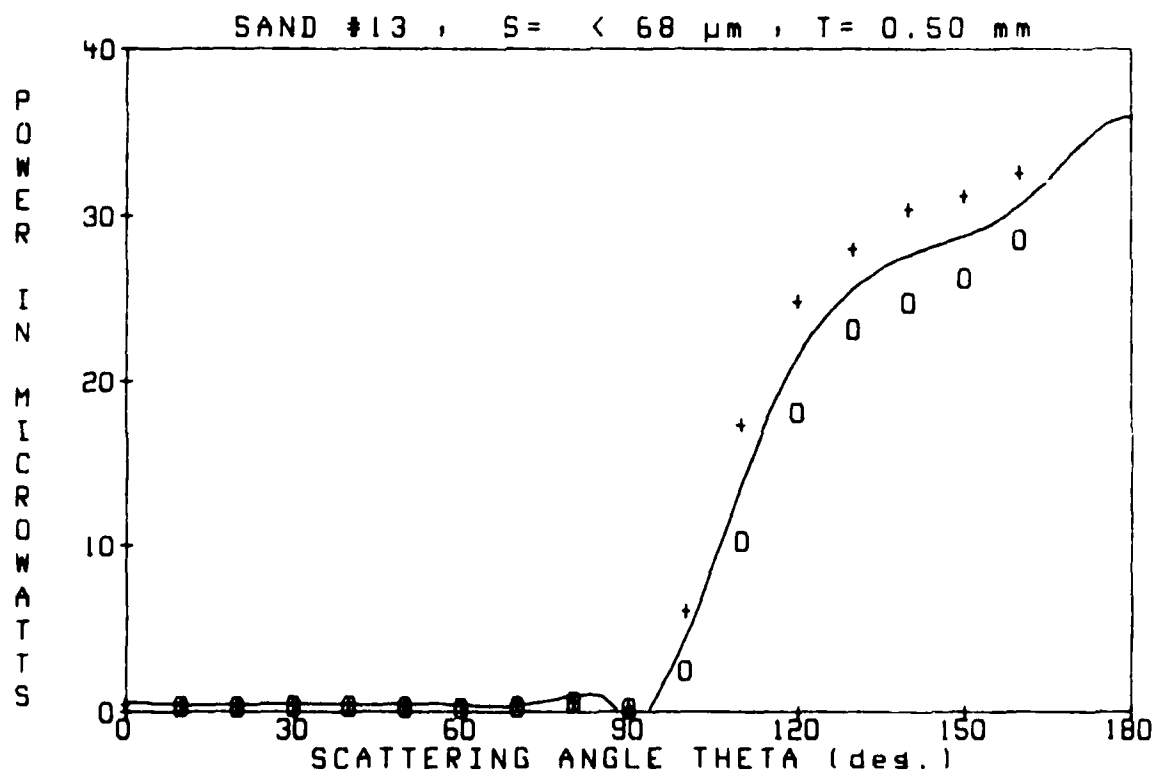
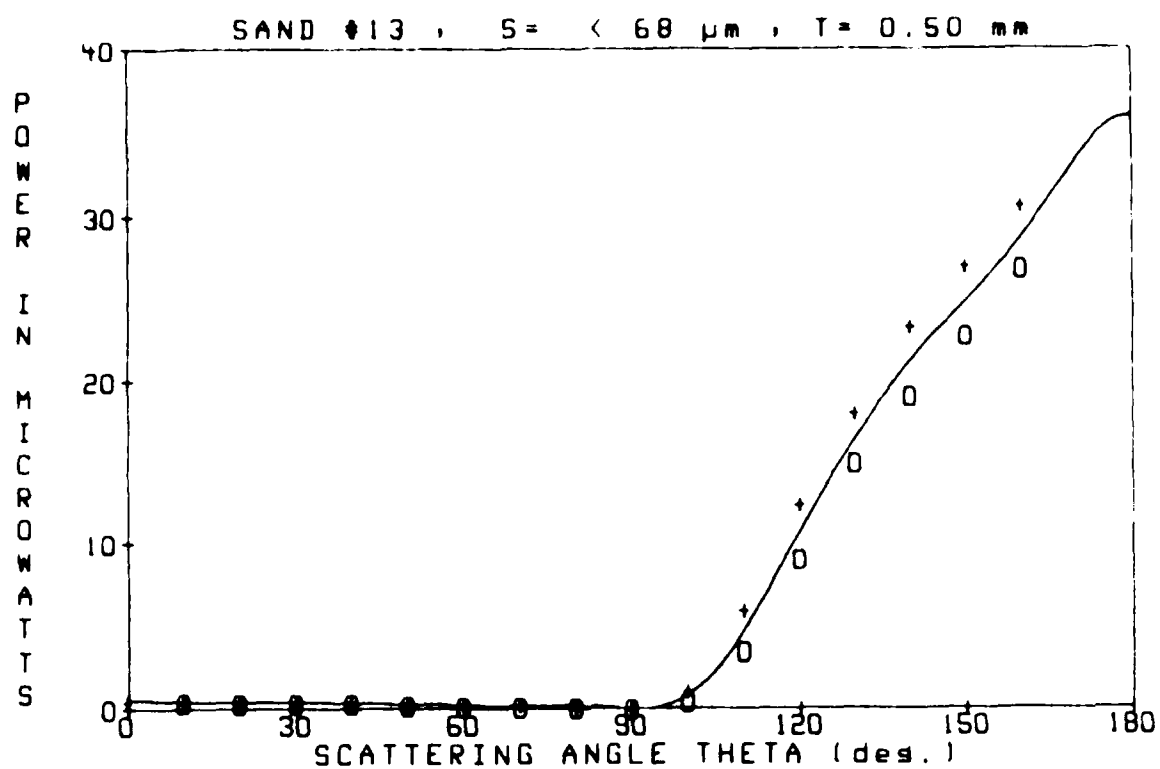


SAND #13

S = < 68 μ m

T = 0.50 mm

SCATTERING ANGLE	DIODE VOLTAGE	POWER (microwatts)
-160	4.41	26.88
-150	3.74	22.80
-140	3.12	19.01
-130	2.44	14.90
-120	1.48	9.06
-110	0.58	3.51
-100	0.07	0.45
-90	0.00	0.00
-80	0.02	0.12
-70	0.02	0.12
-60	0.02	0.15
-50	0.04	0.24
-40	0.06	0.35
-30	0.06	0.35
-20	0.06	0.35
-10	0.07	0.41
0	0.08	0.48
10	0.08	0.51
20	0.07	0.41
30	0.07	0.41
40	0.07	0.41
50	0.04	0.26
60	0.04	0.26
70	0.03	0.21
80	0.02	0.12
90	0.00	0.00
100	0.17	1.07
110	0.97	5.93
120	2.04	12.46
130	2.96	18.03
140	3.83	23.36
150	4.44	27.11
160	5.04	30.72

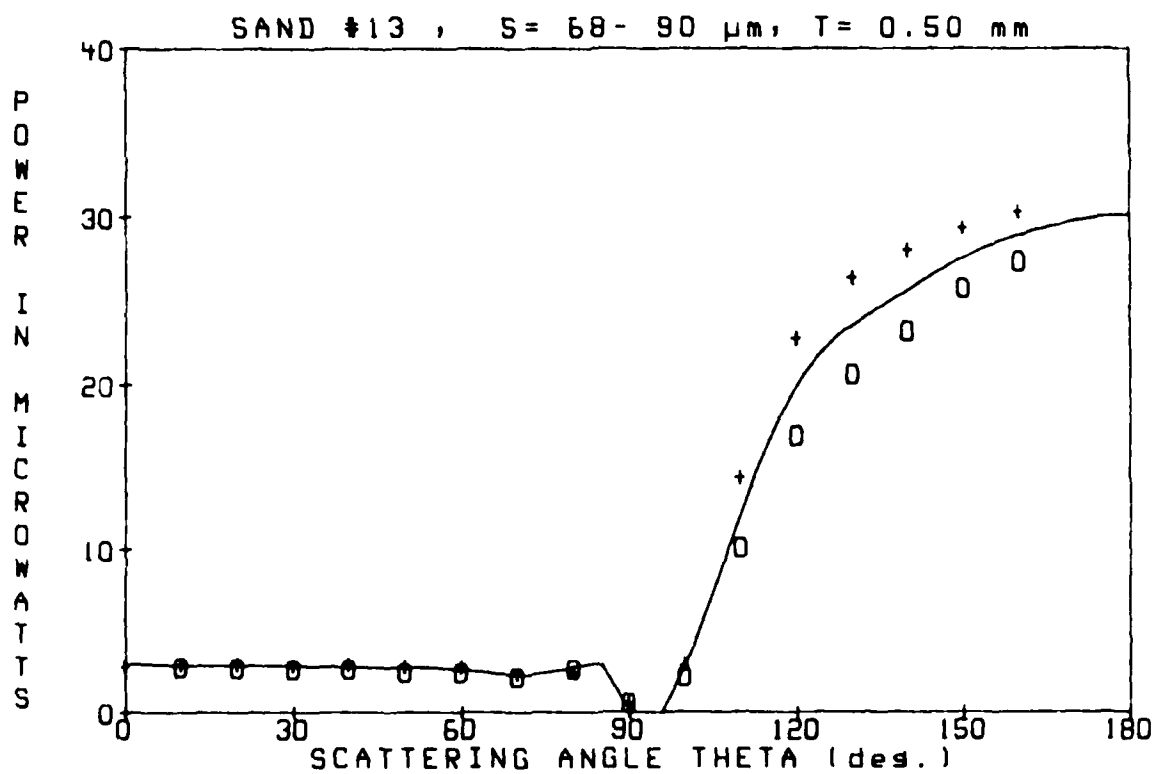
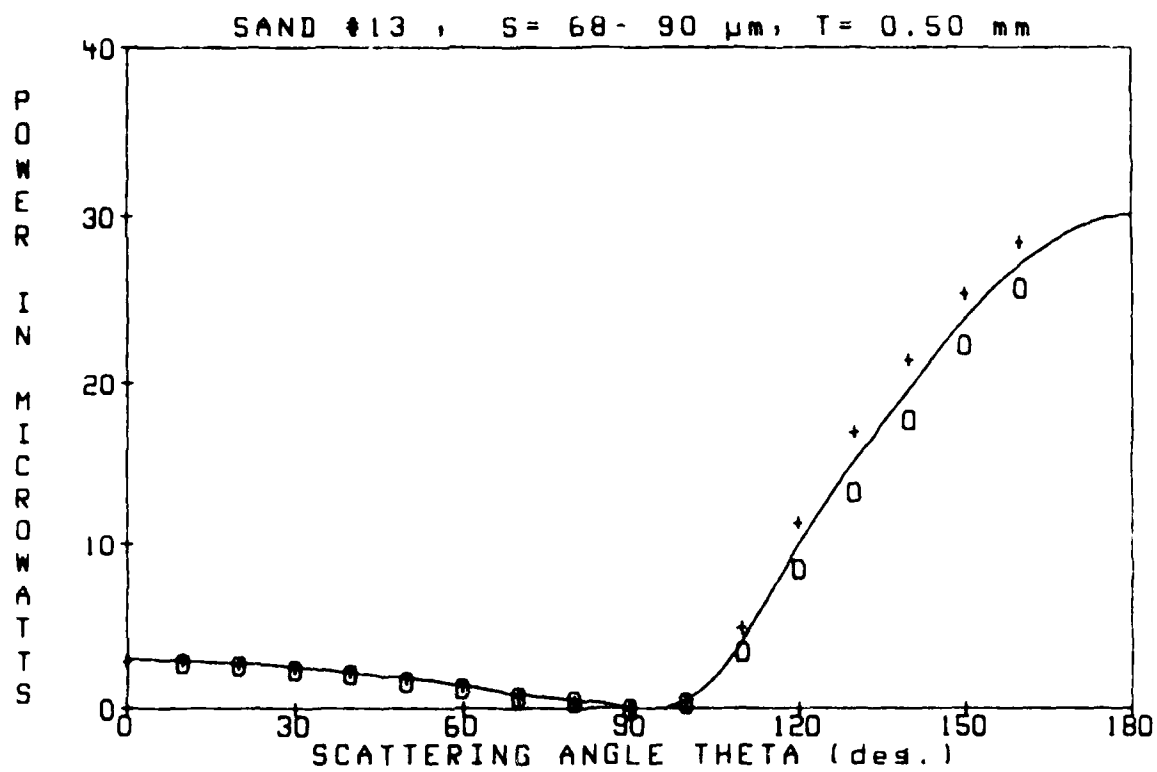


SAND #13

S= 68- 90 μ m

T= 0.50 mm

SCATTERING ANGLE		DIODE VOLTAGE		POWER (microwatts)
-160		4.23		25.80
-150		3.67		22.37
-140		2.92		17.79
-130		2.18		13.29
-120		1.39		8.49
-110		0.57		3.48
-100		0.06		0.38
-90		0.00		0.00
-80		0.08		0.48
-70		0.13		0.77
-60		0.21		1.25
-50		0.27		1.63
-40		0.35		2.11
-30		0.39		2.38
-20		0.44		2.68
-10		0.46		2.83
0		0.49		2.95
10		0.49		3.01
20		0.46		2.83
30		0.43		2.59
40		0.38		2.32
50		0.31		1.87
60		0.24		1.46
70		0.14		0.83
80		0.07		0.45
90		0.00		0.00
100		0.09		0.53
110		0.81		4.94
120		1.87		11.41
130		2.79		17.04
140		3.53		21.51
150		4.18		25.47
160		4.69		28.60

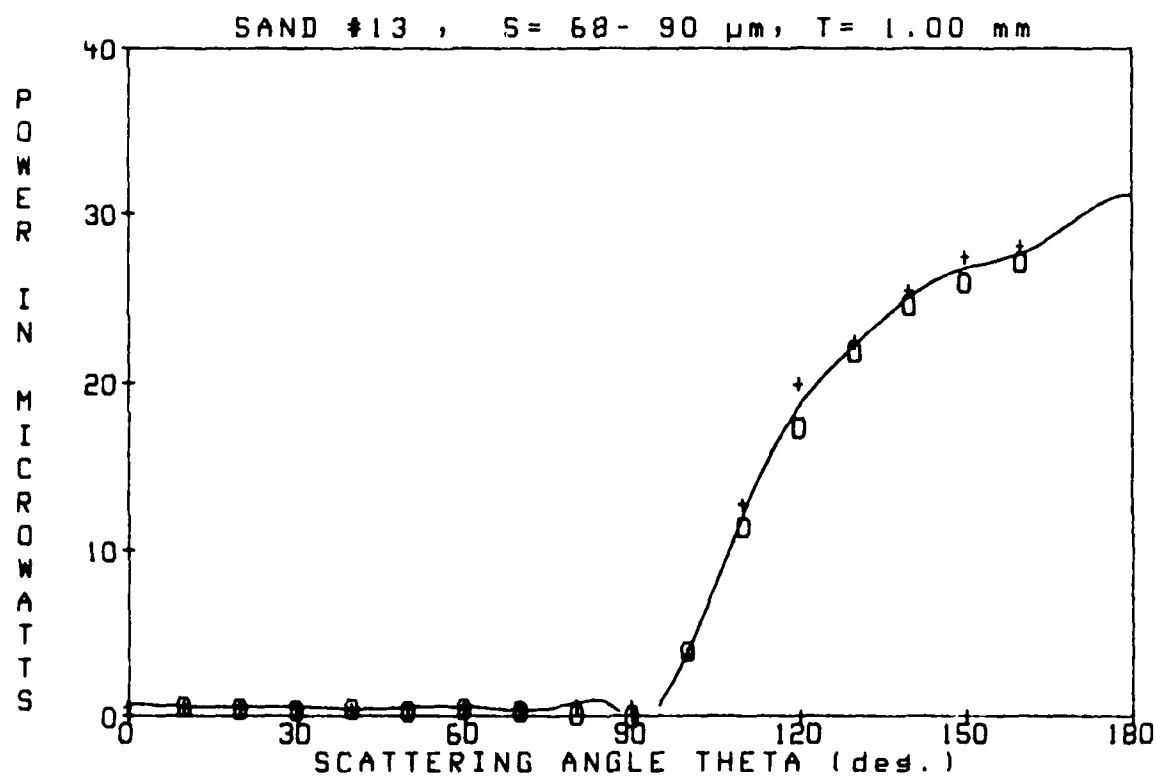
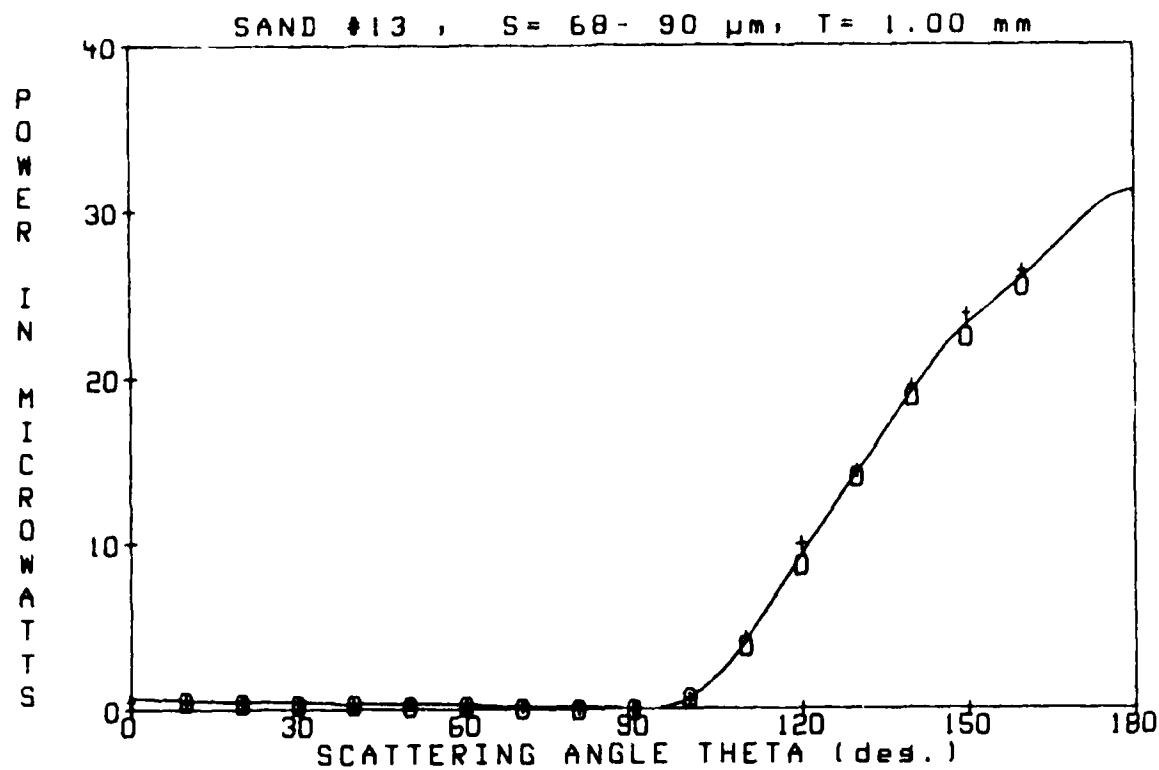


SAND #13

S= 68- 90 μ m

T= 1.00 mm

SCATTERING ANGLE	DIODE VOLTAGE	POWER (microwatts)
-160	4.18	25.50
-150	3.68	22.47
-140	3.10	18.89
-130	2.30	14.06
-120	1.43	8.73
-110	0.64	3.93
-100	0.11	0.68
-90	0.00	0.00
-80	0.00	0.00
-70	0.02	0.12
-60	0.04	0.24
-50	0.04	0.24
-40	0.06	0.38
-30	0.06	0.38
-20	0.07	0.45
-10	0.10	0.59
0	0.10	0.59
10	0.10	0.59
20	0.09	0.53
30	0.08	0.48
40	0.06	0.35
50	0.06	0.35
60	0.04	0.26
70	0.03	0.21
80	0.02	0.12
90	0.00	0.00
100	0.11	0.65
110	0.72	4.41
120	1.64	10.01
130	2.37	14.45
140	3.20	19.54
150	3.90	23.81
160	4.33	26.43

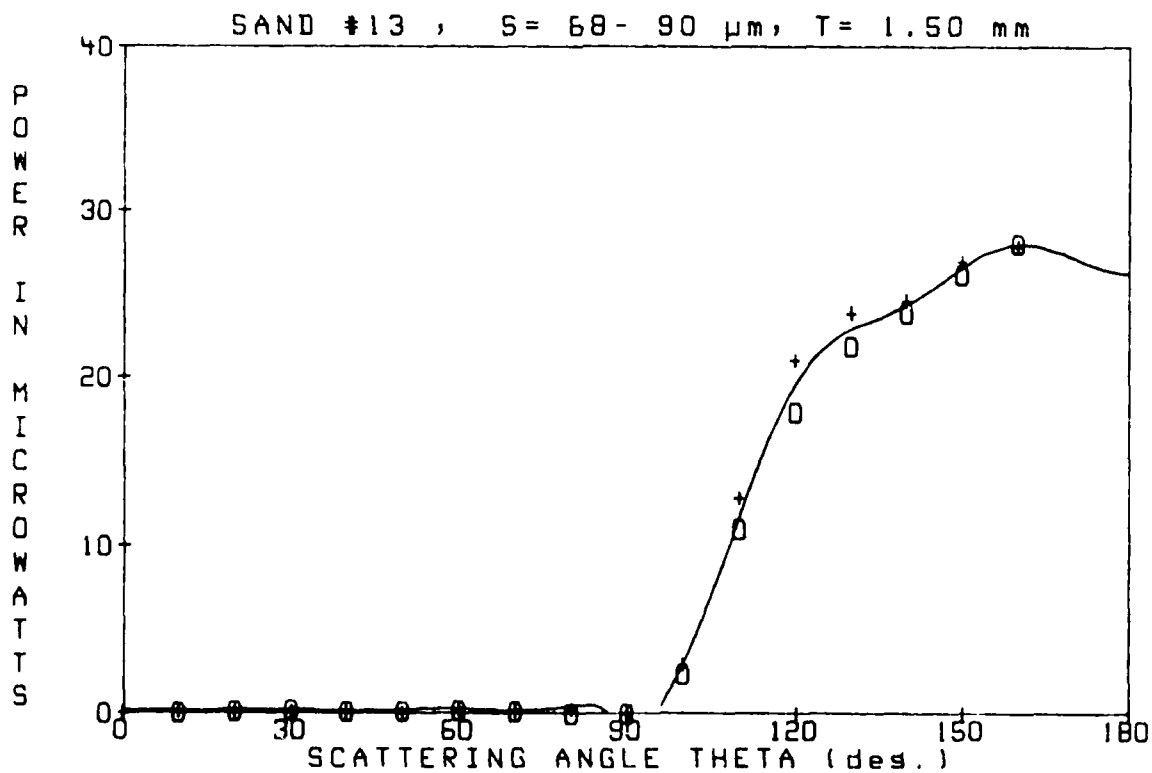
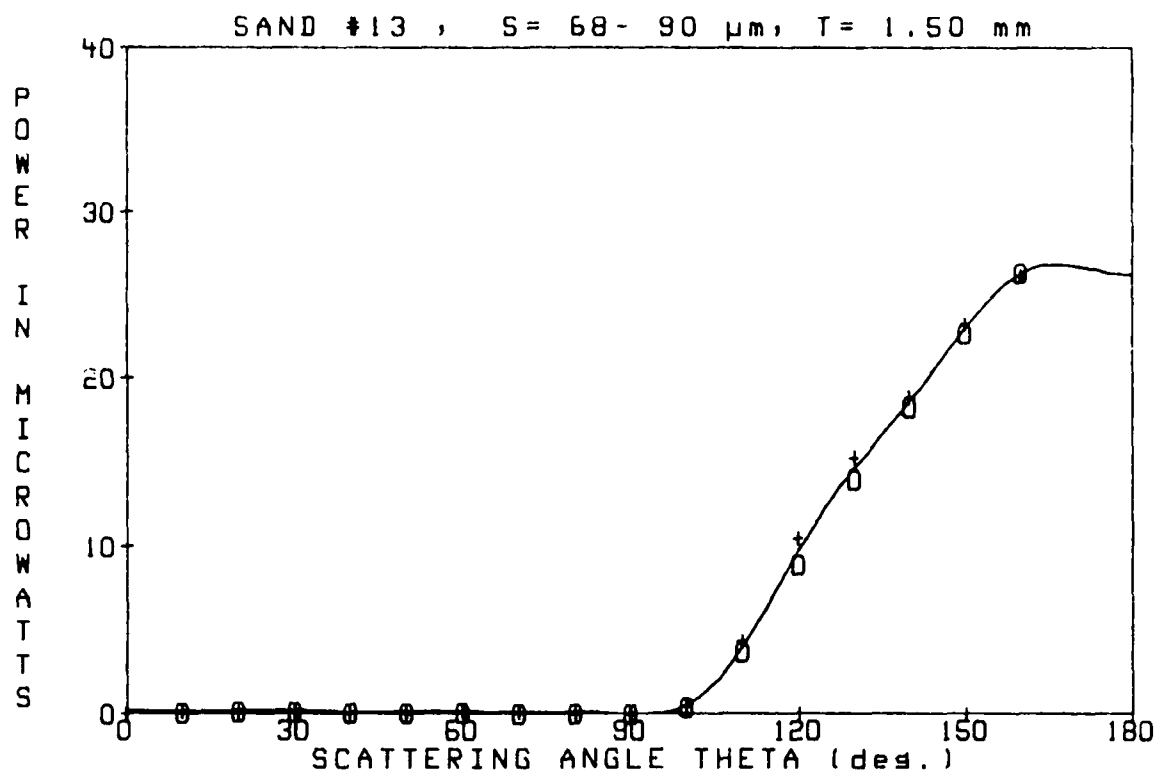


SAND #13

S= 68- 90 μ m

T= 1.50 mm

SCATTERING ANGLE	DIODE VOLTAGE	POWER (microwatts)
-160	4.32	26.34
-150	3.72	22.67
-140	3.00	18.32
-130	2.30	14.06
-120	1.48	9.00
-110	0.62	3.78
-100	0.07	0.41
-90	0.00	0.00
-80	0.00	0.00
-70	0.00	0.00
-60	0.02	0.12
-50	0.02	0.12
-40	0.02	0.12
-30	0.03	0.18
-20	0.03	0.18
-10	0.02	0.12
0	0.02	0.12
10	0.03	0.18
20	0.03	0.18
30	0.02	0.15
40	0.02	0.12
50	0.01	0.09
60	0.02	0.15
70	0.01	0.09
80	0.00	0.00
90	0.00	0.00
100	0.09	0.53
110	0.72	4.41
120	1.73	10.55
130	2.52	15.37
140	3.10	18.89
150	3.83	23.33
160	4.30	26.22

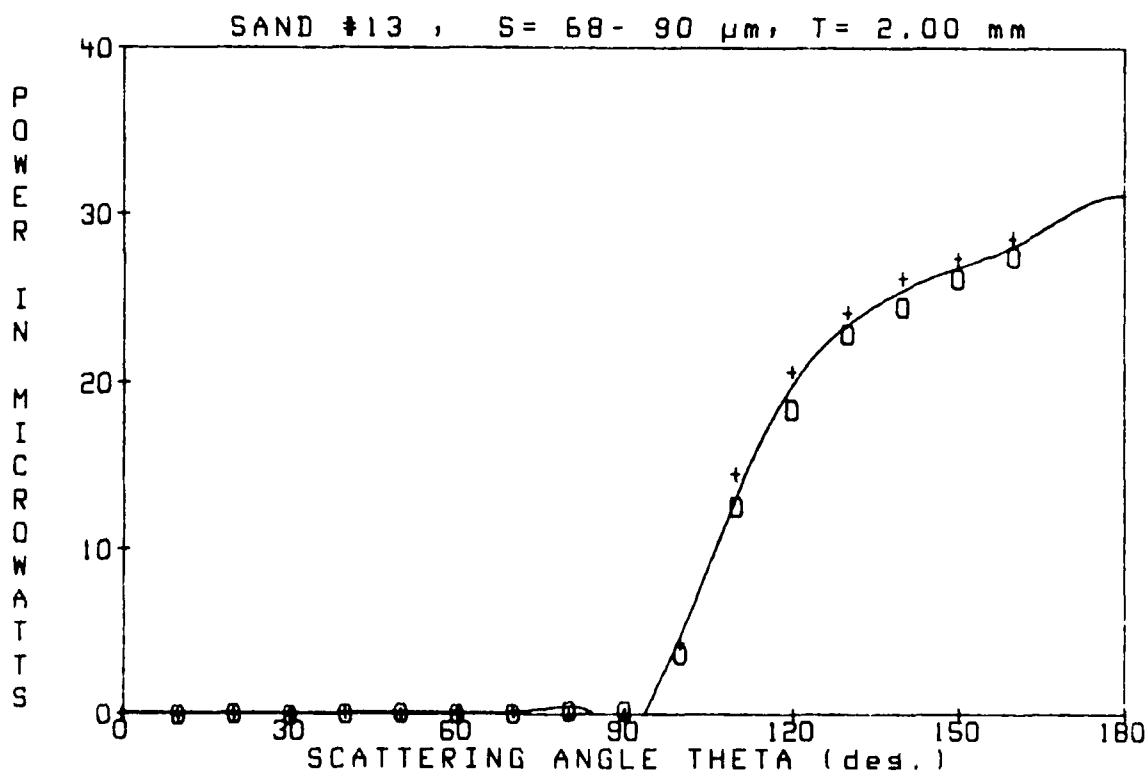
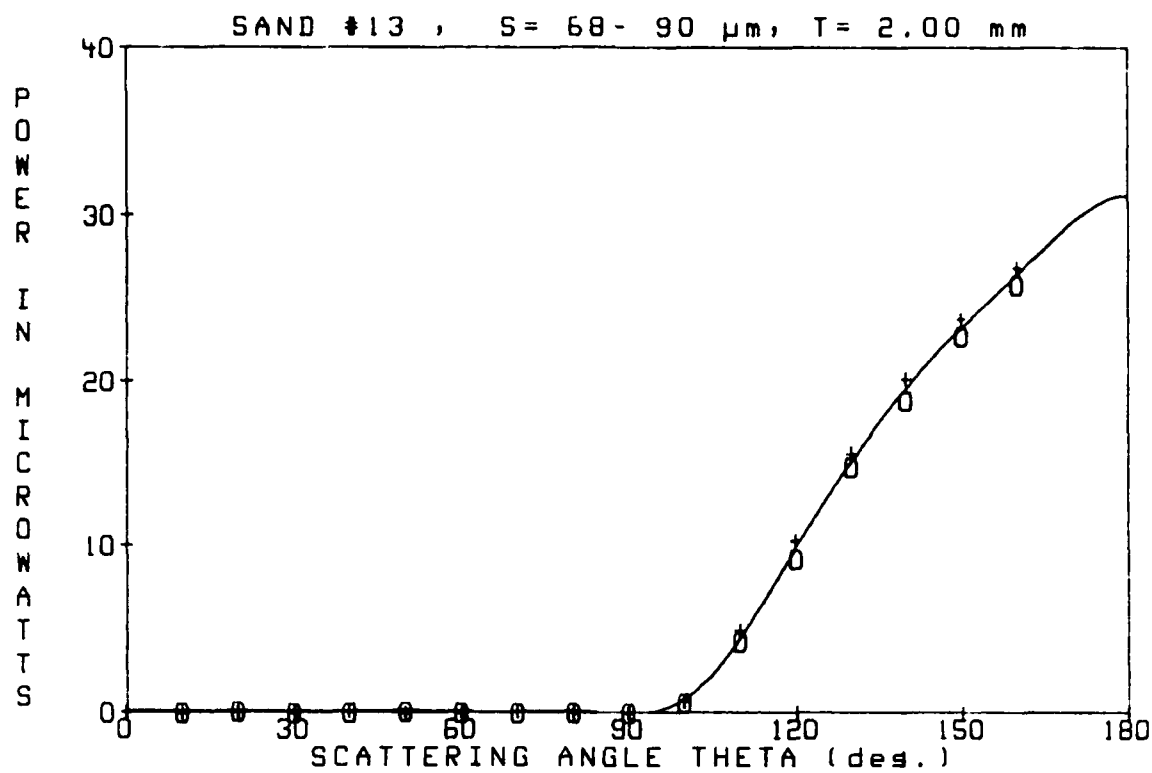


SAND #13

S= 68- 90 μ m

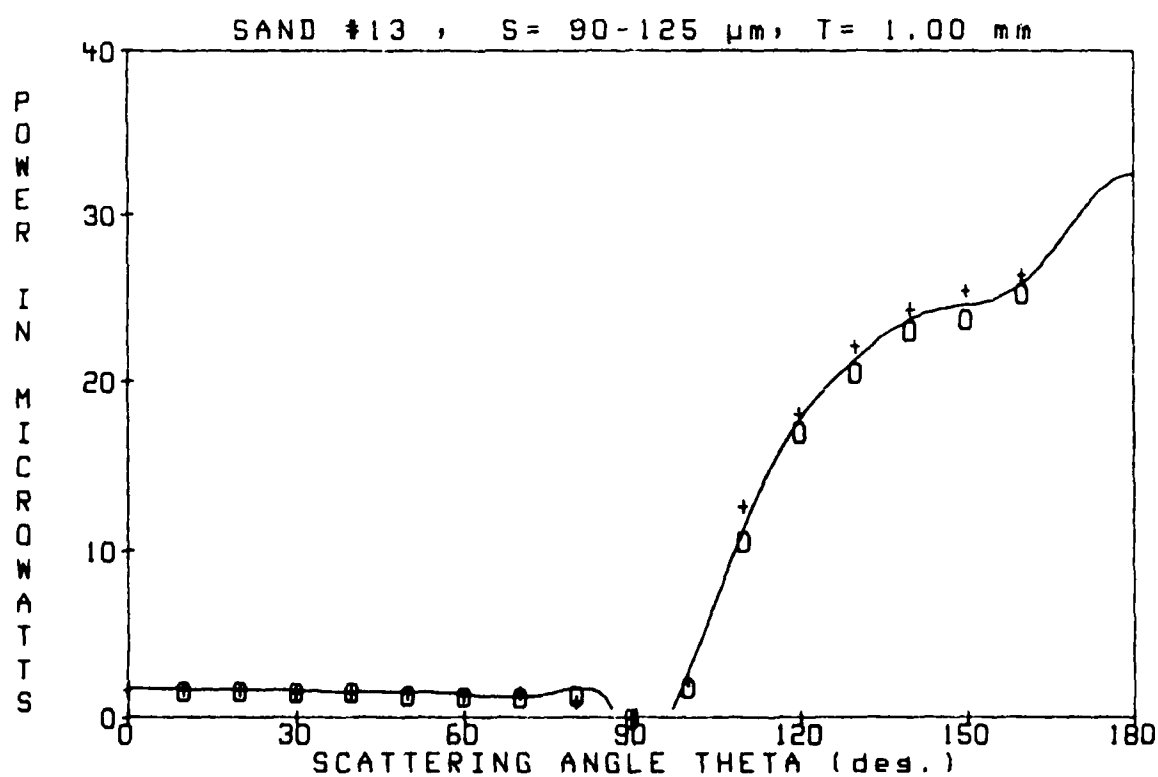
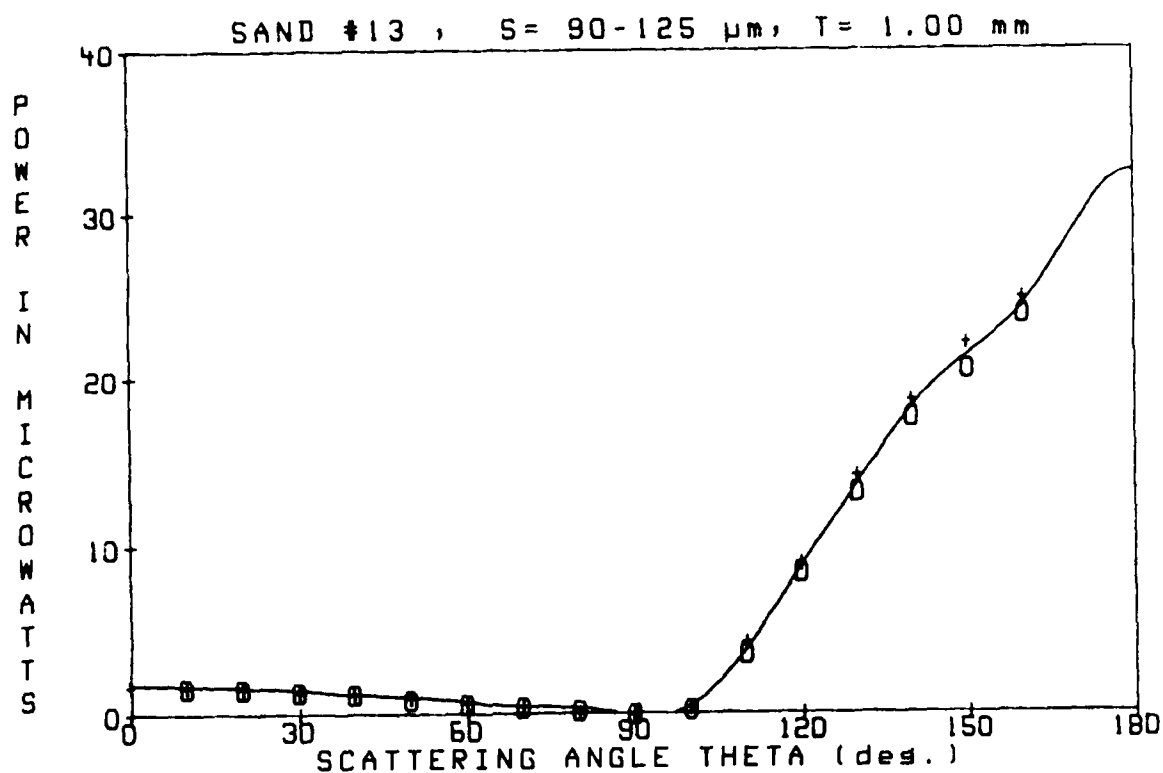
T= 2.00 mm

SCATTERING ANGLE	DIODE VOLTAGE	POWER (microwatts)
-160	4.25	25.92
-150	3.74	22.80
-140	3.09	18.86
-130	2.42	14.78
-120	1.52	9.27
-110	0.71	4.35
-100	0.11	0.65
-90	0.00	0.00
-80	0.00	0.00
-70	0.00	0.00
-60	0.00	0.00
-50	0.02	0.12
-40	0.00	0.00
-30	0.00	0.00
-20	0.02	0.12
-10	0.00	0.00
0	0.02	0.12
10	0.00	0.00
20	0.01	0.09
30	0.00	0.00
40	0.02	0.12
50	0.00	0.00
60	0.00	0.00
70	0.01	0.09
80	0.00	0.00
90	0.00	0.00
100	0.13	0.77
110	0.82	5.00
120	1.70	10.39
130	2.56	15.61
140	3.31	20.20
150	3.90	23.81
160	4.43	26.99



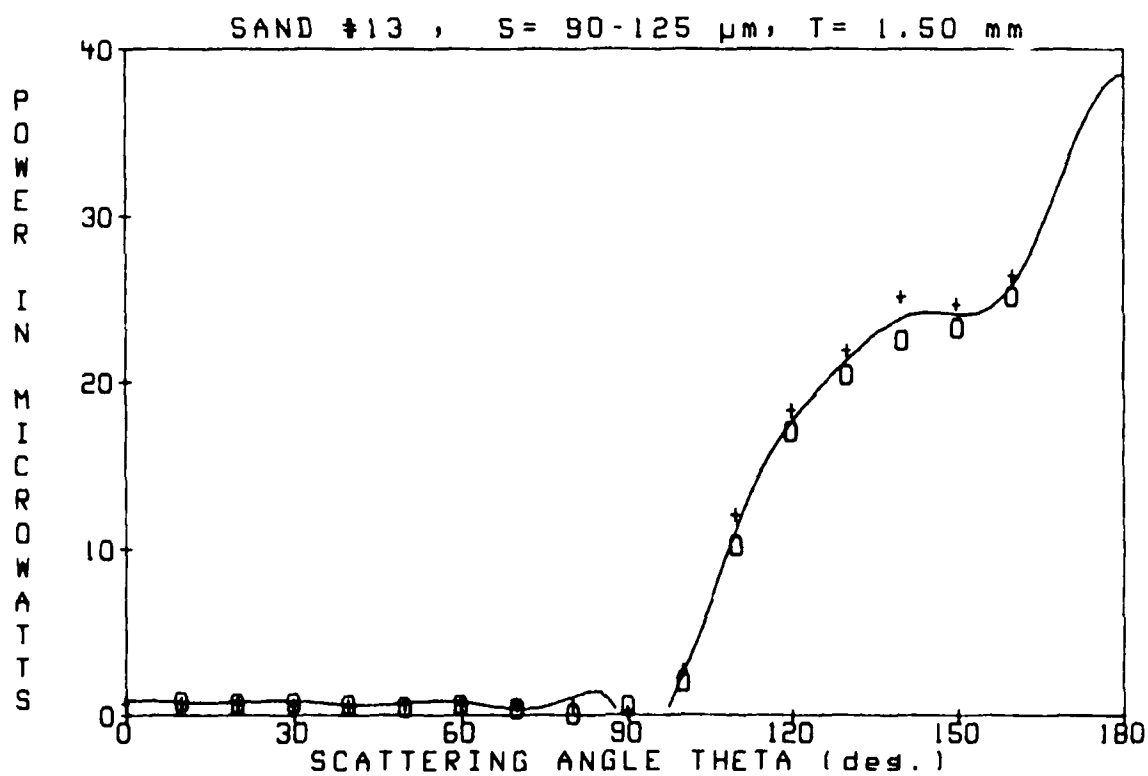
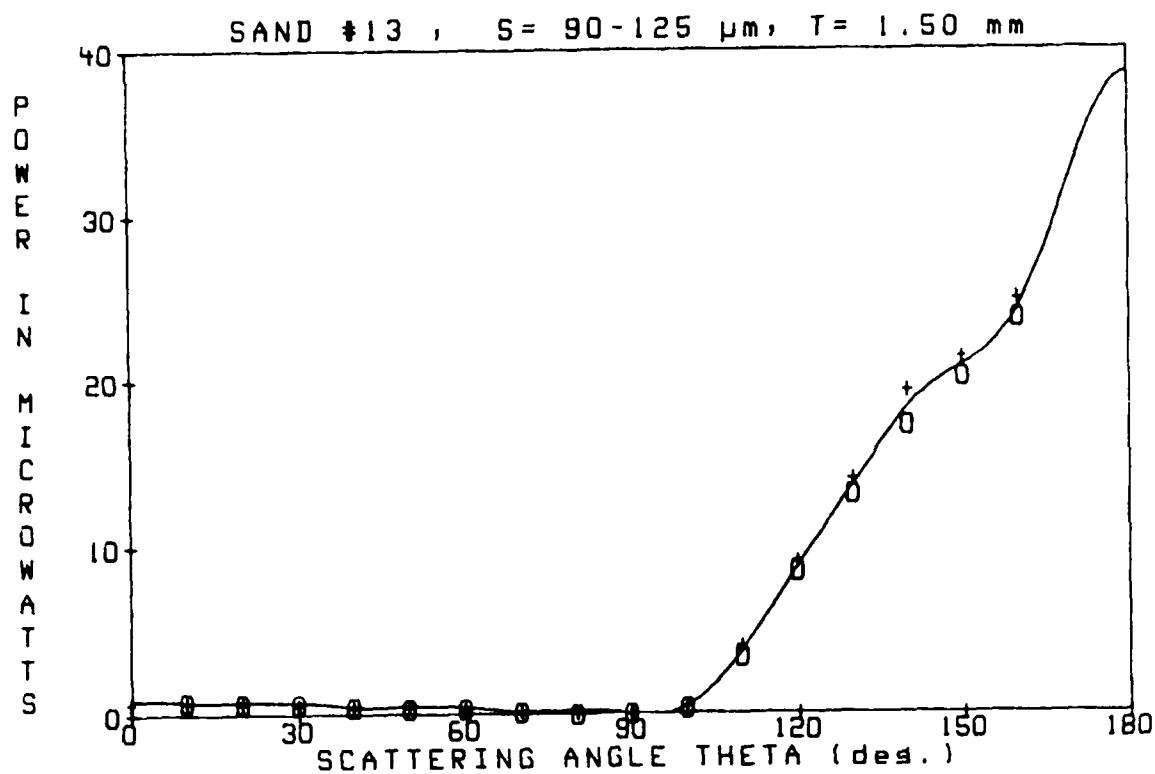
SAND #13 S= 90-125 μ m T= 1.00 mm

SCATTERING ANGLE		DIODE VOLTAGE		POWER (microwatts)
-160		3.89		23.75
-150		3.36		20.50
-140		2.89		17.64
-130		2.17		13.23
-120		1.40		8.52
-110		0.60		3.63
-100		0.05		0.32
-90		0.00		0.00
-80		0.04		0.24
-70		0.07		0.41
-60		0.11		0.65
-50		0.15		0.89
-40		0.20		1.22
-30		0.22		1.34
-20		0.25		1.55
-10		0.26		1.60
0		0.29		1.76
10		0.28		1.73
20		0.27		1.67
30		0.22		1.37
40		0.20		1.22
50		0.17		1.01
60		0.12		0.71
70		0.09		0.53
80		0.03		0.18
90		0.00		0.00
100		0.07		0.41
110		0.71		4.35
120		1.48		9.06
130		2.34		14.24
140		3.06		18.65
150		3.62		22.08
160		4.07		24.85



SAND #13 S= 90-125 μ m T= 1.50 mm

SCATTERING ANGLE	DIODE VOLTAGE	POWER (microwatts)
-160	3.88	23.69
-150	3.31	20.20
-140	2.84	17.31
-130	2.16	13.17
-120	1.40	8.55
-110	0.58	3.51
-100	0.06	0.35
-90	0.00	0.00
-80	0.00	0.00
-70	0.03	0.18
-60	0.06	0.35
-50	0.06	0.38
-40	0.09	0.53
-30	0.12	0.71
-20	0.12	0.71
-10	0.14	0.86
0	0.13	0.77
10	0.14	0.83
20	0.12	0.71
30	0.10	0.62
40	0.08	0.51
50	0.08	0.48
60	0.06	0.35
70	0.04	0.26
80	0.02	0.12
90	0.00	0.00
100	0.08	0.48
110	0.68	4.17
120	1.50	9.17
130	2.32	14.12
140	3.17	19.34
150	3.52	21.45
160	4.08	24.91

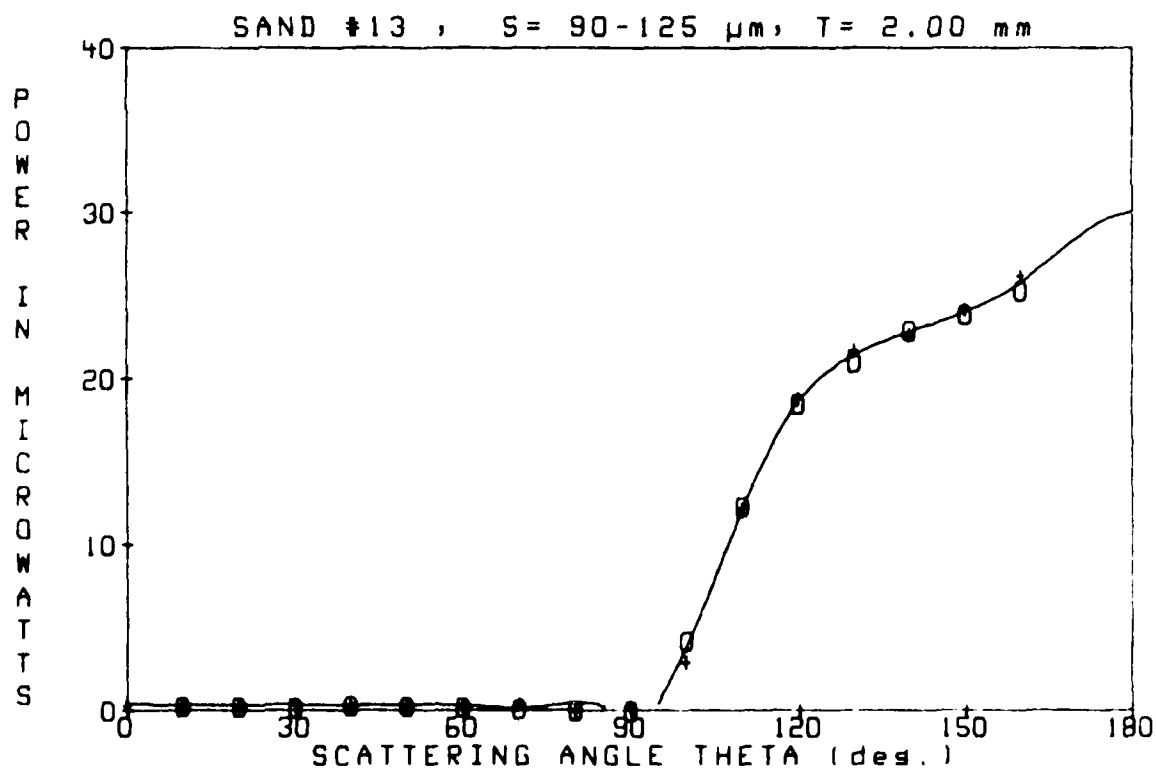
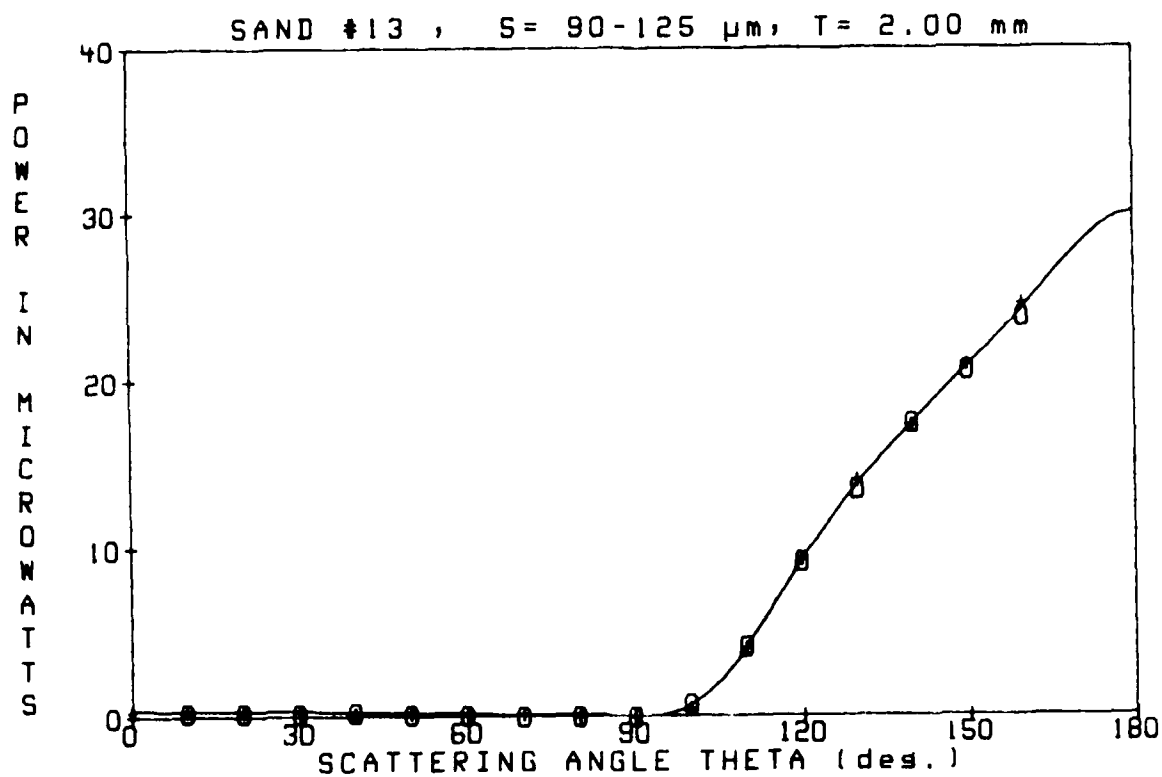


SAND #13

S= 90-125 μ m

T= 2.00 mm

SCATTERING ANGLE	DIODE VOLTAGE	POWER (microwatts)
-160	3.90	23.78
-150	3.38	20.62
-140	2.87	17.52
-130	2.22	13.52
-120	1.51	9.24
-110	0.69	4.23
-100	0.12	0.74
-90	0.00	0.00
-80	0.00	0.00
-70	0.00	0.00
-60	0.02	0.12
-50	0.03	0.18
-40	0.05	0.29
-30	0.03	0.21
-20	0.05	0.29
-10	0.05	0.29
0	0.06	0.35
10	0.06	0.38
20	0.06	0.35
30	0.06	0.35
40	0.04	0.26
50	0.04	0.24
60	0.02	0.15
70	0.03	0.18
80	0.00	0.00
90	0.00	0.00
100	0.09	0.53
110	0.69	4.20
120	1.54	9.41
130	2.30	14.01
140	2.85	17.40
150	3.43	20.95
160	4.04	24.64

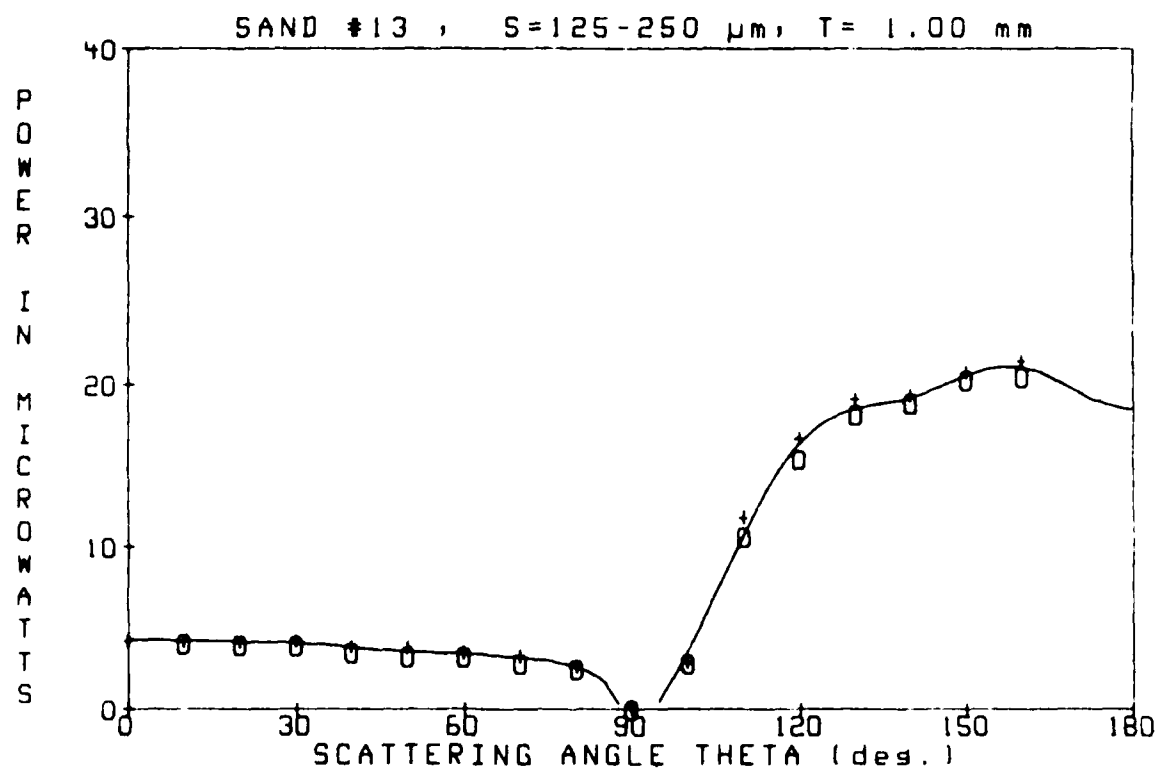
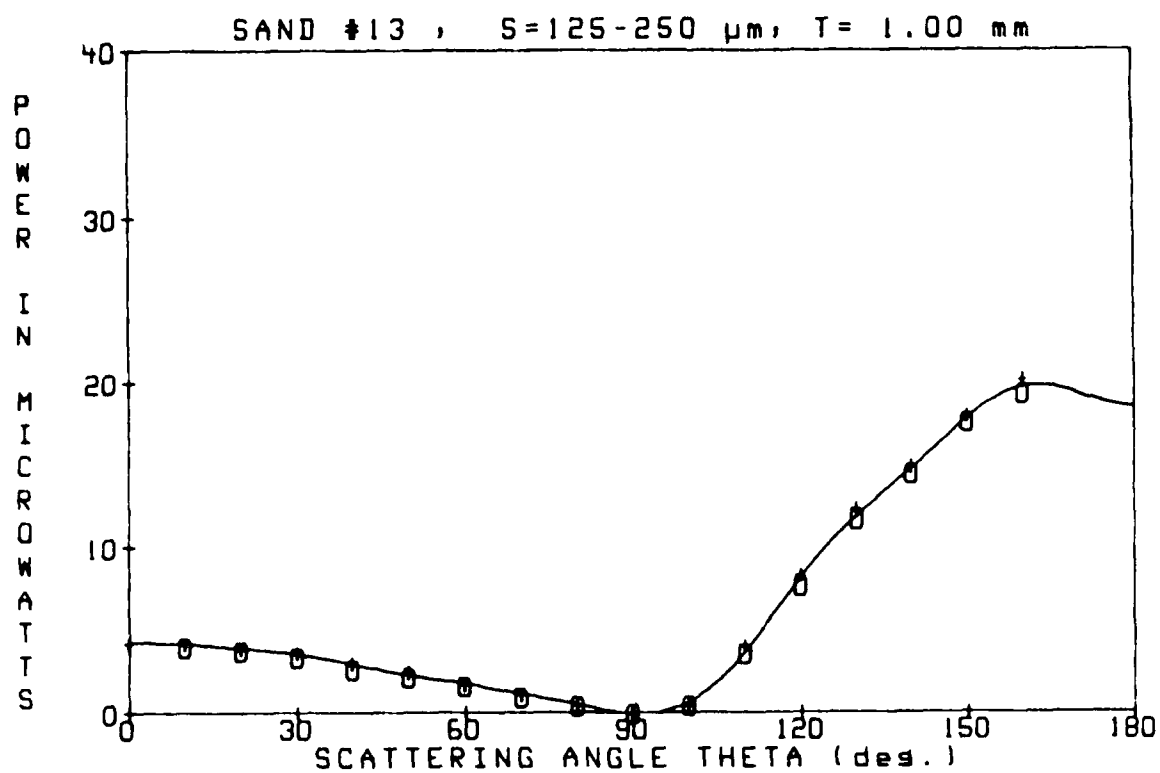


SAND #13

S=125-250 μ m

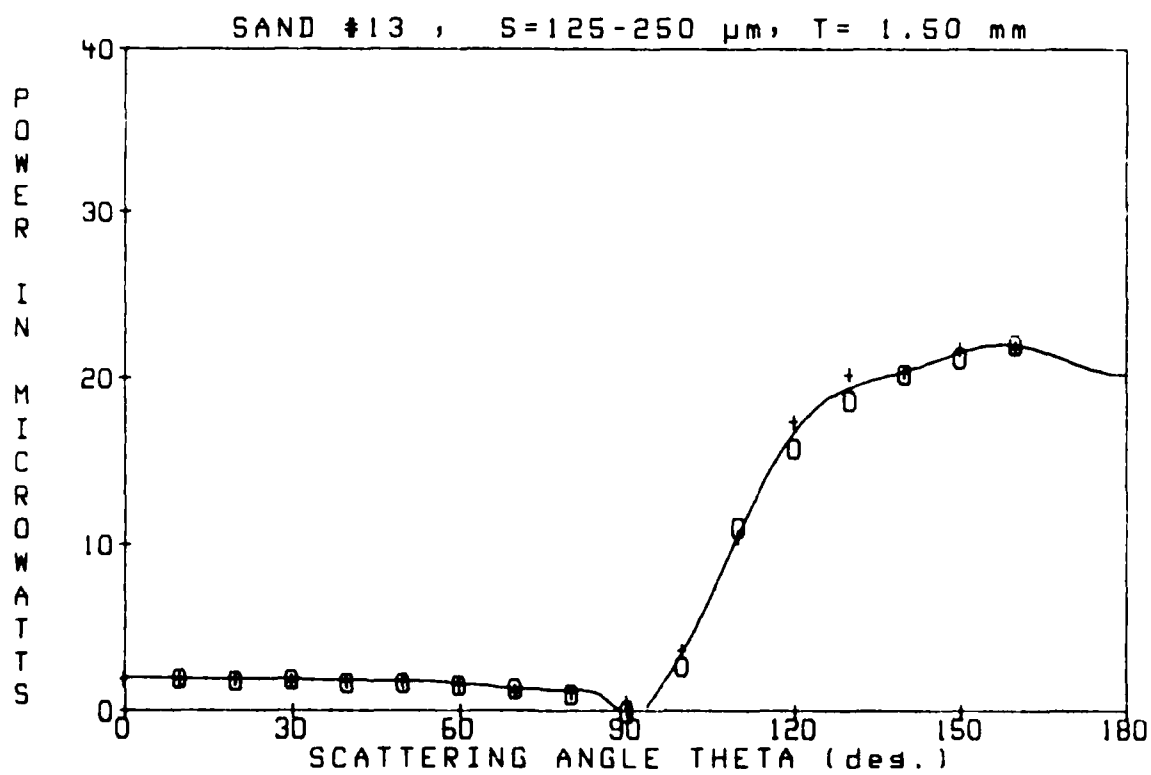
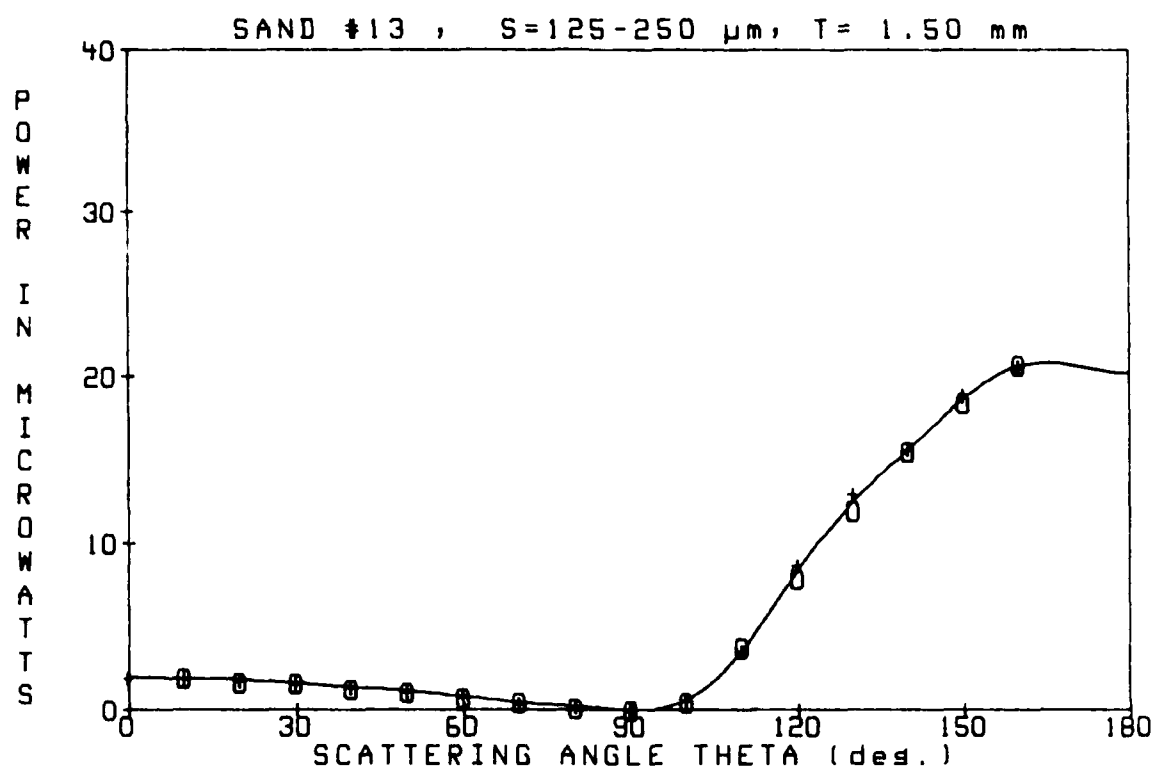
T= 1.00 mm

SCATTERING ANGLE	DIODE VOLTAGE	POWER (microwatts)
-160	3.16	19.28
-150	2.88	17.58
-140	2.36	14.42
-130	1.91	11.68
-120	1.27	7.72
-110	0.60	3.63
-100	0.08	0.51
-90	0.00	0.00
-80	0.07	0.45
-70	0.16	0.98
-60	0.27	1.67
-50	0.35	2.14
-40	0.44	2.71
-30	0.57	3.45
-20	0.63	3.81
-10	0.66	4.05
0	0.70	4.29
10	0.69	4.23
20	0.65	3.96
30	0.61	3.72
40	0.50	3.04
50	0.41	2.50
60	0.29	1.79
70	0.19	1.16
80	0.08	0.48
90	0.00	0.00
100	0.09	0.53
110	0.67	4.08
120	1.37	8.37
130	2.02	12.33
140	2.44	14.90
150	2.96	18.06
160	3.31	20.20



SAND #13 S=125-250 μ m T= 1.50 mm

SCATTERING ANGLE	DIODE VOLTAGE	POWER (microwatts)
-160	3.39	20.68
-150	3.02	18.42
-140	2.55	15.56
-130	1.97	12.04
-120	1.30	7.95
-110	0.63	3.81
-100	0.08	0.48
-90	0.00	0.00
-80	0.03	0.18
-70	0.08	0.48
-60	0.13	0.77
-50	0.18	1.10
-40	0.21	1.28
-30	0.27	1.63
-20	0.28	1.73
-10	0.32	1.96
0	0.32	1.96
10	0.32	1.96
20	0.30	1.84
30	0.26	1.60
40	0.23	1.43
50	0.19	1.16
60	0.14	0.83
70	0.07	0.41
80	0.03	0.21
90	0.00	0.00
100	0.11	0.65
110	0.59	3.61
120	1.44	8.76
130	2.14	13.05
140	2.57	15.67
150	3.10	18.89
160	3.37	20.56

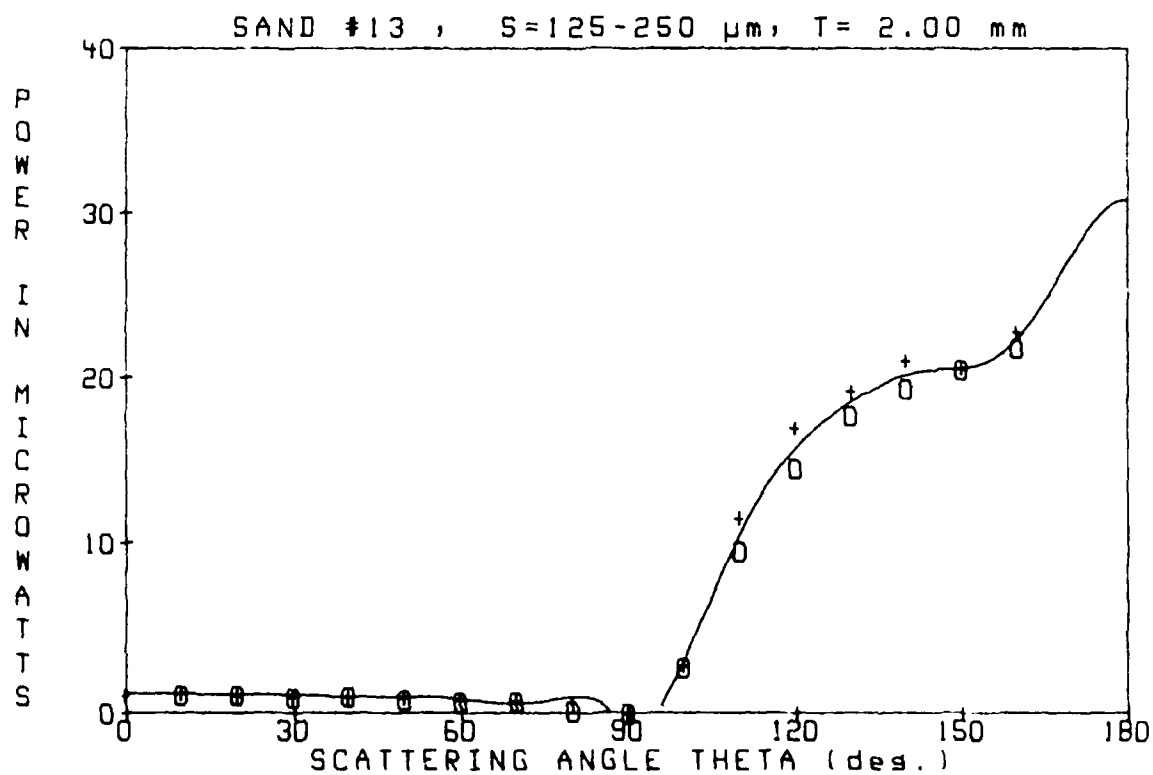
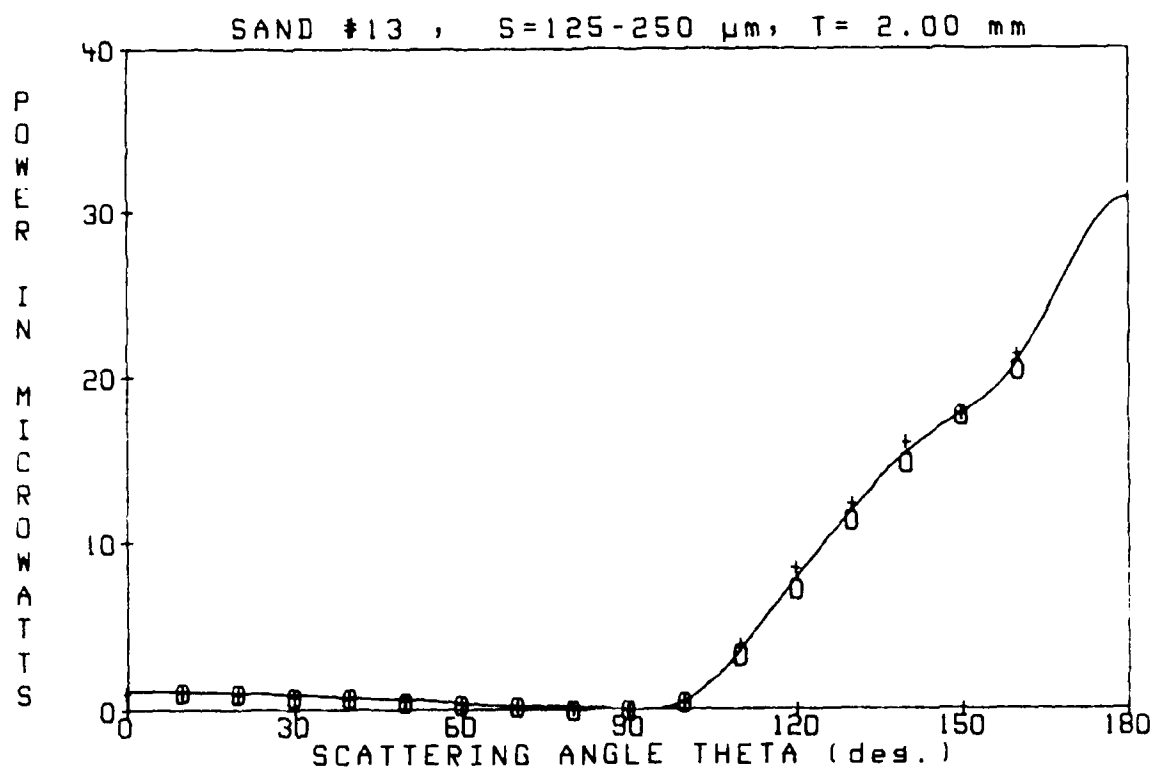


SAND #13

S=125-250 μ m

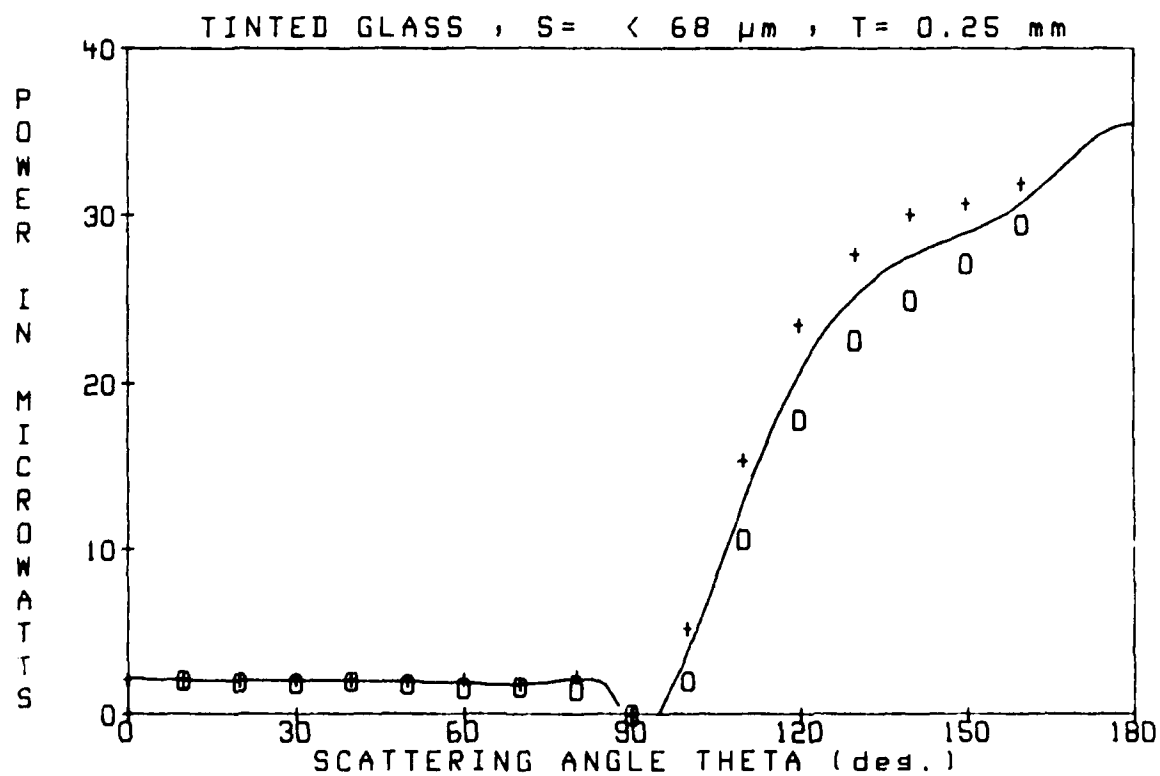
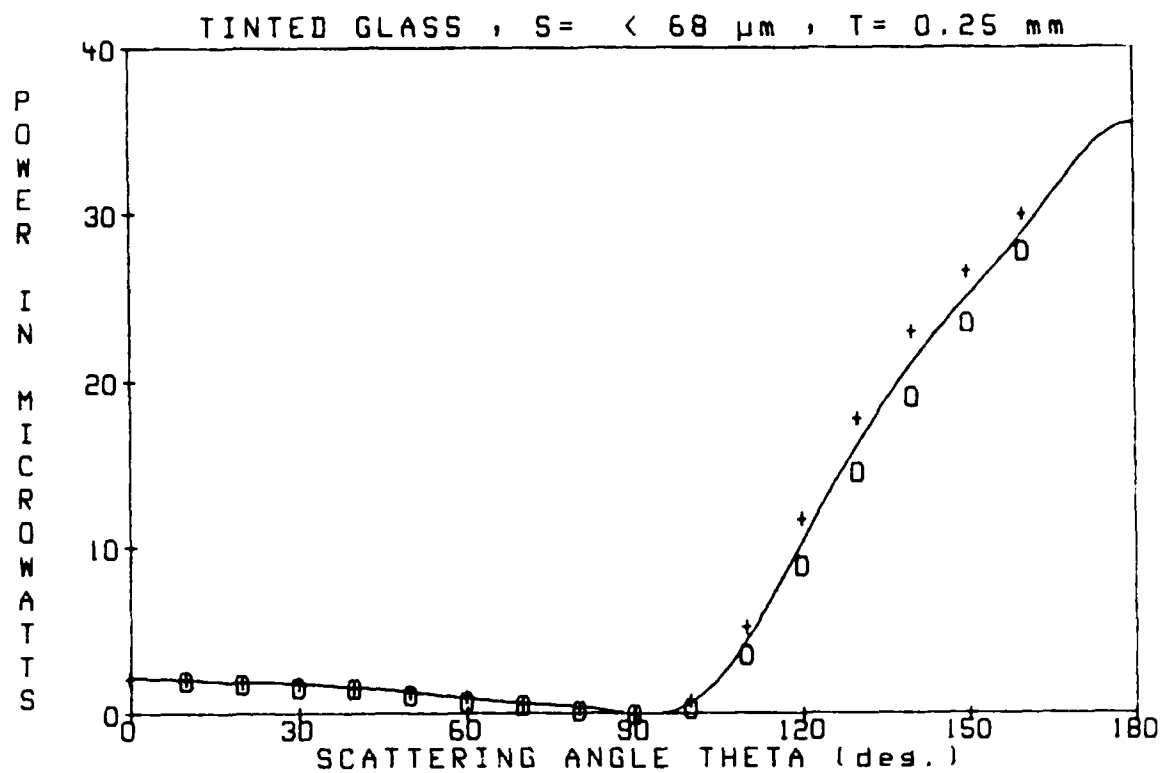
T= 2.00 mm

SCATTERING ANGLE	DIODE VOLTAGE	POWER (microwatts)
-160	3.35	20.44
-150	2.91	17.73
-140	2.42	14.78
-130	1.87	11.38
-120	1.19	7.27
-110	0.54	3.28
-100	0.08	0.48
-90	0.00	0.00
-80	0.00	0.00
-70	0.04	0.24
-60	0.06	0.35
-50	0.09	0.53
-40	0.13	0.77
-30	0.14	0.83
-20	0.17	1.01
-10	0.18	1.10
0	0.18	1.10
10	0.19	1.19
20	0.17	1.04
30	0.15	0.89
40	0.13	0.80
50	0.10	0.62
60	0.07	0.41
70	0.04	0.26
80	0.02	0.12
90	0.00	0.00
100	0.08	0.51
110	0.65	3.96
120	1.40	8.52
130	2.02	12.33
140	2.64	16.09
150	2.92	17.82
160	3.51	21.39



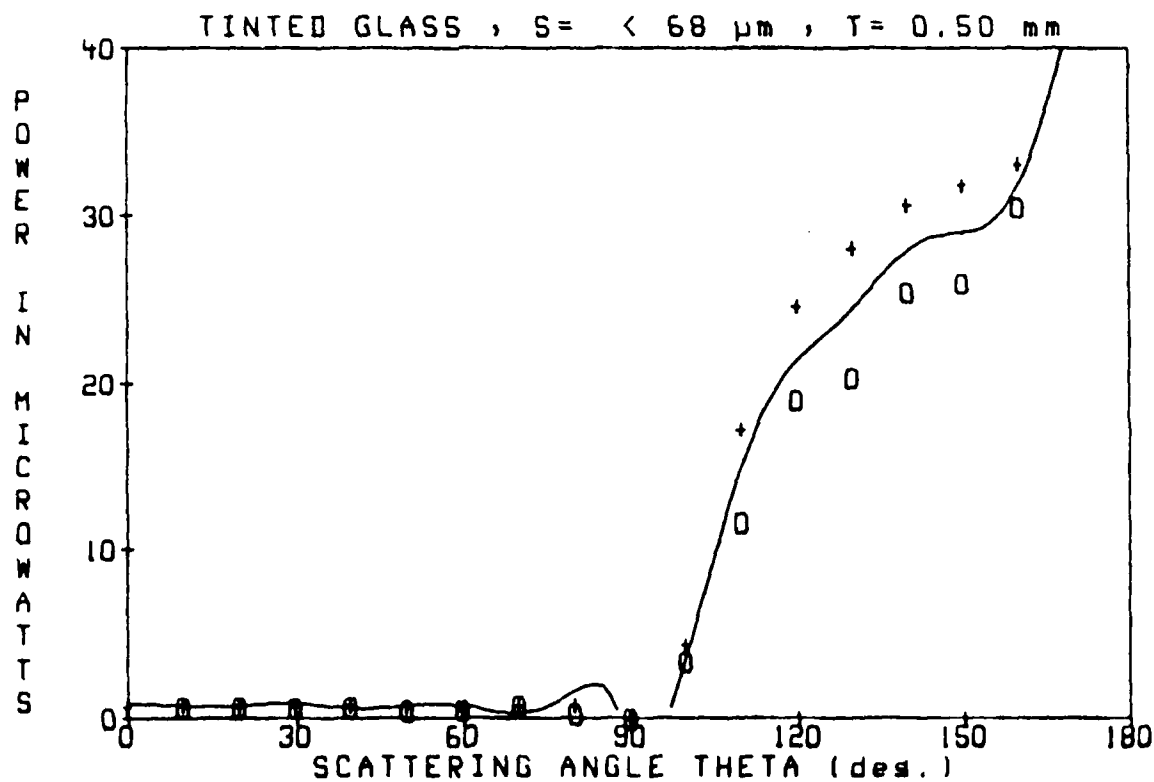
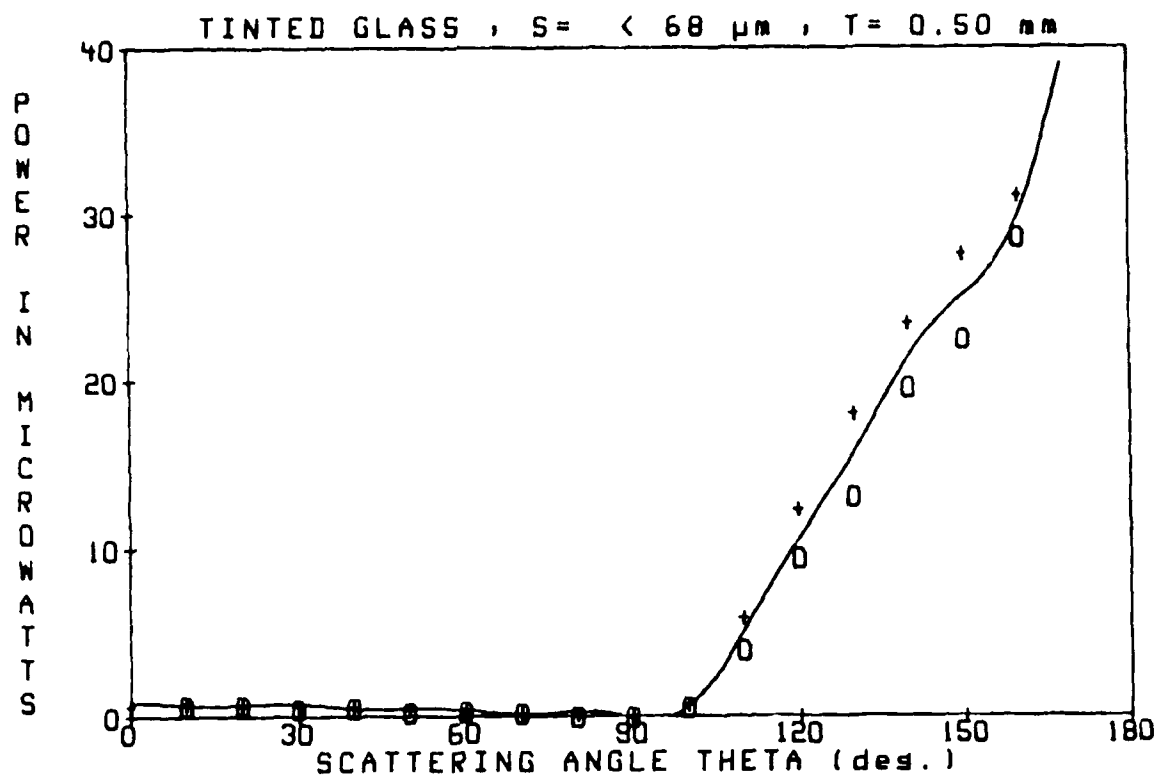
TINTED GLASS S = < 68 μ m T = 0.25 mm

SCATTERING ANGLE	DIODE VOLTAGE	POWER (microwatts)
-160	4.55	27.74
-150	3.85	23.48
-140	3.14	19.13
-130	2.38	14.51
-120	1.46	8.94
-110	0.60	3.63
-100	0.06	0.35
-90	0.00	0.00
-80	0.04	0.26
-70	0.10	0.59
-60	0.13	0.77
-50	0.19	1.16
-40	0.25	1.55
-30	0.27	1.63
-20	0.30	1.84
-10	0.34	2.06
0	0.35	2.14
10	0.35	2.14
20	0.33	1.99
30	0.31	1.87
40	0.27	1.63
50	0.22	1.34
60	0.17	1.07
70	0.11	0.65
80	0.07	0.41
90	0.00	0.00
100	0.15	0.92
110	0.86	5.27
120	1.92	11.74
130	2.92	17.82
140	3.78	23.06
150	4.37	26.64
160	4.92	30.04



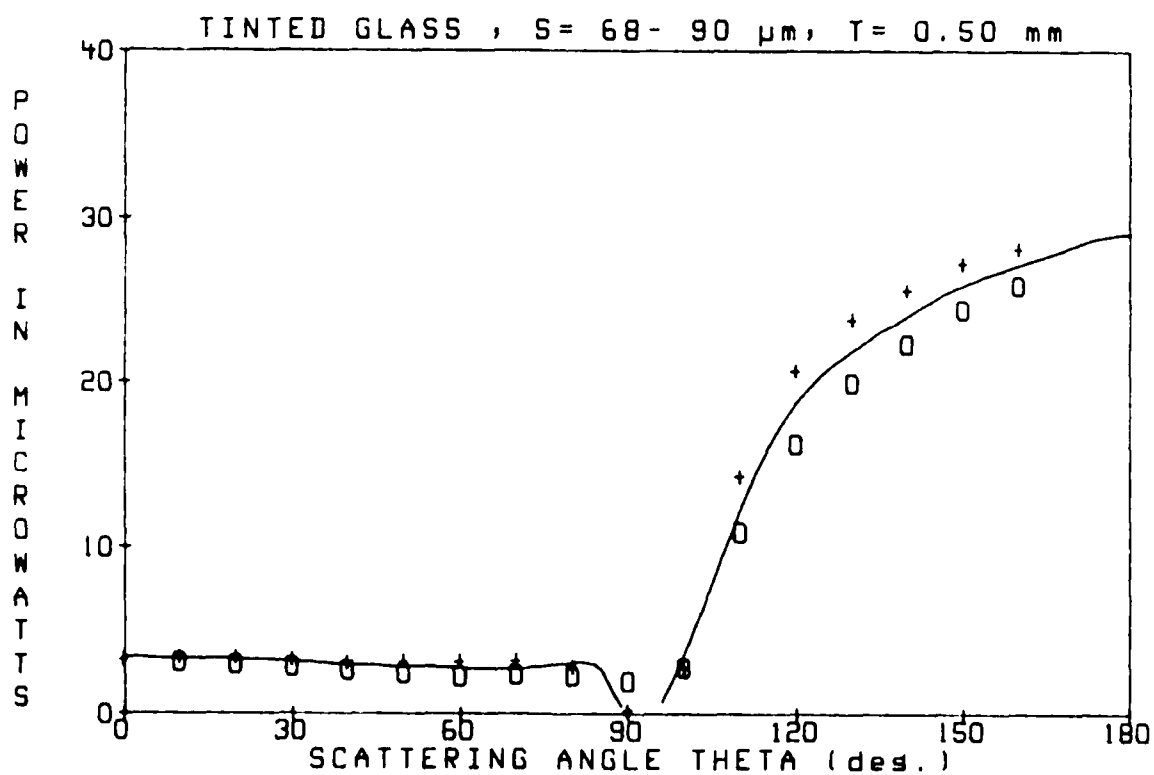
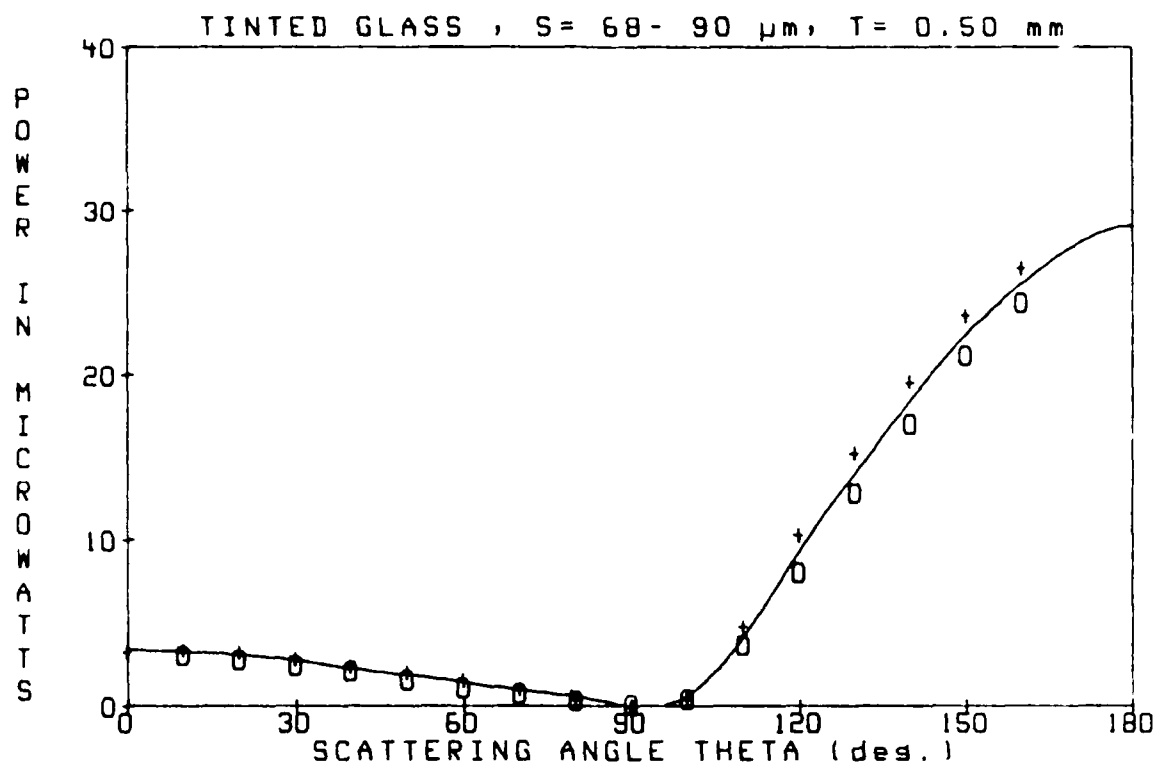
TINTED GLASS S = 68 μ m T = 0.50 mm

SCATTERING ANGLE	DIODE VOLTAGE	POWER (microwatts)
-160	4.70	28.68
-150	3.69	22.53
-140	3.20	19.54
-130	2.14	13.08
-120	1.55	9.47
-110	0.65	3.99
-100	0.10	0.15
-90	0.00	0.00
-80	0.00	0.00
-70	0.04	0.26
-60	0.05	0.29
-50	0.05	0.32
-40	0.09	0.58
-30	0.09	0.53
-20	0.11	0.68
-10	0.11	0.68
0	0.11	0.68
10	0.14	0.83
20	0.12	0.71
30	0.11	0.68
40	0.10	0.62
50	0.08	0.48
60	0.05	0.29
70	0.04	0.26
80	0.02	0.15
90	0.00	0.00
100	0.13	0.77
110	0.97	5.90
120	2.02	12.33
130	2.97	18.09
140	3.85	23.51
150	4.53	27.62
160	5.11	31.20



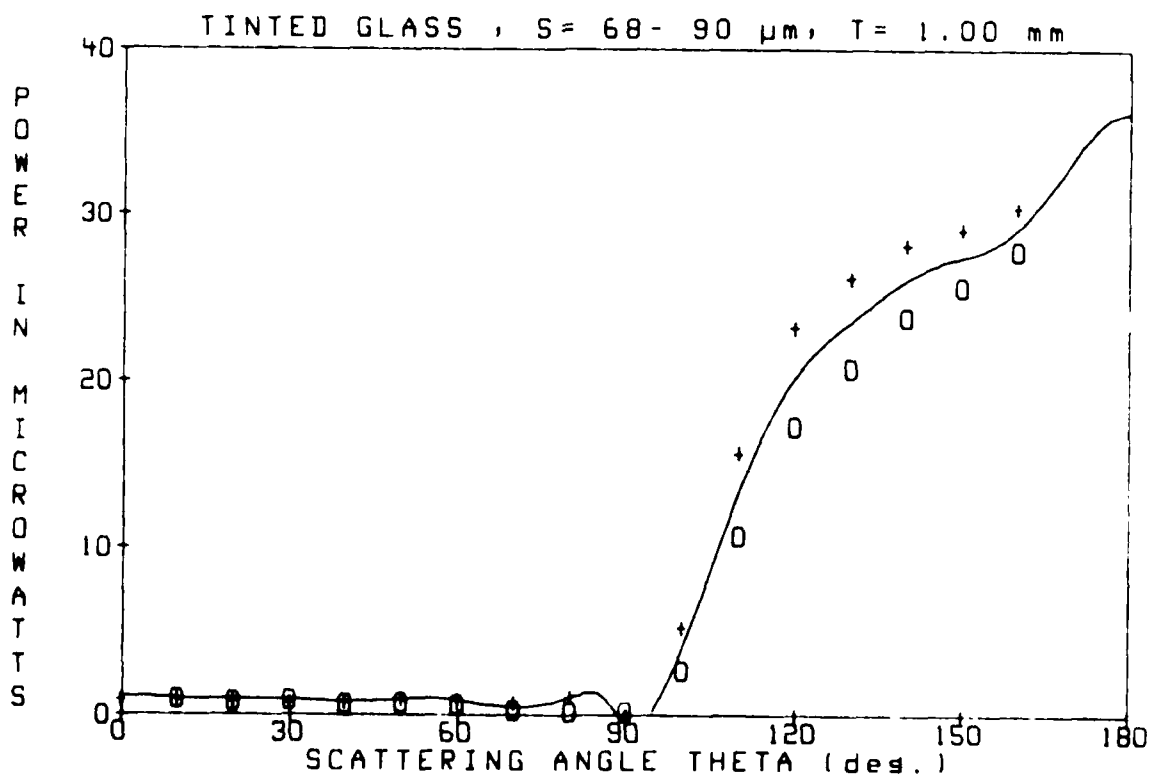
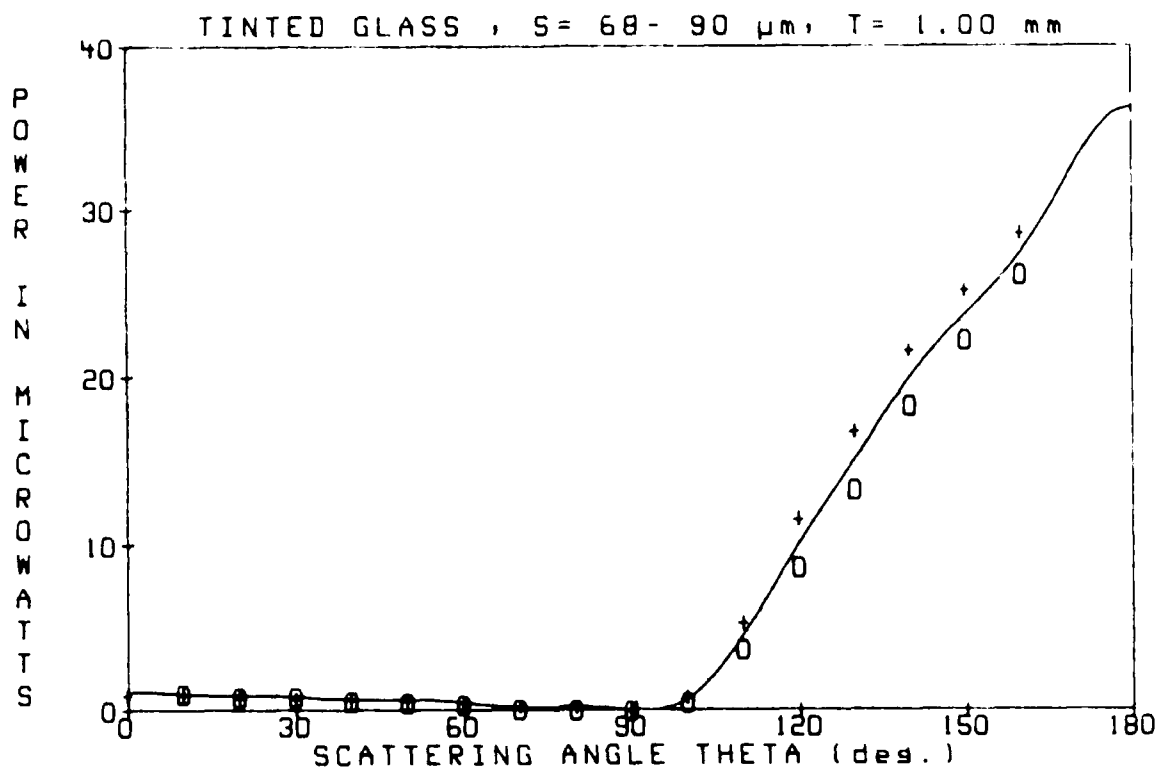
TINTED GLASS S = 68- 90 μ m T = 0.50 mm

SCATTERING ANGLE	DIODE VOLTAGE	POWER (microwatts)
-160	4.01	24.43
-150	3.48	21.25
-140	2.81	17.13
-130	2.11	12.87
-120	1.34	8.16
-110	0.62	3.75
-100	0.08	0.51
-90	0.03	0.18
-80	0.07	0.41
-70	0.14	0.83
-60	0.19	1.16
-50	0.26	1.60
-40	0.35	2.14
-30	0.43	2.59
-20	0.47	2.89
-10	0.52	3.18
0	0.55	3.34
10	0.57	3.45
20	0.54	3.28
30	0.48	2.92
40	0.40	2.44
50	0.34	2.08
60	0.26	1.60
70	0.19	1.13
80	0.08	0.51
90	0.00	0.00
100	0.08	0.51
110	0.80	4.89
120	1.70	10.37
130	2.52	15.37
140	3.22	19.67
150	3.87	23.63
160	4.35	26.52



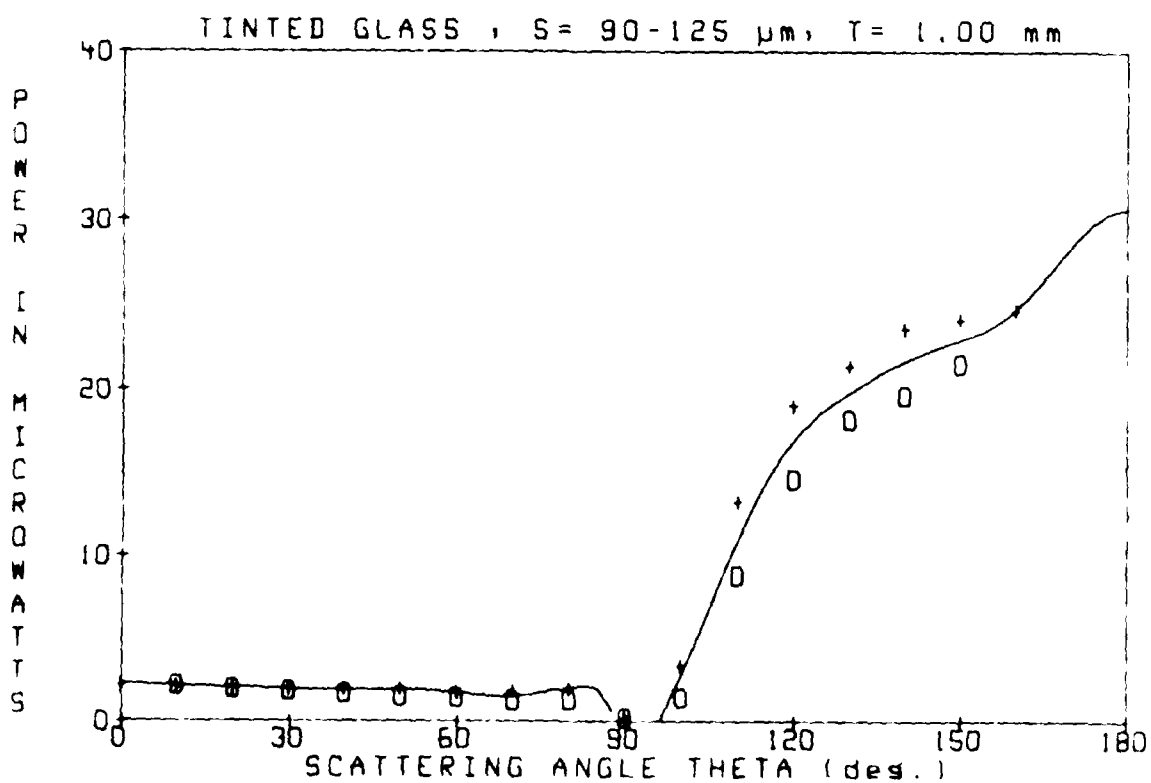
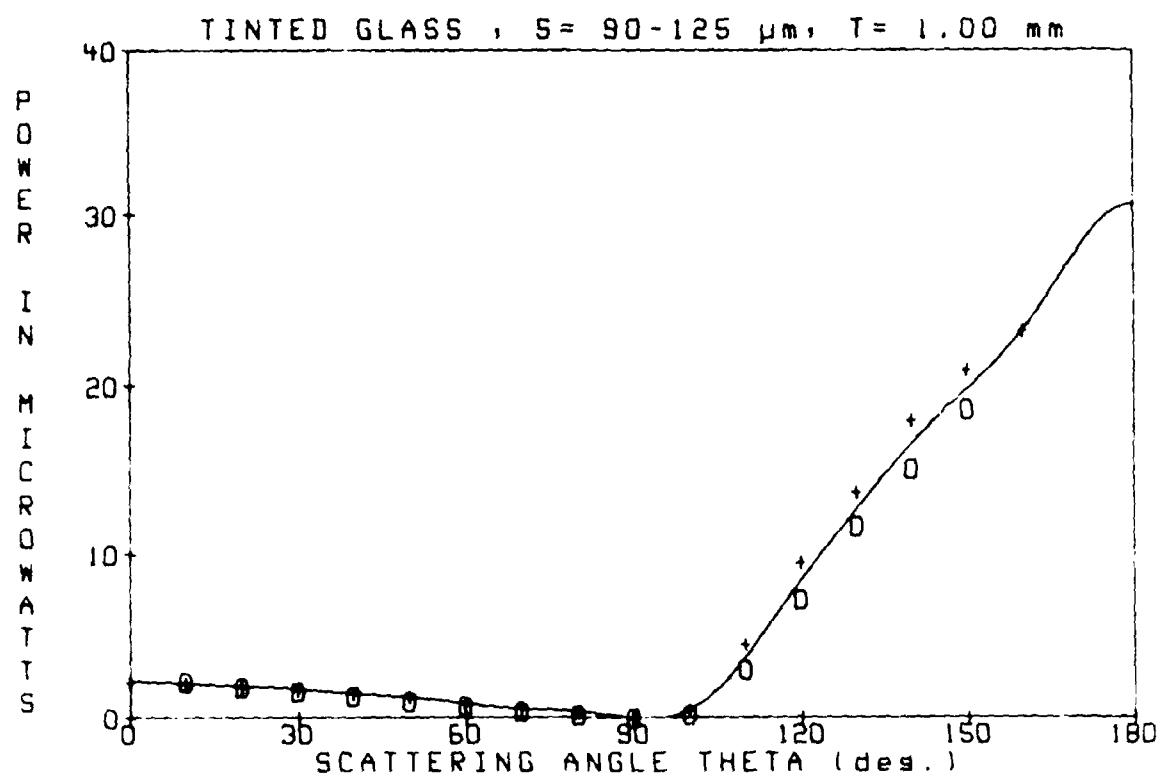
TINTED GLASS S= 68- 90 um T= 1.00 mm

SCATTERING ANGLE	DIODE VOLTAGE	POWER (microwatts)
-160	4.28	26.13
-150	3.64	22.23
-140	3.00	18.29
-130	2.19	13.38
-120	1.43	8.70
-110	0.60	3.69
-100	0.08	0.48
-90	0.00	0.00
-80	0.00	0.00
-70	0.02	0.12
-60	0.06	0.35
-50	0.09	0.53
-40	0.10	0.59
-30	0.14	0.83
-20	0.14	0.83
-10	0.17	1.04
0	0.16	0.98
10	0.17	1.01
20	0.14	0.83
30	0.12	0.74
40	0.11	0.68
50	0.11	0.65
60	0.08	0.48
70	0.05	0.29
80	0.03	0.21
90	0.00	0.00
100	0.15	0.92
110	0.88	5.39
120	1.90	11.62
130	2.77	16.87
140	3.55	21.63
150	4.14	25.24
160	4.70	28.56



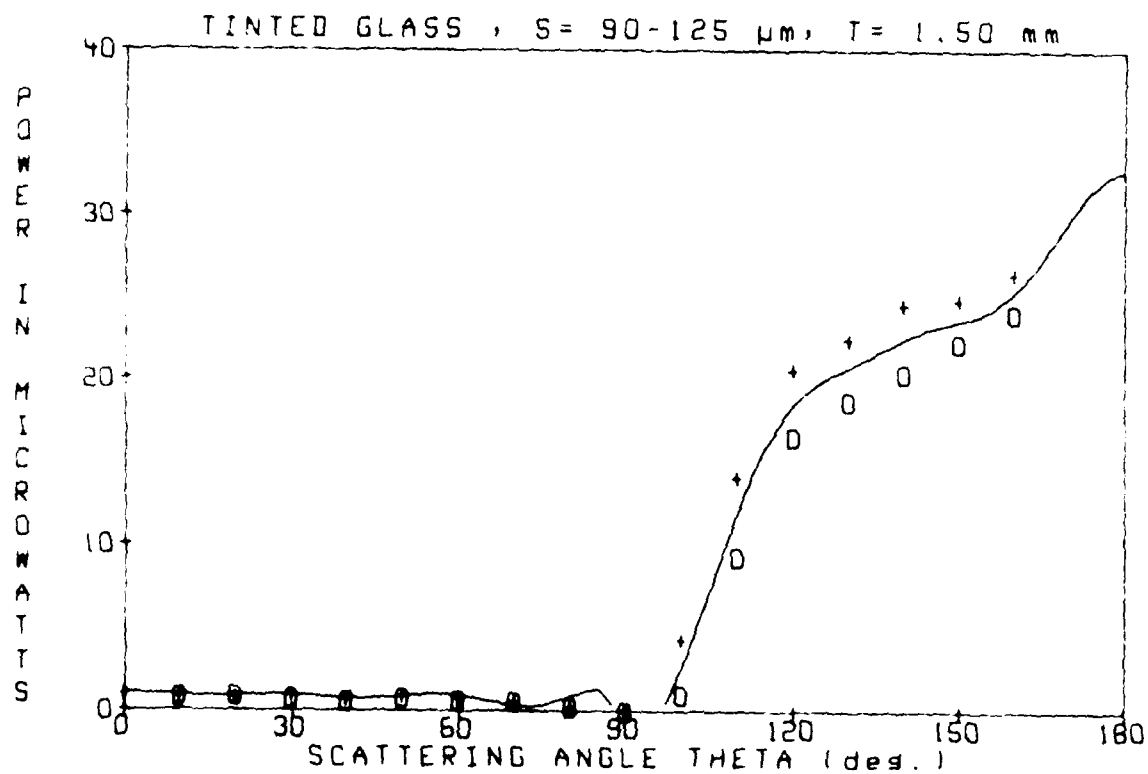
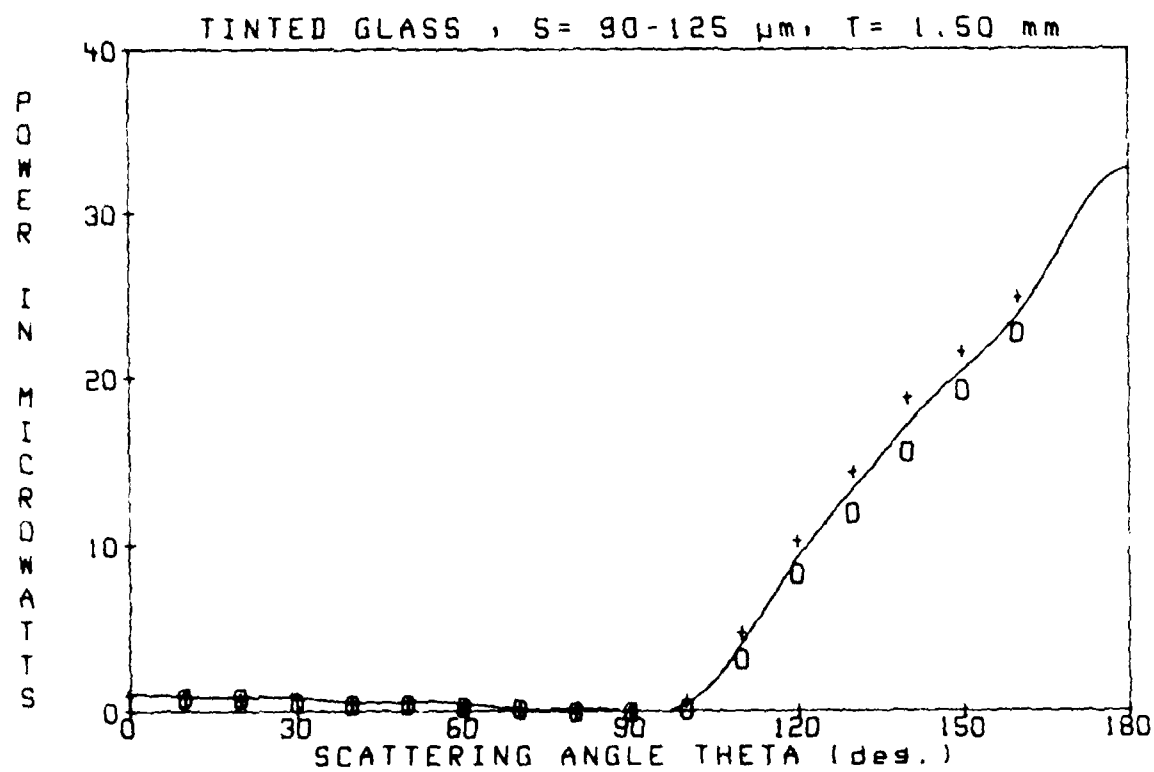
TINTED GLASS S= 90-125 μm T= 1.00 mm

SCATTERING ANGLE	DIODE VOLTAGE	POWER (microwatts)
-160		
-150	3.06	18.65
-140	2.47	15.07
-130	1.92	11.74
-120	1.20	7.33
-110	0.50	3.04
-100	0.04	0.26
-90	0.00	0.00
-80	0.04	0.24
-70	0.07	0.45
-60	0.12	0.74
-50	0.17	1.01
-40	0.22	1.37
-30	0.27	1.63
-20	0.31	1.90
-10	0.36	2.20
0	0.36	2.20
10	0.35	2.14
20	0.32	1.95
30	0.29	1.76
40	0.26	1.57
50	0.22	1.37
60	0.15	0.92
70	0.11	0.65
80	0.06	0.37
90	0.00	0.00
100	0.10	0.59
110	0.75	4.56
120	1.57	9.56
130	2.26	13.76
140	2.96	18.06
150	3.43	20.95
160	3.81	23.24



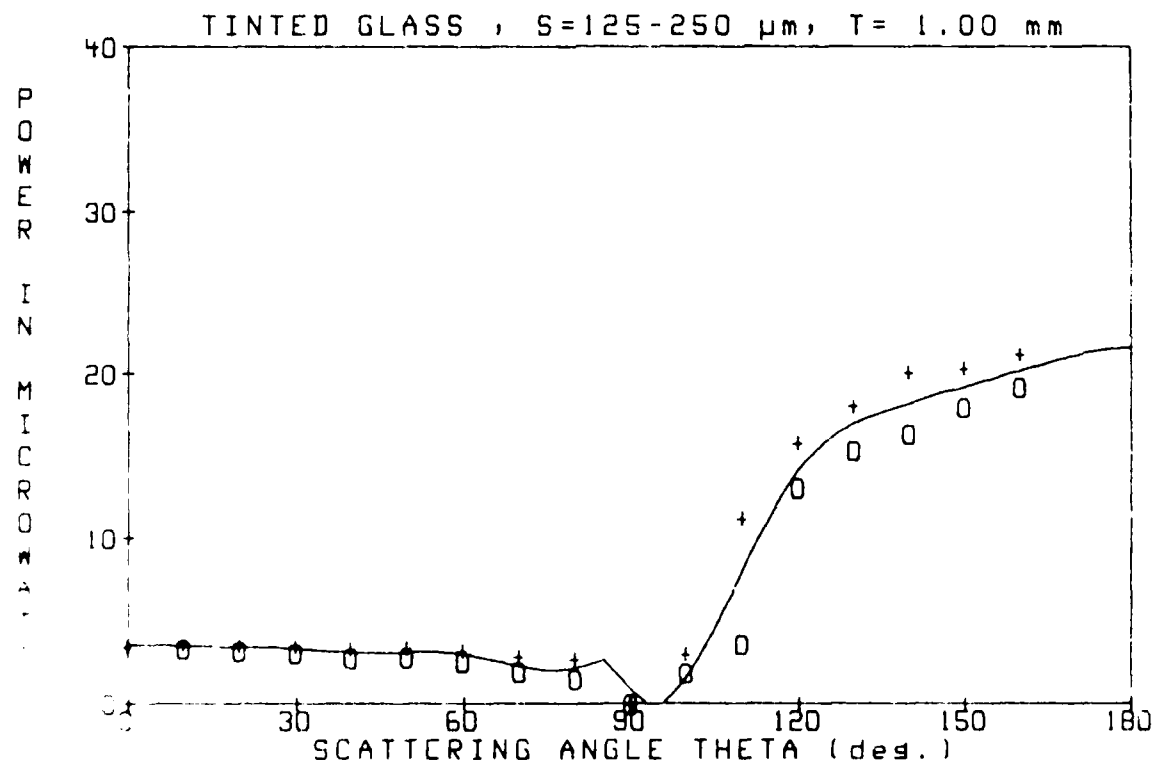
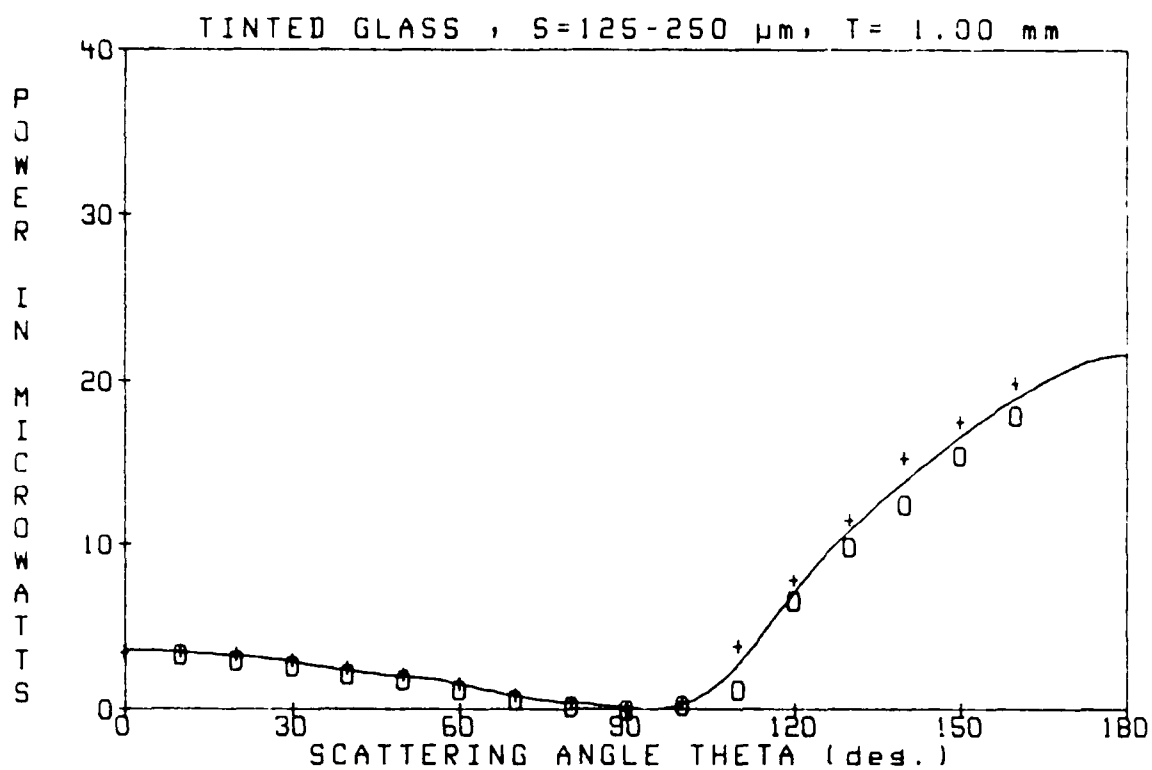
TINTED GLASS S = 90-125 μ m T = 1.50 mm

SCATTERING ANGLE	DIODE VOLTAGE	POWER (microwatts)
-160	3.72	22.87
-150	3.16	19.25
-140	2.56	15.51
-130	1.97	12.04
-120	1.36	8.28
-110	0.53	3.21
-100	0.03	0.18
-90	0.00	0.00
-80	0.00	0.00
-70	0.03	0.21
-60	0.06	0.35
-50	0.09	0.53
-40	0.09	0.53
-30	0.11	0.65
-20	0.15	0.89
-10	0.15	0.89
0	0.17	1.01
10	0.16	0.95
20	0.14	0.86
30	0.15	0.89
40	0.11	0.65
50	0.10	0.62
60	0.07	0.41
70	0.03	0.21
80	0.00	0.00
90	0.00	0.00
100	0.13	0.77
110	0.79	4.83
120	1.69	10.31
130	2.37	14.45
140	3.09	18.83
150	3.54	21.57
160	4.08	24.91



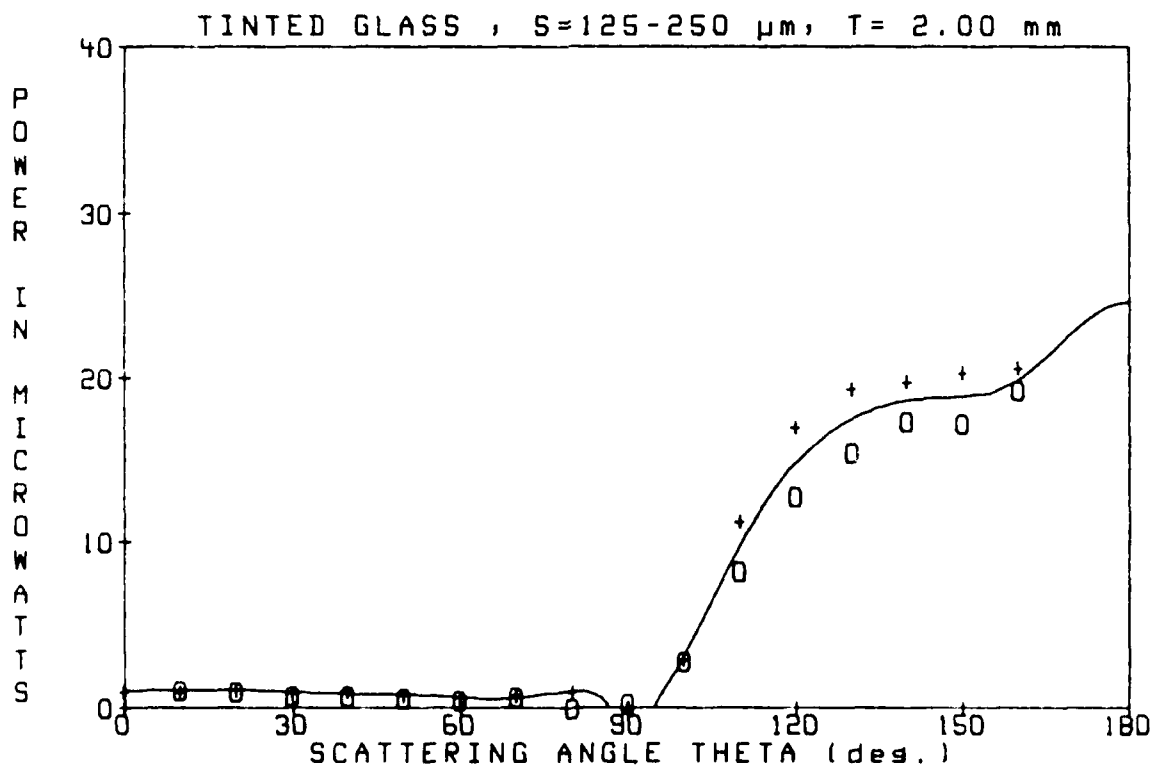
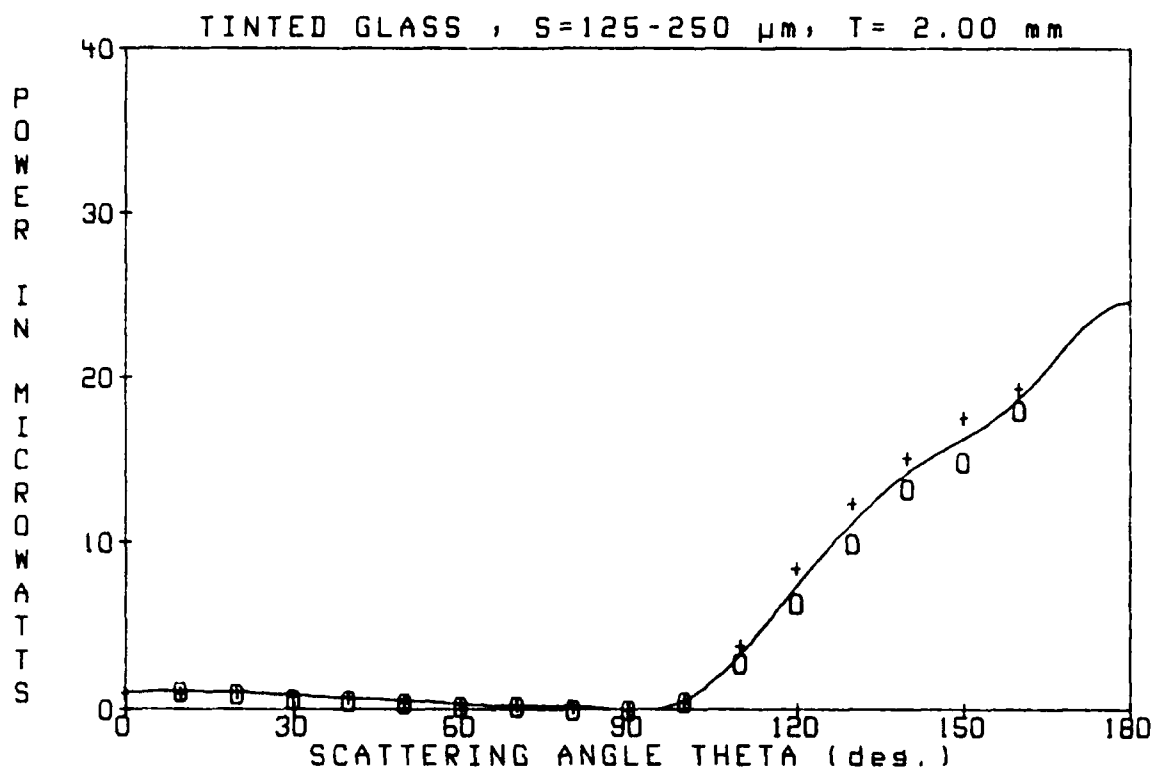
TINTED GLASS S=125-250 μ m T= 1.00 mm

SCATTERING ANGLE	DIODE VOLTAGE	POWER (microwatts)
-160	2.95	18.00
-150	2.55	15.56
-140	2.06	12.54
-130	1.62	9.89
-120	1.07	6.55
-110	0.21	1.25
-100	0.05	0.32
-90	0.00	0.00
-80	0.04	0.26
-70	0.11	0.65
-60	0.21	1.25
-50	0.30	1.84
-40	0.35	2.14
-30	0.44	2.68
-20	0.50	3.04
-10	0.55	3.34
0	0.58	3.51
10	0.59	3.57
20	0.55	3.37
30	0.50	3.04
40	0.42	2.56
50	0.36	2.20
60	0.26	1.60
70	0.16	0.98
80	0.08	0.48
90	0.00	0.00
100	0.09	0.53
110	0.63	3.87
120	1.30	7.92
130	1.91	11.65
140	2.53	15.43
150	2.90	17.67
160	3.27	19.97



TINTED GLASS S=125-250 μm T= 2.00 mm

SCATTERING ANGLE		DIODE VOLTAGE		POWER (microwatts)
-160		2.96		18.06
-150		2.44		14.90
-140		2.18		13.29
-130		1.63		9.95
-120		1.05		6.37
-110		0.46		2.83
-100		0.08		0.51
-90		0.00		0.00
-80		0.00		0.00
-70		0.04		0.24
-60		0.04		0.24
-50		0.07		0.41
-40		0.10		0.59
-30		0.11		0.65
-20		0.16		0.98
-10		0.17		1.07
0		0.17		1.01
10		0.17		1.01
20		0.17		1.07
30		0.14		0.86
40		0.14		0.83
50		0.09		0.53
60		0.06		0.35
70		0.05		0.29
80		0.03		0.18
90		0.00		0.00
100		0.09		0.53
110		0.63		3.87
120		1.40		8.52
130		2.04		12.46
140		2.49		15.20
150		2.90		17.67
160		3.17		19.37



END

8-87

DTIC